State of California
The Resources Agency
Department of Water Resources
Office of State Water Project Planning

METHODOLOGY FOR FLOW AND SALINITY ESTIMATES IN THE SACRAMENTO-SAN JOAQUIN DELTA AND SUISUN MARSH

TWENTY-THIRD ANNUAL PROGRESS REPORT TO THE STATE WATER RESOURCES CONTROL BOARD
In Accordance with Water Right Decision 1485, Order 9

June 2002

Gray Davis
Governor
State of California

Mary D. Nichols
Secretary for Resources
The Resources Agency

Thomas M. Hannigan
Director
Department of Water Resources

FOREWORD

This is the twenty-third annual progress report of the California Department of Water Resources' San Francisco Bay-Delta Evaluation Program, which is carried out by the Delta Modeling Section.

It documents progress in the development and enhancement of the Delta Modeling Section's computer models and reports the latest findings of studies conducted as part of the program. This report was compiled by Michael Mierzwa, with assistance from Jane Schafer-Kramer and Nikki Blomquist, under the direction of Paul Hutton, program manager for the Bay-Delta Evaluation Program.

On-line versions of previous annual progress reports are available at:

http://modeling.water.ca.gov/branch/reports.html

For more information contact:

Tara Smith
tara@water.ca.gov
(916) 653-9885

-or-

Michael Mierzwa
mmierzwa@water.ca.gov
(916) 653-9794

TABLE OF CONTENTS

FOREWORD iii

1 INTRODUCTION 1-1

2 PARTICLE TRACKING MODEL VERIFICATION AND CALIBRATION 2-1

2.1 Introduction 2-1
2.2 Background 2-1
2.3 PTM Theory 2-2
2.3.1 Longitudinal Dispersion 2-3
2.3.2 Longitudinal Diffusion 2-6
2.3.3 Channel Boundaries 2-9
2.3.4 Movement at Junctions 2-10
2.3.5 Movement in and out of Open Water Areas 2-11
2.4 Profile Calibration 2-11
2.4.1 Estimation of Profile Coefficients 2-11
2.4.2 Calibration of Profile Shape Conclusions 2-19
2.5 Verification of PTM in a Single Channel – Static Stage 2-19
2.5.1 Methods 2-20
2.5.2 Results 2-21
2.5.3 Verification Discussion 2-23
2.6 Future Directions 2-23
2.7 References 2-24

3 ANALYSIS AND PREPARATION OF OBSERVED DATA FOR INPUT FILES IN SUPPORT OF DSM2 EXTENDED VALIDATION (1975-1999) 3-1

3.1 Introduction 3-1
3.2 Objectives 3-1
3.3 Description of Analysis and Preparation of Data 3-1
3.3.1 Acquisition of Data 3-1
3.3.2 Analysis and Screening of Input Data for DSM2 Input Files 3-1
3.3.3 Documentation of Delta Events and Activities 3-2
3.4 In Progress and Future Work 3-3

4 CALSIM VERSUS DSM2 ANN AND G-MODEL COMPARISONS 4-1

4.1 Introduction 4-1
4.2 Description of Scenarios 4-1
4.3 Simulation Inputs 4-2
4.3.1 CALSIM 4-2
4.3.2 DSM2 4-3
4.4 Results 4-4
4.4.1 Emmaton 4-4
4.4.2 Jersey Point 4-11
4.4.3 Rock Slough 4-17
4.5 Conclusions 4-23
4.6 References 4-24

5 RELATIONSHIPS BETWEEN DELTA WATER QUALITY CONSTITUENTS AS DERIVED FROM GRAB SAMPLES..... 5-1
5.1 Introduction 5-1
5.2 General Methodology 5-1
5.3 Methodology.....5-2
5.4 A Sample Analysis.....5-3
5.5 Future Directions 5-11
5.6 Reference.....5-11

6 CALIBRATING DSM2-QUAL DISPERSION FACTORS TO PRACTICAL SALINITY 6-1
6.1 Introduction 6-1
6.2 Background 6-1
6.2.1 Calibrating QUAL to EC 6-1
6.2.2 Calibrating QUAL to TDS.....6-4
6.3 Calibrating QUAL to Practical Salinity.....6-6
6.3.1 Practical Salinity Background 6-6
6.3.2 Practical Salinity in the Sacramento-San Joaquin Delta.....6-8
6.3.3 An Alternative Correction to Extend Practical Salinity Scale 1978 Below 1 PPT TDS in the Delta.....6-10
6.3.4 Practical Salinity at Delta Boundaries.....6-13
6.3.5 Practical Salinity of Agricultural Drainage.....6-13
6.3.6 Converting QUAL-Generated Practical Salinity to EC 6-15
6.4 References.....6-18

7 GENERATING MONTHLY DISSOLVED ORGANIC CARBON AND UVA AT DSM2 BOUNDARIES 7-1
7.1 Introduction 7-1
7.2 General Methodology 7-1
7.3 Sacramento River at Greens Landing.....7-2
7.3.1 Dissolved Organic Carbon at Greens Landing 7-2
7.3.2 Ultraviolet Absorbance at Greens Landing 7-8
7.4 San Joaquin River at Vernalis 7-9
7.4.1 Dissolved Organic Carbon at Vernalis.....7-9
7.4.2 Ultraviolet Absorbance at Vernalis.....7-15
7.5 Mokelumne River 7-17
7.5.1 Dissolved Organic Carbon on Mokelumne River.....7-17
7.5.2 Ultraviolet Absorbance on Mokelumne River.....7-21

8 CALSIM WATER QUALITY OPERATING RULES TO MEET DELTA WETLANDS WATER QUALITY MANAGEMENT PLAN..... 8-1
8.1 Introduction 8-1
8.2 CALSIM II 8-3
8.3 Chloride.....8-3
8.3.1 Base Chloride Study 8-5
8.3.2 Project Study Using Chloride Constraints.....8-5
8.4 Total Organic Carbon 8-7
8.4.1 Base DOC Study.....8-8
8.4.2 Project Study Using DOC Constraints 8-8
8.5 Bromate.....8-9
8.6 Total Trihalomethanes (TTHM) 8-9
8.7 Temperature and DOC.....8-10

8.8 References **8-10**

9 DOC GROWTH IN QUAL **9-1**
9.1 Background **9-1**
9.2 Implementation Detail **9-1**
9.2.1 Logistic Equation 9-1
9.2.2 Depth Adjustment 9-2
9.2.3 Timing of Filling and Draining 9-2
9.3 Results **9-2**
9.4 Summary **9-4**
9.5 References **9-4**

10 OPTIMAL CONTROL OF DELTA SALINITY **10-1**
10.1 Introduction **10-1**
10.2 Minimum Water Cost Compliance **10-2**
10.3 Optimal Control Solutions **10-2**
10.3.1 Parameterization 10-3
10.3.2 Regularization 10-3
10.3.3 Comparing Parameterization and Regularization 10-4
10.4 Experiments Using DSM2 ..... **10-7**
10.5 Extensions **10-13**
10.6 References **10-13**

11 16-YEAR DSM2 PLANNING STUDIES WITH ADJUSTED ASTRONOMICAL TIDES AND DAILY HYDROLOGY **11-1**
11.1 Introduction **11-1**
11.2 Preprocessing Planning Runs **11-2**
11.2.1 Changes in HYDRO 11-2
11.2.2 Changes in QUAL 11-3
11.3 Post Processing **11-5**
11.4 Summary **11-7**
11.5 References **11-8**

12 DSM2 DOCUMENTATION **12-1**
12.1 Introduction **12-1**
12.2 Objectives **12-1**
12.2.1 Documenting DSM2 12-1
12.2.2 Standardizing Documentation of DSM2 Studies 12-1
12.3 DSM2 Documentation Overview **12-1**
12.3.1 Volume 1: Formulation and Verification 12-2
12.3.2 Volume 2: Calibration and Validation 12-2
12.3.3 Volume 3: Using DSM2 12-3
12.4 DSM2 Tutorial **12-3**
12.5 Progress and Future Directions **12-4**
12.6 References **12-4**

13 DSM2 INPUT DATABASE AND DATA MANAGEMENT SYSTEM **13-1**
13.1 Introduction **13-1**
13.2 Database and Data Management **13-2**
13.3 Database Structure **13-4**
13.4 Component Sets and Layers **13-7**
13.5 Version Control **13-9**
13.6 Data Validation and the Externalization of Quality Control **13-10**

13.7 Conclusions **13-11**

14 DSM2 FINGERPRINTING METHODOLOGY **14-1**
14.1 Introduction **14-1**
14.2 Conceptualization of Volume Fingerprinting **14-2**
14.3 Conceptualization of Volume and Timing Fingerprinting **14-5**
14.4 Constituent Fingerprinting **14-9**
14.5 Application of Fingerprinting in the Delta using DSM2 ..... **14-9**
14.5.1 Volume Fingerprinting for Conservative Constituents by using Tracer Constituents in QUAL 14-12
14.5.2 Volume and Timing Fingerprinting for Conservative Constituents by using Tracer Constituents in QUAL 14-14
14.5.3 Accuracy of Conservative Constituent Concentration Estimates 14-19
14.5.4 Sample Volume Fingerprinting Results 14-20
14.6 Special Applications of Fingerprinting using DSM2 ..... **14-21**
14.6.1 Constituent Fingerprinting 14-22
14.6.2 Constituent and Timing Fingerprinting 14-23
14.6.3 Constituent or Constituent and Timing Fingerprinting for Conservative Constituents by using an OUTPUTPATHS Section in QUAL Input 14-24
14.7 Summary **14-25**
14.8 References **14-25**

15 SHORT-TERM IMPROVEMENTS TO ARTIFICIAL NEURAL NETWORK IMPLEMENTATION IN CALSIM **15-1**
15.1 Introduction **15-1**
15.2 Objectives **15-1**
15.2.1 Best Input Parameters in ANN 15-1
15.2.2 Better Training Techniques 15-2
15.2.3 Increase the Robustness of the ANN 15-2
15.2.4 Changes in ANN Implementation in CALSIM 15-2
15.3 Current Status **15-3**
15.4 Future Considerations **15-3**

TABLES

Table 2.1: Summary of Profile Coefficients Found from Field Data....2-19
Table 2.2: Range of Parameters Used to Estimate the Dispersion Coefficient....2-20
Table 2.3: Theoretical Bounds on the Dispersion Coefficient....2-20
Table 4.1: Summary of DSM2 Planning Studies....4-1
Table 4.2: Emmaton EC (rounded to nearest 50 umhos/cm)....4-4
Table 4.3: Summary of Emmaton Scatter Plots....4-9
Table 4.4: Jersey Point EC (rounded to nearest 50 umhos/cm)....4-12
Table 4.5: Summary of Jersey Point Scatter Plots....4-15
Table 4.6: Rock Slough EC (rounded to nearest 50 umhos/cm)....4-17
Table 4.7: Summary of Rock Slough Scatter Plots....4-21
Table 5.1: Summary of Data Count for Analysis....5-2
Table 5.2: Summary of Data Available for Analysis of Chloride and Calcium Relationships....5-5
Table 5.3: Preliminary Regressions for Calcium and Chloride Analysis....5-8
Table 6.1: Desired Correction to Delta Practical Salinity....6-11
Table 6.2: Coefficients M_0 and M_1 to Correct Low Practical Salinity in Delta Channels....6-11
Table 6.3: Coefficients M_0 and M_1 to Correct Practical Salinity in Delta Agricultural Drainage....6-13
Table 7.1: Classification of DOC Response to Flow at Greens Landing....7-3
Table 7.2: Generated Monthly DOC at Greens Landing (values in mg/L)....7-7
Table 7.3: Generated Monthly UVA at Greens Landing (values in 1/cm)....7-9
Table 7.4: Classification of DOC Response to Flow at Vernalis....7-11
Table 7.5: Generated Monthly DOC at Vernalis (values in mg/L)....7-15
Table 7.6: Generated Monthly UVA at Vernalis (values in 1/cm)....7-16
Table 7.7: Generated Monthly DOC in Mokelumne River (values in mg/L)....7-20
Table 7.8: Generated Monthly UVA in Mokelumne River (values in 1/cm)....7-21
Table 9.1: DOC Model Input Parameters....9-3
Table 11.1: Comparison between Traditional Monthly Planning Studies and the New Daily Planning Studies....11-8
Table 14.1: Estimation of Conservative Constituent Concentrations using Volume Contributions and Source Concentrations....14-4
Table 14.2: Estimation of Conservative Constituent Concentrations using Volume Contributions, Source Concentrations, and Source Timing....14-7
Table 14.3: Specified Tracer Concentrations for Volume Fingerprinting in the Delta....14-13
Table 14.4: Specified Tracer Concentrations for Volume and Timing Fingerprinting in the Delta....14-16
Table 14.5: Source Month Represented by each Tracer for a Specified Month in the Delta....14-17
Table 14.6: Specified Tracer Concentrations for Constituent Fingerprinting in the Delta....14-22
Table 14.7: Specified Tracer Concentrations for Constituent and Timing Fingerprinting in the Delta....14-23

FIGURES

Figure 2.1: Definition of Dispersion Coefficient, *K* 2-2
Figure 2.2: Coordinate Convention for a Channel 2-3
Figure 2.3: Examples of Vertical Profiles using Different Shape Factors, *s* 2-4
Figure 2.4: Example of Transverse Profiles with Coefficient, *A*, Ranging from 1.2 to 1.6 2-6
Figure 2.5: Diagram of Particle Position Coordinate Convention 2-7
Figure 2.6: PTM Representation of an Irregular Channel where Width is Calculated for a Given Flow Area and Depth 2-9
Figure 2.7: Particles Bounce the Same Projected Distance into the Channel 2-10
Figure 2.8: Probability Based Determination of a Particle Path at a Junction Flow Split 2-11
Figure 2.9: Location of Available ADCP Transects 2-12
Figure 2.10: Creation of Depth Ensembles 2-13
Figure 2.11: ADCP Boat Track and Adjusted Track 2-13
Figure 2.12: Velocity Coverage for a Channel Cross-Section (shown in gray) 2-14
Figure 2.13: Transverse and Vertical Profiles Represent the Depth Averaged and Width Averaged Transect Values 2-15
Figure 2.14: Regression of the Vertical Velocity Profile and Estimation of the von Karman Coefficient, *k*, and Shape Factor, *s* 2-16
Figure 2.15: Theoretical Vertical Profile Compared to Field Velocity and 95% Confidence Intervals 2-17
Figure 2.16: Regression of the Transverse Velocity Profile and Estimation of the Transverse Shape Coefficient, *A* 2-18
Figure 2.17: Theoretical Vertical Profile Comparison to Field Velocity and 95% Confidence Intervals 2-19
Figure 2.18: Theoretical Estimate of PTM Longitudinal Dispersion Coefficient for an Average Velocity of 3.2 ft/s 2-21
Figure 2.19: Theoretical Estimate of PTM Longitudinal Dispersion Coefficient for an Average Velocity of 1.6 ft/s 2-22
Figure 2.20: Theoretical Estimate of PTM Longitudinal Dispersion Coefficient for an Average Velocity of 0.5 ft/s 2-23
Figure 4.1: Study Methodology 4-2
Figure 4.2a: DSM2 versus CALSIM EC at Emmaton for D-1485 using ANN: Water Years 1976-83 4-5
Figure 4.2b: DSM2 versus CALSIM EC at Emmaton for D-1485 using ANN: Water Years 1984-91 4-5
Figure 4.3: Difference in EC at Emmaton for D-1485 using ANN 4-5
Figure 4.4a: DSM2 versus CALSIM EC at Emmaton for D-1485 using G-model: Water Years 1976-83 4-6
Figure 4.4b: DMS2 versus CALSIM EC at Emmaton for D-1485 using G-model: Water Years 1984-91 4-6
Figure 4.5: Difference in EC at Emmaton for D-1485 using G-model 4-6
Figure 4.6a: DSM2 versus CALSIM EC at Emmaton for D-1641 using ANN: Water Years 1976-83 4-7
Figure 4.6b: DSM2 versus CALSIM EC at Emmaton for D-1641 using ANN: Water Years 1984-91 4-7
Figure 4.7: Difference in EC at Emmaton for D-1641 using ANN 4-7
Figure 4.8a: DSM2 versus CALSIM EC at Emmaton for D-1641 using G-model: Water Years 1976-83 4-8
Figure 4.8b: DSM2 versus CALSIM EC at Emmaton for D-1641 using G-model: Water Years 1984-91 4-8
Figure 4.9: Difference in EC at Emmaton for D-1641 using G-model 4-8

Figure 4.10: Scatter Plot of CALSIM with ANN EC versus DSM2 EC for D-1485 at Emmaton 4-10
Figure 4.11: Scatter Plot of CALSIM with G-model EC versus DSM2 EC for D-1485 at Emmaton 4-10
Figure 4.12: Scatter Plot of CALSIM with ANN EC versus DSM2 EC for D-1641 at Emmaton 4-11
Figure 4.13: Scatter Plot of CALSIM with G-model EC versus DSM2 EC for D-1641 at Emmaton 4-11
Figure 4.14: DSM2 versus CALSIM EC at Jersey Point for D-1485 using ANN 4-12
Figure 4.15: Difference in EC at Jersey Point for D-1485 using ANN 4-12
Figure 4.16: DSM2 versus CALSIM EC at Jersey Point for D-1485 using G-model 4-13
Figure 4.17: Difference in EC at Jersey Point for D-1485 using G-model 4-13
Figure 4.18: DSM2 versus CALSIM EC at Jersey Point for D-1641 using ANN 4-13
Figure 4.19: Difference in EC at Jersey Point for D-1641 using ANN 4-14
Figure 4.20: DSM2 versus CALSIM EC at Jersey Point for D-1641 using G-model 4-14
Figure 4.21: Difference in EC at Jersey Point for D-1641 using G-model 4-14
Figure 4.22: Scatter Plot of CALSIM with ANN EC versus DSM2 EC for D-1485 at Jersey Point 4-15
Figure 4.23: Scatter Plot of CALSIM with G-model EC versus DSM2 EC for D-1485 at Jersey Point 4-16
Figure 4.24: Scatter Plot of CALSIM with ANN EC versus DSM2 EC for D-1641 at Jersey Point 4-16
Figure 4.25: Scatter Plot of CALSIM with G-model EC versus DSM2 EC for D-1641 at Jersey Point 4-17
Figure 4.26: DSM2 versus CALSIM EC at Rock Slough for D-1485 using ANN 4-18
Figure 4.27: Difference in EC at Rock Slough for D-1485 using ANN 4-18
Figure 4.28: DSM2 versus CALSIM EC at Rock Slough for D-1485 using G-model 4-18
Figure 4.29: Difference in EC at Rock Slough for D-1485 using G-model 4-19
Figure 4.30: DSM2 versus CALSIM EC at Rock Slough for D-1641 using ANN 4-19
Figure 4.31: Difference in EC at Rock Slough for D-1641 using ANN 4-19
Figure 4.32: DSM2 versus CALSIM EC at Rock Slough for D-1641 using G-model 4-20
Figure 4.33: Difference in EC at Rock Slough for D-1641 using G-model 4-20
Figure 4.34: Scatter Plot of CALSIM with ANN EC versus DSM2 EC for D-1485 at Rock Slough 4-21
Figure 4.35: Scatter Plot of CALSIM with G-model EC versus DSM2 EC for D-1485 at Rock Slough 4-22
Figure 4.36: Scatter Plot of CALSIM with ANN EC versus DSM2 EC for D-1641 at Rock Slough 4-22
Figure 4.37: Scatter Plot of CALSIM with G-model EC versus DSM2 EC for D-1641 at Rock Slough 4-23
Figure 5.1: Locations of Available Data and Sample Groupings for Chloride and Calcium Analysis 5-4
Figure 5.2: Relationship between Chloride and Calcium for West Delta and San Joaquin River Regions. 5-7
Figure 5.3: Relationship between Chloride and Calcium for Franks Tract and Contra Costa Canal Regions 5-9
Figure 5.4: Relationship between Chloride and Calcium for DMC and SWP Intake Regions 5-10
Figure 6.1: EC as a Function of Salinity per Equation 6-1 (Schemel, 2000) 6-2
Figure 6.2: Nonlinear Relationship between EC and TDS from Delta Grab Samples 6-3
Figure 6.3: Nonlinear Relationship between EC and Chloride from Delta Grab Samples 6-3
Figure 6.4: Linear Relationship between Chloride and TDS from Delta Grab Samples 6-3
Figure 6.5: Relationship between TDS and EC at Delta Boundaries 6-5

Figure 6.6: Standard Correction to Practical Salinity Scale 1978 (Hill et al., 1980) 6-8
Figure 6.7: Relationship between Delta Practical Salinity Scale 1978 and Observed Chloride 6-8
Figure 6.8: Relationship between Delta Practical Salinity Scale 1978 and Observed TDS 6-9
Figure 6.9: Deviation of Low Delta Practical Salinity from Valid Regression 6-9
Figure 6.10: Relationship between Delta Practical Salinity and TDS for TDS > 1 ppt 6-10
Figure 6.11: Needed Correction to Delta Practical Salinity for Values with TDS < 1 ppt 6-12
Figure 6.12: Corrected Delta Practical Salinity for Values with TDS < 1 ppt 6-12
Figure 6.13: Corrected Delta Practical Salinity at Delta Boundaries 6-14
Figure 6.14: Regions for Different Corrections to the Practical Salinity of Agricultural Drainage 6-15
Figure 6.15: Needed Correction to Practical Salinity of Delta Agricultural Drainage 6-17
Figure 6.16: Residual in EC after EC – Corrected Practical Salinity – EC Analysis 6-18
Figure 7.1: Observed DOC and Flow at Greens Landing 7-2
Figure 7.2: Observed DOC at Greens Landing, 1987-1997 (Grouped by Month) 7-2
Figure 7.3: Observed DOC at Greens Landing Grouped by Response to Flow (Jun. – Oct. Data Removed) 7-3
Figure 7.4: Observed DOC and Response to Flow at Greens Landing 7-4
Figure 7.5a: Assignment of DOC / Flow Relationship at Greens Landing for Planning Period: 1975-1983 7-4
Figure 7.5b: Assignment of DOC / Flow Relationship at Greens Landing for Planning Period: 1984-1992 7-5
Figure 7.6: Observed and Generated DOC at Greens Landing 7-6
Figure 7.7a: Generated DOC at Greens Landing over the Planning Period: 1975-1983 7-6
Figure 7.7b: Generated DOC at Greens Landing over the Planning Period: 1984-1992 7-7
Figure 7.8: Monthly Average Observed and Generated DOC at Greens Landing 7-8
Figure 7.9: Observed UVA versus Observed DOC at Greens Landing 7-8
Figure 7.10: Monthly Average Observed and Generated UVA at Greens Landing 7-9
Figure 7.11: Observed DOC and Flow at Vernalis 7-10
Figure 7.12: Observed DOC at Vernalis, 1987-1997 (Grouped by Month) 7-10
Figure 7.13: Observed DOC at Vernalis Grouped by Response to Flow (Jun. – Oct. Data Removed) 7-11
Figure 7.14: Historic SJR Flow at Vernalis Categorized by DOC Response to Flow 7-12
Figure 7.15a: Assignment of DOC / Flow Relationship at Vernalis for Planning Period: 1975-1983 7-12
Figure 7.15b: Assignment of DOC / Flow Relationship at Vernalis for Planning Period: 1984-92 7-13
Figure 7.16: Observed and Generated DOC at Vernalis 7-13
Figure 7.17a: Generated DOC at Vernalis over the Planning Period: 1975-1983 7-14
Figure 7.17b: Generated DOC at Vernalis over the Planning Period: 1984-1992 7-14
Figure 7.18: Monthly Average Observed and Generated DOC at Vernalis 7-15
Figure 7.19: Observed UVA versus Observed DOC at Vernalis/Mossdale 7-16
Figure 7.20: Monthly Average Observed and Generated UVA at Vernalis 7-17
Figure 7.21: Observed DOC and Flow in the American River 7-18
Figure 7.22: Observed DOC in the American River, 1987-1997 (Grouped by Month) 7-18
Figure 7.23: Flow and Observed DOC in the American River (Jun. – Oct. Data Removed) 7-19
Figure 7.24a: Generated DOC in the Mokelumne River over the Planning Period: 1975-1983 7-19
Figure 7.24b: Generated DOC in the Mokelumne River over the Planning Period: 1984-1992 7-20
Figure 7.25: Monthly Average Observed and Generated DOC in the Mokelumne River 7-20
Figure 7.26: Observed UVA versus Observed DOC in the Mokelumne River 7-21
Figure 7.27: Monthly Average Observed and Generated UVA in the Mokelumne River 7-22

Figure 8.1: Water Quality Criteria, In-Delta Storage Program (Bindra, 2001) 8-2
Figure 8.2: Water Quality – Project Reservoir Release Constraint Process..... 8-4
Figure 9.1: Time Series Plots of DOC Concentrations and Flow Exchange at Webb Tract 9-3
Figure 9.2: Time Series Plots of the Variations in DOC Concentrations at San Joaquin River Near the Mokelumne River Junction and Flow Exchange at Webb Tract..... 9-4
Figure 10.1: Sample 1-Channel Domain with Salinity Regulation 10-4
Figure 10.2: Regularization Solution to Meet Daily-Averaged Salinity Regulations with Control Trajectory for River Inflow (Q_r) and Pumping (Q_p) 10-5
Figure 10.3: Parameterization Solution to Meet Daily-Averaged Salinity Regulations based on Piecewise Linear Controls for River Inflow (Q_r) and Pumping (Q_p)..... 10-6
Figure 10.4: Bethel Tract Daily-Averaged EC (in mS) in Fall 1994..... 10-7
Figure 10.5: Sacramento River Inflow, Combined Export, and Net Delta Outflow in Fall 1994 10-8
Figure 10.6: Historical and Alternative Delta Outflow Index for DWR O&M Fall 1994 Water Quality Study 10-9
Figure 10.7: Comparison of the Cumulative Water Cost of Historical Operations to the Adjusted Operation for Fall 1994 10-9
Figure 10.8: Salinity Results and Flows for Minimum Water Cost Optimization for two Cases: Average Pumping of 5,000 cfs and Average Pumping of 7,000 cfs..... 10-11
Figure 10.9: Martinez Stage and Tidal Average Using a Godin Filter for Fall 1994 10-12
Figure 11.1: South Delta Flow Control Structures..... 11-2
Figure 11.2: Special Tidal Operation of South Delta Flow Control Structures..... 11-3
Figure 11.3: Typical Monthly Planning Study Flow Output 11-5
Figure 11.4: Typical New Daily Planning Study Flow Output..... 11-6
Figure 11.5: Typical Box and Whisker Plot 11-6
Figure 11.6: Typical Probability of Exceedence Plot..... 11-7
Figure 13.1: Single User Interface for Editing Data and Creating Simulations 13-3
Figure 13.2: Single User Interface in Context of a Local (MS Access) Replicate System and a Remote (Informix) Replication System 13-3
Figure 13.3: Hierarchy of the Channel Table 13-5
Figure 13.4: DSM2 Database Interface (Channels)..... 13-5
Figure 13.5: Input Layers 13-7
Figure 13.6: DSM2 Database Interface (Gates)..... 13-8
Figure 13.7: DSM2 Database Interface (Output Time Series) 13-9
Figure 14.1: Conceptualization of a Stream with Two Tributaries 14-3
Figure 14.2: Conceptualization of Relative Volume Contributions from each Source for Water Sampled from Three Locations..... 14-3
Figure 14.3: Conceptualization of Relative Concentrations Computed from Source Volumes and Source Concentrations for Water Sampled from Three Locations..... 14-5
Figure 14.4: Conceptualization of Two Source Streams with a Long Retention Time after their Confluence..... 14-6
Figure 14.5: Conceptualization of Volume and Timing of Source Contributions in a Water Sample from Two Source Streams with a Long Retention Time 14-6
Figure 14.6: Conceptual Relative Concentrations Computed from Source Volumes, Source Concentrations, and Source Timing 14-8
Figure 14.7: Pie Charts of Relative Contributions of Water Volume or of Conservative Constituent Concentrations using Two Fingerprinting Methods 14-9
Figure 14.8: Conceptualization of Relative Contributions of Six Sources of Water Samples from Two Different Locations in the Delta..... 14-10

Figure 14.9: Typical Fingerprinting Source Locations for the Sacramento-San Joaquin Delta 14-11
Figure 14.10: Specified Tracer Concentrations for a Single Source for Volume and Timing Finger Printing in the Delta 14-17
Figure 14.11: Percent Volume Contributions of the Sacramento and San Joaquin Rivers at the Entrance to Clifton Court Forebay 14-20
Figure 14.12: Percent Volume Contributions of the Sacramento and San Joaquin Rivers at the Entrance to Clifton Court Forebay based on Water Year Types 14-21
Figure 14.13: Monthly Average Percent Volume Contributions of the Sacramento and San Joaquin Rivers at the Entrance to Clifton Court Forebay 14-21

1 Introduction

Over the last nine years, the Delta Modeling Section has been developing and enhancing the Delta Simulation Model 2 (DSM2) and its support tools. The following are brief summaries of work that was conducted during the past year. The names of contributing authors are in parentheses.

Chapter 2 – Particle Tracking Model Verification and Calibration

Last year's annual progress report included a chapter on validation of dispersion using the DSM2 Particle Tracking Model (PTM). Chapter 2 summarizes the Section's work to re-calibrate and verify PTM dispersion in response to (1) a new formulation of the PTM mixing equations and (2) changes in DSM2. Last year's work, which was conducted by Ryan Wilbur, was completed prior to the release of the latest version of DSM2 which includes, among other things, re-calibrated model parameters and modified representations of channel bathymetry and open water areas. *(Aaron Miller)*

Chapter 3 – Analysis and Preparation of Observed Data for Input Files in Support of DSM2 Extended Validation (1975 – 1999)

Last year's annual progress report described the most recent DSM2 calibration and validation, which required the capability to simulate historical hydrodynamics and water quality transport for the period 1990-99. This chapter summarizes the Section's work to acquire, analyze and screen observed data collected prior to 1990, including stage, flow, and electrical conductivity. Work also included gathering information on unusual Delta events (such as levee breaks) and barrier installations prior to 1990. These data will be utilized to eventually extend the historical DSM2 simulation period back to 1975. *(Myint Thein)*

Chapter 4 – CALSIM versus DSM2 ANN and G-model Comparisons

For several years, the Section has been reporting updates on the development of a new flow-salinity model for the Department's statewide planning model. This year, the Section's Artificial Neural Network (ANN) flow-salinity model was implemented in CALSIM II. Through the CALSIM ANN Refinement Team (CART), the Section has been collaborating with staff from the Hydrology and Operations Section and the U.S. Bureau of Reclamation to make improvements to the ANN. Chapter 4 presents some work that was conducted in support of the CART effort, including (1) a robustness test assuming increased Banks Pumping Plant pumping capacity of 10,300 cfs and (2) a comparison with G-model performance. Water quality estimates are presented at three key water quality locations: Emmaton, Jersey Point, and Rock Slough. (*Michael Mierzwa*)

Chapter 5 – Relationships Between Delta Water Quality Constituents as Derived from Grab Samples

In 1986, the Department reported a Delta-wide evaluation of multiple water quality relationships derived from a sizeable grab sample data set. In this study, 34 Bay-Delta locations were independently examined and relationships between electrical conductivity, chloride and total dissolved solids were developed by water year type. This work has been referenced extensively by the Section. Chapter 5 presents the Section's current effort to expand upon this previous study by developing water quality relationships based on regional similarities for electrical conductivity, total dissolved solids and a suite of mineral constituents, including: bromide, chloride, sulfate, calcium, magnesium, potassium, and sodium. In addition to providing expanded ability to relate water quality constituents in the Delta, it is anticipated that this effort will provide insight into some characteristics of the mixing of Delta water and will provide another basis for validating DSM2-QUAL. Preliminary results illustrate regional relationships between chloride and calcium. (*Bob Suits*)

Chapter 6 – Calibrating DSM2-QUAL Dispersion Factors to Practical Salinity

This chapter discusses the background behind practical salinity and how it can be treated as an alternative water quality parameter for calibrating the dispersion factors in DSM2-QUAL. In the most recent calibration and validation of DSM2, EC was used to calibrate dispersion in QUAL. However, EC is not truly a conservative constituent, and at higher concentrations EC tends to underestimate true salinity. As is described in this chapter, use of practical salinity allows EC data to be used for validation, but accounts for the non-conservative behavior of EC at high salinity concentrations. (*Bob Suits*)

Chapter 7 – Generating Monthly Dissolved Organic Carbon and UVA at DSM2 Boundaries

DSM2 planning studies generally employ CALSIM II Delta hydrology and operations as flow boundaries to simulate the 16-year sequence of water years 1976-91. DSM2 planning studies also require specifications for water quality boundary conditions. Chapter 7 describes the Section's recent effort to develop dissolved organic carbon and ultraviolet absorbance boundary conditions for DSM2 planning studies. The resulting dissolved organic carbon boundary conditions, which are based on water quality grab samples collected by the Department's Municipal Water Quality Investigations (MWQI) Program, range between 1.5-5.5 mg/l and 2.4-11.4 mg/l in the Sacramento and San Joaquin Rivers, respectively. The boundary conditions attempt to capture the observed relationships between riverine organic loads and the seasonal "first flush" of watersheds. These boundary conditions were utilized by the Section in its most recent evaluation of the Integrated Storage Investigation (ISI) In-Delta Storage Project and will likely be used in subsequent evaluations of organics transport in the Delta. (*Bob Suits*)

Chapter 8 – CALSIM Water Quality Operating Rules to Meet Delta Wetlands Water Quality Management Plan

CALSIM II uses an Artificial Neural Network (ANN) to characterize Delta flow-salinity relationships under various planning scenarios. However, the ANN assumes an existing Delta configuration and has not been calibrated to predict water quality changes that might result from In-Delta Storage Project diversions and releases. To support the Department's Integrated Storage Investigations Program, the Section collaborated with the Hydrology and Operations Section and others to develop preliminary CALSIM II operating rules. These operating rules, as summarized in Chapter 8, are designed to account for interactions between In-Delta Storage Project operations and water quality at Delta urban diversions. (*Tara Smith*)

Chapter 9 – Implementation of DOC Growth in DSM2-QUAL

The Department's Municipal Water Quality Investigations (MWQI) Program conducted field experiments to determine potential changes in dissolved organic carbon concentrations resulting from peat soil contact. Based on the experimental findings, Marvin Jung proposed a set of logistic type equations to characterize the growth of DOC on flooded Delta islands. DOC growth is assumed to result from soil leaching and microbial decay. Chapter 9 summarizes the methodology used to implement the logistic equations in DSM2 and presents the results used to validate the implemented algorithm. The resulting module was utilized in a recent evaluation of the Integrated Storage Investigation (ISI) In-Delta Storage Project. (*Ganesh Pandey*)

Chapter 10 – Optimal Control of Delta Salinity

This chapter is a summary of Eli Ateljevich's Ph.D. dissertation on the optimal control of Delta salinity. After introducing the concept of optimal control, a simplified flow network was employed to compare two methods of incorporating "consistency" into an optimal control problem. Using one of these consistency methods to optimize a DSM2 simulation, a historical Delta salinity compliance problem (August-September 1994) was examined. Results suggest that salinity control through reservoir releases may be more efficient than was previously thought. Finally, the potential application of optimization methods to operational and planning models was discussed. (*Eli Ateljevich*)

Chapter 11 – 16-Year DSM2 Planning Studies with Adjusted Astronomical Tides and Daily Hydrology

This chapter describes the Section's new 16-year DSM2 planning study setup. In the new setup, the design repeating tide was replaced with an adjusted astronomical tide (described in last year's annual progress report) and the monthly hydrology was replaced with a daily hydrology. The new setup was motivated by a recent enhancement of CALSIM II to compute daily varying Delta hydrology and operations. (CALSIM II was modified in support of the ISI In-Delta Storage Program.) By simulating spring-neap tidal variation and daily varying Delta hydrology and operations, the new DSM2 planning study setup provides more detailed results than the previous DSM2 planning studies. (*Bijaya Shrestha*)

Chapter 12 – DSM2 Documentation

This chapter summarizes the Delta Modeling Section's strategy to improve documentation of the Delta Simulation Model 2 (DSM2). This chapter includes a summary of the documentation objectives, an overview of the planned documentation, an overview of the recently released DSM2 tutorial, and a review of the progress to date and future directions. (*Jamie Anderson*)

Chapter 13 – DSM2 Input Database and Data Management System

Chapter 13 summarizes the recent development of a new DSM2 input database and data management system. The new system, which is driven through a graphical user interface (GUI), will promote increased data standardization. DSM2 currently uses a text based input system, where the same task can be accomplished several different ways. The GUI will reduce potential ambiguities associated with text based input systems, and when coupled with a new data management system, will automate version controlling of the DSM2 input data. (*Eli Ateljevich and Tawnly Pranger*)

Chapter 14 – DSM2 Fingerprinting Methodology

This chapter outlines a DSM2 modeling approach used by the Section to estimate individual source concentrations of any conservative constituent at a given location in the Delta. This methodology, referred to as "fingerprinting", can answer questions such as "What percentage of the dissolved organic carbon at Banks Pumping Plant originated from agricultural drainage?" and "What percentage of the export volume at Tracy Pumping Plant originated from the San Joaquin River?" Use of fingerprinting techniques with DSM2 provides a powerful analysis tool for understanding both hydrodynamics and water quality dynamics in the Delta. (*Jamie Anderson*)

Chapter 15 – Short-Term Improvements to Artificial Neural Network Implementation in CALSIM

Through the CALSIM ANN Refinement Team (CART), the Section is collaborating with the Hydrology and Operations Section and the U.S. Bureau of Reclamation to review and improve the flow-salinity relationships used in CALSIM II. Chapter 15 summarizes the near-term objectives, current status and future considerations of CART. (*Sanjaya Senevirante*)

Methodology for Flow and Salinity Estimates in the Sacramento-San Joaquin Delta and Suisun Marsh

23rd Annual Progress Report
June 2002

Chapter 2:
Particle Tracking Model Verification and Calibration

Author: Aaron Miller

2 Particle Tracking Model Verification and Calibration

2.1 Introduction

The Particle Tracking Model (PTM) is one of three modules of the California Department of Water Resource's Delta Simulation Model 2 (DSM2). DSM2 is a combination of three models: HYDRO, a hydrodynamics model; QUAL, a water quality model; and a particle tracking model PTM. PTM simulates the movement of neutrally buoyant particles using transport principles when given hydrodynamic information from HYDRO.

PTM was last validated early in the year 2000 (Wilbur, 2000). Since this time, two things occurred which warranted another model calibration and validation. First, the hydrodynamic model was recently recalibrated, which resulted in changed flow patterns and updated channel bathymetry (Nader-Tehrani, 2001). The method used to represent open water areas was also changed. Second, the formulation of the mixing equations was modified. The formulation for particle mixing was altered to include point velocities at the location of the particle. Also in this formulation is the inclusion of a particle drift term. This drift term is required to keep the mixing equations consistent with the transport equations.

This chapter describes the process and results for the verification and calibration of the PTM. The formulation of PTM was verified by comparing it with theoretical dispersion. The velocity profiles the model uses to generate quasi 3-dimensional velocity fields were calibrated using field-measured velocity. Validation of the model was completed using the 1997 dye study (Oltmann, 1998).

2.2 Background

The Delta Modeling Section began development of the Particle Tracking Model in 1993. Smith (1993) developed the first model in FORTRAN for DSM1 using a formulation developed by Gib Bogle (Water Engineering and Modeling, 1994). The original model was a quasi 2-dimensional model. It was further modified to a quasi 3-dimensional model. Nicky Sandhu and Ralph Finch (DWR) converted the model to Java in 1997.

Since the first Java version of the model there have been advancements in simulating particle behavior, the incorporation of water quality, and implementation of an enhancement to the mixing formulation. Gib Bogle also developed the enhancement to the mixing with assistance from Richard Denton (Contra Costa Water District). Miller (2000) added this enhancement to the code and has further developed particle behavior sections of the code.

2.3 PTM Theory

The dispersion coefficient, *K*, is defined as one half the change in variance with respect to time. This is shown in Figure 2.1.

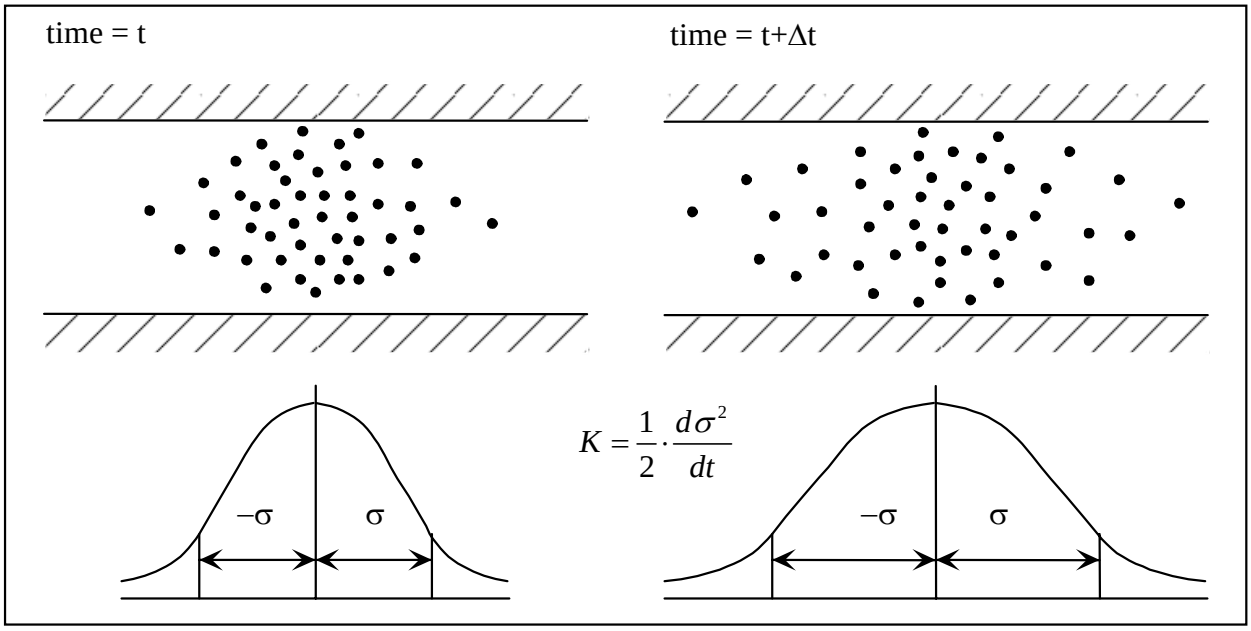

Figure 2.1: Definition of Dispersion Coefficient, *K*.

Equation 2-1 defines the derived dispersion coefficient, *K*.

$$K = \frac{h^2 \overline{u}'^2 I}{\overline{\varepsilon}_t} \qquad \text{[Eqn. 2-1]}$$

where,

K	=	dispersion coefficient,
h	=	characteristic length,
$\overline{u}'$	=	expected squared of the deviation of the depth-averaged velocity,
I	=	dimensionless integral of the velocity profile, and
$\overline{\varepsilon}_t$	=	transverse mixing coefficient.

Fischer et al. (1979) report characteristic lengths that range from half to the full width of the channel cross-section. The integral of the velocity profile is nearly constant for real streams, and ranges from 0.01 to 0.03 (Bogle, 1997). The expected squared of the deviation of the depth-averaged velocity is based on the difference from the actual velocity, u, by the mean velocity, $\overline{u}$, and is described by Fischer et al. (1979) as ranging from $0.03\overline{u}^2$ to $0.20\overline{u}^2$.

2.3.1 Longitudinal Dispersion

To model dispersion, PTM utilizes flow and cross-sectional area provided by HYDRO. This flow is one-dimensional and, when used to calculate velocity, assumes a uniform velocity across a channel cross-section. Using a one-dimensional model for flow and stage calculations is relatively efficient and accurate for the majority of the Delta. However, PTM utilizes the calculated velocity to determine particle movement. PTM depends on differential velocities to simulate dispersion, but a one-dimensional model does not provide a differential velocity field. Thus, theoretical profiles were applied to HYDRO's one-dimensional velocities. The application of these profiles creates a quasi three-dimensional velocity field in the cross section. This velocity field forces particles to move at a speed determined by the combination of the vertical and the transverse profiles. This differential movement in the longitudinal direction creates a dispersive effect.

Equation 2-2 describes the point velocity in the longitudinal direction. Figure 2.2 shows the coordinate convention for a channel.

$$u(y,z) = \bar{u} \cdot F_T(y) \cdot F_V(z) \qquad \text{[Eqn. 2-2]}$$

where,

$\bar{u}$ = mean velocity,
$F_T(y)$ = transverse multiplication factor, and
$F_V(z)$ = vertical multiplication factor.

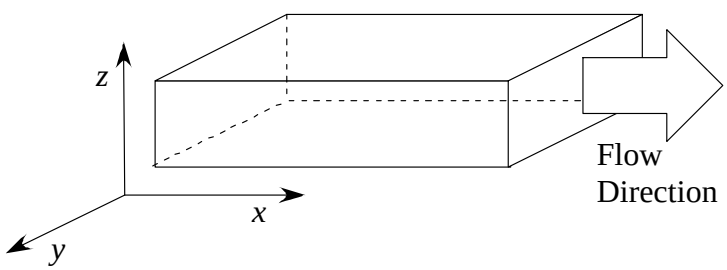

Figure 2.2: Coordinate Convention for a Channel.

When F_V and F_T are equal to one, the particle is traveling at the average velocity of the water in the channel. The functions F_V and F_T represent the profiles used to simulate dispersion. They are described in more detail below.

Vertical Profile

In the vertical direction the velocity profile is described by a von Karman logarithmic function. The von Karman logarithmic profile has been found to be a good approximation of vertical velocity profile in wide two-dimensional channels (Bogle, 1997). Wilbur (2000) added the shape factor to change the profile shape while conserving the von Karman constant.

$$F_V(z) = 1 + \frac{u^*/\bar{u}}{s \cdot k}\left[1 + \ln\left(\frac{z}{d}\right)\right] \qquad \text{[Eqn. 2-3]}$$

where,

u^* = shear velocity,
s = shape factor,
k = von Karman constant (≈0.4),
z = vertical position from the bottom of the channel, and
d = depth of channel from water surface.

The shear velocity used in Equation 2-3 is calculated as the shear velocity for steady flow in an open channel, as shown by Equation 2-4.

$$u^* = \sqrt{g \cdot r_h \cdot S} \qquad \text{[Eqn. 2-4]}$$

where,

g = acceleration due to gravity,
r_h = hydraulic radius, and
S = channel bottom slope.

Figure 2.3 shows examples of vertical profiles using different shape factors. As the shape coefficient, *s*, approaches zero the intercept of the profile moves to 0.37 of the depth and the maximum value of the profile moves towards infinity.

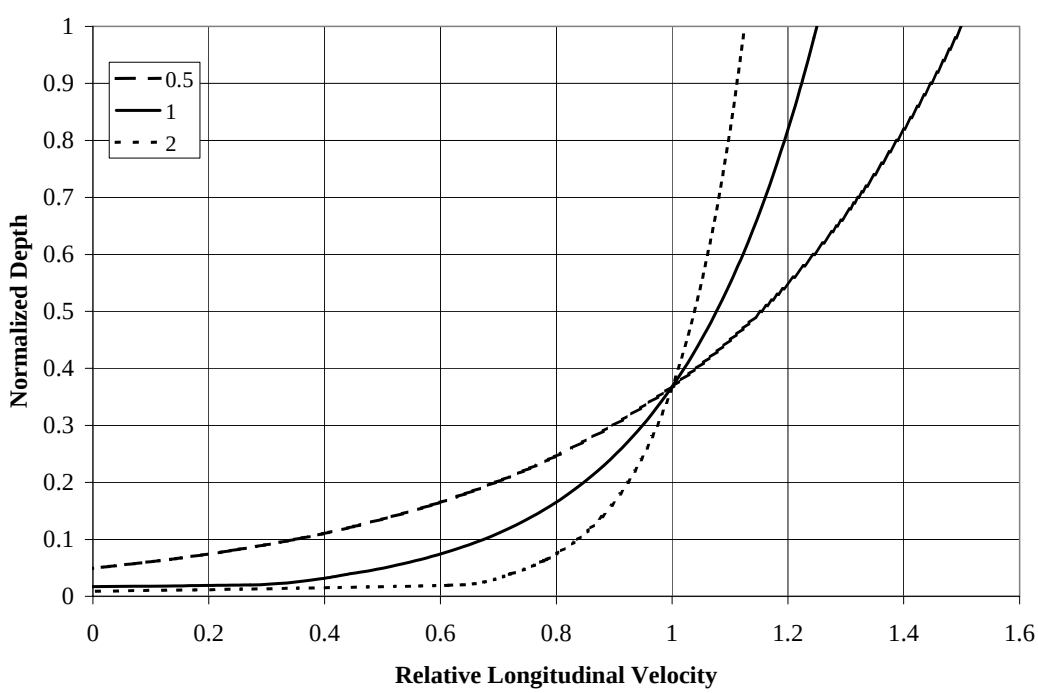

Figure 2.3: Examples of Vertical Profiles using Different Shape Factors, *s*.

Transverse Profile

In the transverse direction the velocity profile is described by a quartic function (Equation 2-5). Bogle (1997) arrived at this function through numerical experiments.

$$F_T(y) = A + B\left(\frac{2y}{w}\right)^2 + C\left(\frac{2y}{w}\right)^4 \qquad \text{[Eqn. 2-5]}$$

where,

A,B,C = profile shape coefficients,
w = channel width, and
y = transverse position from center of the channel.

Given that the velocity at the sides of the channel is equal to zero, Bogle (1997) simplified Equation 2-5 at the middle of the channel ($y = w/2$) to:

$$A + B + C = 0 \qquad \text{[Eqn. 2-6]}$$

To maintain the average velocity, the area of the profile is required to be a value of 1. Integrating Equation 2-5 where y is between $-w/2$ and $w/2$ and by dividing by the width, w, results in:

$$A + \frac{B}{3} + \frac{C}{5} = 1 \qquad \text{[Eqn. 2-7]}$$

When A is used at the free parameter, the maximum velocity occurs along the centerline at $y = 0$. Thus Equations 2-6 and 2-7 can be solved in terms of the remaining coefficients B and C:

$$B = -6A + 7.5 \qquad \text{[Eqn. 2-8]}$$

$$C = 5A - 7.5 \qquad \text{[Eqn. 2-9]}$$

For application in the Sacramento-San Joaquin Delta, A=1.2, B=0.3, and C=-1.5 was found to be representative of the velocity profiles found in the Delta channels (Wilbur, 2000).

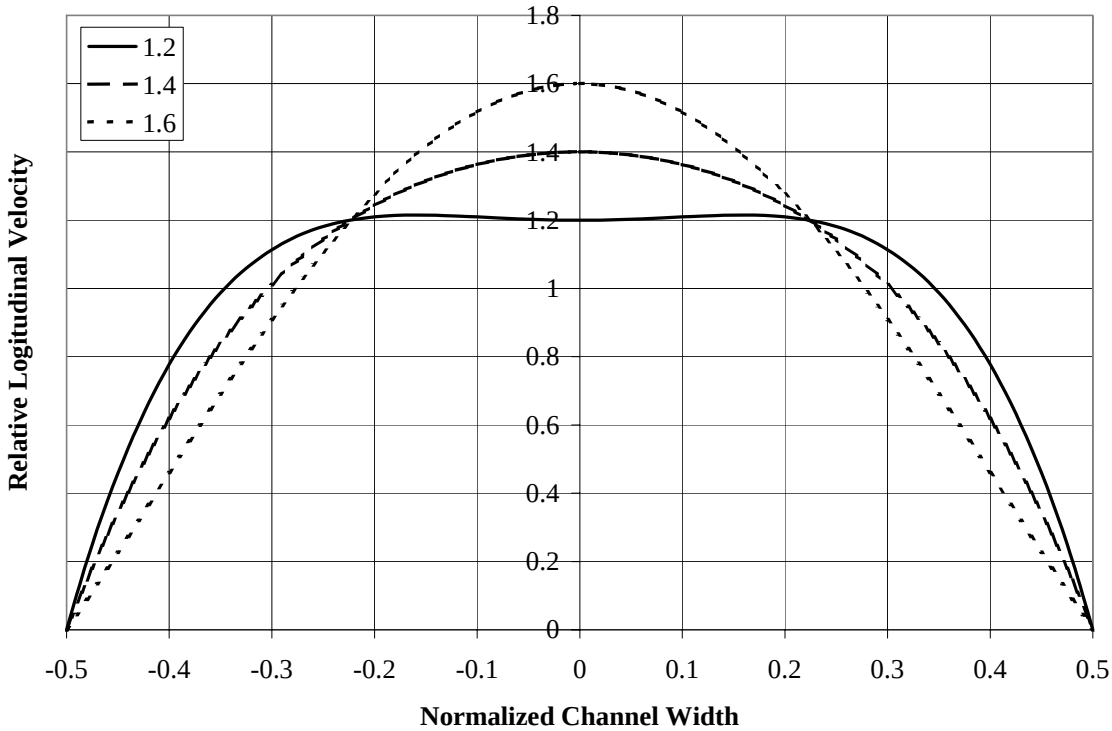

Figure 2.4: Example of Transverse Profiles with Coefficient, *A*, Ranging from 1.2 to 1.6.

Combining Vertical and Transverse Velocity Profiles

The point velocity is a function of the vertical and horizontal position in the channel. A particle at the top center of a channel will have a higher velocity than a particle near the side or bottom. For example, a position near the top center of the channel will have a point velocity around 1.5 times the average velocity for a vertical shape factor of 1 and a transverse shape coefficient *A* of 1.2, using Equation 2-2 and Figures 2.3 and 2.4. A position near the bottom or side of the channel will result in a point velocity approaching zero.

2.3.2 Longitudinal Diffusion

Particle movement within the channel cross section is completed through diffusion. Given a longitudinal velocity a particle will tend to move vertically and horizontally due to turbulent mixing. Because a one-dimensional hydrodynamics model is used for flow and velocity, the movement in the *y* and *z* direction must estimated using empirical equations.

Vertical Mixing

Vertical particle position in a channel is based on the normalized depth of the channel where 0 is the bottom of the channel and 1 is top of the water column (Figure 2.5). Movement in the vertical direction is estimated using a vertical diffusivity coefficient, ε_V, which is defined as one half the derivative of the variance of the vertical distance, σ_z^2, traveled in one time step (Equation 2-10). The empirical form of the vertical diffusivity coefficient, Equation 2-11, is

based on the depth, average velocity, and vertical position in the channel. Fischer (1979) completed the initial derivation, and Wilbur (2000) added the shape factor to change the profile shape and to conserve the von Karman constant.

$$\varepsilon_V = \frac{d\sigma_z^2}{2dt} \qquad \text{[Eqn. 2-10]}$$

$$\varepsilon_V = sku^* z\left(1 - \frac{z}{d}\right) \qquad \text{[Eqn. 2-11]}$$

where,

s = shape factor,
k = von Karman constant,
u^* = shear velocity (see Equation 2-4),
z = vertical position from the bottom of the channel, and
d = depth of the channel from the water surface.

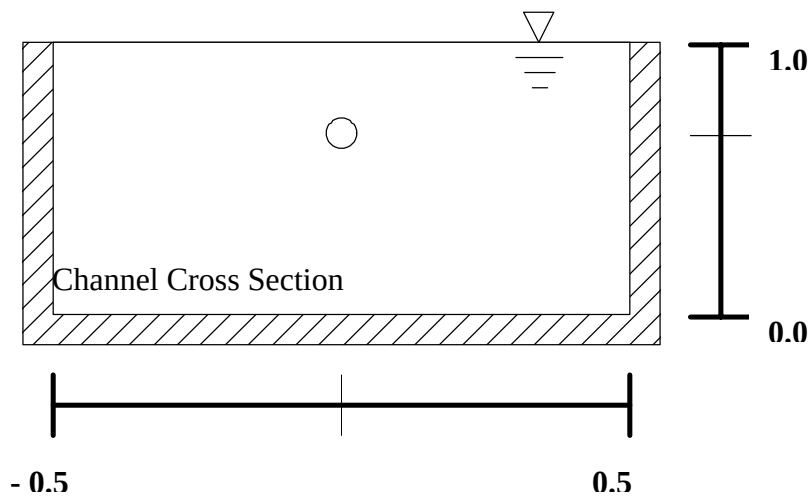

Figure 2.5: Diagram of Particle Position Coordinate Convention.

Smith (1998) showed the derivation of a particle's change in vertical position (Equation 2-10). The particle's change in vertical position, Δz, is then calculated using a Gaussian random number, the diffusivity coefficient, and the time step as described by Equation 2-12.

$$\Delta z = R\sqrt{2\varepsilon_V \Delta t} \qquad \text{[Eqn. 2-12]}$$

where,

R = Gaussian random number, with a mean of 0 and variance of 1, and
Δt = time step.

The current particle position, as given by Equation 2-13, is adjusted using the change in position and the gradient of the diffusivity for the time step. Denton (1995) showed that this gradient contribution was important in reducing particle drift for non-uniform mixing. Particle drift is the phenomena where particles move to certain locations in a channel and stay there. Dimou and Adams (1993) applied a similar gradient contribution or correction factor to a one-dimensional particle tracking model. In addition, this gradient contribution is required to obtain equivalence between the random walk algorithm (Fokker-Planck Equation) and the transport equation.

$$z_1 = z_0 + \Delta z + \frac{d\varepsilon_V}{dz}\Delta t \qquad \text{[Eqn. 2-13]}$$

The gradient of the vertical diffusivity coefficient is defined by Equation 2-14.

$$\frac{d\varepsilon_V}{dz} = sku^*\left(1 - 2\frac{z}{d}\right) \qquad \text{[Eqn. 2-14]}$$

Transverse Mixing

The transverse mixing is similar to the vertical mixing. The position of the particle in the transverse direction is based on the normalized width of the channel where –0.5 is the left bank, 0.5 is the right bank, and 0.0 is the center (Figure 2.5). Transverse movement is estimated using a transverse diffusivity coefficient, ε_T, which, like the vertical diffusivity, is defined as one half the derivative of the variance of the distance traveled in one time step, Equation 2-15. The empirical form of the transverse diffusivity coefficient, Equation 2-16, is based on a flow coefficient, average velocity, channel depth, and transverse velocity profile from Equation 2-5.

$$\varepsilon_T = \frac{d\sigma_y^2}{2dt} \qquad \text{[Eqn. 2-15]}$$

$$\varepsilon_T = C_T u^* d\left[A + B\left(\frac{2y}{w}\right)^2 + C\left(\frac{2y}{w}\right)^4\right] \qquad \text{[Eqn. 2-16]}$$

where,

C_T = flow coefficient,
A,B,C = profile shape coefficient,
y = transverse position from the center of the channel, and
w = channel width.

Smith (1998) showed the derivation of a particle's change in transverse position from Equation 2-15. The particle change in transverse position is then calculated using a Gaussian random number, the transverse diffusivity coefficient, and the time step as shown in Equation 2-17.

$$\Delta y = R\sqrt{2\varepsilon_T \Delta t} \qquad \text{[Eqn. 2-17]}$$

Like the vertical displacement, the current particle position, as given in Equation 2-18, is adjusted using the change in position and the gradient of the diffusivity for the time step. Denton (1995) showed why this gradient contribution was important. Dimou and Adams (1993) applied a similar gradient contribution or correction factor to a one-dimensional particle tracking model.

$$y_1 = y_0 + \Delta y + \frac{d\varepsilon_T}{dy}\Delta t \qquad \text{[Eqn. 2-18]}$$

The gradient of the transverse diffusivity coefficient was found to be defined by Equation 2-19.

$$\frac{d\varepsilon_T}{dy} = C_T u^* d \frac{2y}{w^2}\left[4B + 8C\left(\frac{2y}{w}\right)^2\right] \qquad \text{[Eqn. 2-19]}$$

2.3.3 Channel Boundaries

Currently PTM is not able to incorporate irregular cross-sections as HYDRO does. Irregular cross-sections are cross-sections that are not rectangular. PTM obtains cross-sectional information from HYDRO, and then builds a representative rectangular cross-section. As illustrated in Figure 2.6, PTM assumes the same depth as an irregular cross-section in HYDRO and then calculates the width for the given cross-sectional area.

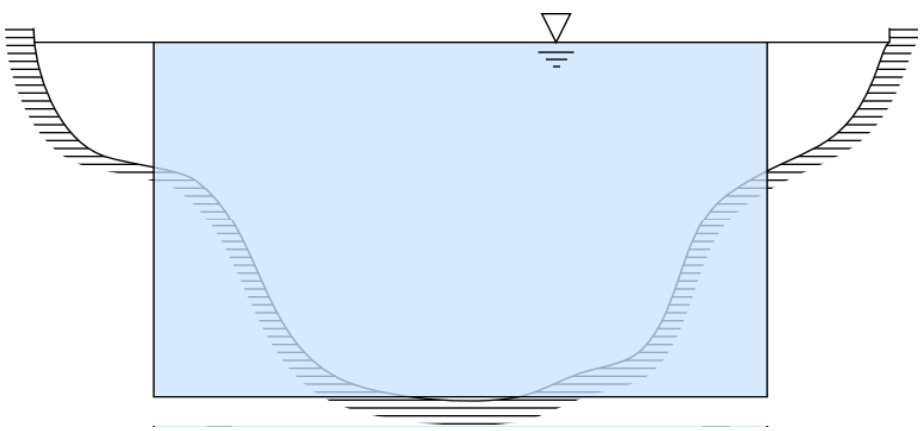

Figure 2.6: PTM Representation of an Irregular Channel where Width is Calculated for a Given Flow Area and Depth.

The PTM simulates the movement of particles within this rectangular cross-section. While calculating the particle movement, there are times when the calculated distance a particle should travel would result in the particle moving outside the boundary of this rectangle. In cases like this the particles “bounce” back into the channel the same projected distance as shown in Figure 2.7.

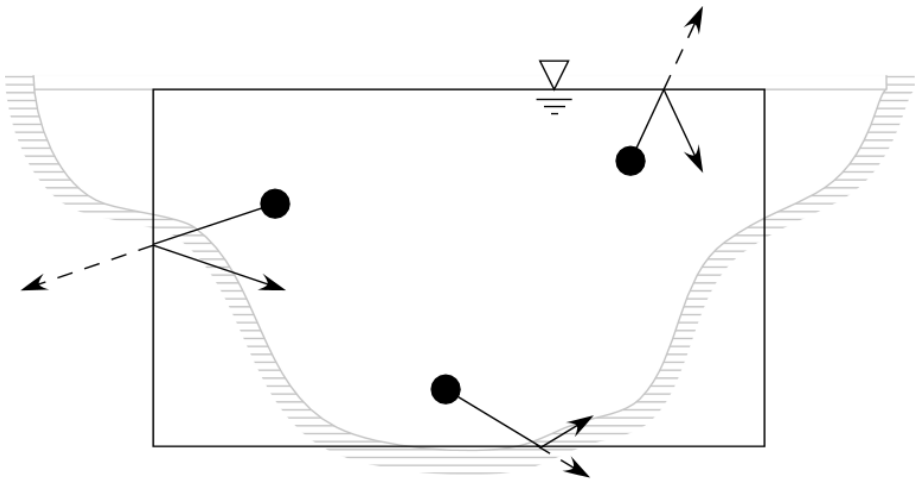

Figure 2.7: Particles Bounce the Same Projected Distance into the Channel.

Excessive bouncing occurs when particle movement is simulated with long time steps. With long time steps a particle movement may be calculated so that it is required to bounce off of the channel boundaries many times. Use of sub-time steps eliminates excessive bouncing. Sub-time steps are calculated by utilizing the channel depth or width, the velocity, and the mixing coefficient. The model currently does not allow the particle to move (and therefore bounce) more than 10% of the width or depth within one sub-time step.

2.3.4 Movement at Junctions

Decisions are made at various points within the simulation. At a junction the particle must decide which path to take. The path may lead to another channel, open water area, agricultural diversion, or an export. As illustrated in Figure 2.8, the path of a particle is determined randomly based on the proportion of flow. The proportion of flow determines the probability of movement into each reach (Equation 2-20). A random number based on this determined probability then determines where the particle will go.

$$P\left(\textit{particle entering water body}\right) = \frac{\textit{flow entering water body}}{\textit{total flow @ junction}} \qquad \text{[Eqn. 2-20]}$$

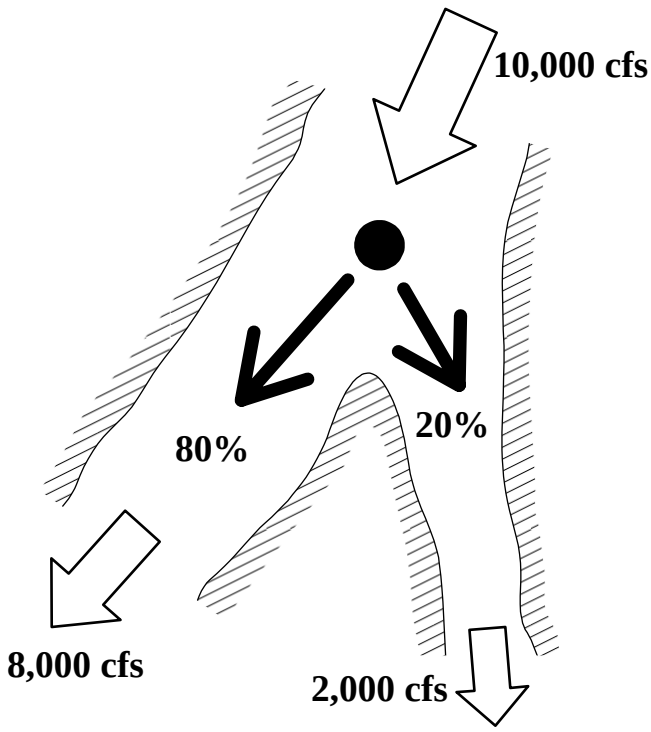

Figure 2.8: Probability Based Determination of a Particle Path at a Junction Flow Split.

2.3.5 Movement in and out of Open Water Areas

A particle that moves into an open water area, such as a reservoir, no longer retains its position information. A DSM2 open water area is considered a fully mixed reactor. The path out of the open water area is a decision based on the volume in the open water area, the time step, and the flow out of the area as shown in Equation 2-21.

$$P\left(\textit{particle entering water body}\right) = \frac{\textit{flow entering water body} \times \textit{time step}}{\textit{open water area total volume}} \qquad \text{[Eqn. 2-21]}$$

2.4 Profile Calibration

2.4.1 Estimation of Profile Coefficients

Profile coefficients were determined for both the transverse and vertical profiles using Acoustic Doppler Current Profiler (ADCP) transect data. The profile equations were simplified using the transect information. The transect information included average velocity, width, depth, and position in the channel. To simplify these equations into univariate relationships the coefficients were estimated using linear regression.

Transverse and vertical profile coefficients were determined by linear regression between simplified profile equations and measured field velocities. The measured velocities were

obtained from United States Geological Survey (USGS) ADCP transects. These transects represent the three-dimensional velocity across a channel cross section at a time in history. Figure 2.9 shows the locations of the transect data used in this analysis. This process is explained in greater detail in the following paragraphs.

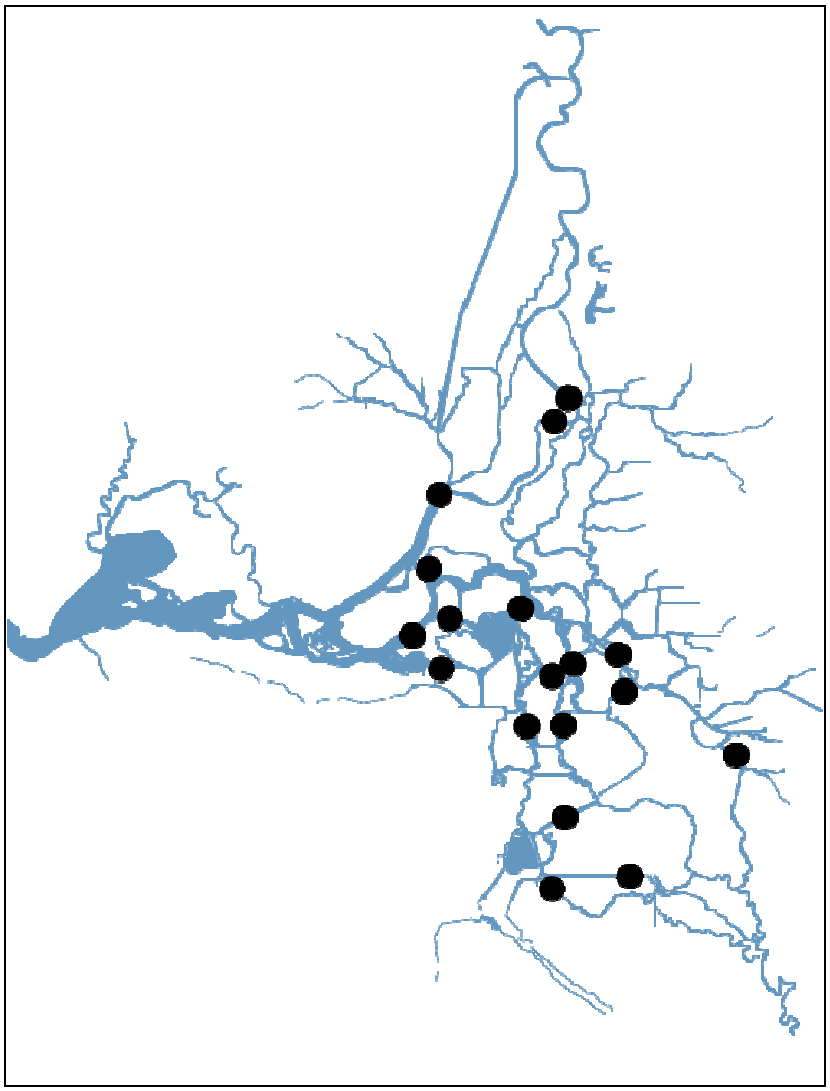

Figure 2.9: Location of Available ADCP Transects.

Field Measured Velocity

The field measurements used in estimating the velocity profile coefficients were provided by the USGS in the form of velocity transects. As shown in Figure 2.10, a transect is typically obtained by a boat-mounted ADCP that moves across a channel while taking several vertical velocity profile measurements (RD Instruments, 1995). The ADCP makes several velocity or *depth cell* measurements and then averages these into *ensembles*. Each *ensemble* then represents the average velocity for a 25 to 50 cm distance. The combination of *ensembles* then makes up a vertical velocity profile at the current ADCP position. The distance between the vertical velocity profiles is dependant on the speed of the boat and the time between samples.

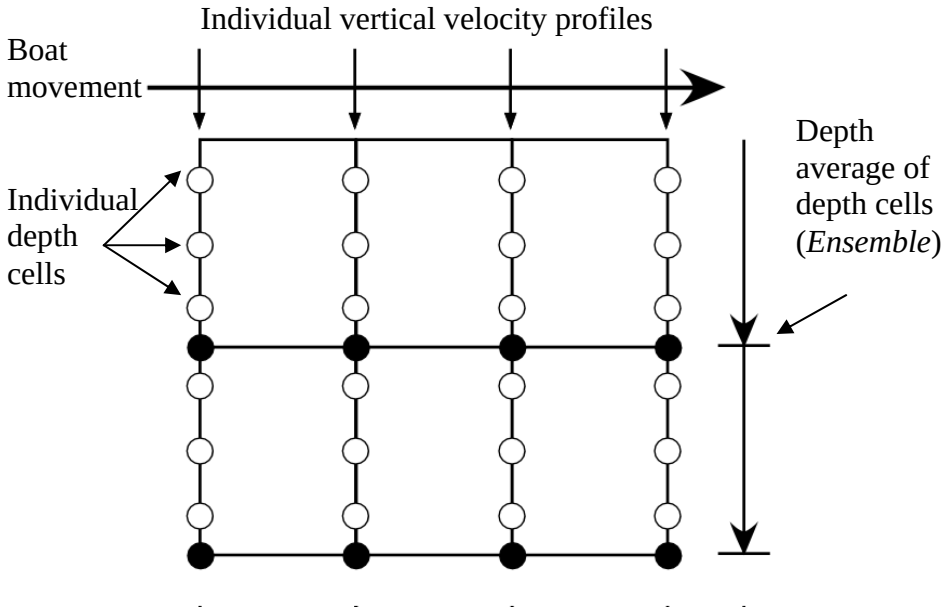

Figure 2.10: Creation of Depth Ensembles.

Data Manipulation

The data was adjusted for two main factors: 1) the distance between measured velocity profiles, and 2) the direction of the velocity vector. When the boat carrying the ADCP crosses a channel, the boat captain attempts to make the boat path as straight and perpendicular to the channel bank as possible. However, this is a difficult task especially in higher flows and the path tends to be less than perfect. As shown in Figure 2.11 the boat track can be straightened. In this process the starting and ending points of the boat track are preserved and the vertical velocity profiles are adjusted to the new reference line.

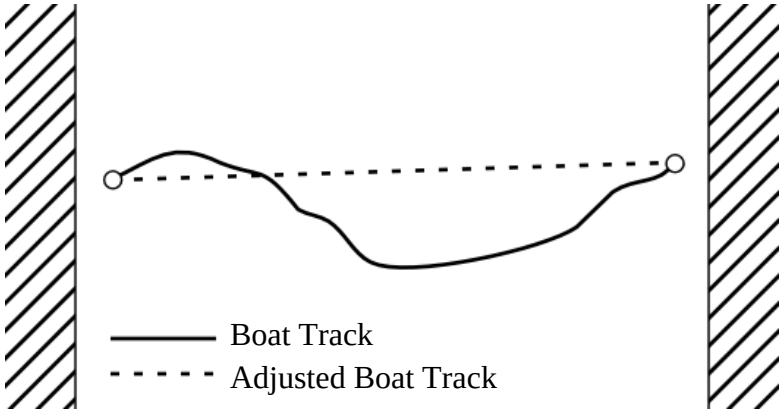

Figure 2.11: ADCP Boat Track and Adjusted Track.

The ADCP reports the velocities in a vertical profile as a series of three-dimensional vectors. To relate these data to PTM, these three-dimensional data were converted to one-dimension. A resultant vector was calculated for each transect to find the average direction of flow. This direction was then used to adjust the velocity vector direction and magnitude in the flow field. The adjusted boat track and the adjusted velocity direction are not necessarily perpendicular.

The transects provide a good coverage of velocity across a given channel. However, the transects lack the ability to capture detail at the top, the bottom, or the sides of a channel. The top of the cross-section is not included because the ADCP is submerged below the surface of the water. Typically the top one meter of the cross-section is lost, but this loss is not necessarily bad. The topmost portion of the water column can be heavily influenced by environmental conditions, such as wind. The velocities at the bottom of the transect are not recorded. The distance not recorded varies by cross section. This loss of velocity information at the bottom is essential for keeping track of the ADCP position with respect to the bottom of the channel. The velocity at the sides of the channel is also lost due to the inability of boat to safely reach the bank. The operators of the boat estimate the distance from the start and end of the boat track to the bank. Figure 2.12 illustrates the availability of data within a given cross-section. The gray squares represent the location and averaging that occurs when an ADCP is collecting data and creating the *ensembles*.

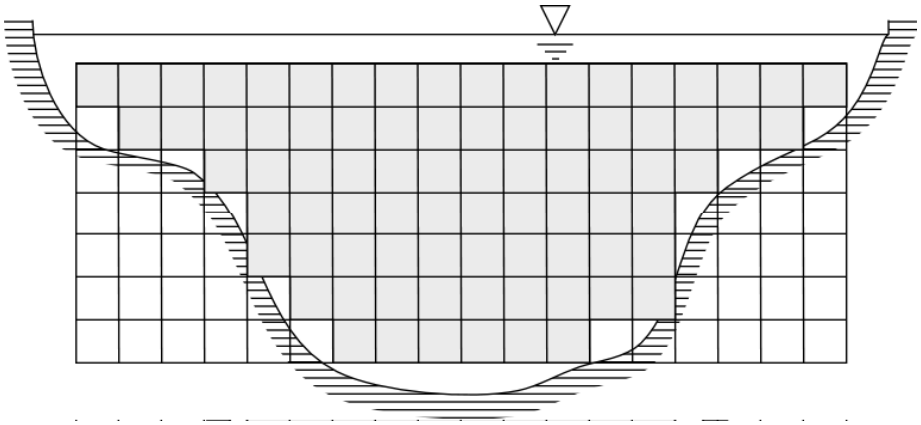

Figure 2.12: Velocity Coverage for a Channel Cross-Section (shown in gray).

For estimating the transverse profile coefficients the depth-averaged velocity was used. Similarly the vertical profile coefficients used the width-averaged velocity.

As illustrated in Figure 2.13, the width and the depth of the channel were estimated. The width of the channel includes both the straight-line distance of the transect and estimates from the transect start and end points to the channel banks. This total length was used in estimating the transverse profile coefficient. The depth of the channel was estimated using the ADCP. The estimated distance from the last velocity value in the profile to the bottom of the channel was calculated using ADCP estimated bottom error.

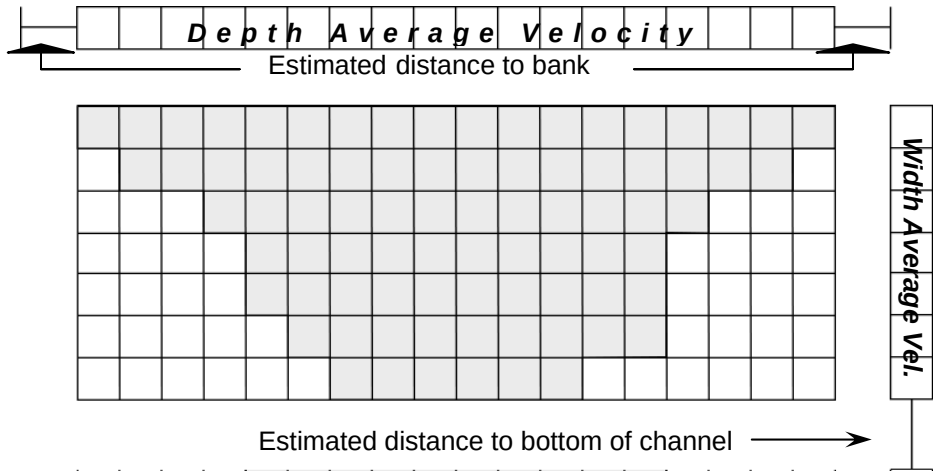

Figure 2.13: Transverse and Vertical Profiles Represent the Depth Averaged and Width Averaged Transect Values.

Filtering Data

The data for each cross section was examined and filtered before being added to the regression. Only data from cross sections with an average velocity greater than 0.25 ft/s were used. The solution for the coefficient of both the vertical and transverse profiles becomes unstable as the average velocity approaches zero. Also, profiles with lower velocities are typically in a flow transition, such as moving from flood to ebb tide. This flow transition is important in the dispersion process, but the velocities in these types of transects are very complex and difficult to model. Transects with average velocities greater than 0.25 ft/s typically have, or are in the process of forming, a velocity profile, which can be estimated more easily.

Additional limitations were placed on the data for the vertical profile. For each transect the shape coefficient was determined and data were used only if the coefficient was found to be greater than 0.5. This limitation was implemented to reduce the amount of outliers and eliminate unreasonable data. As the shape coefficient moves towards zero, the intercept of the profile moves to around 0.37 of the depth and the maximum value of the profile goes toward infinity (Figure 2.3).

For the transverse profile, like the vertical profile, a limitation was placed on the coefficient. For each transect the coefficient was determined and the data were not used if the coefficient was less than 1.25 or greater than 1.87. Values less than 1.25 describe profiles that are concave in the center. Values greater than 1.87 describe profiles that become negative near the sides.

Estimating Vertical Profile Coefficients

To estimate the vertical velocity coefficient, Equations 2-2 and 2-3 were combined. Combining these equations and assuming a width averaged velocity ($F_T(y) = 1$), the point velocity is then described by Equation 2-22. For each cross-section the width averaged velocity is used in the estimation of a vertical velocity profile. The point velocity (u) was the width averaged velocity at each layer. The average velocity ($\bar{u}$) was the average velocity of the average vertical velocity

profile. The vertical position (z) was the height of the velocity layer above the bottom of the channel. The depth (d) was estimated using ADCP data. The unknown, von Karman constant, can be estimated using a $y=Ax$ model linear regression.

$$u-\bar{u}=\frac{1}{sk}u^{*}\left[1+\ln\left(\frac{z}{d}\right)\right] \qquad \text{[Eqn. 2-22]}$$

Estimation of the vertical profile shape factor was obtained by regressing both sides of Equation 2-22 for a number of cross-sections. Figure 2.14 is a graphical solution of Equation 2-22 where $1/sk$ is the slope; hence sk is the inverse of the slope.

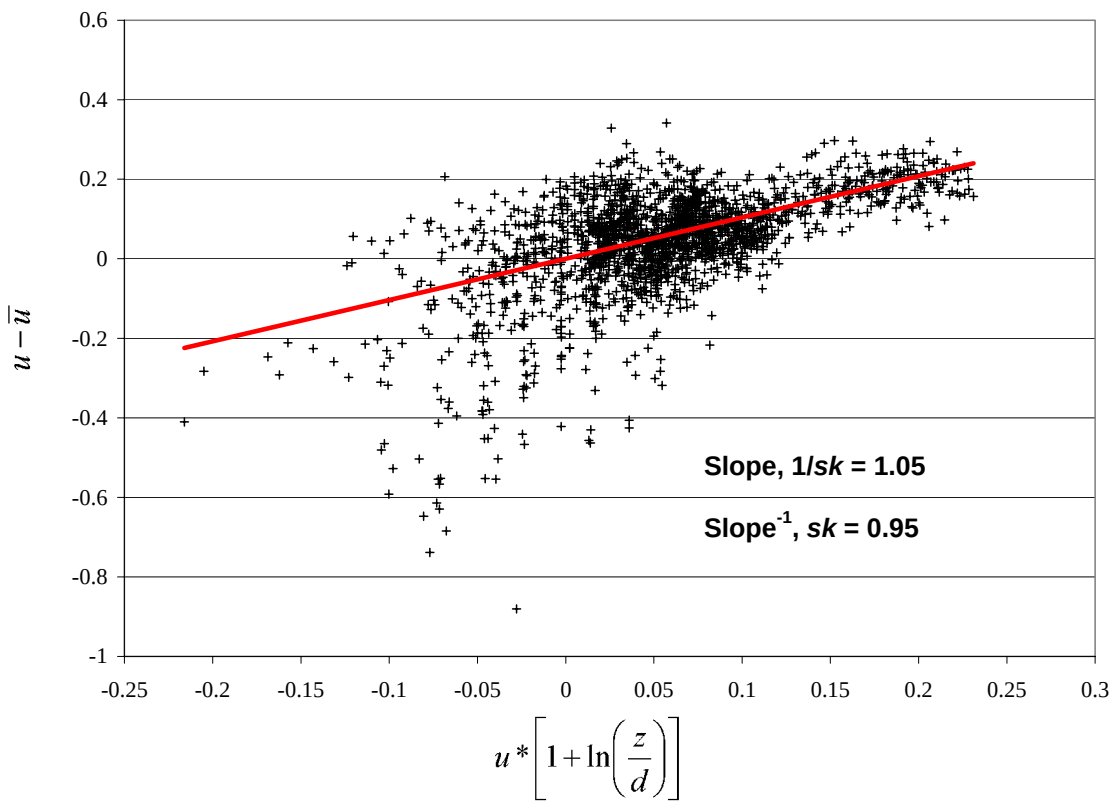

Figure 2.14: Regression of the Vertical Velocity Profile and Estimation of the von Karman Coefficient, *k*, and Shape Factor, *s*.

The regression of the graphical solution of Equation 2-22 was completed with 1928 data points and 90 individual profiles. The product of the shape factor (s) and von Karman (k) coefficient was found to be 0.95. Comparing a sample cross-section with the theoretical profile (Figure 2.15) shows a good representation. However, the 95 percent confidence interval illustrates the vast uncertainty in the point velocity across a give cross-section.

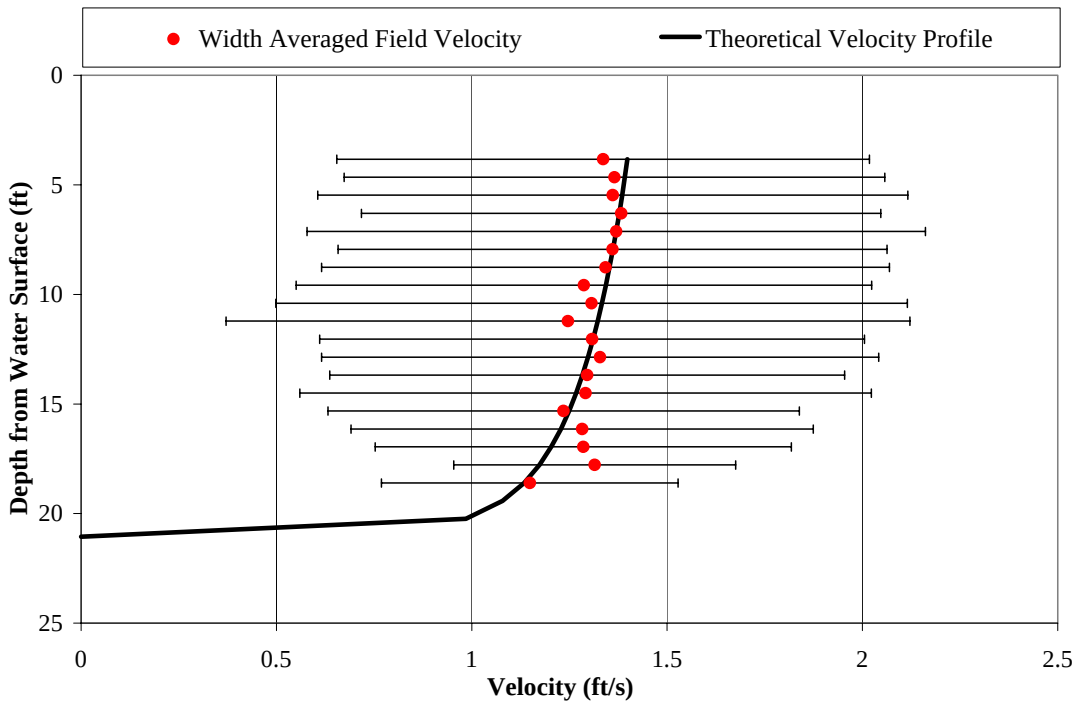

Figure 2.15: Theoretical Vertical Profile Compared to Field Velocity and 95% Confidence Intervals.

Estimating Transverse Profile Coefficients

Equations 2-2 and 2-5 were combined to estimate the transverse velocity coefficient. Assuming a depth averaged velocity ($F_V(z) = 1$), the longitudinal velocity across a channel can be described with Equation 2-23.

$$u(y) = \bar{u}\left[A + B\left(\frac{2y}{w}\right)^2 + C\left(\frac{2y}{w}\right)^4\right] \qquad \text{[Eqn. 2-23]}$$

Substituting in Equations 2-8 and 2-9, the following relationship is obtained:

$$\frac{u}{\bar{u}} - 7.5\left[\left(\frac{2y}{w}\right)^2 - \left(\frac{2y}{w}\right)^4\right] = A\left[1 - 6\left(\frac{2y}{w}\right)^2 + 5\left(\frac{2y}{w}\right)^4\right] \qquad \text{[Eqn. 2-24]}$$

For each cross-section, the depth averaged velocity is used in the estimation of a transverse velocity profile by regressing both sides of Equation 2-24. The point velocity (u) was the depth averaged velocity at each location across the cross-section. The average velocity ($\bar{u}$) was the average velocity of the average transverse velocity profile. The horizontal position (y) was the normalized distance across the channel with zero falling in the center of the channel. The width (w) was estimated using the starting point and ending point of the transect and the estimated distance to the bank.

The transverse velocity profile data used in Equation 2-24 provides an estimate for the transverse velocity profile shape coefficient, *A*. In Figure 2.16, the slope of the regression, which is the transverse shape coefficient *A*, was found to be about 1.34. The regression used 11894 data points from 149 profiles. Using Equation 2-8 the *B* coefficient was found to be -0.54 and using Equation 2-9 the *C* coefficient was found to be -0.8.

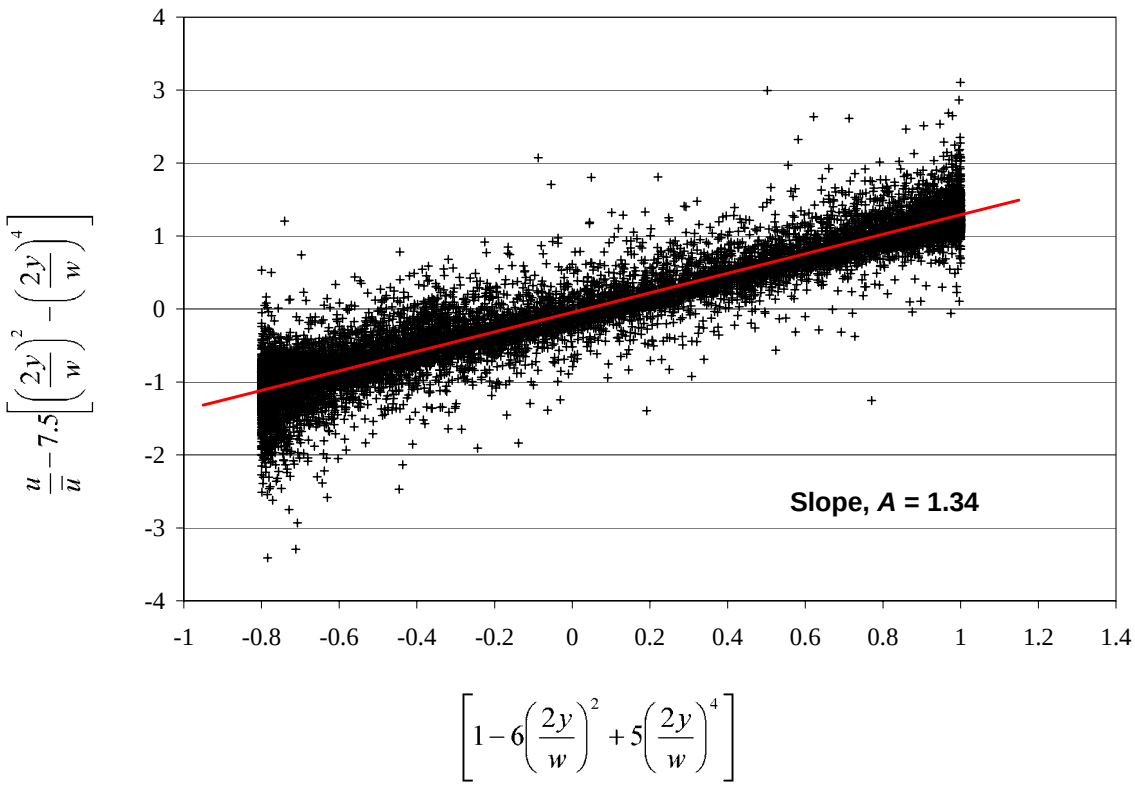

Figure 2.16: Regression of the Transverse Velocity Profile and Estimation of the Transverse Shape Coefficient, *A*.

A comparison of the theoretical profile and field profile (Figure 2.17) shows that the coefficients are a good representation of the velocity profile at this location. However, the 95 percent confidence interval illustrates the vast uncertainty in the point velocity across a give cross-section.

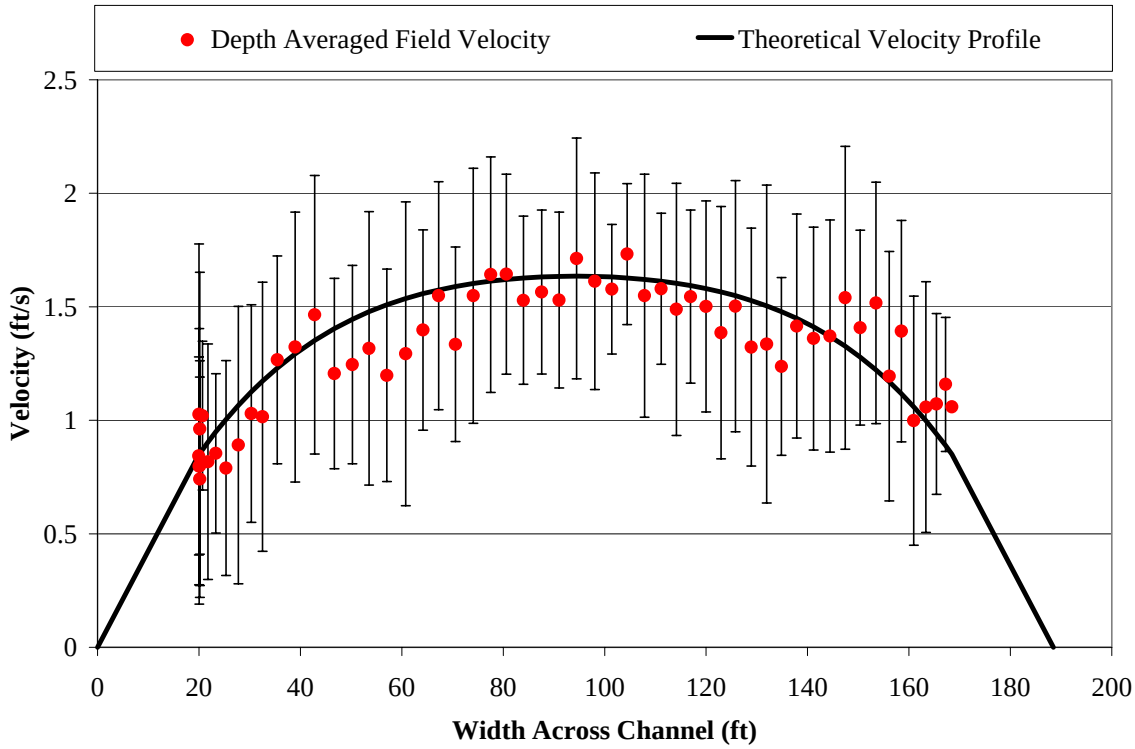

Figure 2.17: Theoretical Vertical Profile Compared to Field Velocity and 95% Confidence Intervals.

Calibration of Profile Shape Conclusions

The coefficients for the vertical and transverse profiles were found and are summarized in Table 2.1.

Table 2.1: Summary of Profile Coefficients Found from Field Data.

Coefficient	***Value***
Transverse *A*	1.34
Transverse *B*	-0.54
Transverse *C*	-0.80
Vertical *s*	2.38

2.5 Verification of PTM in a Single Channel – Static Stage

The longitudinal dispersion of the Particle Tracking Model was calculated using a simple channel with a steady flow. Dispersion coefficients for natural systems have been found to be quite varied and the theoretical range is enormous. This process is simply to show that the model is simulating dispersion within theoretical bounds.

2.5.1 Methods

Verification of dispersion used a theoretical 150,000 ft long channel with a width of 500 ft and a 0% bottom slope. Stage at the downstream boundary was set at 40 ft. The upstream boundary was forced with three separate positive flows, 10,000, 32,000, and 64,000 cfs, giving an average velocity in the channel of 0.5, 1.6, and 3.2 ft/s respectively.

Parameters assumed for the model were: transverse flow coefficient, C_T, of 0.6; shear velocity, u/u*, of 0.1; vertical profile shape coefficient, *s*, of 2.375 (Table 2.1); and transverse *A*, *B* and *C* shape coefficients of 1.34, -0.54, and -0.8 (Table 2.1).

The model was compared to the theoretical values using Equation 2-1. Because it is difficult to determine the actual parameters that represent the Sacramento – San Joaquin Delta, theoretical parameters, which bracket the higher and lower bounds of dispersion, are shown in Table 2.2.

Table 2.2: Range of Parameters Used to Estimate the Dispersion Coefficient.

Parameter	Value(s)	Reference
C_T	0.6	Fischer (1979)
u/u*	0.1	Fischer (1979)
h	1.0W to 0.5W	Fischer (1979)
$\overline{u}'^2$	$0.03\overline{u}^2$ to $0.2\overline{u}^2$	Fischer (1979)
I	0.01 to 0.03	Bogle (1997)

Applying these assumptions results in two equations that bound the theoretical range of dispersion. Using I = 0.01, h = 0.5 W, and $\overline{u}'^2 = 0.03\overline{u}^2$ for the lower bound, the following equation can then be deduced:

$$K = \frac{0.00125\overline{u}W^2}{d} \qquad \text{[Eqn. 2-25]}$$

Using I = 0.03, h = 1.0 W, and $\overline{u}'^2 = 0.2\overline{u}^2$ for the upper bound, the following equation can then be deduced:

$$K = \frac{0.1\overline{u}W^2}{d} \qquad \text{[Eqn. 2-26]}$$

Results from the calculation of the upper and lower bounds of the dispersion coefficient for each of the flow scenarios is shown in Table 2.3.

Table 2.3: Theoretical Bounds on the Dispersion Coefficient.

Flow (cfs)	Velocity (ft/s)	Lower Bound (ft^2/s)	Upper Bound (ft^2/s)
64,000	3.2	25	2000
32,000	1.6	13	1000
10,000	0.5	4	312

For each of the three simulations particles were randomly inserted at the upstream end of the long channel. The longitudinal distance along the channel for each particle was collected every five minutes. The variance of the particle plume was calculated for each time step. The respective dispersion for each time step was then determined by half the slope (half of the derivative of the variance) (Figure 2.1).

2.5.2 Results

The results of the dispersion verification resulted in consistent results for the three flow scenarios with respect to the upper and lower bounds.

The 64,000 cfs flow scenario resulted in an average velocity of 3.2 ft/s. The simulation ended after 700 minutes (Figure 2.18) when the first particle reached the end of the theoretical channel. Theoretical longitudinal dispersion for this channel and velocity ranged from 25 to 2000 ft^2/s. The particles became fully dispersed within 60 minutes of simulation. However, after the first 60 minutes, the dispersion coefficient continued to rise from around 600 to 900 ft^2/s.

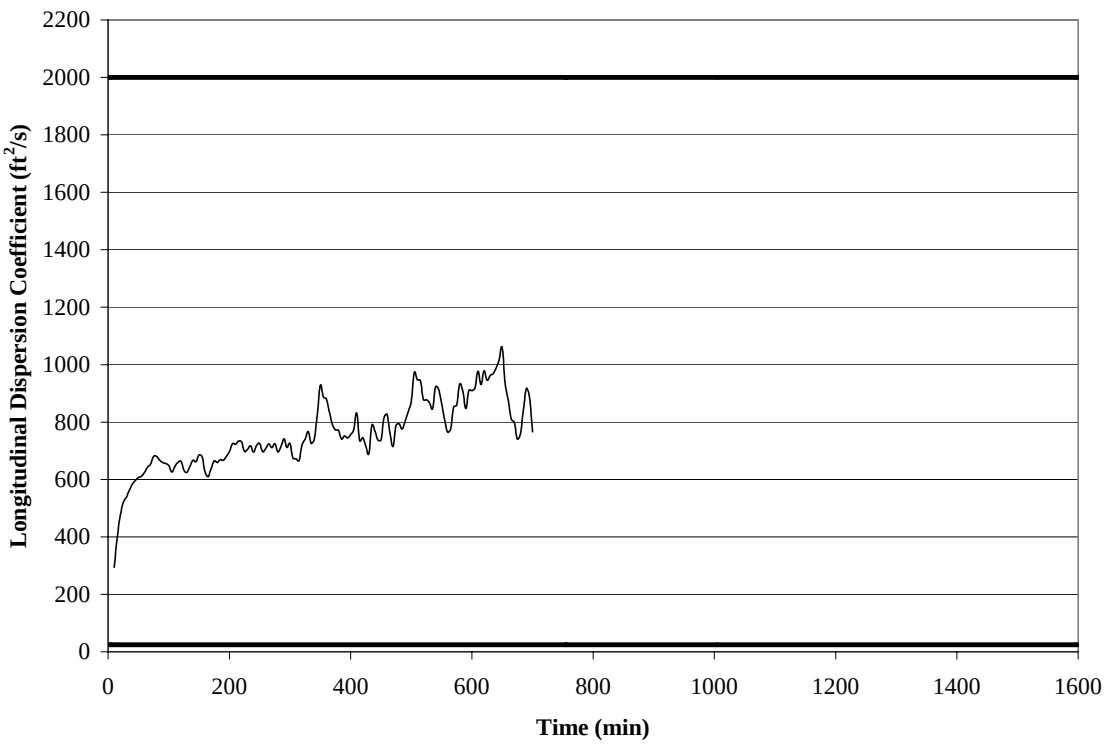

Figure 2.18: Theoretical Estimate of PTM Longitudinal Dispersion Coefficient for an Average Velocity of 3.2 ft/s.

The 32,000 cfs flow scenario resulted in an average velocity of 1.6 ft/s. The simulation ended after 1330 minutes (Figure 2.19) when the first particle reached the end of the channel. Theoretical longitudinal dispersion ranged from 13 to 1,000 ft^2/s. The particles became fully dispersed within 80 minutes of simulation. The dispersion coefficient at a velocity of 1.6 ft/s for PTM is approximately 400 ft^2/s.

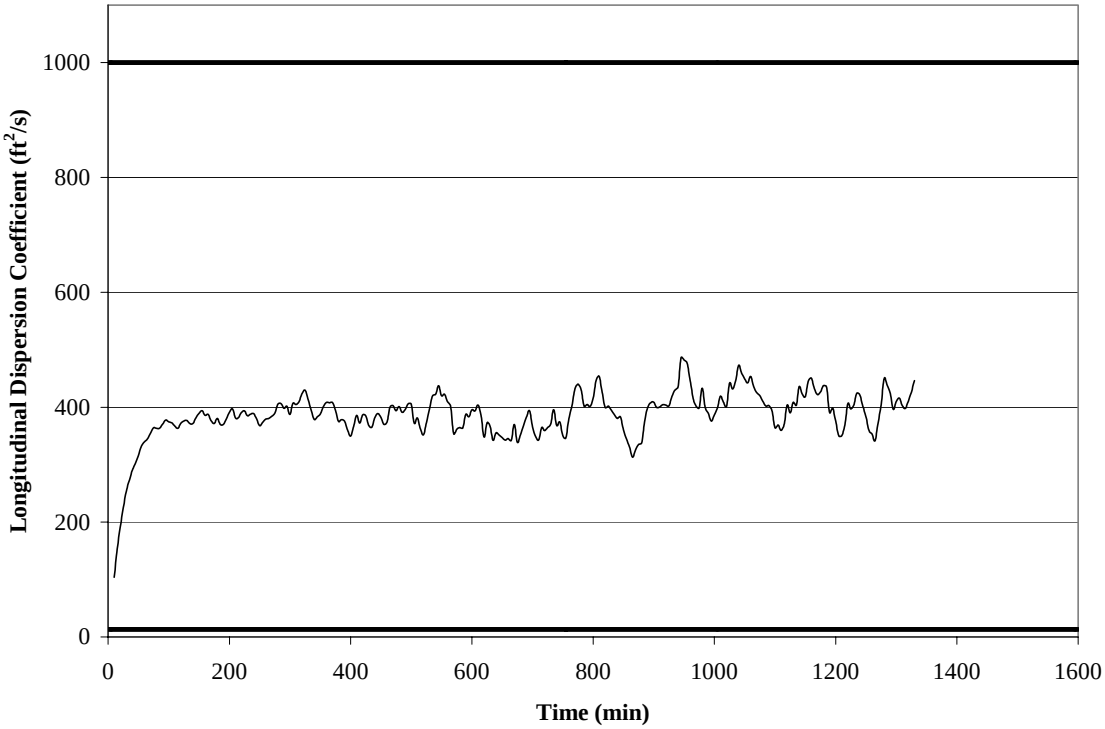

Figure 2.19: Theoretical Estimate of PTM Longitudinal Dispersion Coefficient for an Average Velocity of 1.6 ft/s.

The 10,000 cfs flow scenario resulted in an average velocity of 0.5 ft/s. The simulation was run for 1440 minutes (Figure 2.20). At that point all particles remained within the channel. Theoretical longitudinal dispersion ranged from 4 to 312 ft^2/s. Full dispersion occurred within 200 minutes of the simulation. At a velocity of 0.5 ft/s for PTM, the dispersion coefficient was approximately 125 ft^2/s.

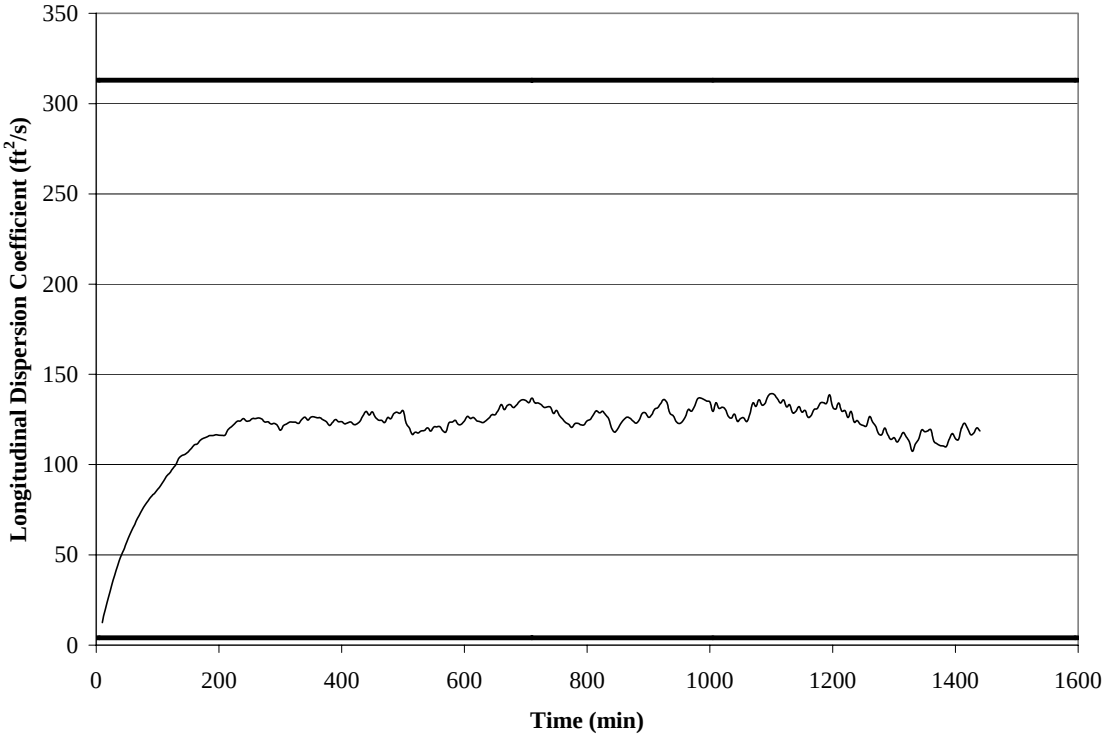

Figure 2.20: Theoretical Estimate of PTM Longitudinal Dispersion Coefficient for an Average Velocity of 0.5 ft/s.

2.5.3 Verification Discussion

The process of verifying the dispersion of PTM has produced successful results. PTM has proven to simulate dispersion in a consistent manner. For the three different velocity scenarios, the dispersion coefficient was consistently found to be between the lower and upper bounds.

2.6 Future Directions

The validation of the model is being completed. There are a number of physical studies for which PTM may simulate in the validation process. These studies include the:

- 1997 Dye Study.

  In the spring of 1997 the USGS (Oltmann, 1998) conducted a dye study where rhodamine WT dye was inserted into the San Joaquin river near Mossdale bridge. The dye concentration was monitored at various locations in the Delta.

- 1993 striped bass egg data.

  In late 1993 during the striped bass spawn, egg densities were collected along the

Sacramento River. Striped bass lay their eggs at the surface of the water column. The eggs then slowly sink as they move downstream due to being slightly more dense than the water.

- 2000 Delta Cross Channel study.

  In fall 2000 the USGS, DWR, U.S. Fish and Wildlife Service (USFWS), and others participated in a study of the flow around the Delta Cross Channel. From this study resulted in an extensive data set that shows the movement of water around the cross channel for many different flow conditions.

2.7 References

Bogle, G. (1997). "Stream Velocity Profiles and Longitudinal Dispersion." *Journal of Hydrologic Engineering.* American Society of Civil Engineers. 123 (9).

Bogle, G. (1994). "Simulation of Dispersion in Streams by Particle Tracking." *Draft Report*. Water Engineering & Modeling.

Denton, R. (1995). "Particle Tracking with Non-Uniform Cross-Sectional Mixing." Presentation given at the Bay-Delta Modeling Forum. Monterey, CA.

Dimou, K. Nadia and Adams, E. Eric (1993). "A Random-walk, Particle Tracking Model for Well Mixed Estuaries and Coastal Waters." *Estuarine, Coastal and Shelf Science.*

Fischer, H.B., E.J. List, R.C.Y. Koh, J. Imberger, N.H. Brooks. (1979). Mixing in Inland and Coastal Waters. Academic, New York.

Miller, Aaron. (2000). "Chapter 5: DSM2 Particle Tracking Model Development." *Methodology for Flow and Salinity Estimates in the Sacramento-San Joaquin Delta and Suisun Marsh. 21st Annual Progress Report to the State Water Resources Control Board.* California Department of Water Resources. Sacramento, CA.

Nader-Tehrani, P. (2001). "Chapter 2: DSM2 Calibration and Validation." *Methodology for Flow and Salinity Estimates in the Sacramento-San Joaquin Delta and Suisun Marsh. 22nd Annual Progress Report to the State Water Resources Control Board.* California Department of Water Resources. Sacramento, CA.

Oltmann, R. N. (1998). *Measured Flow and Tracer – Dye Data Showing Anthropogenic Effects on the Hydrodynamics of South Sacramento – San Joaquin Delta, California, Spring 1996 and 1997.* United States Geological Survey, Open File Report 98-285.

RD Instruments. (1995). ADCP River Discharge Measurement Manual.

Smith, T. (1993). "Chapter 2: Particle Tracking Model for the Delta." *Methodology for Flow and Salinity Estimates in the Sacramento-San Joaquin Delta and Suisun Marsh. 14th Annual Progress Report to the State Water Resources Control Board.* California Department of Water Resources. Sacramento, CA.

Smith, T. (1998). "Chapter 4: DSM2 PTM." *Methodology for Flow and Salinity Estimates in the Sacramento-San Joaquin Delta and Suisun Marsh. 19th Annual Progress Report to the State Water Resources Control Board.* California Department of Water Resources. Sacramento, CA.

Wilbur, R. (2000). *Validation of Dispersion Using the Particle Tracking Model in the Sacramento-San Joaquin Delta*. M.S. Thesis. University of California, Davis.

Methodology for Flow and Salinity Estimates in the Sacramento-San Joaquin Delta and Suisun Marsh

23rd Annual Progress Report
June 2002

Chapter 3:
Analysis and Preparation of Observed Data for Input Files in Support of DSM2 Extended Validation (1975-1999)

Author: Myint Thein

3 Analysis and Preparation of Observed Data for Input Files in Support of DSM2 Extended Validation (1975-1999)

3.1 Introduction

This chapter summarizes the work done analyzing and preparing the observed 1975-1999 data for DSM2 input files that will be used in a forthcoming DSM2 Extended Validation Project.

3.2 Objectives

The primary objectives of the analysis and preparation of the data for DSM2 input files are to:

- Check the observed data for errors,
- Organize an accurate data set conformable to the required format of DSM2, and
- Convert and link this data set to the DSM2 input files.

3.3 Description of Analysis and Preparation of Data

3.3.1 Acquisition of Data

The historical raw data of stage, flow, and electrical conductivity at 11 boundary-condition sites and 64 Delta-interior sites were downloaded from the Interagency Ecological Program (IEP) website (http://iep.water.ca.gov/dss/). Additionally, historical information on barrier installations and island floodings were obtained from various DWR bulletins (DWR Bulletin 132: Appendix E series; DWR Bulletin 69 series; and DWR Bulletin 160 series).

3.3.2 Analysis and Screening of Input Data for DSM2 Input Files

To improve the accuracy and quality of the input data and also to conform to the requirements of the DSM2 input format, the downloaded raw data were screened for missing data and for inaccuracies. One of the vital requirements of the data provided to the DSM2 input files is that data must be continuous. During the screening process, the raw data were checked for missing values, errors, and questionable data. If unchecked, the inaccurate data will affect the accuracy of DSM2's simulation results. Missing values and errors in data can occur for various reasons, including:

- Mechanical or electrical breakdown of the data acquisition equipment.

- Data collection devices damaged by passing marine vehicles or debris.

- Abnormally high currents, flows, or sediment movement that are beyond the device's ability to measure or that could damage the device.

- Errors that occurred in the data due to the incorrect post processing of the collected data by the collecting agency.

Using the data analysis and visualizing tool, VISTA, the raw data were classified in five different ways: Unscreened, OK, Missing, Questionable, and Reject. The unscreened data flag indicates that the data have not been reviewed for errors. The OK data flag indicates that the data are correct. The missing data flag indicates missing data. The questionable data flag indicates that the data are suspicious but not obviously in error. Finally, the reject data flag indicates that the data are in error and should not be used as input or for comparison. Later in the preprocessing of the data, the flagged missing, reject, and questionable data will be filled in and/or replaced by data generated by a filling function.

3.3.3 Documentation of Delta Events and Activities

During the data analysis, it was observed that some of the data were strongly affected by natural events and man-made remedial activities in the Delta. The comprehensive knowledge of the events and activities that occurred in the Delta is beneficial to understanding which data to flag as rejected or questionable. In order to gather information about the Delta events and activities the published bulletins and reports were sought and studied. The notable events, activities, and changes that occurred in the Delta were documented.

The information has helped to explain the predominant and/or probable causes behind the abruptly changing values and abnormally high or low values of data. Some examples of the documented events and activities are:

- Naturally occurring undesirable events, such as levee breaks, island floods, and droughts.
  e.g., On Aug 23, 1982, the west levee of McDonald Island broke at 3 a.m. The break widened to 600 feet and later deepened to 85 feet, flooding 5,800 acres.

- Irregular or temporary closures of channels and sloughs (to mitigate the water quality issues).
  e.g., On Sep 1, 1976, a temporary closure in Sutter Slough was built to increase the transfer of Sacramento River water to the central Delta via the Delta Cross Channel and to help reduce the flow-reversal in the San Joaquin River.

- Seasonal installation of temporary rock-barriers.
  e.g., The fall-installation of the Head of Old River Barrier depends primarily upon the water quality in the San Joaquin River near Stockton. In some years, the Old River Barrier was installed September through December. In other years, it was not installed and an alternative solution (such as curtailment of exports) was carried out.

- Trial measures to improve the Delta water quality.
  e.g., In September 1977, a Dutch Slough Barrier was installed (with siphons and flap gates) to mitigate salinity intrusion to the central and south Delta. It was removed three months later and not installed again.

- Occasional installations of barriers.
  e.g., In March 1977, an Indian Slough Barrier was installed to allow northward one-way flow of low salinity water. It was removed in March 1978.

- Irregular operations of SWP and CVP pumps.
  e.g., In June 1976, California Aqueduct deliveries were interrupted and State Water Project (SWP) pumping operation ceased. Also, in May 1981, the California Aqueduct failed and consequently SWP pumping was reduced and later increased dramatically to make up the loss in export.

- The State Water Resources Control Board's (SWRCB) relaxation on Delta water quality standards during critical water years.
  e.g., During the severe drought of 1977, SWRCB modified and/or temporarily suspended required water quality standards at various sites in the Delta and Suisun Marsh. It also imposed emergency regulations and export restrictions on the SWP and CVP.

3.4 In Progress and Future Work

Presently, 15-minute stage data for DSM2's downstream boundary at Martinez has been prepared. The historical configuration of gates and barriers in the Delta has been collected. However, work still in progress includes:

- Formatting the gate and barrier information for use in DSM2.

- Completing documentation of events and activities that historically occurred in the Delta.

Future work includes:

- Filling and merging the screened and flagged stage, flow, and EC data for the DSM2 interior boundary conditions.

- Collecting and updating the most accurate information on Delta Island Consumptive Use.

- Running the historical simulations of DSM2 Model (1975 to 1999).

- Reviewing and analyzing the simulation results.

- Comparing the simulation results with the observed data.

- Documenting the DSM2 Extended Validation (1975 to 1999).

Methodology for Flow and Salinity Estimates in the Sacramento-San Joaquin Delta and Suisun Marsh

23rd Annual Progress Report
June 2002

Chapter 4:
CALSIM versus DSM2 ANN and G-model Comparisons

Author: Michael Mierzwa

4 CALSIM versus DSM2 ANN and G-model Comparisons

4.1 Introduction

DWR's Delta Modeling Section has developed an Artificial Neural Network (ANN) trained on a series of DSM2 simulations to estimate salinity within CALSIM II. Wilbur et al. (2001) provided a detailed description of how this ANN was integrated into CALSIM II. Prior to use of the ANN within CALSIM, the G-model was used to estimate the Delta's flow-salinity relationships. Since the ANN is trained on various flow regimes and Delta Cross Channel position, it may represent both existing and new Delta configurations. However, the current ANN was not trained for high Banks Pumping Plant export conditions.

Four DSM2 planning studies were run based on different monthly CALSIM studies, where the maximum Banks pumping capacity was increased to 10,300 cfs. Two of these CALSIM studies used the ANN to estimate the Delta flow-salinity relationships, and the other two CALSIM studies used the G-model. DSM2-HYDRO was run using a design repeating tide, and then DSM2-QUAL was used to determine if salinity was being over- or underestimated in CALSIM. The results of these four 16-year studies are presented in this report for three water quality locations: Emmaton, Jersey Point, and Rock Slough.

4.2 Description of Scenarios

All four CALSIM II scenarios considered the maximum pumping capacity at Banks Pumping Plant (SWP) to be 10,300 cfs and to have a 2020 level of development for the system demands. Two of the CALSIM II scenarios were optimized to meet the D-1485 water quality standards, and the remaining two CALSIM II scenarios optimized the D-1641 water quality standards. One of the D-1485 CALSIM II scenarios used the DSM2 ANN to estimate salinity, while the other D-1485 CALSIM II scenario used the G-model. Similarly, one of the D-1641 CALSIM scenarios used the DSM2 ANN to estimate salinity, while the remaining scenario was based on G-model salinity estimates.

Table 4.1: Summary of DSM2 Planning Studies.

DSM2 Study	CALSIM II Study		CALSIM II Salinity Model	
	D-1485	D-1641	ANN	G-model
1	•		•	
2	•			•
3		•	•	
4		•		•

These four DSM2 studies were then used to calculate the difference in salinity (converted to EC in CALSIM and modeled directly as EC in DSM2) between CALSIM and DSM2 using a

methodology illustrated in Figure 4.1. First, two CALSIM simulations were run using D-1485 operations. One of these CALSIM simulations used the ANN to estimate EC standards in the Delta, while the other CALSIM simulation used the G-model. The resulting Delta hydrology and operations from each CALSIM simulation was then used to run DSM2. Next, the theoretical water quality results from DSM2 were subtracted from the estimated water quality results that were calculated by each model within CALSIM. These differences were then used to compute several statistical measures in order to compare the ANN versus the G-model.

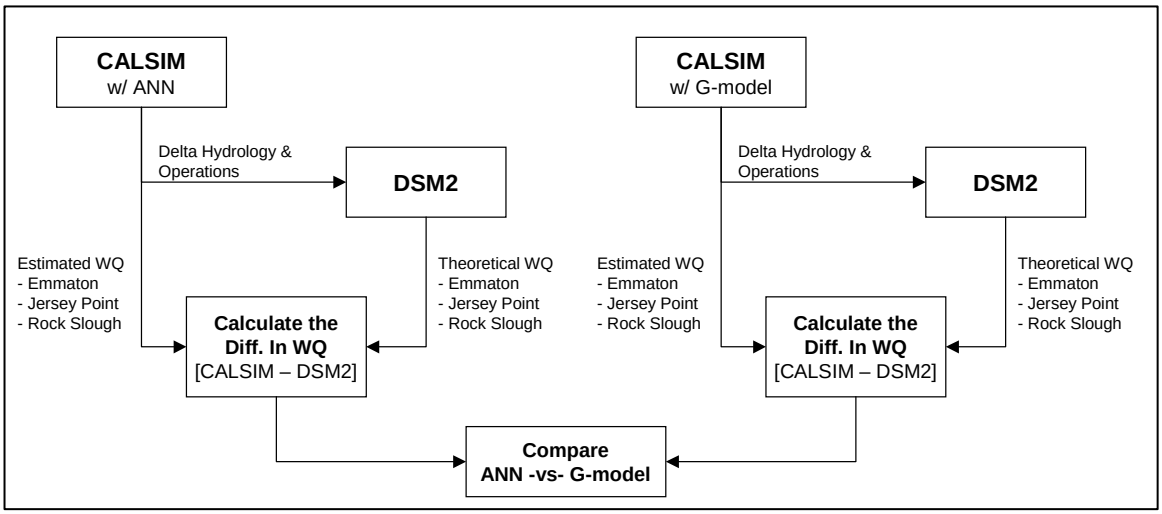

Figure 4.1: Study Methodology.

4.3 Simulation Inputs

The basic simulation inputs / constraints for the two different models used, CALSIM and DSM2, are described below.

4.3.1 CALSIM

Two different Bay-Delta standards, State Water Resources Control Board (SWRCB) D-1485 and D-1641, were used to establish the priorities of water allocation within CALSIM. Although these are daily salinity standards for both D-1485 and D-1641, CALSIM makes its decisions based on an equivalent monthly averaged EC. CALSIM used either the G-model or an ANN trained specifically for use within CALSIM D-1485 studies to estimate EC at Emmaton, Jersey Point, and Rock Slough.[1] The estimated EC from these models was then used as an operating constraint within CALSIM for both the D-1485 and D-1641 studies, such that CALSIM would optimize its water allocation decisions without violating Delta salinity standards.

[1] The CALSIM D-1485 G-model and ANN routines also estimate EC at Collinsville, Antioch, and Mallard Island. However, water quality violations rarely occur at these three locations and, due to the close proximity of these three locations to the ocean, the differences between the G-model and ANN at these locations is small.

The methods used to estimate EC and chloride by the G-model and ANN in CALSIM are summarized below.

G-model

EC (umhos/cm) for Emmaton and Jersey Point were calculated directly as functions of the G-model (Denton and Sullivan, 1993). Chloride (mg/l) at Contra Costa's Pumping Plant #1 in Rock Slough was then calculated as a function of the current (t) and previous (t-1) month's Jersey Point EC as is described in Equation 4-1:

$$Cl_{CCPP\#1_t} = 0.061 EC_{JP_t} + 0.050 EC_{JP_{t-1}} \qquad \text{[Eqn. 4-1]}$$

ANN

EC (umhos/cm) for Emmaton and Jersey Point were calculated directly using the ANN. EC at the entrance to Rock Slough on the Old River was then calculated as a function of the current (t) and previous (t-1) month's Jersey Point EC, as is described in Equation 4-2:

$$EC_{RS_t} = 0.188 EC_{JP_t} + 0.1401 EC_{JP_{t-1}} + 142.25 \qquad \text{[Eqn. 4-2]}$$

EC at the entrance to Rock Slough was then converted to chloride for Contra Costa's Pumping Plant #1, based on Equation 4-3 (see Wilbur et al., 2001):

$$Cl_{CCPP\#1_t} = 0.268 EC_{RS_t} - 23.6 \qquad \text{[Eqn. 4-3]}$$

When Equation 4-2 is combined with Equation 4-3, the relationship between chloride at Contra Costa's Pumping Plant #1 and EC calculated from the ANN at Jersey Point is described as:

$$Cl_{CCPP\#1_t} = 0.050 EC_{JP_t} + 0.038 EC_{JP_{t-1}} + 14.5 \qquad \text{[Eqn. 4-4]}$$

4.3.2 DSM2

A design repeating tide was used as the downstream boundary condition at Martinez.[2] The monthly hydrology (including the rim flows, exports, and diversions) was provided by CALSIM II. The CALSIM II studies assumed a 2020 level of development, thus 2020 DICU data used in previous DSM2 studies were used. The consumptive use in the Delta did not change for any of the four DSM2 studies. No South Delta Barriers were modeled. The Delta Cross Channel position was taken from the CALSIM II simulations.

Salinity was modeled as EC in DSM2. Martinez EC was generated using an ANN trained on net delta outflow.[3] Tidal variations in the Martinez EC are constructed using Kristof coefficients. The EC time series for the San Joaquin boundary condition was taken from CALSIM II

[2] The DSM2 monthly repeating tide does not account for the Spring-Neap variation.
[3] The ANN used to estimate EC at the Martinez boundary is different than the ANN used within CALSIM.

estimates. EC for the Sacramento River, Yolo Bypass, and Eastside streams was fixed at 150, 150, and 125 umhos/cm respectively.

4.4 Results

This report focuses on the relationship between CALSIM's ANN and G-model derived EC and the EC as simulated by DSM2-QUAL for three locations: Emmaton, Jersey Point, and Old River at Rock Slough. Both the ANN and G-model EC estimates used within CALSIM are used within CALSIM to make operations decisions. In turn, 16-years of CALSIM operations are used as the hydrologic boundary conditions for DSM2.

4.4.1 Emmaton

The time series of EC at Emmaton calculated by both DSM2 and CALSIM II is shown for all four studies in Figures 4.2, 4.4, 4.6, and 4.8. The total exports (combined flow through Banks Pumping and Tracy Pumping Plants) for each of the four DSM2 studies are different and are shown on a secondary axis of each of the time series plots. Time series of the difference of the CALSIM salinity estimates from the modeled DSM2 EC are shown in Figures 4.3, 4.5, 4.7, and 4.9.

A summary of all of time series plots is listed below in Table 4.2. The maximum absolute difference in EC between CALSIM and DSM2 does not always correspond with the maximum EC values listed. DSM2 and CALSIM EC were higher in both G-model studies. The G-model over predicted the maximum EC in both studies (i.e., CALSIM EC is greater than DSM2 EC). Furthermore, the absolute difference in EC was lower when the ANN was used to estimate EC in CALSIM.

Table 4.2: Emmaton EC (rounded to the nearest 50 umhos/cm).

DSM2 Study	DSM2 Max EC (umhos/cm)	CALSIM Max EC (umhos/cm)	Max Absolute Diff. in EC* (umhos/cm)
1485 w/ ANN	4150	4300	1000
1485 w/ G-model	4500	5200	1450
1641 w/ ANN	4250	4150	950
1641 w/ G-model	4650	4900	1500

* This is the maximum absolute value of the difference in EC, and does not correspond with the timing of the maximum EC.

The Mean Squared Error (MSE) was calculated as the sum of the squares of the differences between CALSIM and DSM2 EC and is also shown on Figures 4.3, 4.5, 4.7, and 4.9. The estimated standard deviation, σ, for CALSIM EC was then calculated based on the MSE. The MSE (and σ) for the ANN was lower than the MSE (and σ) for the G-model.

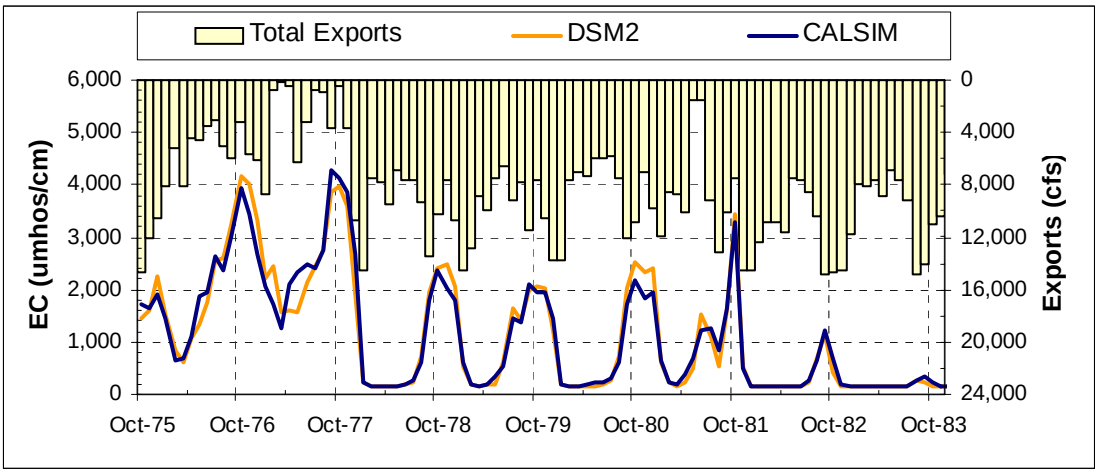

Figure 4.2a: DSM2 versus CALSIM EC at Emmaton for D-1485 using ANN: Water Years 1976-83.

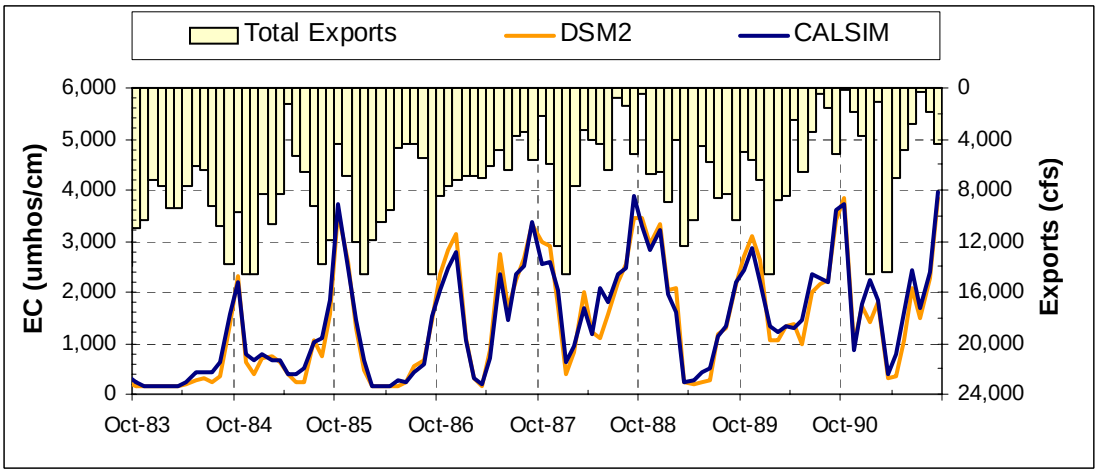

Figure 4.2b: DSM2 versus CALSIM EC at Emmaton for D-1485 using ANN: Water Years 1984-91.

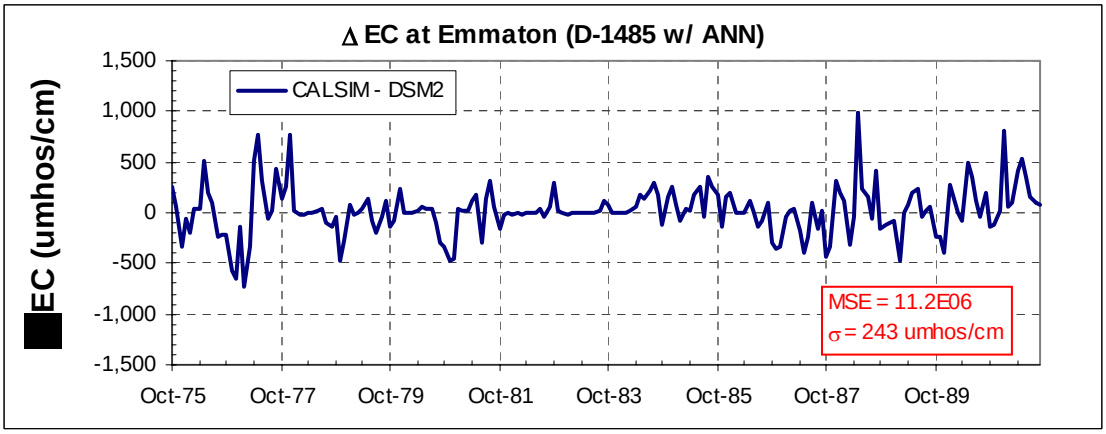

Figure 4.3: Difference in EC at Emmaton for D-1485 using ANN.

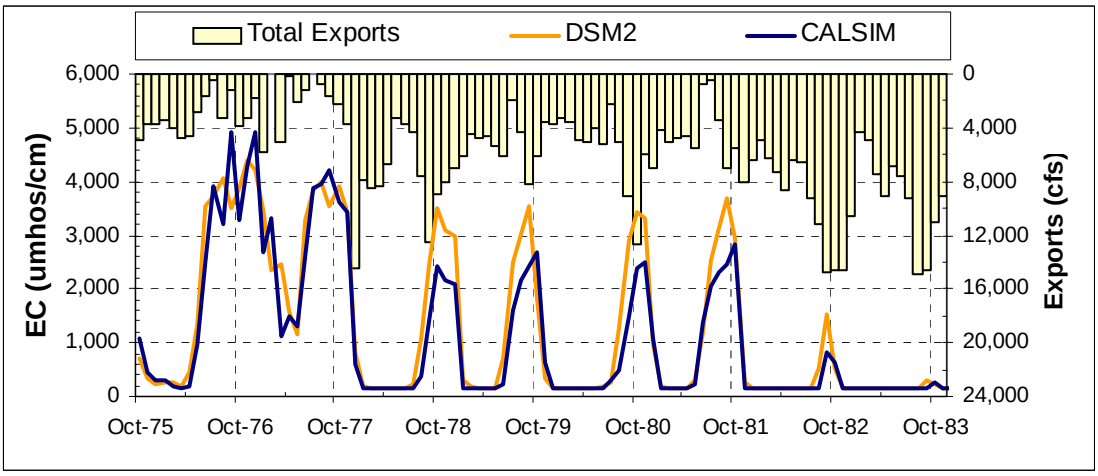

Figure 4.4a: DSM2 versus CALSIM EC at Emmaton for D-1485 using G-model: Water Years 1976-83.

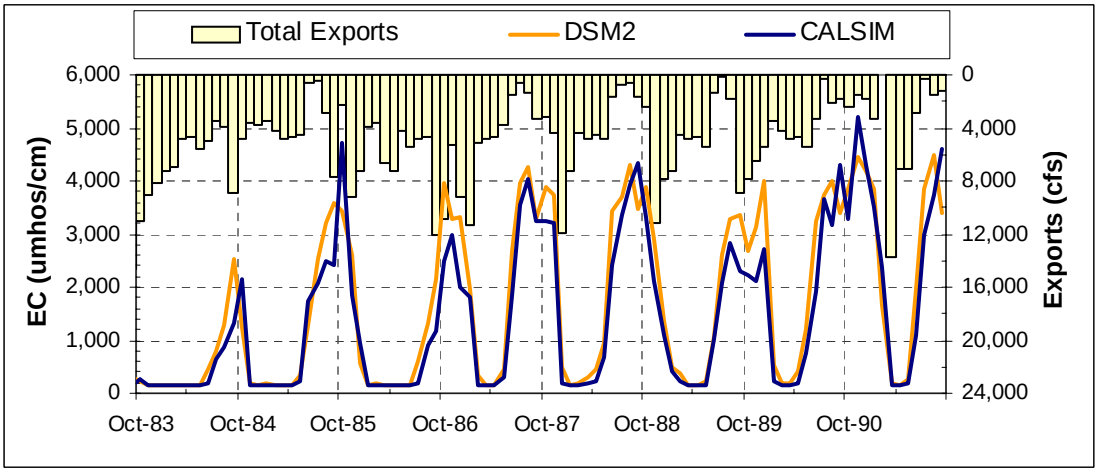

Figure 4.4b: DSM2 versus CALSIM EC at Emmaton for D-1485 using G-model: Water Years 1984-91.

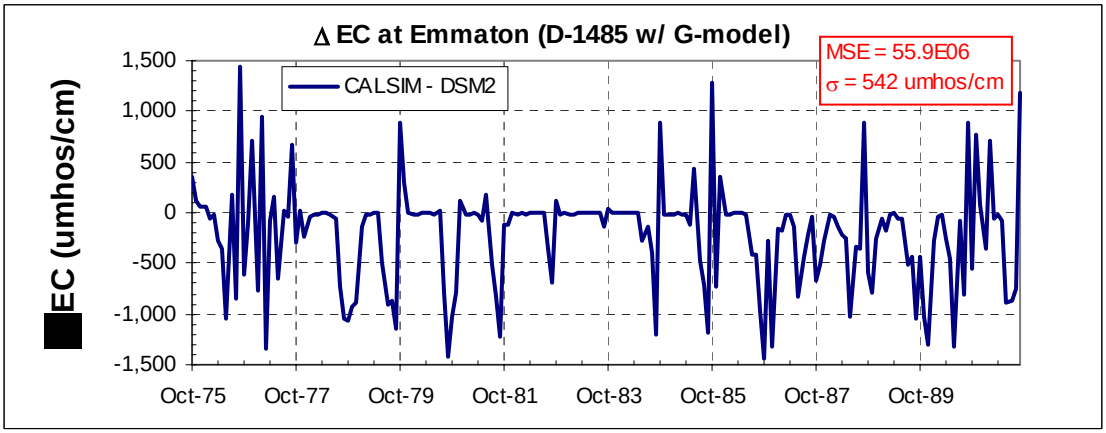

Figure 4.5: Difference in EC at Emmaton for D-1485 using G-model.

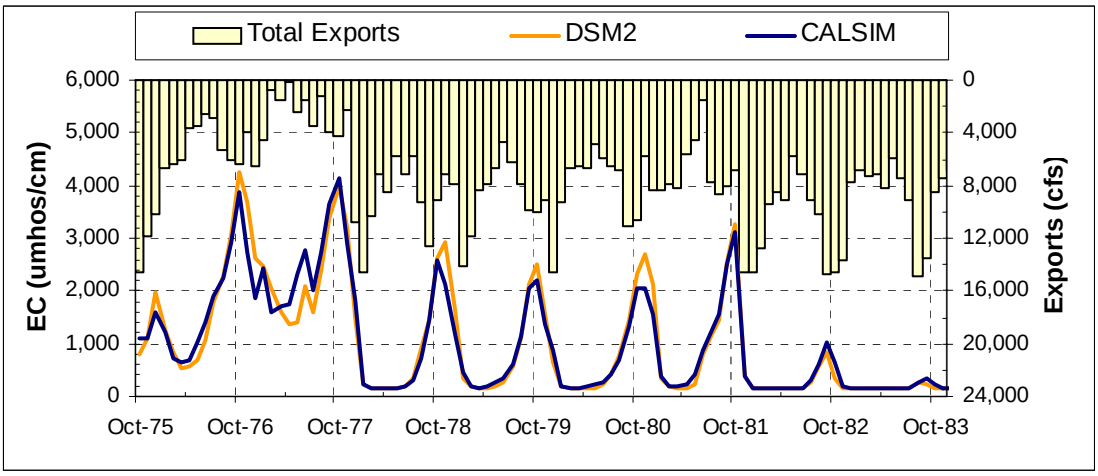

Figure 4.6a: DSM2 versus CALSIM EC at Emmaton for D-1641 using ANN: Water Years 1976-83.

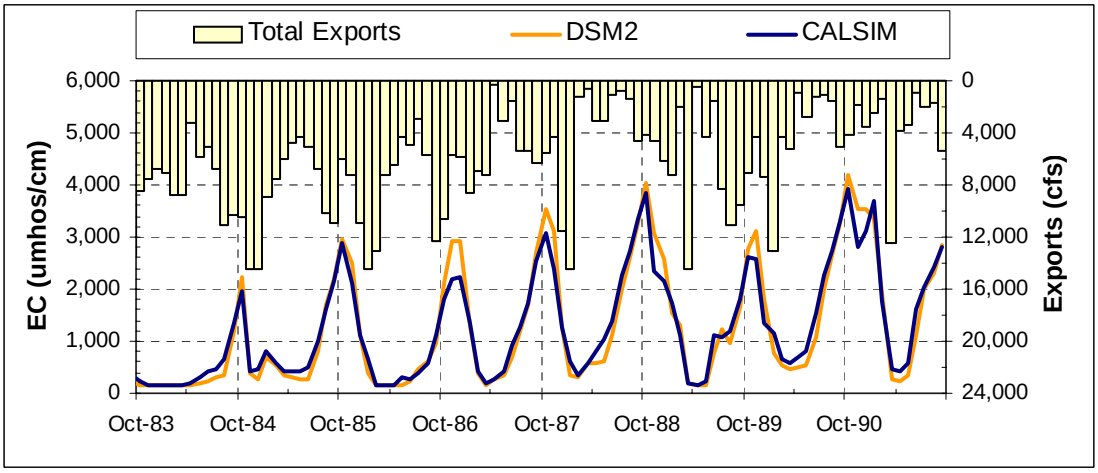

Figure 4.6b: DSM2 versus CALSIM EC at Emmaton for D-1641 using ANN: Water Years 1984-91.

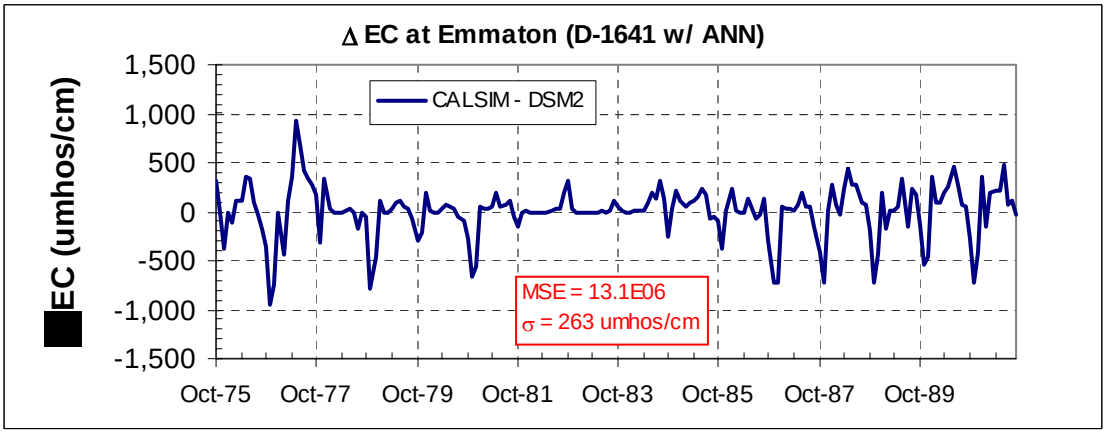

Figure 4.7: Difference in EC at Emmaton for D-1641 using ANN.

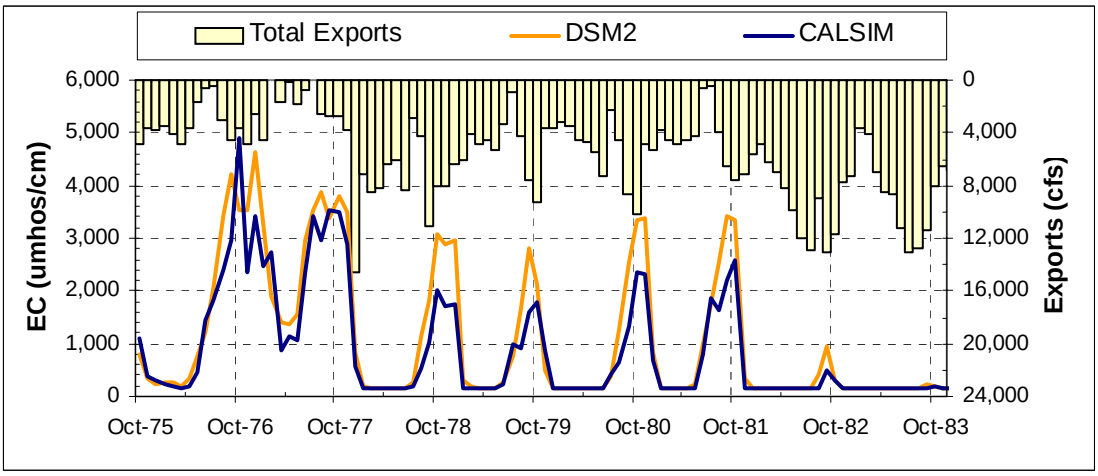

Figure 4.8a: DSM2 versus CALSIM EC at Emmaton for D-1641 using G-model: Water Years 1976-83.

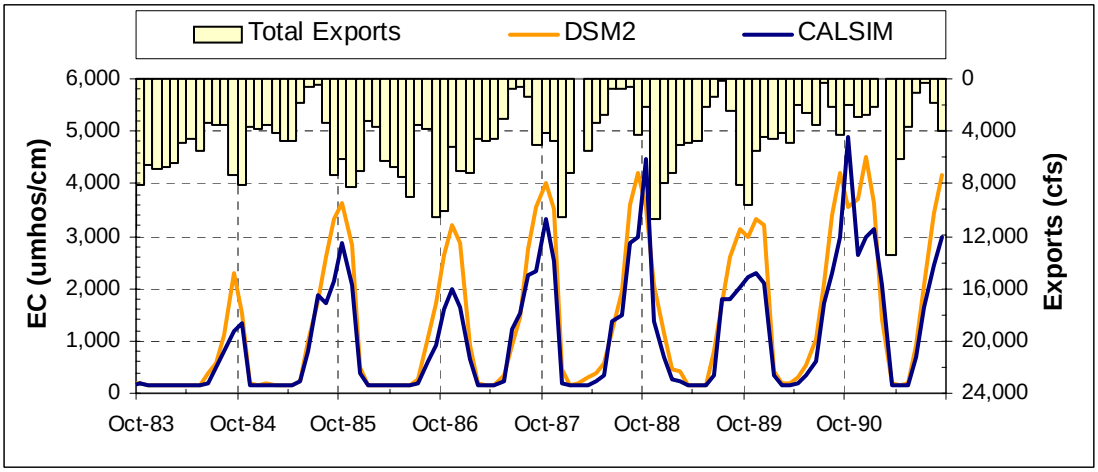

Figure 4.8b: DSM2 versus CALSIM EC at Emmaton for D-1641 using G-model: Water Years 1984-91.

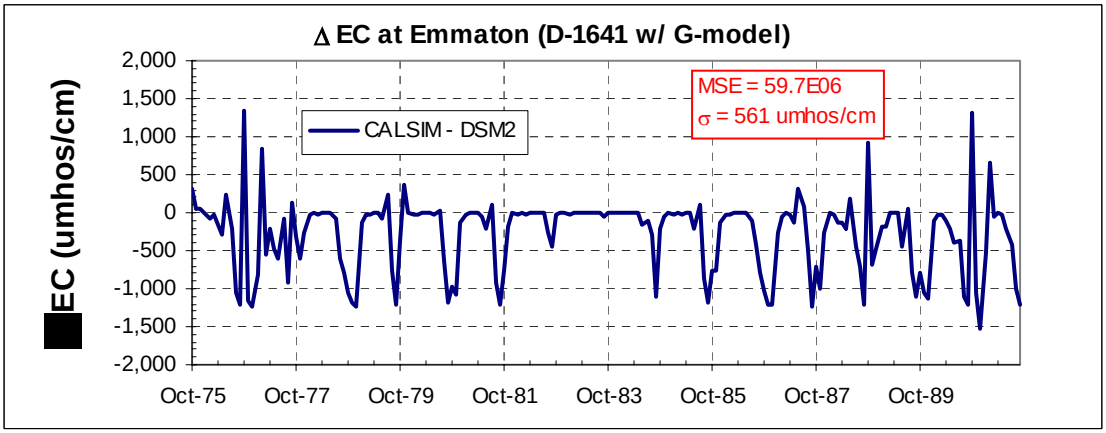

Figure 4.9: Difference in EC at Emmaton for D-1641 using G-model.

Scatter plots illustrating the relationship between DSM2 EC and CALSIM EC at Emmaton for each of the four studies are shown in Figures 4.10 – 4.13. An equivalent EC line (the 1:1 sloped line) is shown on each figure. This line represents the point where the estimated CALSIM EC matches the simulated DSM2 EC. The CALSIM EC is illustrated as a function of the DSM2 EC. The data will fall above the equivalent EC line when CALSIM is over predicting DSM2 EC. Similarly, the data will fall below the equivalent EC line when CALSIM is under predicting DSM2 EC. Estimates representing two standard deviations above and below this equivalent EC line are also shown and can be used as a measure of scatter of the data about the equivalent EC line. Best-fit lines based on simple linear regressions of the EC data, along with the regression statistics, are also shown on each plot.

A summary of the regression statistics for all of the Emmaton scatter plots is shown in Table 4.3. The MSE and estimated standard deviation, σ, were calculated from the difference between CALSIM and DSM2 EC. The MSE represents a measure of the scatter of the CALSIM EC data about the predicted EC. The slope of the best-fit line represents the bias of the linear regression from the equivalent EC line. When the slope of the best-fit line is less than 1.0, the general trend in the CALSIM data is to underestimate EC. As the slope decreases, this underestimation is more pronounced. The R^2 value for the best-fit line (which should not be confused with the MSE based on the actual difference between CALSIM and DSM2) represents a measure of the scatter of the data about the best-fit line. As R^2 approaches 1.0, the data will have a tighter fit about the best-fit line.

Table 4.3: Summary of Emmaton Scatter Plots.

DSM2 Study	MSE	σ (umhos/cm)	Slope of best-fit line	R^2 of best-fit line
1485 w/ ANN	11.2E06	243	0.94	0.95
1485 w/ G-model	55.9E06	542	0.88	0.89
1641 w/ ANN	13.1E06	263	0.89	0.95
1641 w/ G-model	59.7E06	561	0.76	0.89

For both water quality base studies (D-1485 and D-1641) at Emmaton the ANN best-fit lines more closely matched the equivalent EC lines. The G-model results systematically underestimate the EC as calculated by DSM2. The MSE (and σ) for the ANN was lower than the MSE (and σ) for the G-model.

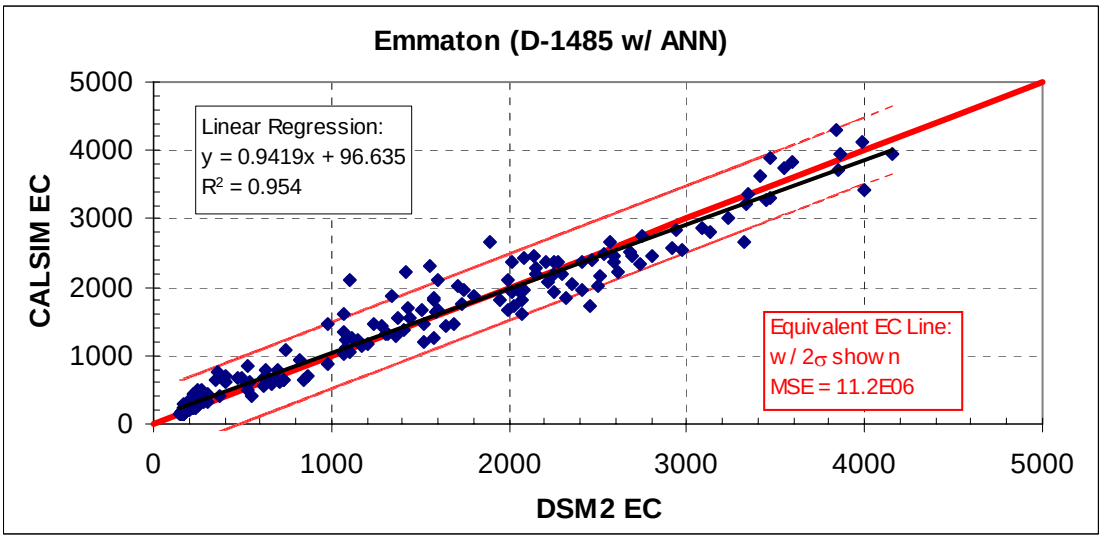

Figure 4.10: Scatter Plot of CALSIM with ANN EC versus DSM2 EC for D-1485 at Emmaton.

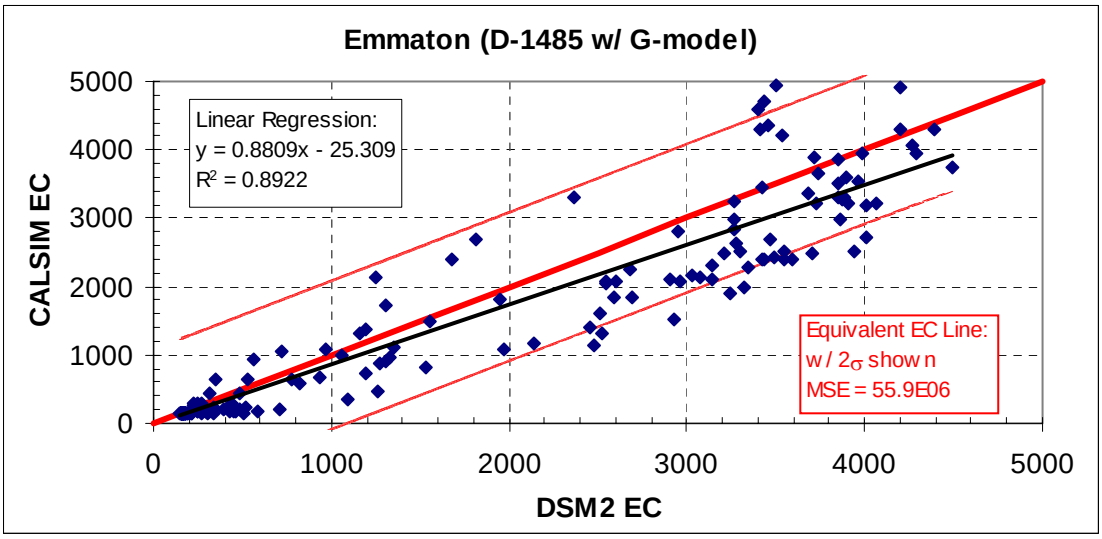

Figure 4.11: Scatter Plot of CALSIM with G-model EC versus DSM2 EC for D-1485 at Emmaton.

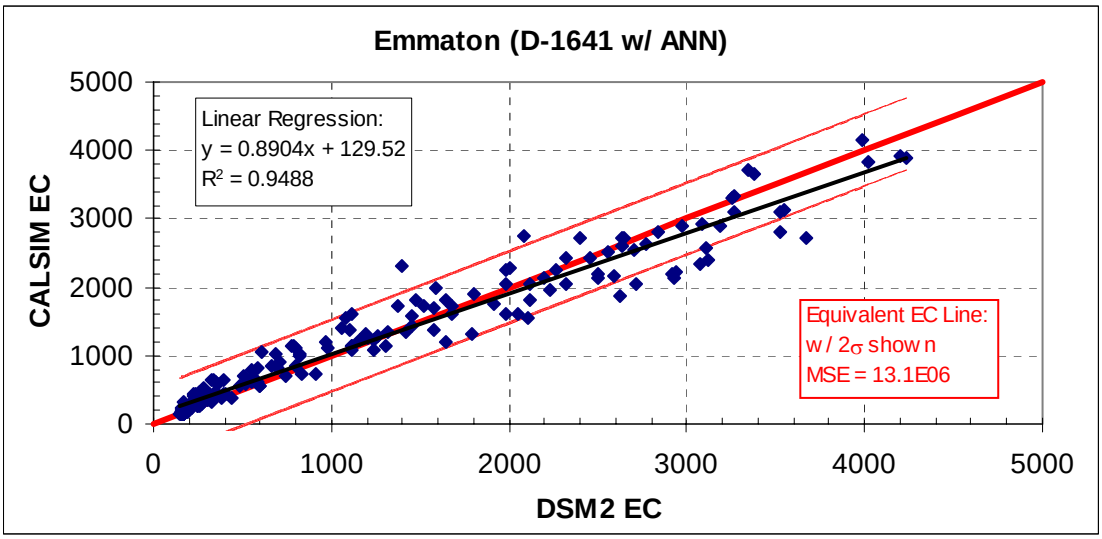

Figure 4.12: Scatter Plot of CALSIM with ANN EC versus DSM2 EC for D-1641 at Emmaton.

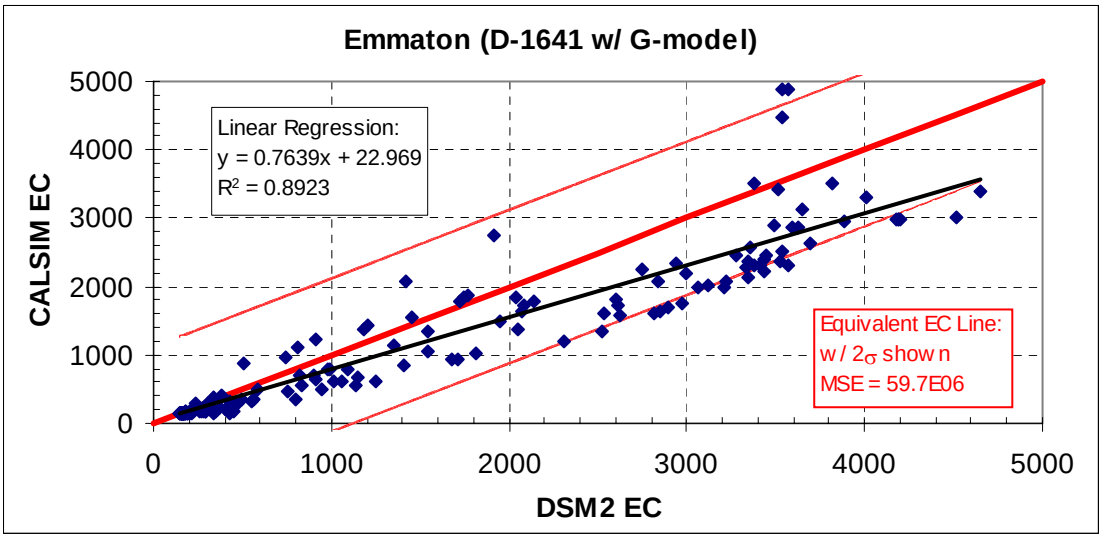

Figure 4.13: Scatter Plot of CALSIM with G-model EC versus DSM2 EC for D-1641 at Emmaton.

4.4.2 Jersey Point

The time series of EC at Jersey Point calculated by both DSM2 and CALSIM II is shown for all four studies in Figures 4.14, 4.16, 4.18, and 4.20. The combined exports are shown on Figures 4.2, 4.4, 4.6, and 4.8 (Section 4.4.1). Time series of the difference of the CALSIM salinity estimates from the modeled DSM2 EC are shown in Figures 4.15, 4.17, 4.19, and 4.21. A summary of all of time series plots is listed below in Table 4.4.

Table 4.4: Jersey Point EC (rounded to the nearest 50 umhos/cm).

DSM2 Study	DSM2 Max EC (umhos/cm)	CALSIM Max EC (umhos/cm)	Max Absolute Diff. in EC* (umhos/cm)
1485 w/ ANN	4000	3000	1850
1485 w/ G-model	4550	2200	2800
1641 w/ ANN	3050	2950	900
1641 w/ G-model	3500	2200	1500

* This is the maximum absolute value of the difference in EC, and does not correspond with the timing of the maximum EC.

As shown in Table 4.4 for Jersey Point, G-model under predicted the maximum EC in both studies (i.e., CALSIM EC is less than DSM2 EC), while the ANN under predicted the maximum EC in the D-1485 study. For both studies, the maximum absolute difference between CALSIM and DSM2 was lower when the ANN was used to estimate EC in CALSIM. However, this difference when the G-model was used in the D-1641 study was lower than the difference from the ANN comparison of the D-1485. In other words, CALSIM generally performed better in the D-1641 study.

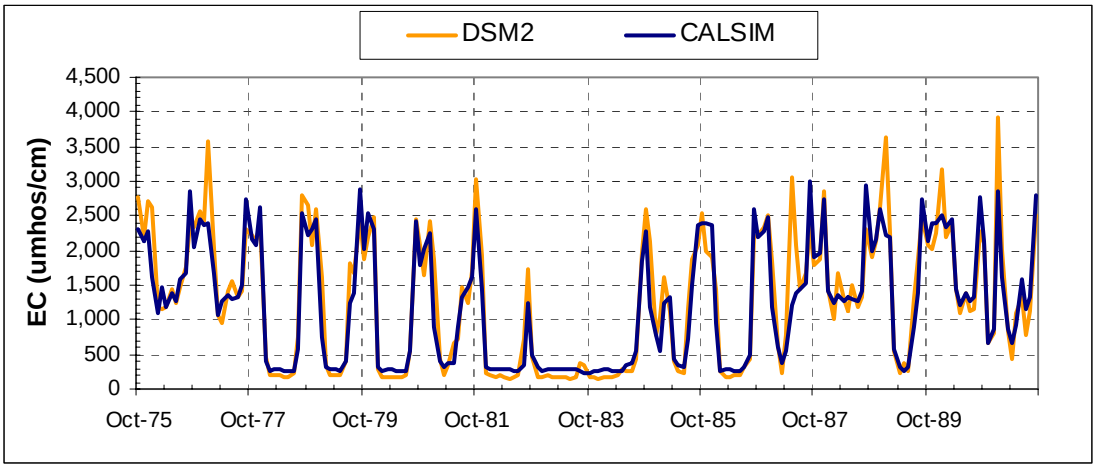

Figure 4.14: DSM2 versus CALSIM EC at Jersey Point for D-1485 using ANN.

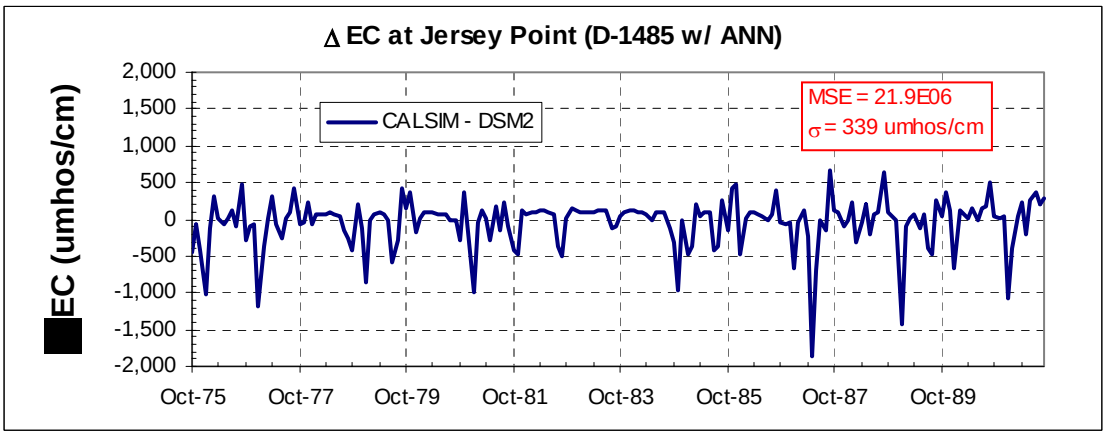

Figure 4.15: Difference in EC at Jersey Point for D-1485 using ANN.

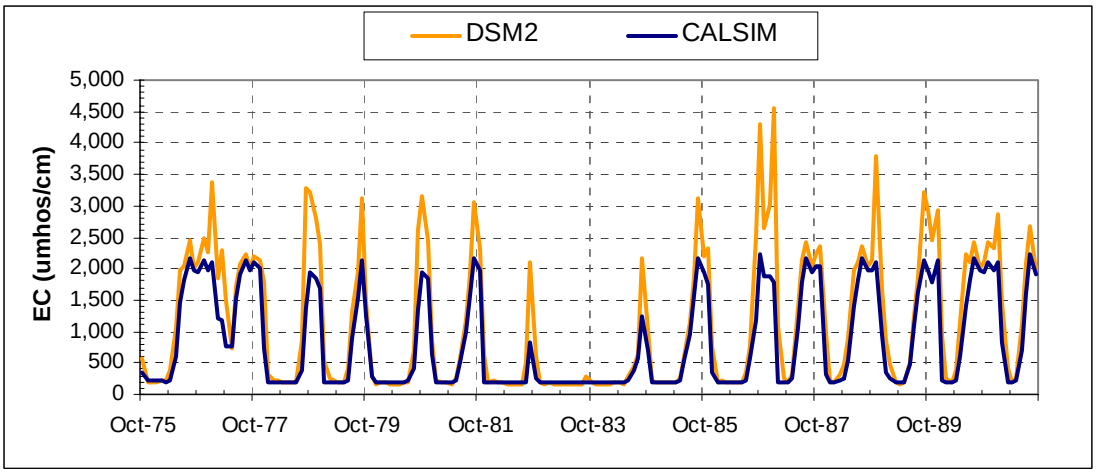

Figure 4.16: DSM2 versus CALSIM EC at Jersey Point for D-1485 using G-model.

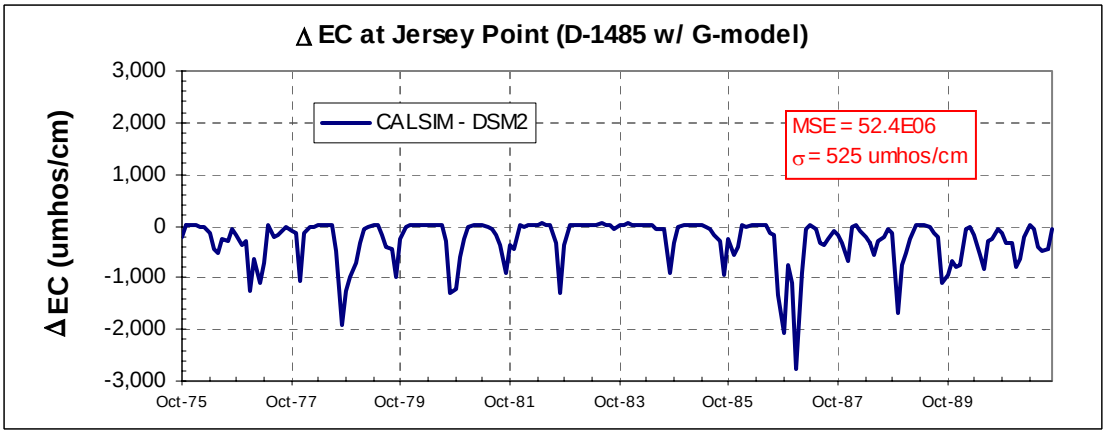

Figure 4.17: Difference in EC at Jersey Point for D-1485 using G-model.

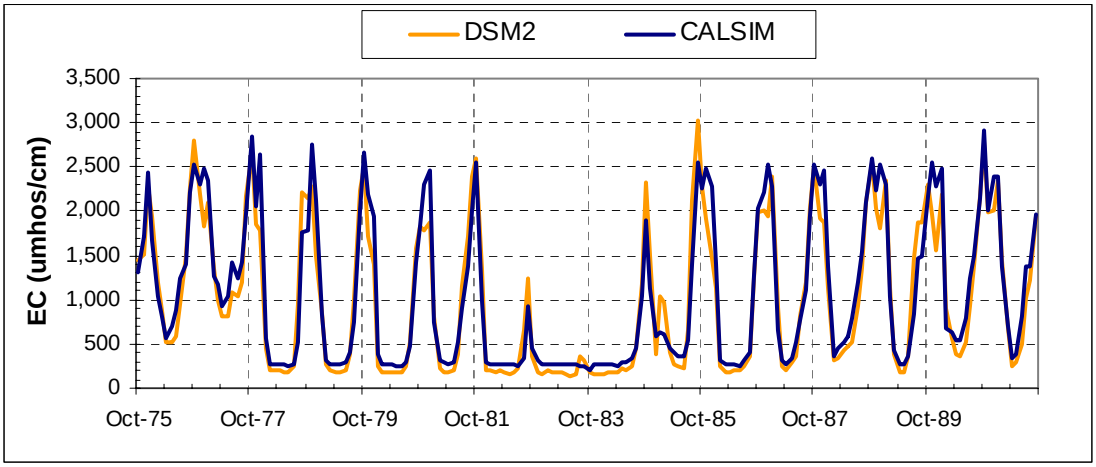

Figure 4.18: DSM2 versus CALSIM EC at Jersey Point for D-1641 using ANN.

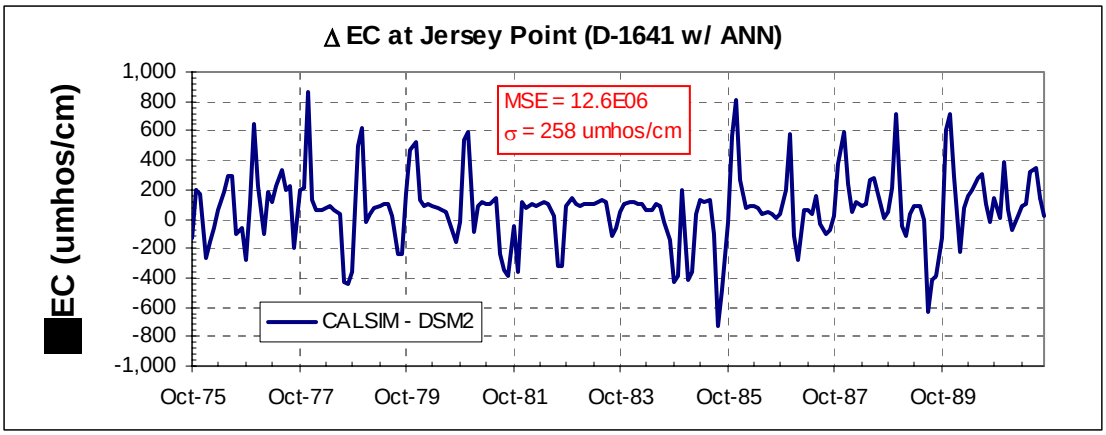

Figure 4.19: Difference in EC at Jersey Point for D-1641 using ANN.

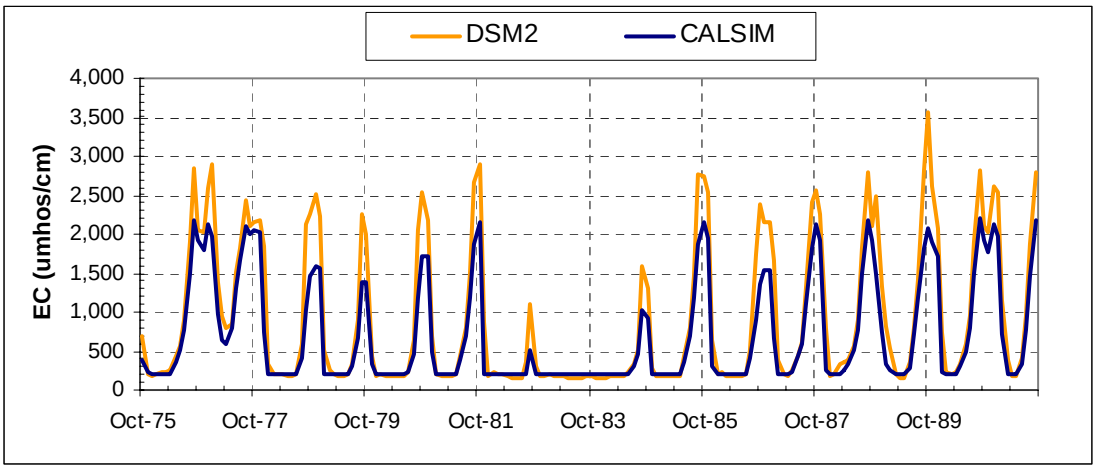

Figure 4.20: DSM2 versus CALSIM EC at Jersey Point for D-1641 using G-model.

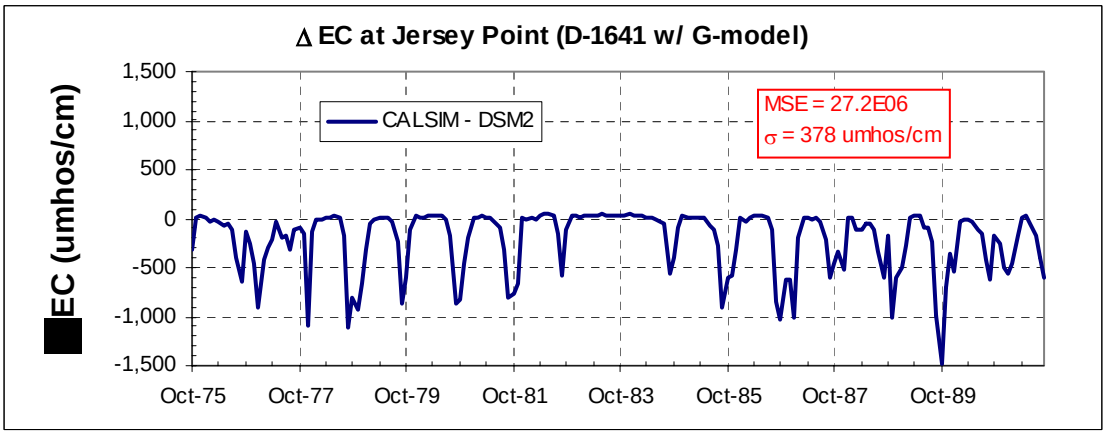

Figure 4.21: Difference in EC at Jersey Point for D-1641 using G-model.

Scatter plots illustrating the relationship between DSM2 EC and CALSIM EC at Jersey Point for each of the four studies are shown in Figures 4.22 – 4.25. An equivalent EC line is shown on each figure. Data will fall above the equivalent EC line when CALSIM is over predicting DSM2

EC. Similarly, data will fall below the equivalent EC line when CALSIM is under predicting DSM2 EC. Estimates representing two standard deviations above and below this equivalent EC line are also shown and can be used as a measure of scatter of the data about the equivalent EC line. Best-fit lines based on simple linear regressions of the EC data, along with the regression statistics, are also shown on each plot.

A summary of the regression statistics for all of the Jersey Point scatter plots is shown in Table 4.5. A complete discussion of how these regression statistics were calculated and what they represent is described in Section 4.4.1.

Table 4.5: Summary of Jersey Point Scatter Plots.

DSM2 Study	MSE	σ (umhos/cm)	Slope of best-fit line	R^2 of best-fit line
1485 w/ ANN	21.9E06	339	0.86	0.87
1485 w/ G-model	52.4E06	525	0.68	0.88
1641 w/ ANN	12.6E06	258	0.98	0.91
1641 w/ G-model	27.2E06	378	0.71	0.94

For both base studies (D-1485 and D-1641) at Jersey Point the slope of the best-fit lines for the ANN results more closely match the equivalent EC line. The scatter associated with D-1485 is about the same using both the ANN and G-model. The scatter associated with the G-model results about the best-fit lines is less (as seen by higher R^2 values) than the ANN scatter for the D-1641 study. However, as shown in Figures 4.23 and 4.25, while the G-model results generally represent a marginally tighter fit to the best-fit line, the G-model systematically underestimates EC for both studies. Furthermore, as discussed above, the MSE for the ANN is significantly lower in both studies than the MSE for the G-model results. Overall, the ANN resulted in a better fit of the equivalent EC line than the G-model.

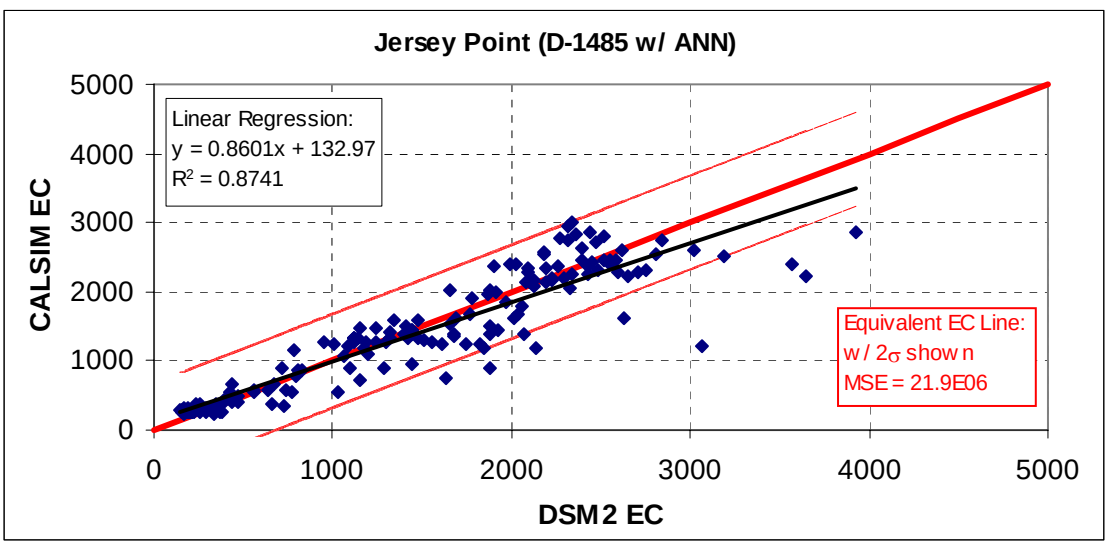

Figure 4.22: Scatter Plot of CALSIM II with ANN EC versus DSM2 EC for D-1485 at Jersey Point.

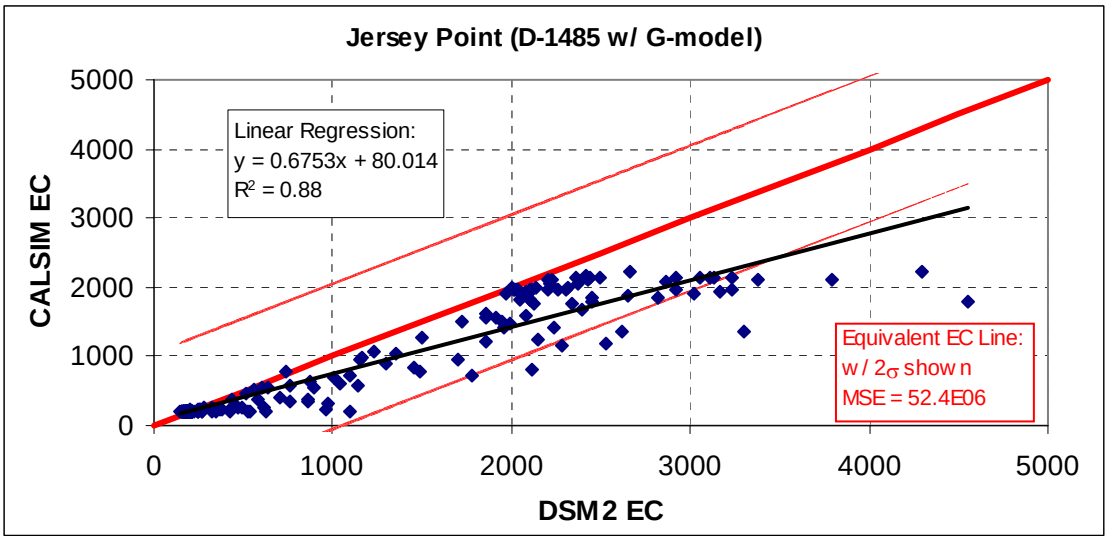

Figure 4.23: Scatter Plot of CALSIM with G-model EC versus DSM2 EC for D-1485 at Jersey Point.

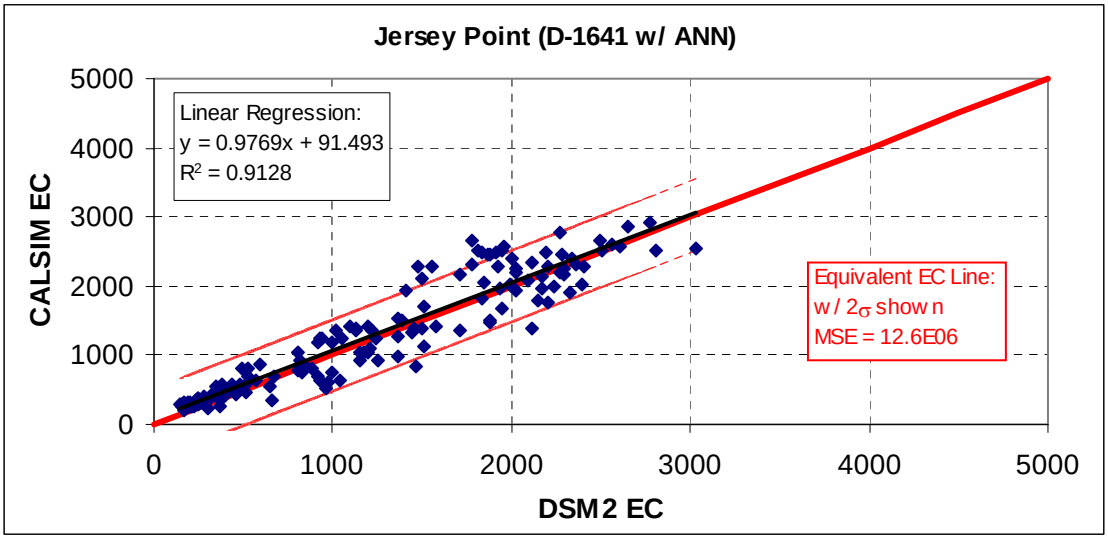

Figure 4.24: Scatter Plot of CALSIM with ANN EC versus DSM2 EC for D-1641 at Jersey Point.

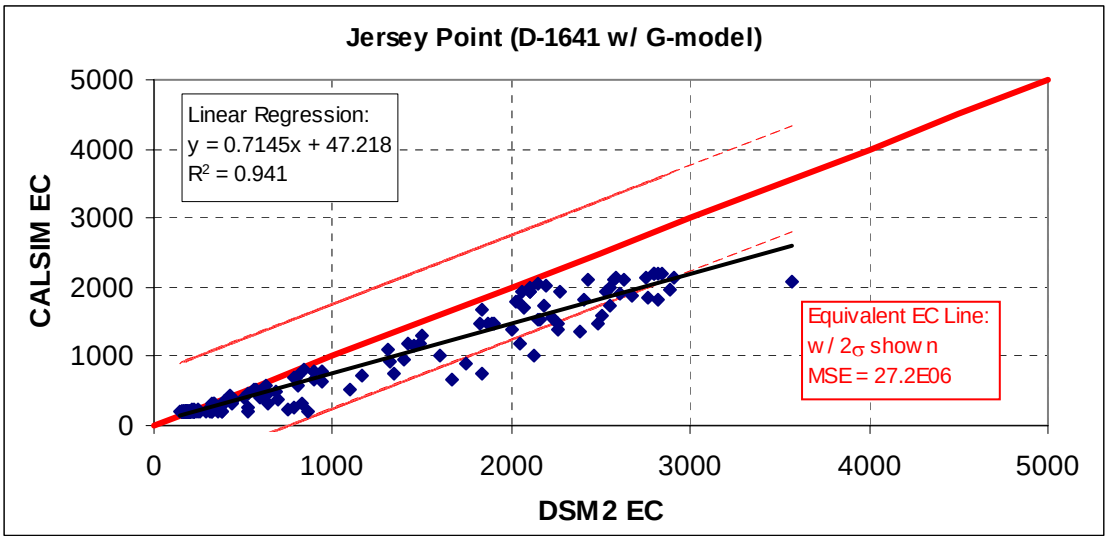

Figure 4.25: Scatter Plot of CALSIM with G-model EC versus DSM2 EC for D-1641 at Jersey Point.

4.4.3 Rock Slough

The time series of EC at Rock Slough calculated by both DSM2 and CALSIM II is shown for all four studies in Figures 4.26, 4.28, 4.30, and 4.32. Time series of the difference of the CALSIM salinity estimates from the modeled DSM2 EC are shown in Figures 4.27, 4.29, 4.31, and 4.33. A summary of all of time series plots is listed in Table 4.6.

Table 4.6: Rock Slough EC (rounded to the nearest 50 umhos/cm).

DSM2 Study	DSM2 Max EC (umhos/cm)	CALSIM Max EC (umhos/cm)	Max Absolute Diff. in EC* (umhos/cm)
1485 w/ ANN	1950	950	1100
1485 w/ G-model	2000	950	1150
1641 w/ ANN	1000	1000	400
1641 w/ G-model	1300	950	350

* This is the maximum absolute value of the difference in EC, and does not correspond with the timing of the maximum EC.

As shown in Table 4.6 for Rock Slough, both the ANN and G-model predicted maximum EC from CALSIM is about the same for both studies. As was discussed in Section 4.3.1, this is due to the fact that CALSIM uses the Rock Slough salinity standard as one of its salinity constraints while making water allocation decisions. However, as shown by the maximum EC in both D-1485 studies, CALSIM underestimated the DSM2 EC. The maximum absolute difference in EC between CALSIM and DSM2 was significantly lower in D-1641.

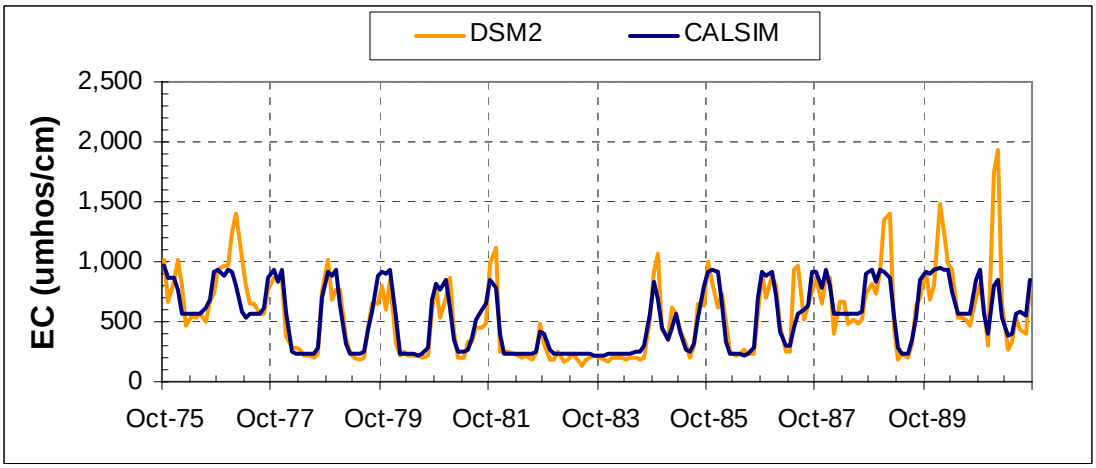

Figure 4.26: DSM2 versus CALSIM EC at Rock Slough for D-1485 using ANN.

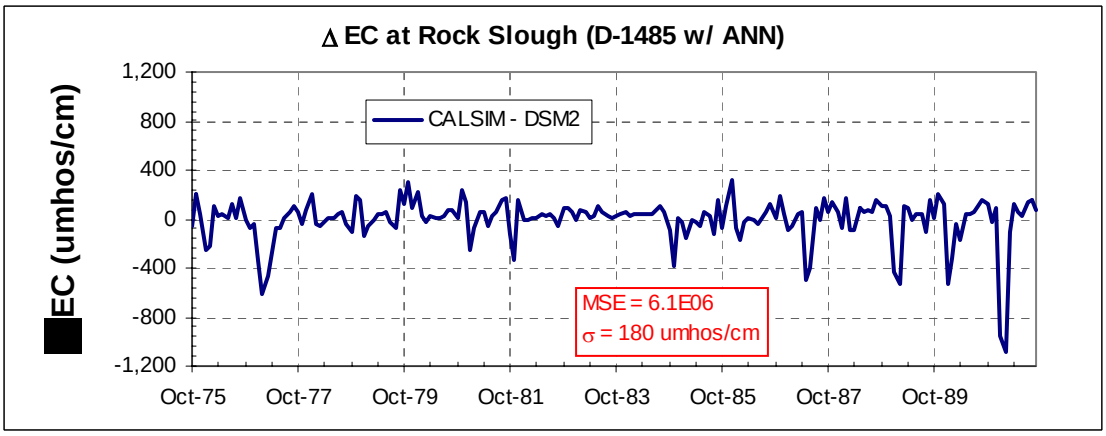

Figure 4.27: Difference in EC at Rock Slough for D-1485 using ANN.

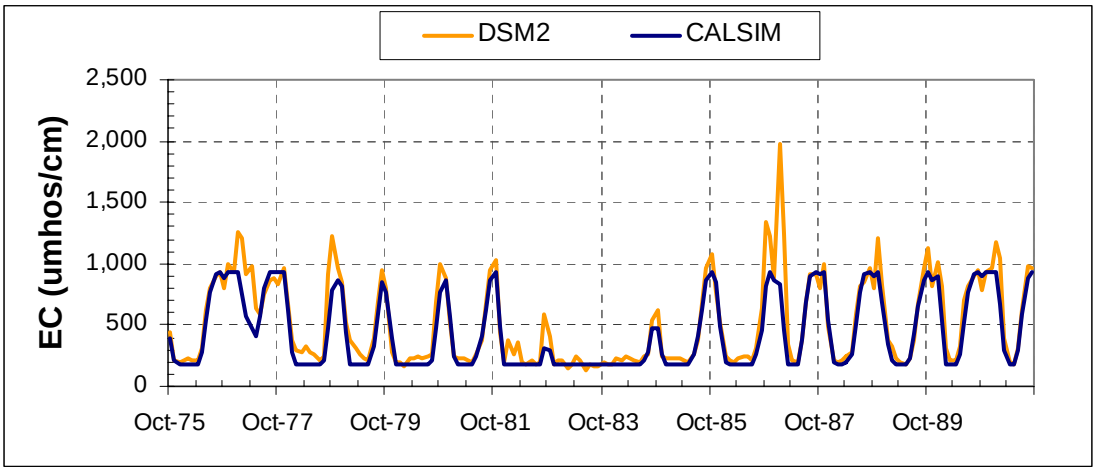

Figure 4.28: DSM2 versus CALSIM EC at Rock Slough for D-1485 using G-model.

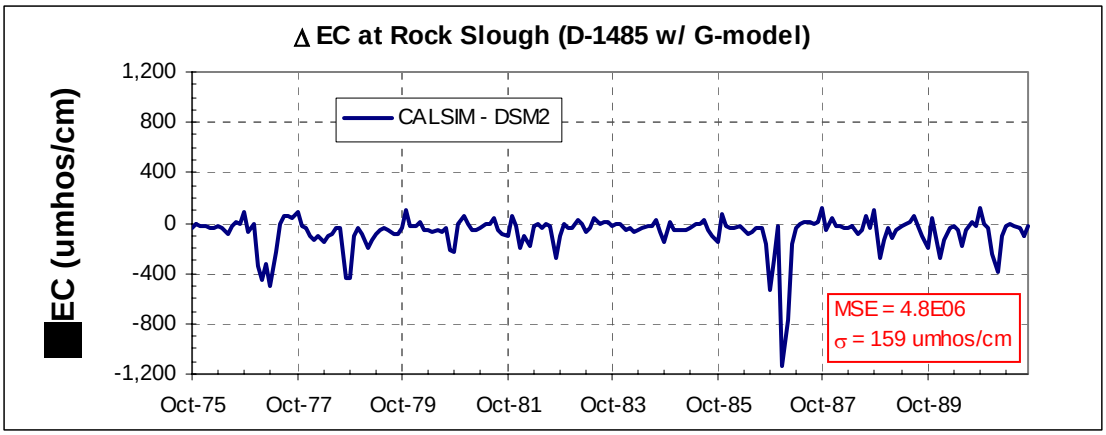

Figure 4.29: Difference in EC at Rock Slough for D-1485 using G-model.

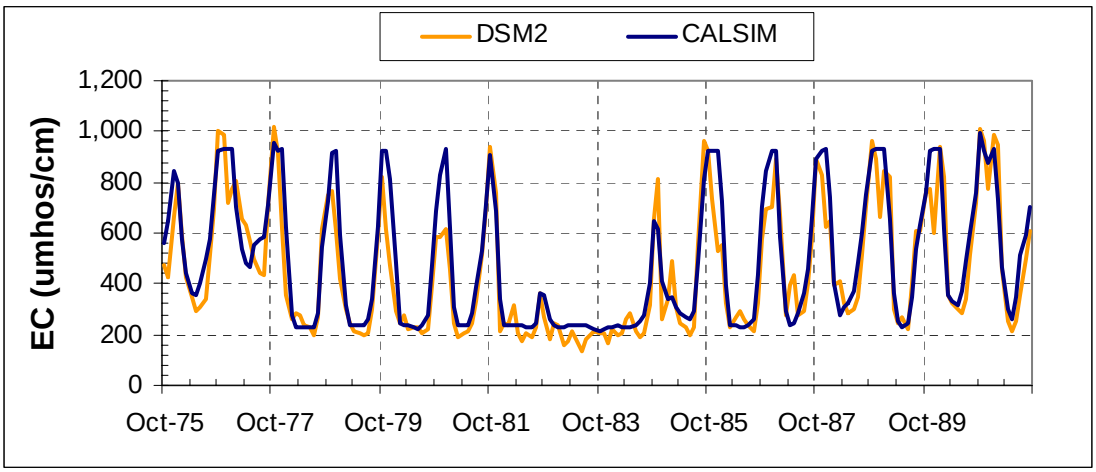

Figure 4.30: DSM2 versus CALSIM EC at Rock Slough for D1641 using ANN.

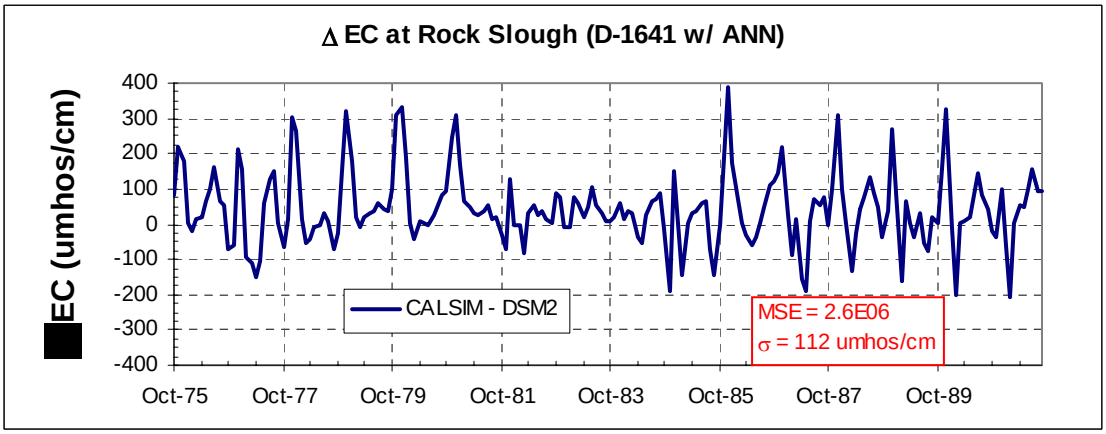

Figure 4.31: Difference in EC at Rock Slough for D-1641 using ANN.

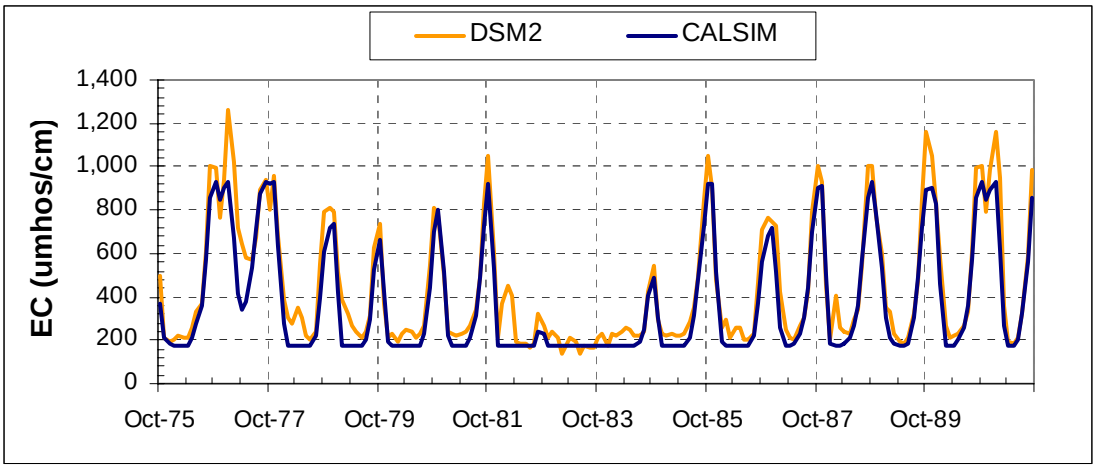

Figure 4.32: DSM2 versus CALSIM EC at Rock Slough for D-1641 using G-model.

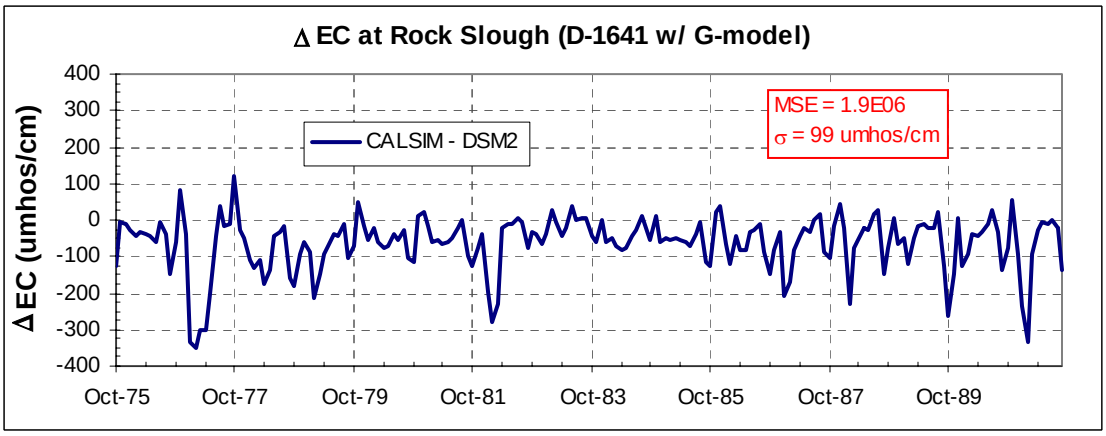

Figure 4.33: Difference in EC at Rock Slough for D-1641 using G-model.

Scatter plots illustrating the relationship between DSM2 EC and CALSIM EC at Rock Slough for each of the four studies are shown in Figures 4.34 – 4.37. An equivalent EC line is shown on each figure. Data will fall above the equivalent EC line when CALSIM is over predicting DSM2 EC. Similarly, data will fall below the equivalent EC line when CALSIM is under predicting DSM2 EC. Estimates representing two standard deviations above and below this equivalent EC line are also shown. Best-fit lines based on simple linear regressions of the EC data, along with the regression statistics, are also shown on each plot.

A summary of the regression statistics for all of the Rock Slough scatter plots is shown in Table 4.7. A complete discussion of how these regression statistics were calculated and what they represent is described in Section 4.4.1.

Table 4.7: Summary of Rock Slough Scatter Plots.

DSM2 Study	MSE	σ (umhos/cm)	Slope of best-fit line	R^2 of best-fit line
1485 w/ ANN	6.1E06	180	0.67	0.71
1485 w/ G-model	4.8E06	159	0.79	0.84
1641 w/ ANN	2.6E06	112	0.97	0.84
1641 w/ G-model	1.9E06	99	0.89	0.93

For both studies (D-1485 and D-1641) at Rock Slough the G-model resulted in a tighter fit of the MSE and estimated standard deviation of EC about the equivalent EC line. However, the MSE for the ANN for D-1641 was lower than the MSE for the G-model for D-1485. Overall, D-1641 had a much lower MSE and estimated standard deviation. The scatter associated with the G-model results about the best-fit lines also is less (as seen by higher R^2 values) than the ANN scatter for both studies. While the slope of the best-fit line for the G-model results is closer to the equivalent EC line for D-1485, the ANN results represent a better fit to the equivalent EC line for D-1641.

In the D-1485 study at Rock Slough both the G-model and ANN had some obvious outliers (see Figures 4.34 and 4.35). Removal of these outliers would shift the slope of the best-fit line closer to the equivalent EC lines as well as increase the R^2 value closer to 1.0.

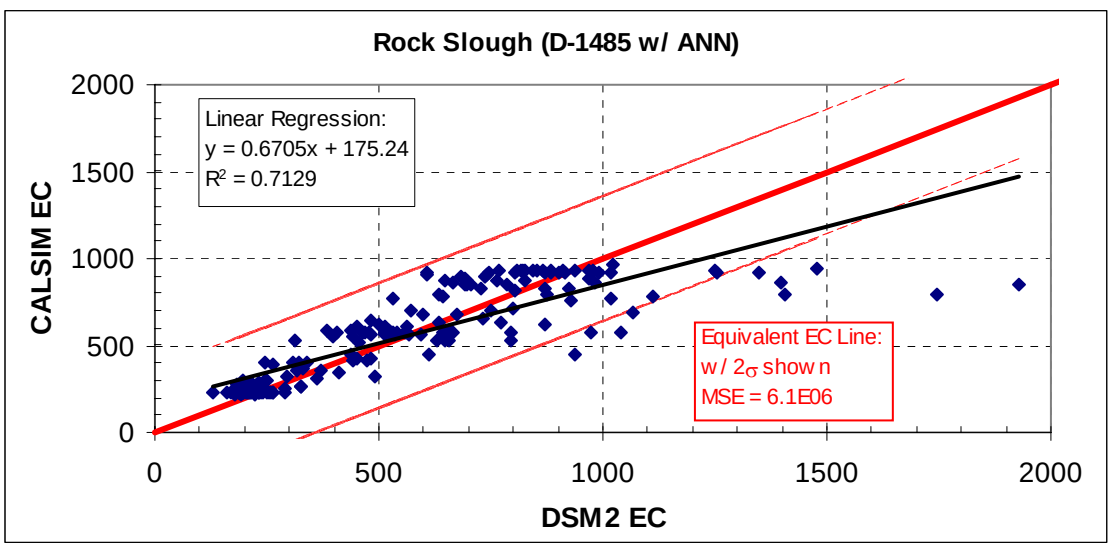

Figure 4.34: Scatter Plot of CALSIM with ANN EC versus DSM2 EC for D-1485 at Rock Slough.

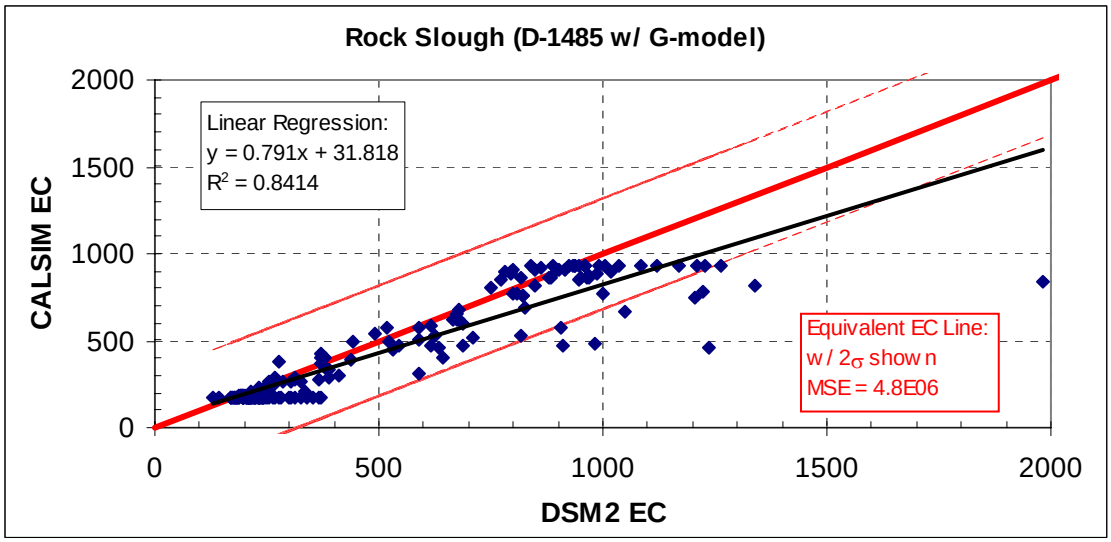

Figure 4.35: Scatter Plot of CALSIM with G-model EC versus DSM2 EC for D-1485 at Rock Slough.

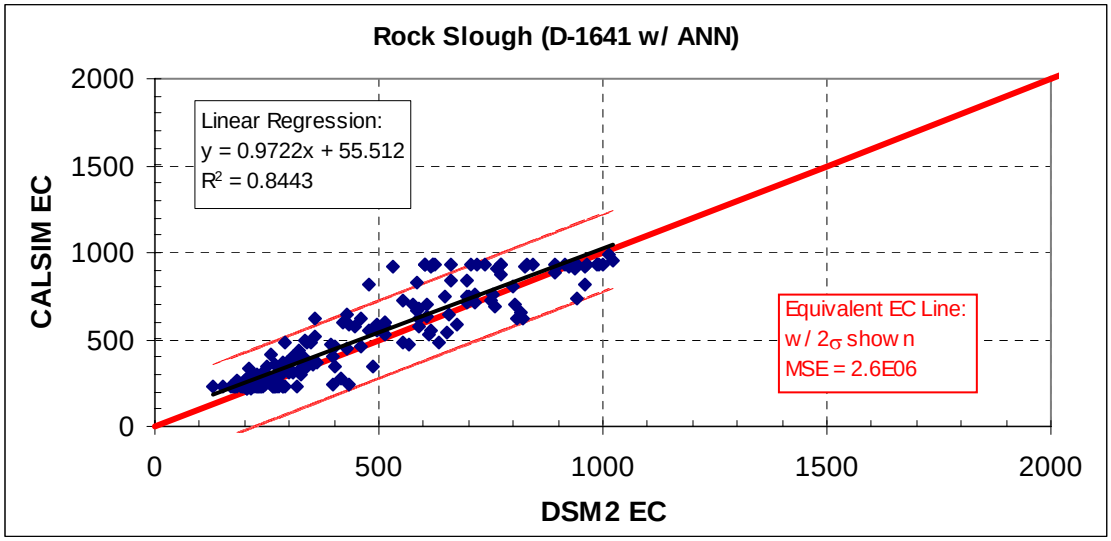

Figure 4.36: Scatter Plot of CALSIM with ANN EC versus DSM2 EC for D-1641 at Rock Slough.

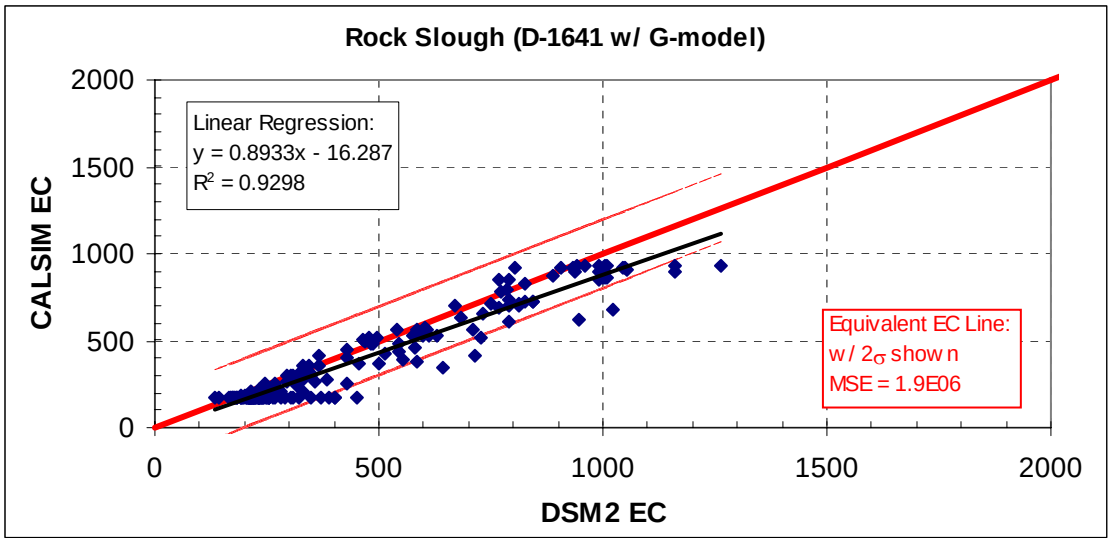

Figure 4.37: Scatter Plot of CALSIM with G-model EC versus DSM2 EC for D-1641 at Rock Slough.

4.5 Conclusions

The results presented in this study focused on comparing the statistical results of the EC estimated in CALSIM by the G-model with the results of the EC estimated in CALSIM by an ANN that has been trained using DSM2. The hydrology from each CALSIM study was then input into DSM2. The EC simulated by DSM2 was considered the theoretical EC, thus allowing the differences between the DSM2 EC to be taken from the CALSIM estimated EC for each simulation. The resulting statistics of these differences were then used to compare the impact of using the ANN versus the G-model to estimate EC within CALSIM.

A summary of the results for each location is presented below:

Emmaton

- The D-1485 CALSIM study using the ANN had the lowest MSE of the difference of EC, 11.2E06; the lowest estimated standard deviation, σ, 243 umhos/cm; best slope, 0.94; and tightest fit about the best-fit line, with a R^2 value of 0.95.

- For both water quality studies, D-1485 and D-1641, the ANN provided a better fit than the G-model to the equivalent EC line (point at which CALSIM and DSM2 are equal).

- The G-model results systematically underestimated the theoretical EC calculated by DSM2.

Jersey Point

- The D-1641 CALSIM study using the ANN had the lowest MSE of the difference of EC, 12.6E06; the lowest estimated standard deviation, σ, 258 umhos/cm; and best slope, 0.98.

- The D-1641 CALSIM study using the G-model had tightest fit about the best-fit line, with a R^2 value of 0.94.

- For both water quality studies, D-1485 and D-1641, the ANN provided a better fit than the G-model to the equivalent EC line (point at which CALSIM and DSM2 are equal).

- The G-model results systematically underestimated the theoretical EC calculated by DSM2.

Rock Slough

- The D-1641 CALSIM study using the G-model had the lowest MSE of the difference of EC, 1.9E06, the lowest estimated standard deviation, σ, 99 umhos/cm, and tightest fit about the best-fit line, with a R^2 value of 0.93.

- The D-1641 CALSIM study using the ANN had best slope fit about the best-fit line, 0.97.

- Though the G-model provided a tighter fit to its estimated best-fit lines than the ANN model did to its own best-fit lines for both studies, the presence of outliers in the D-1485 study make it difficult to critique the performance of either model for that study.

- The G-model results still underestimated the theoretical EC calculated by DSM2.

At all three locations the G-model systematically underestimated EC. With the exception of Rock Slough, the ANN results represented a tighter fit about the theoretical EC values, as measured by lower MSE values. At Rock Slough, the G-model did provide a better fit to the theoretical EC values; however, it is important to note that the differences of the estimated standard deviations between the G-model (99 umhos/cm for D-1641) and ANN (112 umhos/cm for D-1641) were small. It is interesting to note that although the ANN was trained on D-1485 operations, that generally D-1641 operations resulted in better estimations of EC for both the G-model and ANN.

4.6 References

Denton, R. and G. Sullivan. (1993.) *Antecedent Flow-Salinity Relationships: Applications to Delta Planning Models*. Contra Costa Water District.

Wilbur, R., and A. Munevar. (2001). "Chapter 7: Integration of CALSIM and Artificial Neural Network Models for Sacramento-San Joaquin Delta Flow-Salinity Relationships." *Methodology for Flow and Salinity Estimates in the Sacramento-San Joaquin Delta and Suisun Marsh. 22nd Annual Progress Report to the State Water Resources Control Board.* California Department of Water Resources. Sacramento, CA.

Methodology for Flow and Salinity Estimates in the Sacramento-San Joaquin Delta and Suisun Marsh

23rd Annual Progress Report
June 2002

Chapter 5:
Relationships between Delta Water Quality Constituents as Derived from Grab Samples

Author: Bob Suits

5 Relationships between Delta Water Quality Constituents as Derived from Grab Samples

5.1 Introduction

Delta grab samples are being analyzed to establish relationships between various water quality constituents. Wherever justified, relationships are developed for discrete regions rather than for individual locations. The purpose of this study is to replace published Delta relationships between total dissolved solids (TDS), chloride, and electrical conductivity (EC); provide insight into some characteristics of the mixing of Delta water; and to provide another basis for validating DSM2-QUAL. This chapter presents a brief background and methodology for this ongoing project.

5.2 General Methodology

Relationships between Delta water quality constituents are routinely developed to support Delta modeling activities. One recent example was developing relationships between EC and chloride at export locations in order to check model results that were in EC against water quality standards in chloride. Often the only source of data available to do such analysis is historic grab samples. Grab samples, collected by various programs, will usually be analyzed for multiple constituents, most commonly EC, TDS, and chloride. However, many other constituents may also be evaluated, depending upon the purpose of the monitoring. The last time DWR conducted a Delta-wide evaluation of multiple relationships derived from grab sample data was presented in a 1986 Department memo (Guivetchi, 1986). This analysis was a compilation of regressions generated between EC and chloride, EC and TDS, and chloride and TDS. Thirty-four locations in the Bay-Delta system were independently examined and relationships were broken down by water year type (dry years, normal years, wet years, and all years), with water year classification being defined according to State Water Resources Quality Control Board Decision 1485 (D-1485).

The current project differs from the previous study in several ways. First, the scope of the analysis is substantially larger. Previously, only samples collected by U.S. Bureau of Reclamation and DWR from 1968 through 1981 as part of the D-1485 monitoring program were used, and only TDS, chloride, and EC were evaluated. The current project expands the data used to include grab samples collected by DWR's Operations and Maintenance (O&M) and Municipal Water Quality Investigations (MWQI), and draws upon data through 1999. Data from the now-defunct Water Information Monitoring System (WIMS) are also considered. WIMS data come from a variety of mostly undocumented sources and date back to 1955. The use of WIMS data in this project is relatively limited and more recent data from the other three sources are given precedence.

The current project also expands the number of constituents evaluated. In addition to finding relationships among EC, chloride, and TDS, the project will also add calcium, sulfate, potassium,

magnesium, sodium, and bromide to the list of constituents to be evaluated. Table 5.1 summarizes the amount of data available for the analysis. The data are stored in ACCESS and flagged for redundancy and obvious error. Delta inflow and export values from DAYFLOW, also stored in the database, allow ACCESS queries to return pairs of constituent values and daily average Delta inflows and exports.

Table 5.1: Summary of Data Count for Analysis.

Constituent	D-1485	MWQI	WIMS	O & M	TOTAL
Calcium	0	1521	3047	606	5174
EC	10948	1920	7598	903	21369
CL	8362	1919	8760	895	19936
TDS	6702	998	4676	837	13213
Na	0	1910	5921	875	8706
SO4	0	0	2136	828	2964
Br	0	1430	1	153	1584
K	0	1194	2824	159	4177
Mg	0	1521	3385	607	5513
ALK	0	995	6325	247	7567
TOTAL	26584	13408	44673	6110	90775

The present study's focus is different from the 1986 effort. Previously, relationships between EC, TDS, and chloride were presented for 34 locations and were broken down by water year classification. This approach had two shortcomings. First, the 1986 analysis' breakdown of regression by water year type is misleading. Since the relationship between constituents may be different for different sources of water and different flow patterns result in different mixing, it is reasonable to attempt to associate relationships between water quality constituents at any location in the Delta with Delta flow conditions. However, using the water year type as a surrogate for Delta flow conditions is over-simplistic. Second, the 1986 analysis fails to generalize Delta mixing characteristics by region.

In comparison, the current study does not differentiate relationships by water year type, rather it attempts to identify regions within the Delta that may be described by a single relationship between any two constituents. Trends in patterns of mixing of source water might hopefully then be inferred. Also, regional relationships should provide an additional source for validation of DSM2-QUAL. The extent that QUAL produces patterns of relationships between modeled constituents that are consistent with those derived from observed historic grab samples should indicate how well QUAL simulates the gross mixing of Delta water. Finally, because the focus of this study is analysis to support evaluating DSM2, only regions within DSM2's boundaries are being considered.

5.3 Methodology

Grab data compiled from the sources mentioned above have been screened to include only surface water samples (depth of 4 feet or less). At any one site, most data was sampled monthly. When more frequent sampling occurred, the data was screened to maintain a minimum of 10

days between samples. In areas of the Delta where flows and subsequent mixing of water may be affected by SWP exports, only data after 1971 was used, effectively eliminating the use of WIMS data from Old River. The purpose of this study is to identify mixing patterns of water under conditions that DSM2 will simulate for validation purposes. Thus, evaluating pre-SWP conditions for this study is beyond the scope of the project. A separate analysis is underway examining if the relationships between water quality constituents, and thus perhaps mixing patterns, have changed since SWP operations in the Delta began. For any pair of constituents, a separate regression is found for regions as close as possible to a DSM2 boundary: in the west Delta starting at Carquinez Strait at Martinez and moving west, in the San Joaquin River starting at Vernalis and moving downstream, and in the Sacramento River starting at Sacramento and moving downstream. At each boundary location, data from adjacent sites are incrementally added as long as the data are judged to display the same relationship. A single regression is eventually developed for each grouping of sample sites.

Other sites within the Delta are grouped according to the consistent relationships between the pair of constituents and then compared for reference to the regressions for the boundary groups. For any pair of constituents, the San Joaquin River group and the Sacramento River group usually display similar but different relationships, while the west Delta group may also be similar or radically different, depending upon the particular constituents. The relationship between the constituents at interior Delta locations can typically be described in approximately 12 discrete regions.

5.4 A Sample Analysis

As an example of the procedure described above, a preliminary analysis with chloride and calcium is presented. This particular analysis is illustrative in that chloride and calcium sampling can effectively reveal mixing trends in the Delta; certain regions in the Delta display a predictable mixing while others reveal a complexity that will require DSM2 modeling to understand. Fresh waters such as Delta inflows from rivers and streams tend to have a relatively high portion of TDS from calcium and less from chloride, thus the ratio of calcium to chloride is typically high (2 to 3 in the Sacramento and San Joaquin rivers). For ocean water, on the other hand, much more of TDS comes from chloride and the calcium to chloride ratio is low, typically around 0.02. Therefore, Delta water samples will reveal ratios of calcium to chloride ranging between 0.02 to 3, depending upon the mixing of the sources of the constituents.

Figure 5.1 shows where the data is available for these constituents. Also shown is how the west Delta, Sacramento River, and San Joaquin River groups are formed, as well as the interior regions. Table 5.2 describes the data available for the analysis. Figure 5.2 shows the relationships between chloride and calcium for the San Joaquin River and west Delta regions and Figure 5.3 shows the relationships in the Contra Costa Canal and Franks Tract regions. Table 5.3 presents the regressions shown in these figures.

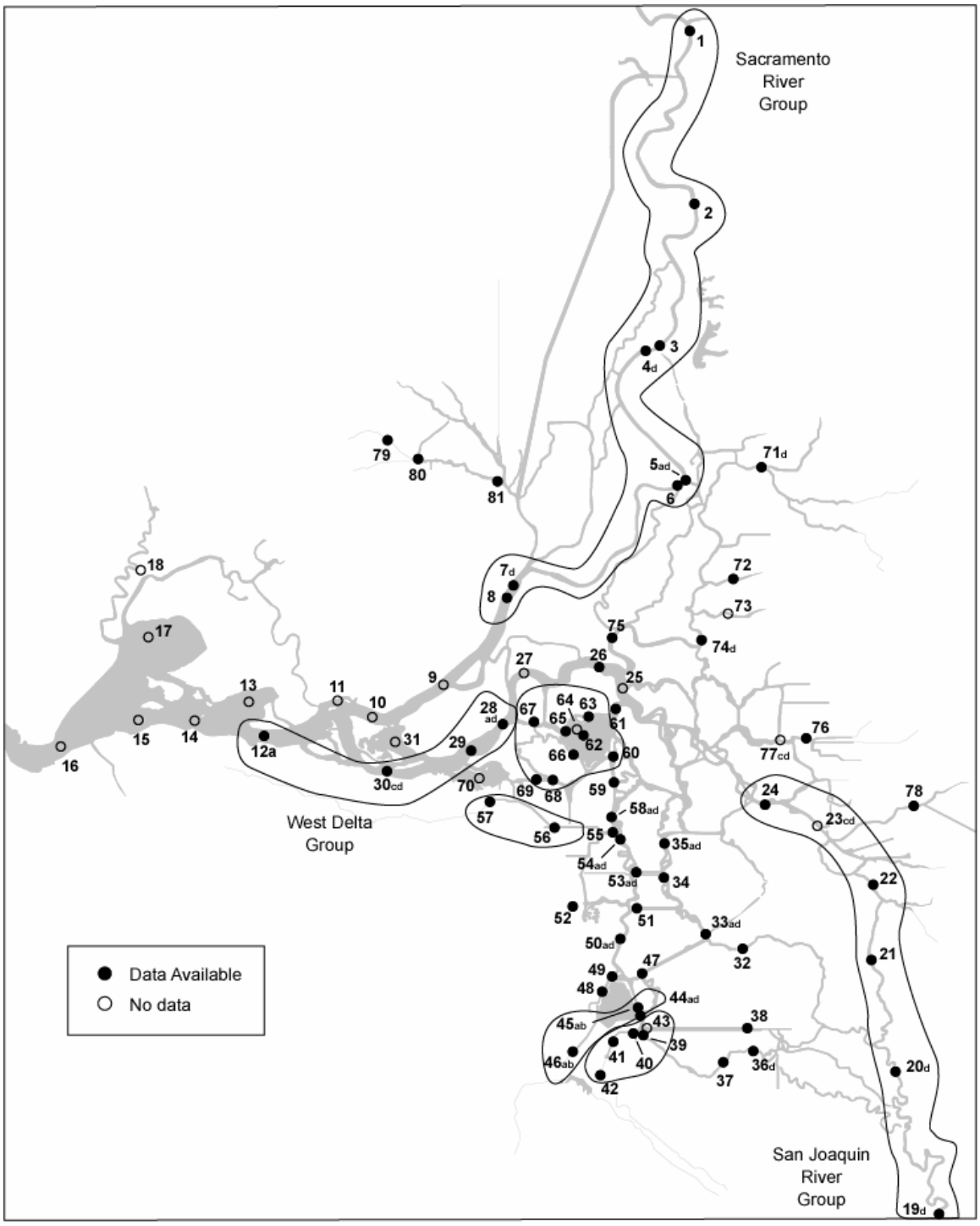

Figure 5.1: Locations of Available Data and Sample Groupings for Chloride and Calcium Analysis.

Table 5.2: Summary of Data Available for Analysis of Chloride and Calcium Relationships.

Site	Description	Source	# samples	Chloride (mg/L) Min	Max	Avg	Calcium (mg/L) Min	Max	Avg
1	Sacramento River at Sacramento	WIMS	38	1	13	5	5	17	11
2	Sacramento River at Freeport	WIMS	65	2	15	6	7	18	12
3	Sacramento River at Snodgrass Slough	WIMS	103	1	23	9	4	25	13
4 d	Sacramento River at Greens Landing	WIMS	156	2	14	6	6	16	11
5 a	Delta Cross Channel at west end	MWQI	21	1	12	7	8	16	12
5 d	Delta Cross Channel at west end	WIMS	41	1	17	8	6	18	12
6	Sacramento River at Walnut Grove	WIMS	46	3	16	8	7	17	12
7 d	Sacramento River at Rio Vista	WIMS	15	4	13	9	10	18	14
8	Sacramento River at Rio Vista	WIMS	6	[illegible]	15	8	9	88	16
12 a	Sacramento River at Chipps Island	MWQI	143	7	6060	2182	8	138	58
19 d	San Joaquin River near Vernalis	WIMS	186	6	312	115	7	75	35
20 d	San Joaquin River at Mossdale	WIMS	162	6	307	129	8	82	39
21	San Joaquin River at Brandt Bridge	WIMS	104	14	195	79	8	50	28
22	San Joaquin River at Highway 4	WIMS	40	11	182	92	8	54	30
24	San Joaquin River at Rindge Tract	WIMS	40	14	152	68	10	50	24
26	San Joaquin River nr San Andreas Lndg	WIMS	92	2.8	133	20	6	24	15
28 a	San Joaquin River at Jersey Point	MWQI	54	13	746	304	12	30	20
28 d	San Joaquin River at Jersey Point	WIMS	11	11	178	46	10	19	15
29	San Joaquin River at Blind Point	WIMS	7	15	637	162	11	30	16
30 d	San Joaquin River at Antioch	WIMS	53	12	1620	247	9	56	20
32	Middle River at Tracy Road Bridge	WIMS	7	31	144	92	14	39	26
33 a	Middle River at Victoria Canal	MWQI	93	12	139	57	10	30	18
33 d	Middle River at Victoria Canal	WIMS	17	15	110	47	10	30	19
34	Middle River at Mokelumne Aqueduct	WIMS	103	12	92	36	8	30	16
35 a	Middle River at Bacon Island	MWQI	80	11	133	64	10	28	19
35 d	Middle River at Bacon Island	WIMS	10	26	135	74	15	21	18
36 d	Old River at Tracy Road Bridge	WIMS	105	14	228	96	9	81	34
37	Old River near Tracy	WIMS	41	17	258	126	1	67	38
38	Grant Line Canal at Tracy Road Bridge	WIMS	35	12	232	146	10	62	41
39	Old River upstream of temporary barrier	MWQI	50	38	177	109	14	54	26
40	Delta-Mendota Canal Intake	MWQI	113	16	179	87	9	52	24
41	Delta-Mendota Canal at Byron Road	WIMS	163	17	256	90	8	62	27
42	Delta-Mendota Canal near Tracy	WIMS	67	18	224	81	6	65	25
43	Grant Line Canal near Old River	MWQI	48	36	180	111	14	63	29
44 a	Old River near Clifton Court Intake	MWQI	46	37	181	106	14	47	23
44 d	Old River at Clifton Court Ferry	WIMS	40	14	188	71	10	52	23
45 a	Clifton Court Forebay Intake	MWQI	51	13	185	89	11	38	20
45 a	West Canal at Clifton Court Forebay	MWQI	56	5	177	100	11	42	20

Preliminary

Table 5.2 (continued)

Site	Description	Source	# samples	Chloride (mg/L) Min	Max	Avg	Calcium (mg/L) Min	Max	Avg
45 b	Clifton Court Forebay Entrance	O&M	158	11	176	57	8	39	18
46 a	Banks Pumping Plant	MWQI	116	15	185	86	9	30	19
46 b	Banks Pumping Plant	O&M	374	12	305	66	2	45	18
47	North Canal near Old River	MWQI	51	3	155	78	13	26	19
48	Italian Slough	WIMS	64	15	328	82	8	49	22
49	Italian Slough	WIMS	23	16	175	71	10	51	25
50 a	Old River at Highway 4	MWQI	85	6	211	90	10	28	17
50 d	Old River at Highway 4	WIMS	26	22	293	100	11	49	23
51	North Victoria Canal near Old River	MWQI	50	3	213	98	13	25	18
52	Indian Slough near Brentwood	WIMS	41	22	390	99	11	102	33
53 a	Old River at SantaFe Railroad	MWQI	51	27	220	103	13	24	18
53 d	Old River at SantaFe Railroad	WIMS	40	14	164	59	9	53	20
54 a	Old River upstream of Rock Slough	MWQI	26	8	192	43	9	22	14
54 d	Old River near Rock Slough	WIMS	136	10	244	49	8	39	15
55	Rock Slough near Old River	MWQI	68	12	257	126	10	29	17
56	Rock Slough at CCC intake	WIMS	40	13	193	63	9	53	21
57	Contra Costa Canal Pumping Plant #1	MWQI	69	11	233	97	8	39	18
58 a	Old River downstream of Rock Slough	MWQI	57	10	257	133	10	23	17
58 d	Old River downstream of Rock Slough	WIMS	18	29	451	158	15	28	20
59	Old River at Holland Tract	WIMS	5	19	134	59	9	26	17
60	Sandmound Slough at Old River	MWQI	57	10	245	132	10	23	17
61	Old River at Mandeville Island	WIMS	39	10	181	44	10	38	18
62	Franks Tract at Russo Landing	WIMS	8	13	206	52	11	19	15
63	False River at Webb Pump	WIMS	4	12	59	36	7	18	14
65	False River at southmost tip of Webb Tract	MWQI	48	12	540	200	12	26	18
66	Piper Slough at Bethel Tract	WIMS	79	11	420	75	7	25	14
67	False River below Piper Slough	WIMS	9	46	543	215	15	30	20
68	Dutch Slough at Bethel Island Bridge	WIMS	6	30	273	89	10	23	18
69	Dutch Slough at Jersey Island Bridge	WIMS	9	38	712	275	14	36	24
71 d	Mokelumne River near Thorton	WIMS	10	0.2	7	3	3	13	7
72	Hog Slough	WIMS	13	24	212	89	14	60	32
74 d	Little Potato Slough at Terminous	WIMS	47	8	42	19	5.2	20	14
75	Mokelumne River at Highway 12	WIMS	8	9	15	11	10	16	14
76	Disappointment Slough near Lodi	WIMS	13	5	69	23	11	33	19
78	Calaveras River at Stockton	WIMS	29	3	46	8	8.3	40	20
79	North Bay Aqueduct	O&M	45	8	67	28	8	28	18
80	Lindsay Slough at Hastings Cut	WIMS	46	6	79	38	4	26	19
81	Lindsey Slough near Rio Vista	WIMS	75	6	35	15	3	25	15

Preliminary

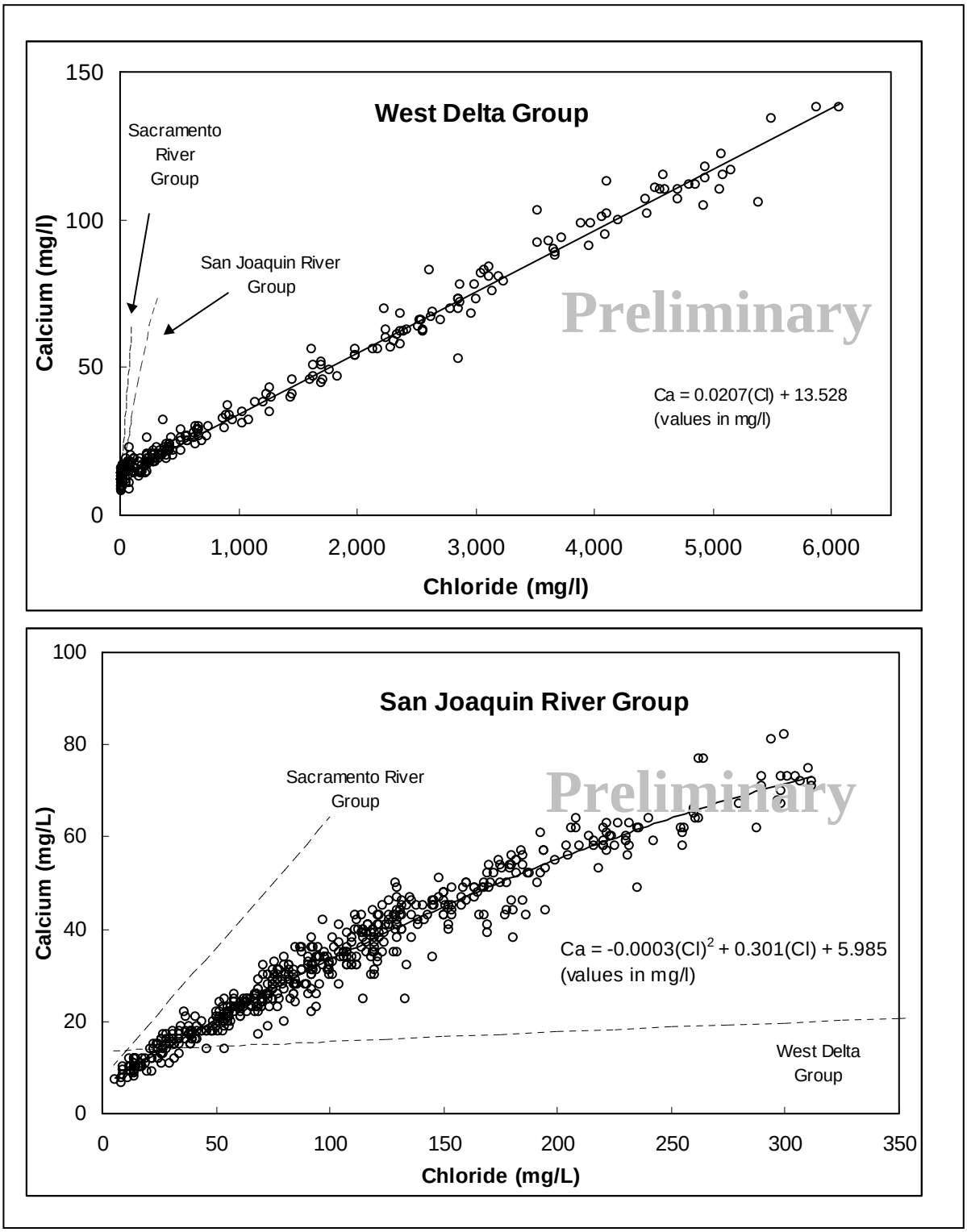

Figure 5.2: Relationship Between Chloride and Calcium for West Delta and San Joaquin River Regions.

Table 5.3: Preliminary Regressions for Calcium and Chloride Analysis.

Location	Total # Samples	Cl (mg/L) Min	Cl (mg/L) Max	Ca (mg/L) Min	Ca (mg/L) Max	X^2 Coeff	X Coeff	Intercept	R^2	SE (mg/L)
Sacramento River Group Sacramento to Rio Vista (1,2,3,4d,5a,5d,6,7d,8)	511	1	23	4	88	none	0.565	7.71	0.48	1.86
West Delta Group Jersey Point to Chipps Island (12a,12c,28a,28c,28d,29,30c,30d)	268	7	6060	8	138	none	0.0207	13.53	0.99	3.77
San Joaquin River Group Vernalis to Rindge Tract (19c,19d,20c,20d,21,22,24)	531	6	505	7	105	-0.00027	0.301	5.99	0.95	3.43

As Figure 5.3 shows, the relationship between chloride and calcium in these regions follows that of the San Joaquin River group up to 50 to 100 mg/l chloride, and then follows the west Delta regression at higher chloride concentrations. It is likely that during low chloride concentrations, when the Delta outflow is high, the main source of water in the Contra Costa Canal and Franks Tract regions are the Sacramento and San Joaquin rivers. Relationships between constituents during high Delta outflow simply reflect the source of water. As the concentration of chloride increases, Delta outflow decreases and the source of water increasingly is the west Delta.

Figure 5.4 shows the relationships at the DMC and SWP intakes. The complex relationship between chloride and calcium in the DMC group implies substantial mixing of water; however, the data is roughly bounded between the San Joaquin River group and the west Delta group regressions. The relationship between the two constituents in the SWP intake group at times follows the west Delta group and at other times is consistent with the San Joaquin River group. The trends for these two groups demonstrate that further work is needed to explain the mixing of water at the DMC and SWP intakes.

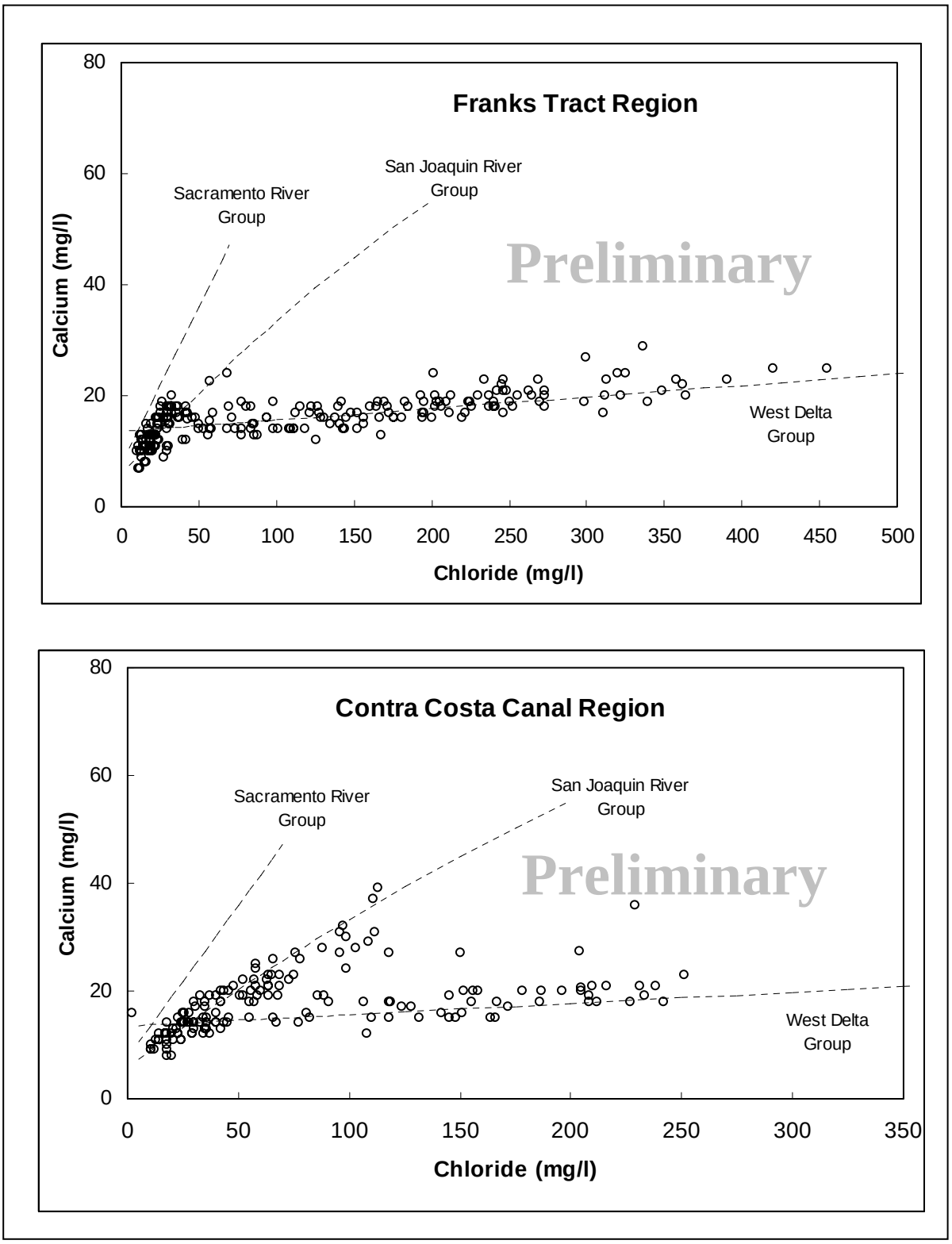

Figure 5.3: Relationship Between Chloride and Calcium for Franks Tract and Contra Costa Canal Regions.

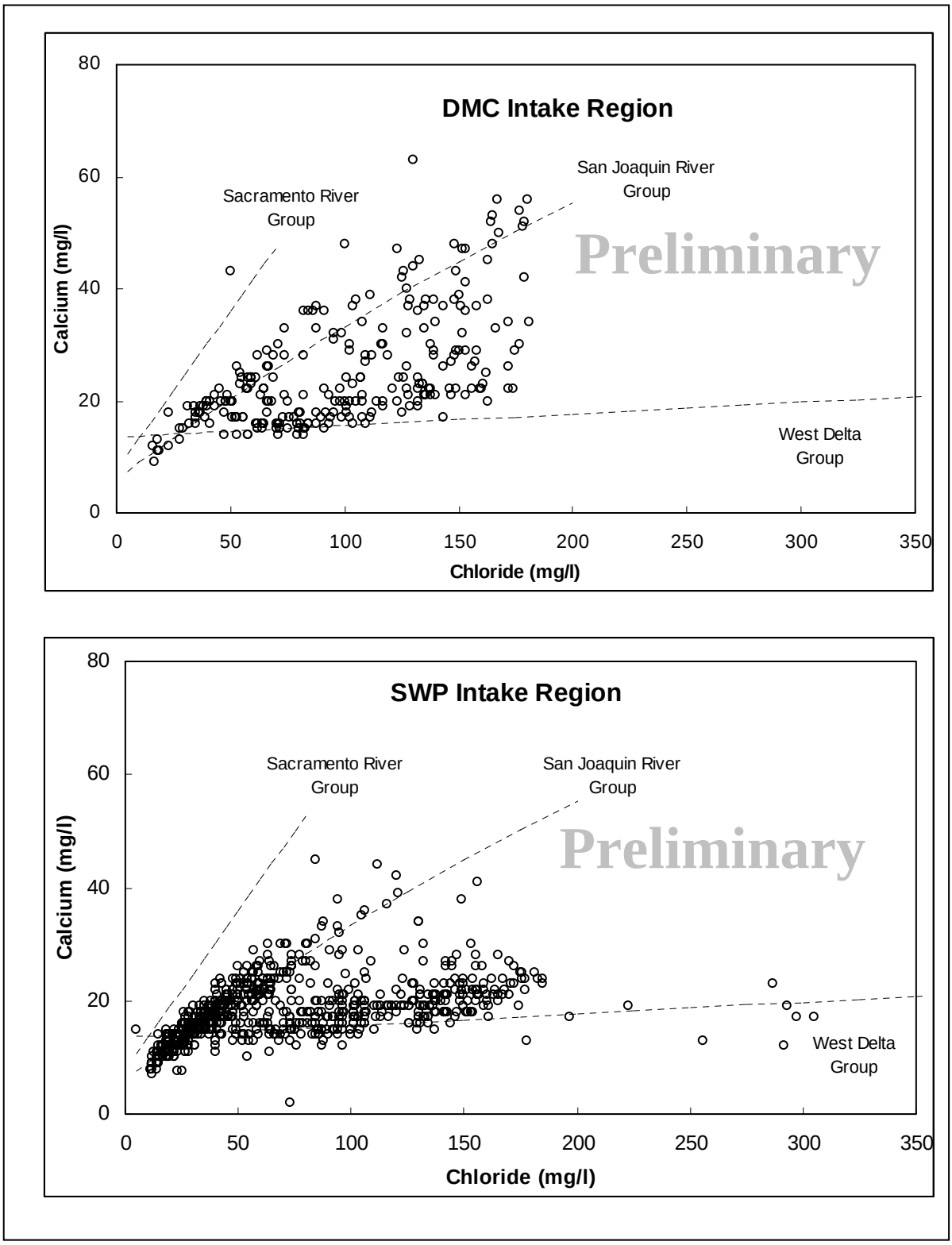

Figure 5.4: Relationship Between Chloride and Calcium for DMC and SWP Intake Regions.

5.5 Future Directions

At the time of this writing, much of the analysis has been done and is being summarized. For regions on the periphery of the Delta where water mixing is less complex, this analysis will be directly applicable to QUAL validation. At interior Delta locations, complex mixing of west Delta, Sacrament River, and San Joaquin River sources occurs and the current analysis does not explain or predict this. What is possible to predict for such regions is bounding the expected relationship between any two constituents as modeled by QUAL. Future analysis with grab sample data and concurrent Delta flow patterns may give insight on predicting how relationships between two constituents may change based upon hydrologic conditions. Sufficient data should already exist to both develop and test some simple predictive models.

5.6 Reference

Guivetchi, K. (1986). *Salinity Unit Conversion Equations*. Memorandum. California Department of Water Resources. Sacramento, CA.

Methodology for Flow and Salinity Estimates in the Sacramento-San Joaquin Delta and Suisun Marsh

23rd Annual Progress Report
June 2002

Chapter 6:
Calibrating DSM2-QUAL Dispersion Factors to Practical Salinity

Author: Bob Suits

6 Calibrating DSM2-QUAL Dispersion Factors to Practical Salinity

6.1 Introduction

DSM2-QUAL's current set of dispersion factors that are used in simulating the transport of salinity in the Delta were calibrated to measured electrical conductivity (EC). Concerns have been raised about using EC for this purpose due to its failure to behave as a truly conservative indicator of salinity. This chapter briefly discusses this problem and presents practical salinity, as derived from EC, as an alternative water quality parameter for calibrating dispersion factors.

6.2 Background

In past development of Delta water quality simulation models, DWR has used both total dissolved solids (TDS) and EC to calibrate and validate models for the transport of conservative mass. Both approaches have advantages and disadvantages and are briefly summarized below.

6.2.1 Calibrating QUAL to EC

The IEP DSM2 Project Work Team established the set of dispersion factors currently used by DSM2-QUAL (QUAL) in 2000 as part of the most recent calibration and validation of DSM2 (Nader-Tehrani, 2001). EC was chosen for calibrating the dispersion factors for conservative mass transport primarily because of its availability at DSM2 boundaries and at important interior Delta locations. EC is recorded every 15 minutes or hourly at multiple sites within the Delta and data extend back to the 1980s or earlier, depending upon the site. Other potential constituents for calibration, such as chloride and TDS, are far less available in the Delta and would have to be inferred from relationships to EC.

An important drawback to using EC to calibrate dispersion factors is its acknowledged failure to behave as a truly conservative constituent of salinity. As salinity and ionic concentration increases, electrical conductance increases. For high concentrations, however, the proximity of ions to each other depresses their activity and consequently their ability to transmit electrical current. As a result, EC increasingly underestimates true salinity at higher concentrations, a trend manifest in a nonlinear relationship between EC and any conservative constituent. This behavior is described by Hem (1985) as typical for all salts. As an example, Hem presents the case of KCl at a concentration of 7,460 mg/L which displays a conductance of 12,880 μS/cm instead of the expected 14,000 μS/cm , an under measurement of 8%. It was also explicitly presented in an equation developed by Poisson (1980) relating EC to salinity for diluted standard seawater and simplified by Schemel (2000) for surface data taken at 25 ^{0}C (Figure 6.1):

$$EC = \left(\frac{S}{S_{Seawater}}\right)\left(EC_{Seawater}\right) + S\left(S - S_{Seawater}\right)\left(J_1 + J_2 S^{1/2} + J_3 S + J_4 S^{3/4}\right) \qquad \text{[Eqn. 6-1]}$$

where S is practical salinity (dimensionless) or salinity in parts per thousand (ppt), and:

$S_{seawater}$ = 35
$EC_{seawater}$ = 53,087 µS/cm
J_1 = -16.072
J_2 = 4.1495
J_3 = -0.5345
J_4 = 0.0261

Figure 6.1: EC as a Function of Salinity per Equation 6-1 (Schemel, 2000).

EC's non-conservative behavior is also evident when viewing the nonlinear relationship between Delta EC and TDS and Delta EC and chloride, considering that TDS and chloride are generally considered conservative (Figures 6.2 and 6.3). These figures are consistent with the relationship of EC to TDS and chloride from the Gila River in Arizona presented by Hem (1985). In contrast to EC, Figure 6.4 shows that Delta TDS and chloride are linearly related. The data for these figures and much of the analysis in this chapter come from grab samples collected by DWR over the past 30 years for various programs, primarily the Municipal Water Quality Investigations Program and D-1485 Water Quality Monitoring Program. TDS and chloride have been converted from mg/l to parts per thousand (ppt) by dividing values by sample density, ρ, estimated by:

$$\rho = 1 + \left[\frac{X_s}{X_{sw}}\right]\left(\rho_{sw} - 1\right) \qquad \text{[Eqn. 6-2]}$$

where:

X_s is sample concentration (either TDS or chloride) in mg/l,
X_{sw} is concentration of seawater (19,370 mg/l chloride or 35,000 mg/l TDS), and
ρ_{sw} is the density of seawater, assumed to be 1.0243.

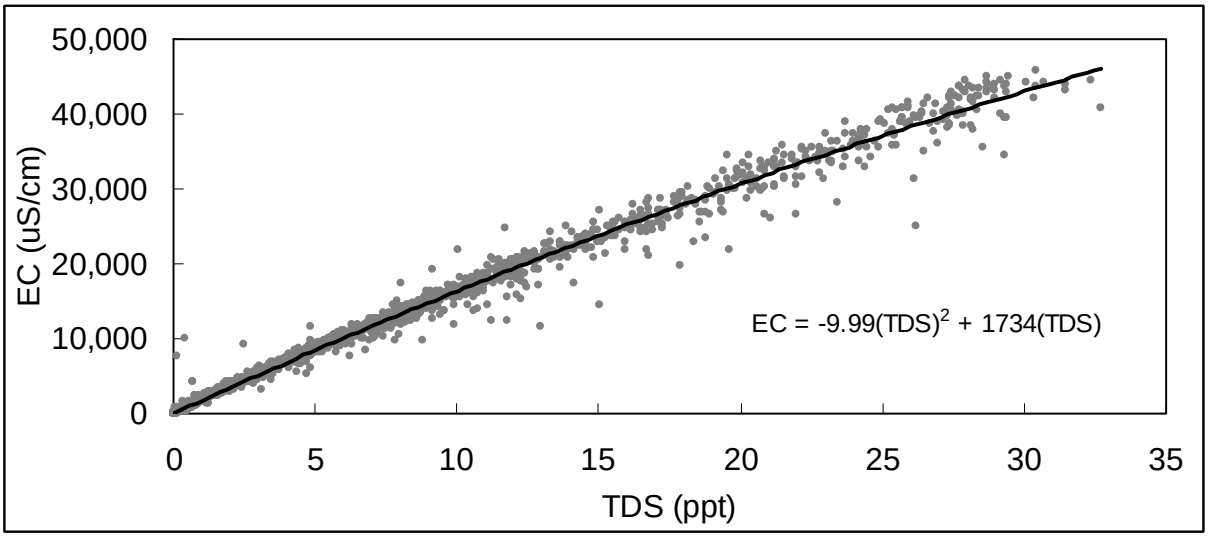

Figure 6.2: Nonlinear Relationship between EC and TDS from Delta Grab Samples.

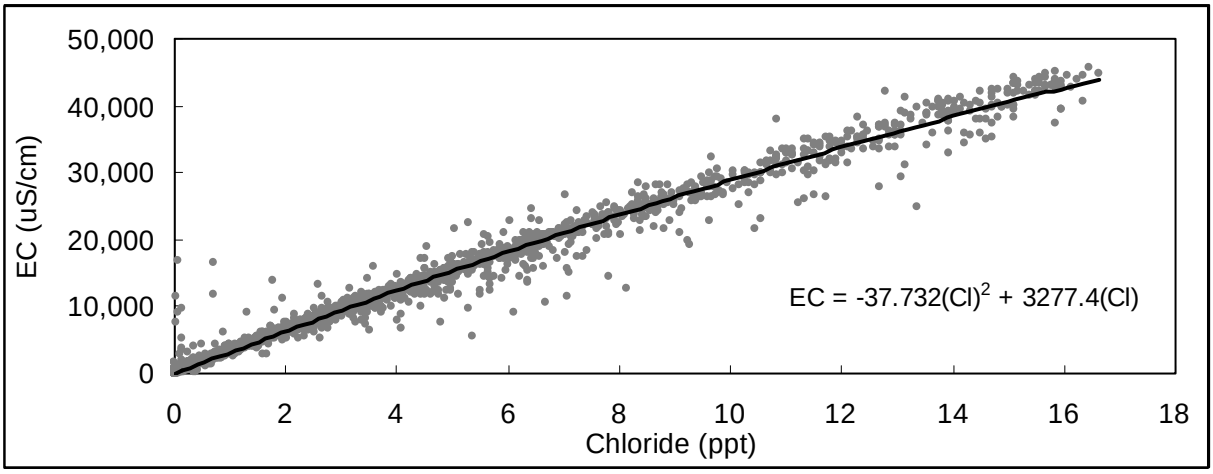

Figure 6.3: Nonlinear Relationship between EC and Chloride from Delta Grab Samples.

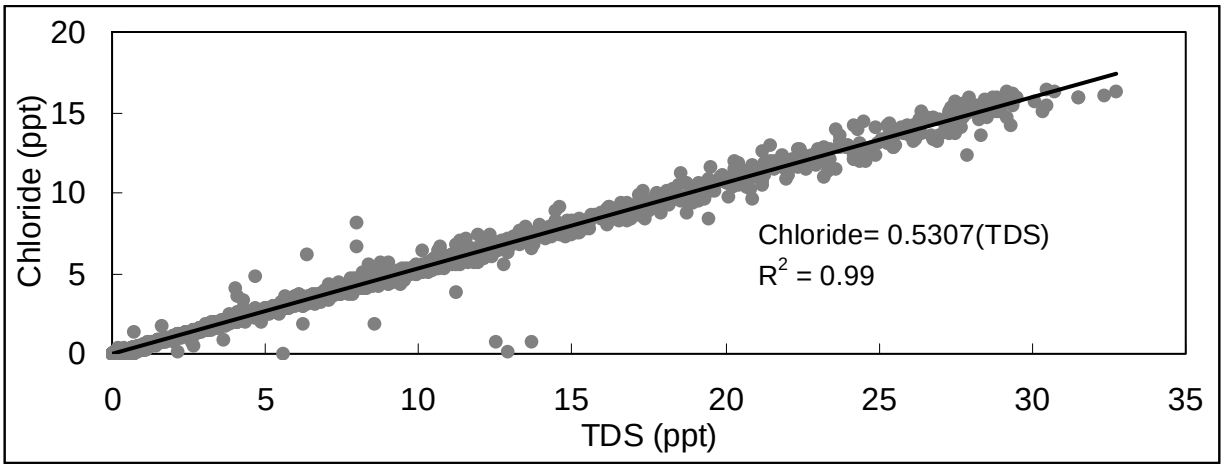

Figure 6.4: Linear Relationship between Chloride and TDS from Delta Grab Samples.

Delta values go up to 17 ppt for chloride, 33.5 ppt for TDS, and 45,800 uS/cm for EC. These ranges relate to the location and tidal and hydrologic conditions at the time the sample is taken. However, samples with higher salinity tend to have been collected in the Suisun Bay, nearer to DSM2's downstream boundary. The non-conservative property of EC may be insignificant for relatively fresh water, but in Suisun Bay EC can exceed 30,000 µS/cm . Using EC as an indicator of relative salinity may be problematic and has implications for the calibration of dispersion factors. Higher measured EC in Suisun Bay and DSM2's downstream boundary of Carquinez Strait at Martinez, will tend to be too low relative to true salinity while lower EC values at interior Delta locations will more accurately reflect actual salinity. As a result, calibrating DSM2 for salinity transport with measured EC will cause dispersion factors in Suisun Bay to be set artificially high in order to transport sufficient EC into the Delta to match more accurate interior EC values.

The current dispersion factors in DSM2 are therefore probably higher in Suisun Bay than would be calculated if a truly conservative transport constituent was used for calibration. However, as long as EC is simulated in QUAL, model results are probably valid, although a bias for overestimating EC during wetter conditions is possible. Total organic carbon (TOC) simulations are also probably valid since downstream boundary contribution is trivial. In calibrating QUAL, dispersion factors are typically adjusted until annual peak salinity at upstream locations is reproduced in the late summer or fall. Thus, calibration naturally focuses on periods when boundary EC will be highest. Wetter conditions when EC in Suisun Bay is much lower, and thus a more accurate representation of salinity, will still use the same dispersion factors and too much inland transport of mass could conceivably occur. However, such a bias of over predicting interior EC in wetter periods is not readily apparent in the current validation of DSM2 (http://iep/dsm2pwt/dsm2pwt.html).

6.2.2 Calibrating QUAL to TDS

TDS is another water quality constituent that is used to calibrate dispersion factors in mass transport models. TDS has been collected in the Delta, along with many other constituents, in monthly or semi-monthly grab samples. While this data is insufficient to use directly as boundary input for simulating a historic period for calibrating or validating DSM2, sufficient samples exist to establish relationships between EC and TDS at the boundaries (Figure 6.5). Boundary conditions for any calibration period that are based on such relationships will introduce additional error to the simulated values. In addition, historical EC field measurements from internal Delta channels would need to be converted to TDS in order to compare modeled results while calibrating and validating the model. Such modification of historically measured data in order to document model validation is viewed as undesirable.

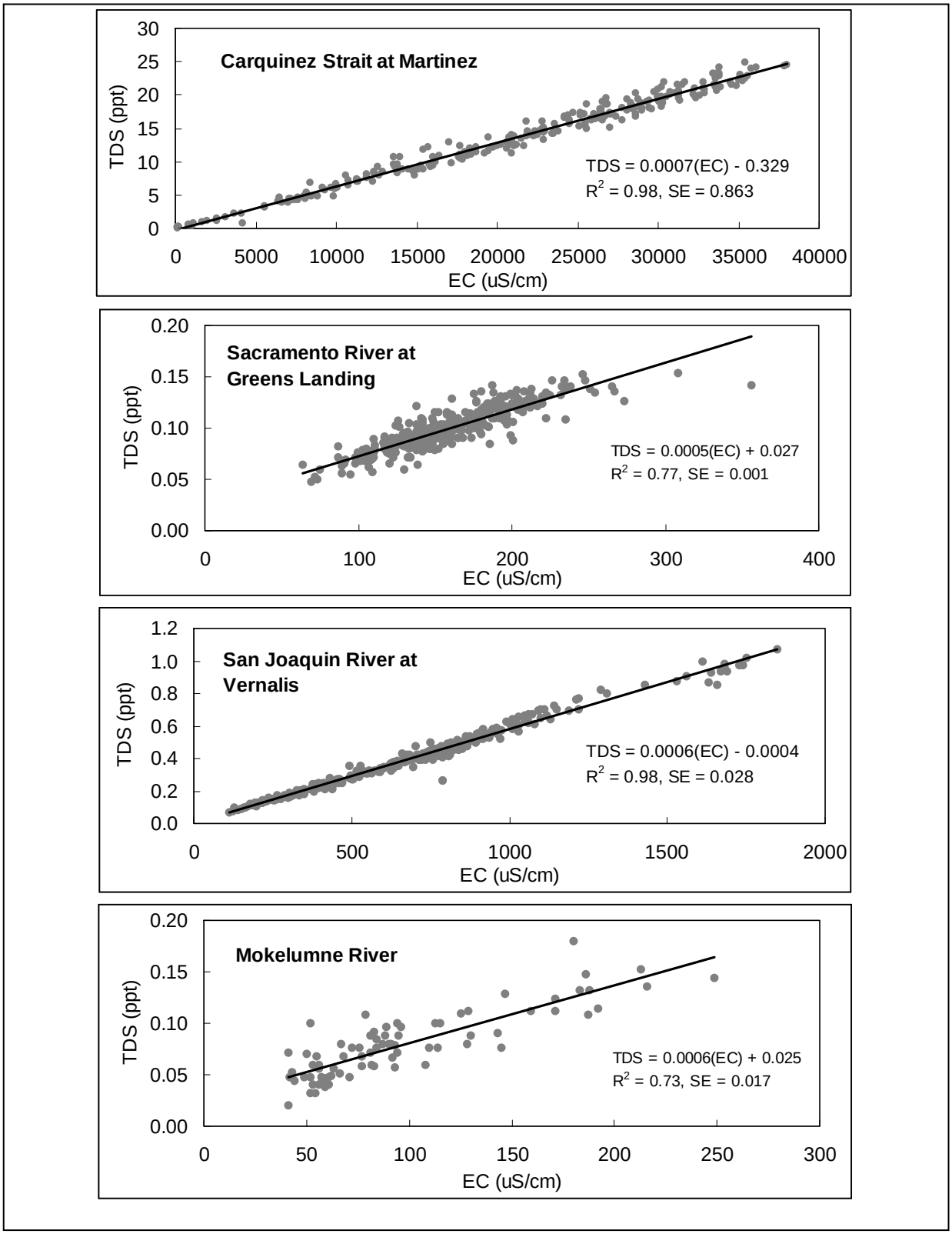

Figure 6.5: Relationship between TDS and EC at Delta Boundaries.

6.3 Calibrating QUAL to Practical Salinity

An alternative approach to using EC or TDS to calibrate QUAL was sought that would both correct for the non-conservative behavior of EC at high salinity concentrations and allow for field EC data to be used unaltered for validation. Using practical salinity to calibrate QUAL is now presented as an alternative.

6.3.1 Practical Salinity Background

A standard expression of salinity is the Practical Salinity Scale 1978, first proposed by Lewis (1980). This scale converts *in situ* electrical conductivity readings into salinity. Practical salinity is defined as a function of electrical conductivity and temperature (and assuming any pressure component to be negligible):

$$S = a_0 + a_1 R_T^{1/2} + a_2 R_T + a_3 R_T^{3/2} + a_4 R_T^2 + a_5 R_T^{5/2} + \frac{(T-15)}{1+k(T-15)}\left\{b_0 + b_1 R_T^{1/2} + b_2 R_T + b_3 R_T^{3/2} + b_4 R_T^2 + b_5 R_T^{5/2}\right\} \qquad \text{[Eqn. 6-3]}$$

where:

$a_0 =$ 0.0080	$b_0 =$ 0.0005	$k = 0.0162$
$a_1 =$ -0.1692	$b_1 =$ -0.0056	
$a_2 =$ 25.3851	$b_2 =$ -0.0066	
$a_3 =$ 14.0941	$b_3 =$ -0.0375	
$a_4 =$ -7.0261	$b_4 =$ 0.0636	
$a_5 =$ 2.7081	$b_5 =$ -0.0144	

$$\sum a_i = 35.0000; \qquad \sum b_i = 0.0000$$

$$R_T = \left(\frac{EC_{sample}}{EC_{seawater}}\right)_{TemperatureT}; \qquad -2^oC \le T \le 35^oC$$

Practical salinity is commonly expressed as dimensionless or as parts per thousand.
Equation 6-3 is based upon analysis of data obtained by diluting standard seawater with distilled water or evaporating by weight. As formulated above, the Practical Salinity Scale 1978 is valid over the range of 2 - 42, which roughly corresponds to EC values in the Delta in excess of 4,000 µmhos/cm .

Electrical conductivity data recorded at various monitoring stations within the Delta are typically collected at shallow depths and are normalized to a standard temperature of 25 ^oC. Schemel (2000) provided a simplified equation for calculating practical salinity from EC data. Assuming T = 25 ^oC and atmospheric pressure,

$$S = K_0 + K_1 R_T^{1/2} + K_2 R_T + K_3 R_T^{3/2} + K_4 R_T^2 + K_5 R_T^{5/2} \qquad \text{[Eqn. 6-4]}$$

where:

$K_0 =$ 0.0120
$K_1 =$ -0.2174
$K_2 =$ 25.3283
$K_3 =$ 13.7714
$K_4 =$ -6.4788
$K_5 =$ 2.5842

R_T is as defined in Equation 6-3. Schemel (2000) assumed $EC_{seawater}$ to be 53,097 µS/cm .

As previously mentioned, the Practical Salinity Scale 1978 as originally formulated was valid for the range from 2 to 42, with seawater at 35. Hill et al. (1986) developed a standard correction to Equation 6.3 to extend the Practical Salinity Scale 1978 to salinity below 2. This correction is expressed by:

$$\text{Standard Correction} = -\frac{a_0}{1+1.5x+x^2} - \frac{b_0 f(T)}{1+y^{1/2}+y+y^{3/2}} \qquad \text{[Eqn. 6-5]}$$

where:

$$f(T) = \frac{(T-15)}{1+k(T-15)}$$

x = $400R_T$
y = $100R_T$
$a_0 =$ 0.008
$b_0 =$ 0.0005
k = 0.0162

This correction approaches 0 at a practical salinity of 2, leaving the original equation, Equation 6-3, intact while forcing the practical salinity to equal 0 when the conductivity is equal to the value for pure water (Figure 6.6). The standard correction to practical salinity below 2 is based on dilutions of standard seawater and is only strictly applicable to waters that have the major ions in the same proportions as standard seawater. This correction does not necessarily apply to coastal waters diluted by land drainage such as occurs in the Delta (Hill, 1986). The American Public Health Association et al. (1995) state that the standard correction can be used, with some limitations, with estuarine water. Buchanan et al. (2001) apply the standard correction to Practical Salinity Scale 1978 as derived from *in situ* EC collected from the San Francisco Bay-Delta as part of USGS's standard methodology. In contrast, Kimmerer et al. (1998) makes no mention of a correction but suggests limiting use of the Practical Salinity Scale 1978 in the San Francisco Bay-Delta to salinity values above 2. Still others state that Practical Salinity Scale 1978 values calculated from fresh water EC need no correction if EC values have already been corrected to 25 ^{0}C (Schemel, 2000; Seabird, 2001). Other literature on estuarine salinity where practical salinity values below 2 are presented are mute on this issue

(Blanton et al. 2001; Schoellhamer, 2001). The issue of applying a correction to the Standard Salinity Scale 1978 for low salinity Delta water is further explored below.

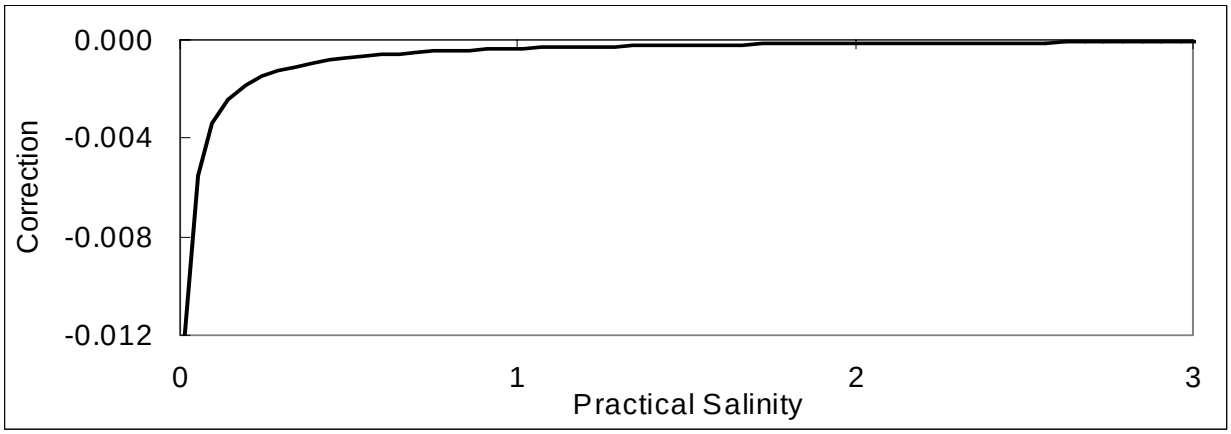

Figure 6.6: Standard Correction to Practical Salinity Scale 1978 (Hill et al., 1986).

6.3.2 Practical Salinity in the Sacramento-San Joaquin Delta

EC from DWR grab samples throughout the Delta collected the past 30 years was converted to practical salinity by the Practical Salinity Scale 1978 (Equation 6.4) and plotted against the chloride that was simultaneously measured (Figure 6.7). When extreme outliers are removed, the resulting relationship, practical salinity / chloride, is found to be 1.78. This is consistent with a published relationship of 1.81 between salinity and chlorinity (Lewis, 1980; Cox et al., 1967).

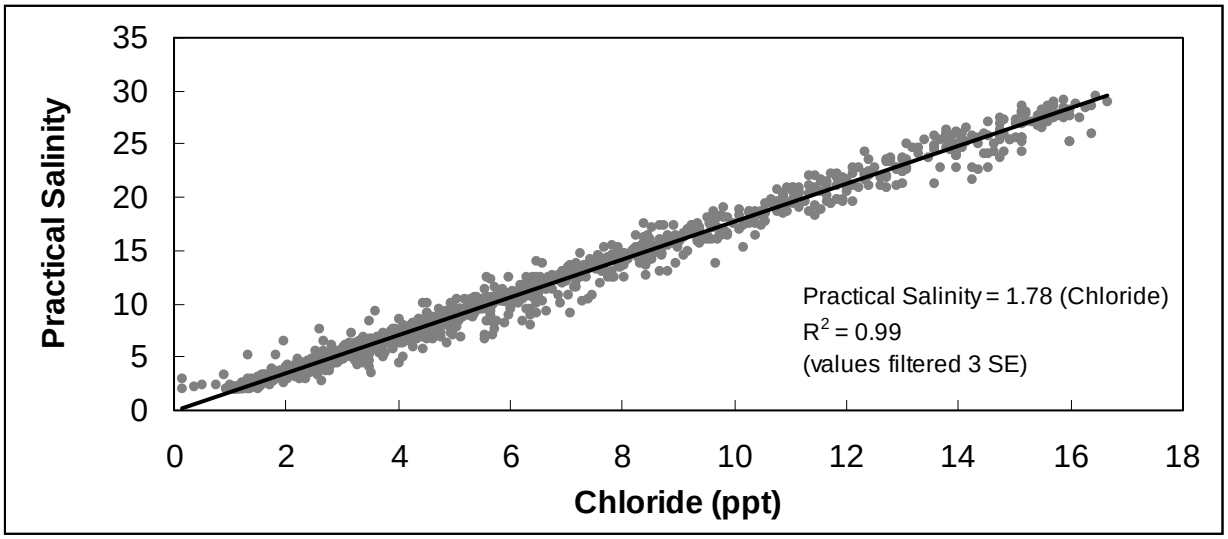

Figure 6.7: Relationship between Delta Practical Salinity Scale 1978 and Observed Chloride.

Practical salinity was also plotted against TDS, again collected from grab samples (Figure 6.8). As Figure 6.8 shows, the overall relationship between practical salinity and TDS is linear, correcting EC's non-conservative behavior. However, examination of practical salinity at low salinity (TDS < 1.2 ppt) shows that the validity of calculating practical salinity in the range of 0

to 2 remains an issue (Figure 6.9). If the Practical Salinity Scale 1978 is valid for all the data, practical salinity in the range of 0 to 2 will fall along the extended regression for the practical salinity range of 2 to 42. However, Figure 6.9 shows that the uncorrected practical salinity data calculated from Delta EC, in fact, deviates from this regression. The linear relationship between practical salinity and TDS actually holds down to a TDS of 1 ppt (Figure 6.10), but below this level, the influence of the Sacramento and San Joaquin rivers and perhaps agricultural drainage apparently causes the Practical Salinity Scale 1978 to err. The Delta water quality samples seem to display behavior inferred by Hill et al. (1986) who cautioned that the assumption of constancy with seawater of relative composition does not apply to coastal waters diluted by land drainage.

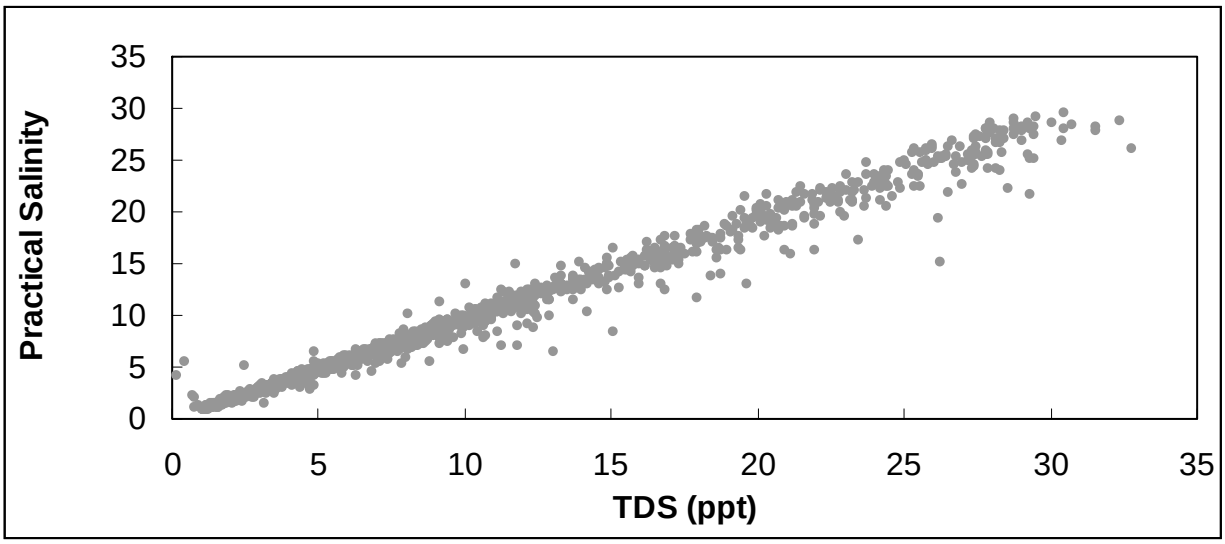

Figure 6.8: Relationship between Delta Practical Salinity Scale 1978 and Observed TDS.

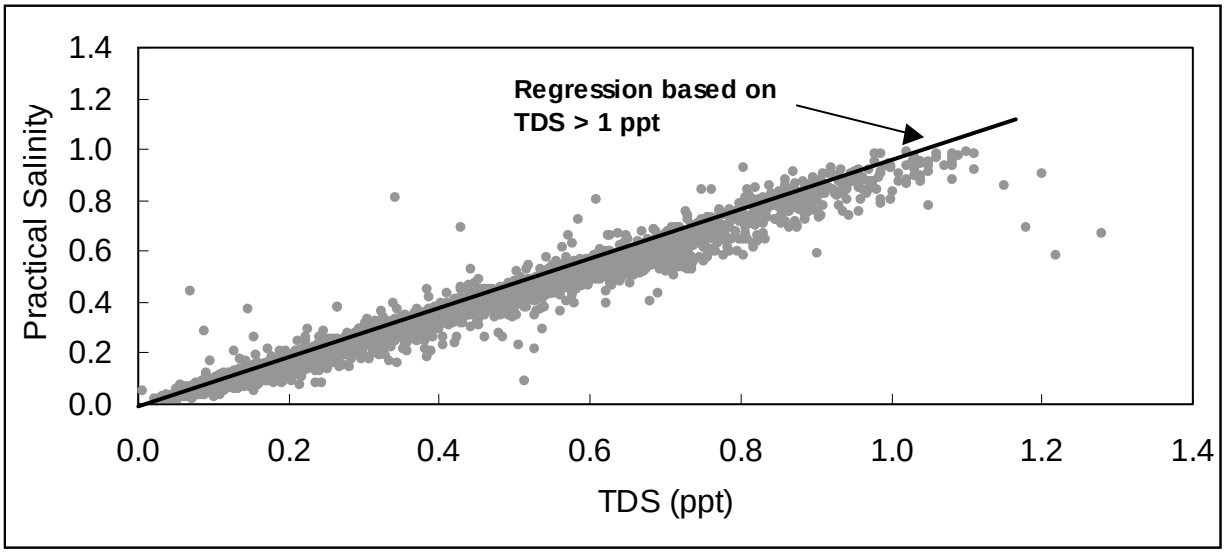

Figure 6.9: Deviation of Low Delta Practical Salinity from Valid Regression.

Applying the standard correction to the Practical Salinity Scale 1978 presented in Equation 6-5 had essentially no effect upon the results. As Schemel (2000) points out, the standard correction

is very small with respect to the generated values. An alternative correction, specific to the conditions in the Sacramento-San Joaquin Delta and the sources of fresh water, is needed.

6.3.3 An Alternative Correction to Extend Practical Salinity Scale 1978 Below 1 PPT TDS in the Delta

Examination of Delta grab sample data shows that practical salinity derived from Delta EC holds a linear relationship with TDS down to a value of approximately 1 ppt TDS (practical salinity of about 0.92). As Figure 6.10 shows, when outliers are removed, this relationship is expressed by:

$$\text{practical salinity} = 0.9528\ (\text{TDS}) \qquad \text{[Eqn. 6-6]}$$

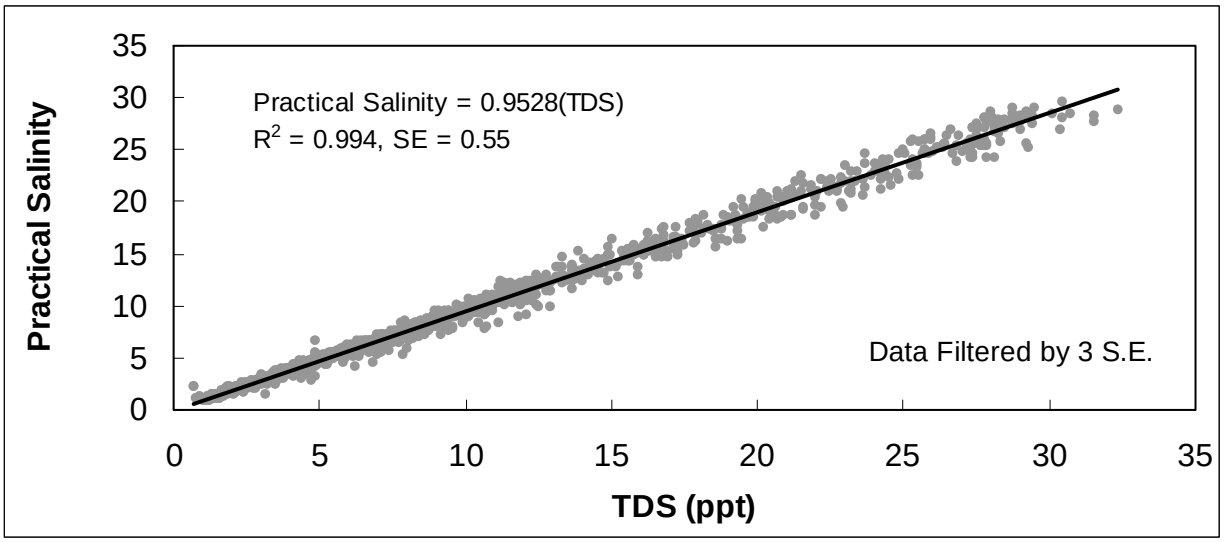

Figure 6.10: Relationship between Delta Practical Salinity and TDS for TDS > 1 ppt.

This regression is assumed to be the valid relationship between practical salinity and TDS in the Delta. Lower practical salinity values would fall along this regression if Equations 6-3 or 6-4 held for all values below 1 ppt TDS. The deviation from this regression is thus assumed to be the needed correction to Delta practical salinity. Figure 6.11 shows how this correction can be approximated by partitioning the range of 0 to 1 ppt TDS (0 to 0.92 practical salinity) into three intervals. The correction to practical salinity will then vary linearly over each interval (Table 6.1) and apply Deltawide since the data in Figure 6.11 come from locations throughout the Delta.

Table 6.1: Desired Correction to Delta Practical Salinity.

TDS (ppt)	EC (uS/cm)	Practical Salinity	Practical Salinity Correction
0	0	0	0
0.175	302	0.145	0.027
0.750	1346	0.671	0.052
1	1824	0.923	0

This correction can then be incorporated directly into the simplified Practical Salinity Scale 1978 for surface water at 25 ^{0}C:

$$S = M_0 + M_1\left(K_0 + K_1 R_T^{1/2} + K_2 R_T + K_3 R_T^{3/2} + K_4 R_T^2 + K_5 R_T^{5/2}\right) \qquad \text{[Eqn. 6-7]}$$

where,

K_0, K_1, K_2, K_3, K_4, and K_5 defined as in Equation 6-4, R_T as defined earlier, and M_0, M_1 as specified in Table 6.2.

Table 6.2: Coefficients M_0 and M_1 to Correct Low Practical Salinity in Delta Channels.

TDS Range (ppt)	EC Range uS/cm	Practical Salinity Range	M0	M1	Corrected Practical Salinity Range
< 0.175	< 302	< 0.145	0	1.1880	< 0.172
0.175 - 0.75	302 - 1346	0.145 - 0.671	0.0205	1.0470	0.172 - 0.723
0.75 - 1.0	1346 - 1824	0.671 - 0.923	0.1903	0.7939	0.723 - 0.923
> 1.0	> 1824	> 0.923	0	1	> 0.923

Practical Salinity from Delta-wide EC data was recalculated according to Equation 6-4 or Equation 6-7 and again compared to TDS. As shown in Figure 6.12, the corrected practical salinity over the range of 0 to 1 ppt TDS essentially falls along the desired regression of practical salinity = 0.9528(TDS), validating Equation 6-7.

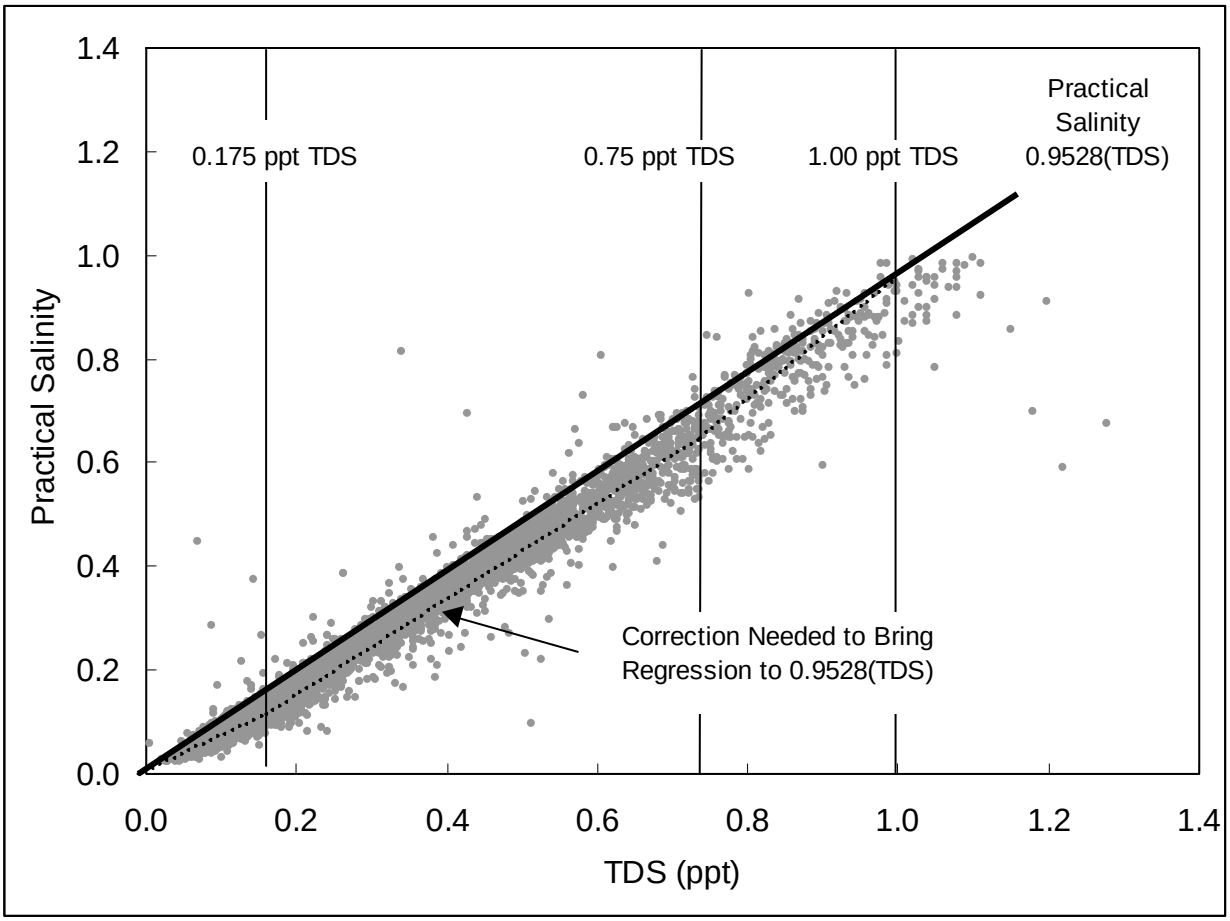

Figure 6.11: Needed Correction to Delta Practical Salinity for Values with TDS < 1 ppt.

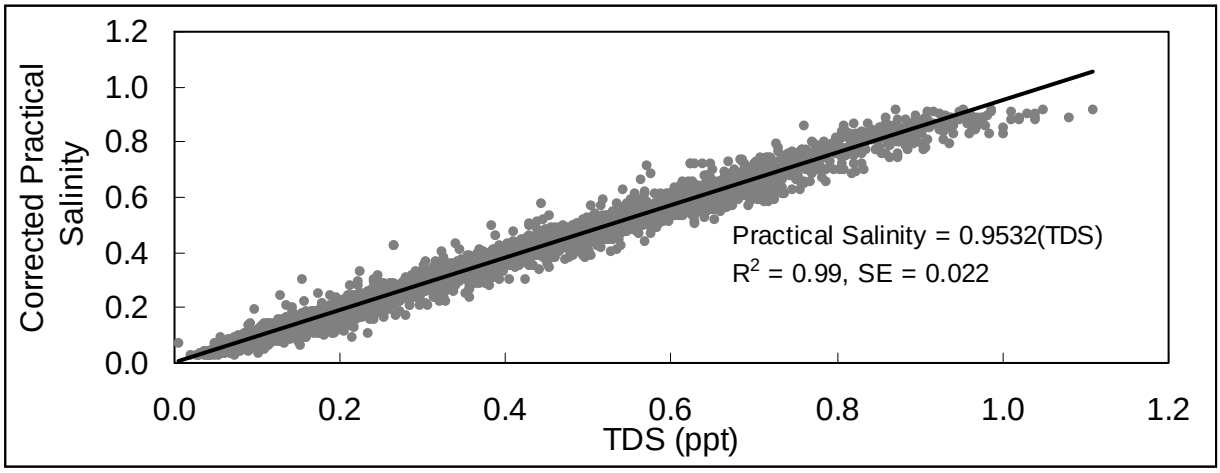

Figure 6.12: Corrected Delta Practical Salinity for Values with TDS < 1 ppt.

6.3.4 Practical Salinity at Delta Boundaries

TDS and EC field data from throughout the Delta were used to generate the correction coefficients in Table 6.2. The actual relationship between practical salinity and TDS that is used to calculate a correction may vary somewhat by location; however, this variability is hidden in Table 6.2. Equation 6-7 was applied separately to EC data at the Delta boundaries. As shown in Figure 6.13, Equation 6-7 holds well at the important boundaries of Carquinez Strait at Martinez and the Sacramento and San Joaquin rivers.

6.3.5 Practical Salinity of Agricultural Drainage

Corrections to practical salinity for agricultural drainage were established separately from the global correction for Delta channel salinity. The relationship between EC and TDS for agricultural drainage appears substantially different from that seen from Delta channels, probably due to the exchange chemistry of soil-water interactions in drainage. In addition, there is no need to convert back from practical salinity to EC for agricultural drainage as there may be for salinity from Delta channels. Agricultural drainage water quality is grouped and evaluated according to the three regions shown in Figure 6.14. This grouping is the same as used in DWR's Delta Island Consumptive Use Model for describing the water quality of Delta agricultural drainage. Figure 6.15 compares uncorrected practical salinity to TDS in each region. The needed correction to practical salinity for agricultural drainage then is calculated as: 0.9528/(slope of regression of TDS-practical salinity relationship). Coefficients M_0 and M_1 for Equation 6-7 then can be expanded to include agricultural drainage (Table 6.3).

Table 6.3: Coefficients M_0 and M_1 to Correct Practical Salinity in Delta Agricultural Drainage.

	Delta Region		
	West	**South-East**	**North**
M_0	0	0	0
M_1	1.1665	1.1165	1.2687

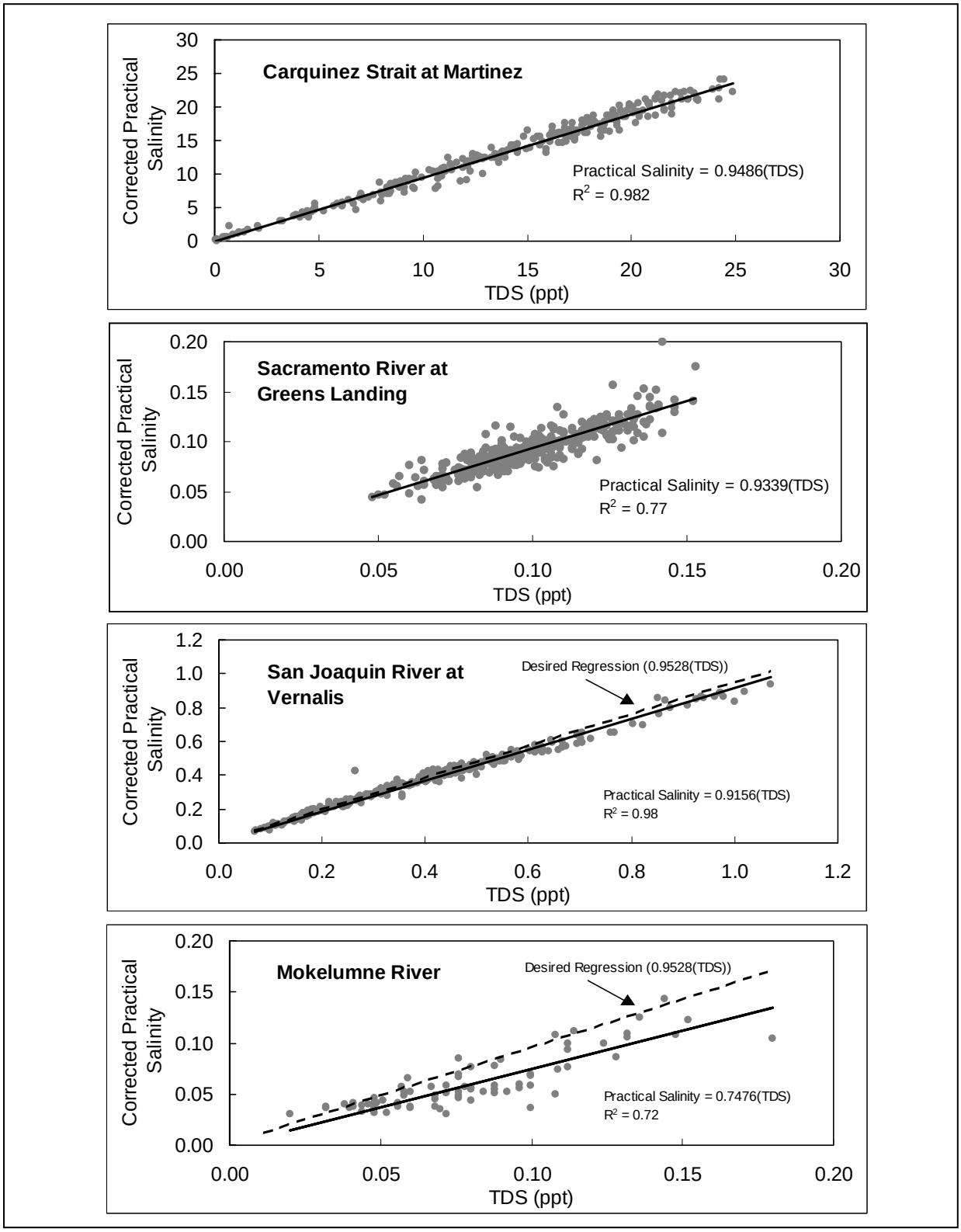

Figure 6.13: Corrected Delta Practical Salinity at Delta Boundaries.

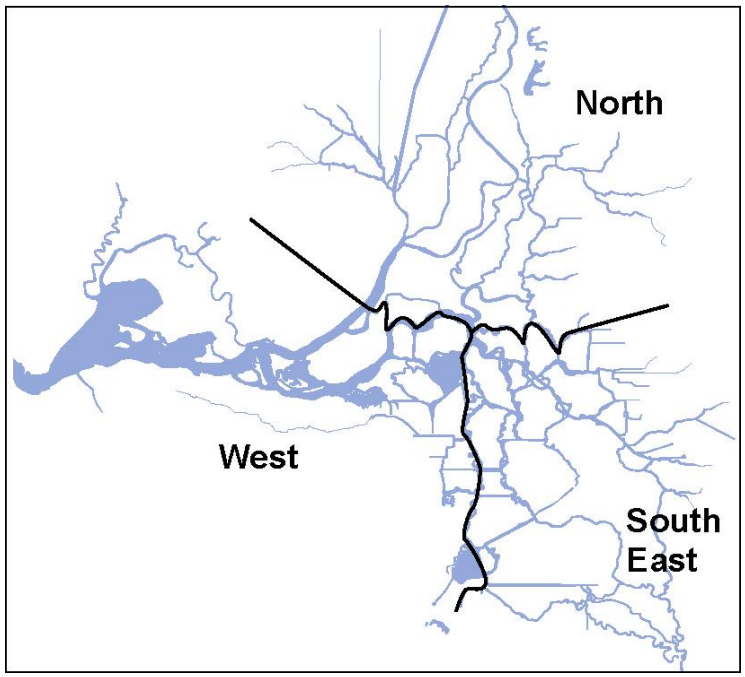

Figure 6.14: Regions for Different Corrections to the Practical Salinity of Agricultural Drainage.

6.3.6 Converting QUAL-Generated Practical Salinity to EC

Calibrating QUAL to practical salinity as calculated in Section 6.3.5 should result in dispersion factors appropriate for simulating transport of any conservative mass. However, Delta EC is still often needed for analysis and presentation of study results. Methods for converting from practical salinity back to EC were therefore explored. Expressing practical salinity in terms of EC requires two steps: removing the global correction to low practical salinity values that would be embedded in QUAL-generated values, then converting this practical salinity back to EC. Delta practical salinity with the correction removed is expressed by:

$$S_u = \frac{S - M_0}{M_1} \qquad \text{[Eqn. 6-8]}$$

where S_u is uncorrected practical salinity, S is corrected practical salinity, M_0 and M_1 are as defined in Tables 6.2 and 6.3.

Poisson (1980) presents an equation for converting from practical salinity to EC (Equation 6-1). This equation is based on a set of samples diluted from standard seawater. A full-circle analysis can be done to validate the use of Equation 6-1: convert Delta EC to corrected practical salinity by Equation 6-7, convert to uncorrected practical salinity by Equation 6-8, and finally convert back to EC by Equation 6-1. Figure 6.16 shows the residuals of EC after performing this check. Errors in converting from practical salinity to EC range from 0 to 30 μS/cm . As mentioned before, Equation 6-1 was based on variations of standardized seawater. As an alternative approach, an equation was developed that directly relates EC from Delta samples and uncorrected practical salinity as calculated from the same EC data and Equation 6-5:

$$EC = h_0 + h_1 S_u^{1/2} + h_2 S_u + h_3 S_u^{3/2} + h_4 S_u^{2} + h_5 S_u^{5/2} \qquad \text{[Eqn. 6-9]}$$

where EC is electrical conductivity (μS/cm), S_u is uncorrected practical salinity, and:

h_0 = -39.1632
h_1 = 170.6825
h_2 = 1953.7171
h_3 = -125.4956
h_4 = 11.5454
h_5 = -0.6103

A full-circle analysis with Equation 6-9 in shows that the equation reduces the maximum error to 2 μS/cm (Figure 6.16). Combining Equations 6-8 and 6-9 then yields a method for converting QUAL-generated practical salinity in the Delta to EC:

$$EC = h_0 + h_1\left(\frac{S - M_0}{M_1}\right)^{1/2} + h_2\left(\frac{S - M_0}{M_1}\right) + h_3\left(\frac{S - M_0}{M_1}\right)^{3/2} + h_4\left(\frac{S - M_0}{M_1}\right)^{2} + h_5\left(\frac{S - M_0}{M_1}\right)^{5/2} \qquad \text{[Eqn. 6-10]}$$

where S is QUAL-generated practical salinity, M_0 and M_1 are defined as in Table 6.2, and h_0, h_1, h_2, h_3, h_4, and h_5 are defined as in Equation 6-9.

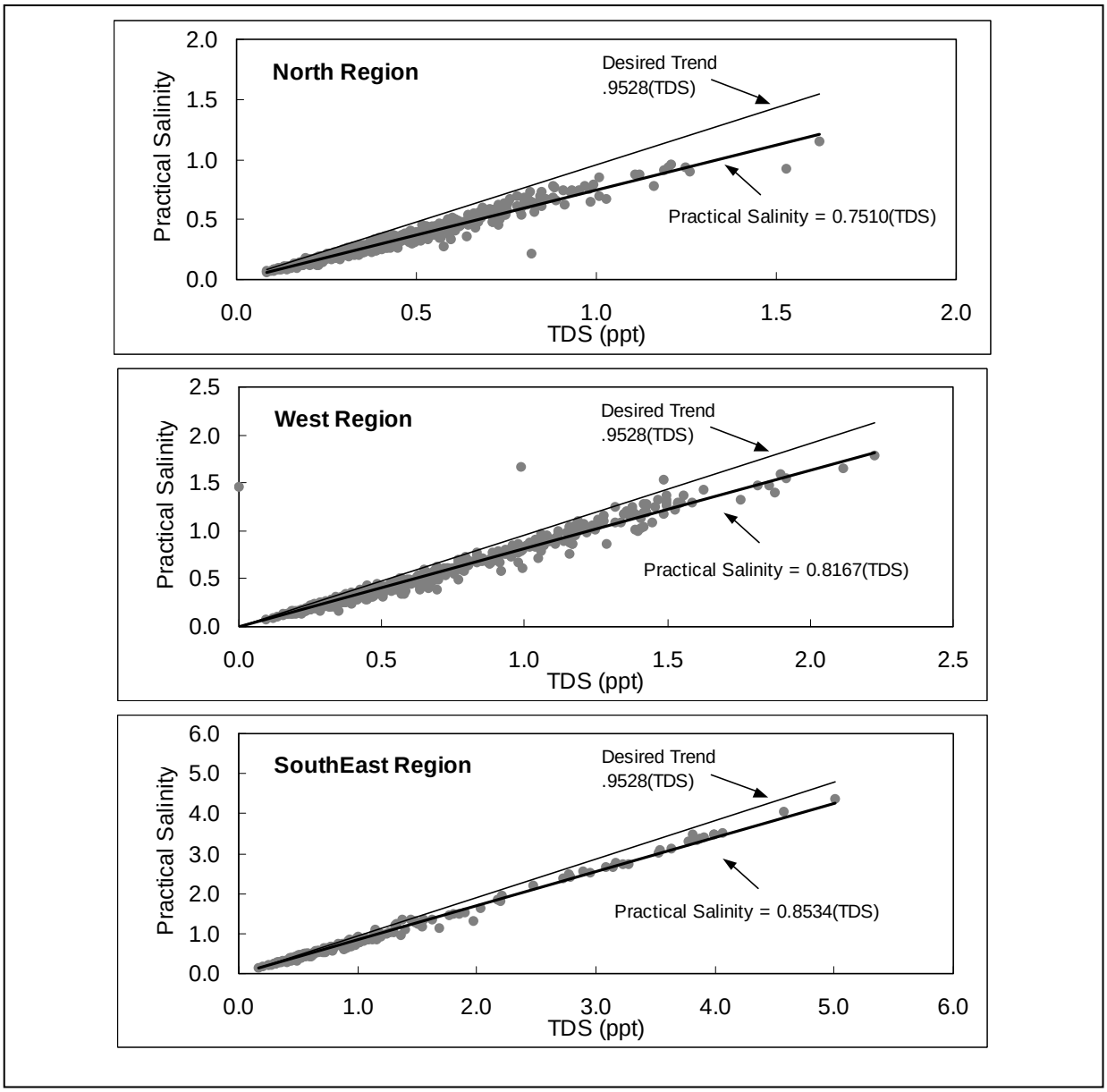

Figure 6.15: Needed Correction to Practical Salinity of Delta Agricultural Drainage.

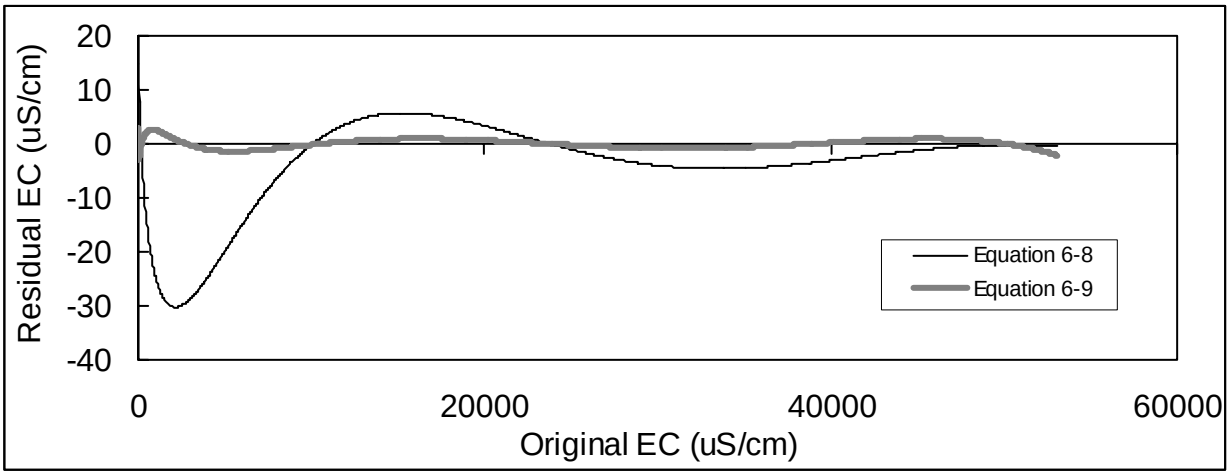

Figure 6.16: Residual in EC after EC - Corrected Practical Salinity - EC Analysis.

6.4 References

American Public Health Association, American Water Works Foundation, and Water Environment Federation. (1995). *Standard Methods for the Examination of Water and Wastewater.*

Blanton, J., A. Merryl, and J. Sheldon. (2001). *Salinity Response of the Satilla River Estuary to Seasonal Changes in Freshwater Discharge*. Proceedings of the 2001 Georgia Water Resources Conference.

Buchanan, P., C.A. Ruhl, and D. Schoellhamer. (2001). *Continuous Monitoring in San Francisco Bay and Delta: Data Collection Methods and Procedures*. Access USGS. http://sfports.wr.usgs.gov/Fixed_sta/DataCollection/data_collect.html

Cox, R.A., F. Culkin, and J.P. Riley. (1967). *The Electrical Conductivity/Chlorinity Relationship in Natural Seawater*. Deep Sea Research, 17. pp. 679-89.

Hem, J.D. (1985). *Study and Interpretation of Chemical Characteristics of Natural Water*. U.S. Geological Survey Water-Supply Paper 2254. pp. 66-9. http://water.usgs.gov/pubs/wsp/wsp2254/html/pdf.html

Hill, K.D., T.M. Dauphinee, and D.J. Woods. (1986). *The Extension of the Practical Salinity Scale 1978 to Low Salinities*. IEEE Journal of Oceanic Engineering OE-11 (1). pp. 109-12.

Kimmerer, W., F. Nichols, P. Lehman, B. Cole, B. Thompson, and E. Cummings. (1998). *Estuarine System Production: Lower Trophic Levels*. CALFED CMARP Paper.

Lewis, E.L. (1980). *The Practical Salinity Scale 1978 and Its Antecedents*. IEEE Journal of Oceanic Engineering OE-5:3-8.

Nader-Tehrani, P. (2001). "Chapter 2: DSM2 Calibration and Validation." *Methodology for Flow and Salinity Estimates in the Sacramento-San Joaquin Delta and Suisun Marsh. 22nd Annual Progress Report to the State Water Resources Control Board.* California Department of Water Resources. Sacramento, CA.

Poisson, A. (1980). *Conductivity/Salinity/Temperature Relationship of Diluted and Concentrated Standard Seawater*. IEEE Journal of Oceanic Engineering OE-5 (1). pp. 41-50.

Seabird Company Document. (2001). *SeFresh Water Conductivity Measurements using the SBE 19 (not 19plus) SEACAT Profiler.* Application Note No. 30. http://www.seabird.com/application_notes/AN30.htm

Schemel, L. (2000). *Simplified Conversions Between Specific Conductance and Salinity Units for Use with Data from Monitoring Stations.* Interagency Ecological Program Newsletter. U.S. Geological Survey.

Schoellhamer, D.H. (2001). *Influence of Salinity, Bottom Topography, and Tides on Locations of Estuarine Turbidity Maxima in Northern San Francisco Bay*. Coastal and Estuarine Fine Sediment Transport Processes: Elsevier Science B.V. pp. 343-57.

Methodology for Flow and Salinity Estimates in the Sacramento-San Joaquin Delta and Suisun Marsh

23rd Annual Progress Report
June 2002

Chapter 7:
Generating Monthly Dissolved Organic Carbon and UVA at DSM2 Boundaries

Author: Bob Suits

7 Generating Monthly Dissolved Organic Carbon and UVA at DSM2 Boundaries

7.1 Introduction

Dissolved organic carbon (DOC) and ultraviolet light absorbance (UVA) have been developed for the Sacramento River at Greens Landing, the San Joaquin River at Vernalis, and the Mokelumne River at I-5 for the 1975–1991 planning simulation period. This chapter presents these data and details the methodology used.

7.2 General Methodology

DOC for the planning period was developed using two different methods. In the first method, due to a small variation in historical data, constant monthly DOC values were used for June through October. These values were calculated using data from 1987 through 1998. The second method was applied to the remaining months (November–May). These months have a greater variation in data over the historical period so in this method, relationships between DOC and flow were developed. These relationships are discussed in detail in the following paragraphs.

The averaged observed DOC from June through October (approximately from 1987 through 1998) was assigned as monthly DOC for the same months over the planning period. In order to generate DOC for the remaining months, relationships between observed DOC and flow were established and then applied to the historic flows over the planning period.

Relationships between DOC and flow were found by first partitioning observed DOC into three or four categories according to the ratio of observed DOC to historic flow. The categories were presented as containing data exhibiting “low”, “moderate”, or “high” DOC response to flow. Regressions were then found between DOC and flow for each category of data. Historic patterns of DOC / flow values were then examined to determine the conditions under which low, moderate, or high DOC response to flow occurred in the past. General trends in the historic data were used to assign each month in the planning period with low, moderate, or high DOC / flow values. Each month then was assigned a constant DOC (for June through October) or a regression was applied to the flow to obtain DOC. Finally, any generated DOC was limited to falling within minimum and maximum observed DOC at that location.

UVA over the planning period was generated at the three sites by applying regressions between historic UVA and DOC to the generated DOC.

Historic DOC and UVA was available from once or twice-per-month grab samples collected over the approximate period of 1987 through 1998 by the Department’s Municipal Water Quality Investigations (MWQI). DOC and UVA in the American River were used as a surrogate for the Mokelumne River. Multiple values of DOC or UVA in any given month were averaged together

to yield one value per month. Monthly average flows in the Sacramento, San Joaquin, and American rivers were determined using DAYFLOW.

7.3 Sacramento River at Greens Landing

7.3.1 Dissolved Organic Carbon at Greens Landing

Figure 7.1 shows historic DOC and flow in the Sacramento River at Greens Landing. DOC from June through October was averaged to yield a single value of 1.81 mg/L to approximate monthly DOC from June through October for the planning period (Figure 7.2). DOC in other months exhibited a pattern of high values associated with the first large flows of the fall/winter and low values after sustained high flows. Figure 7.3 and Table 7.1 show that, after excluding the June-October data, partitioning DOC according to DOC / flow ratio, yielded reasonable regressions between DOC and flow.

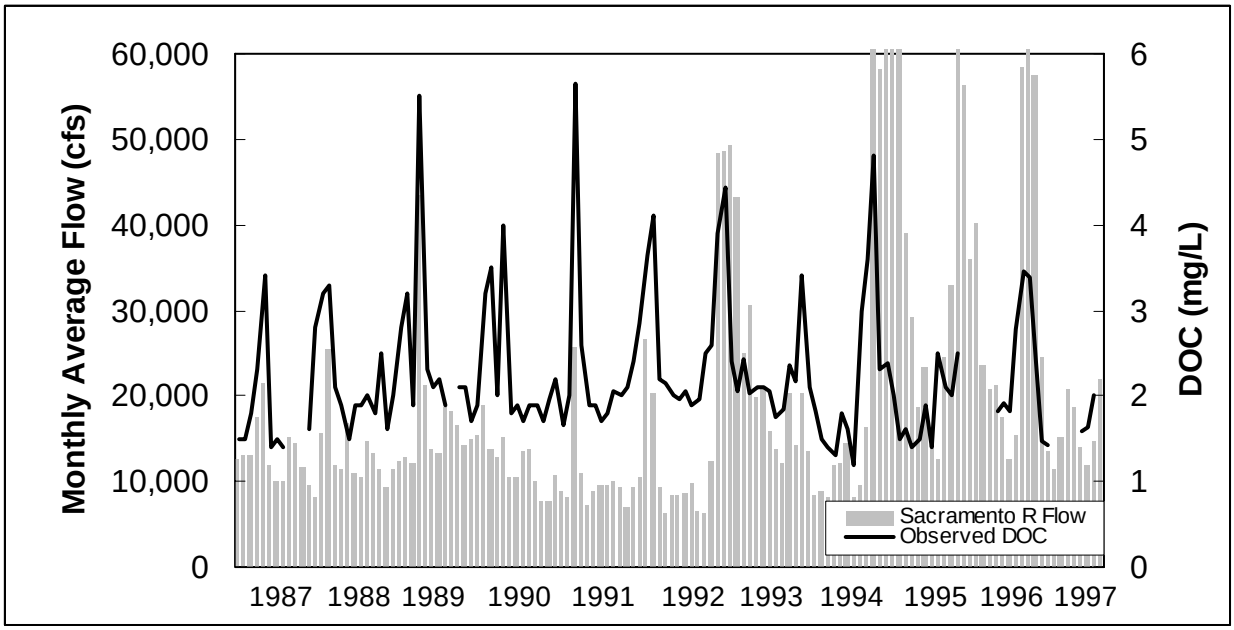

Figure 7.1: Observed DOC and Flow at Greens Landing.

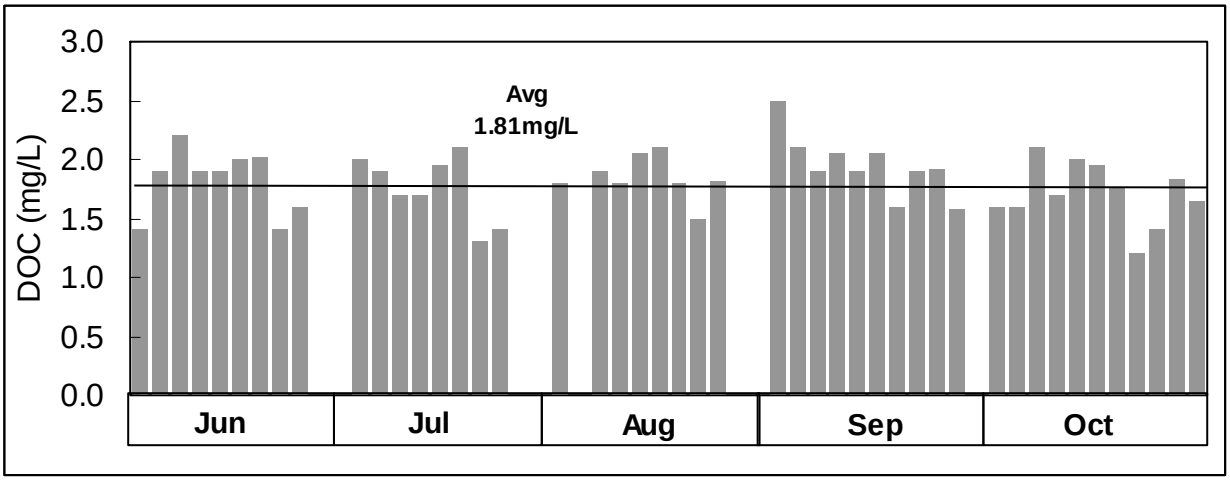

Figure 7.2: Observed DOC at Greens Landing, 1987–1997 (Grouped by Month).

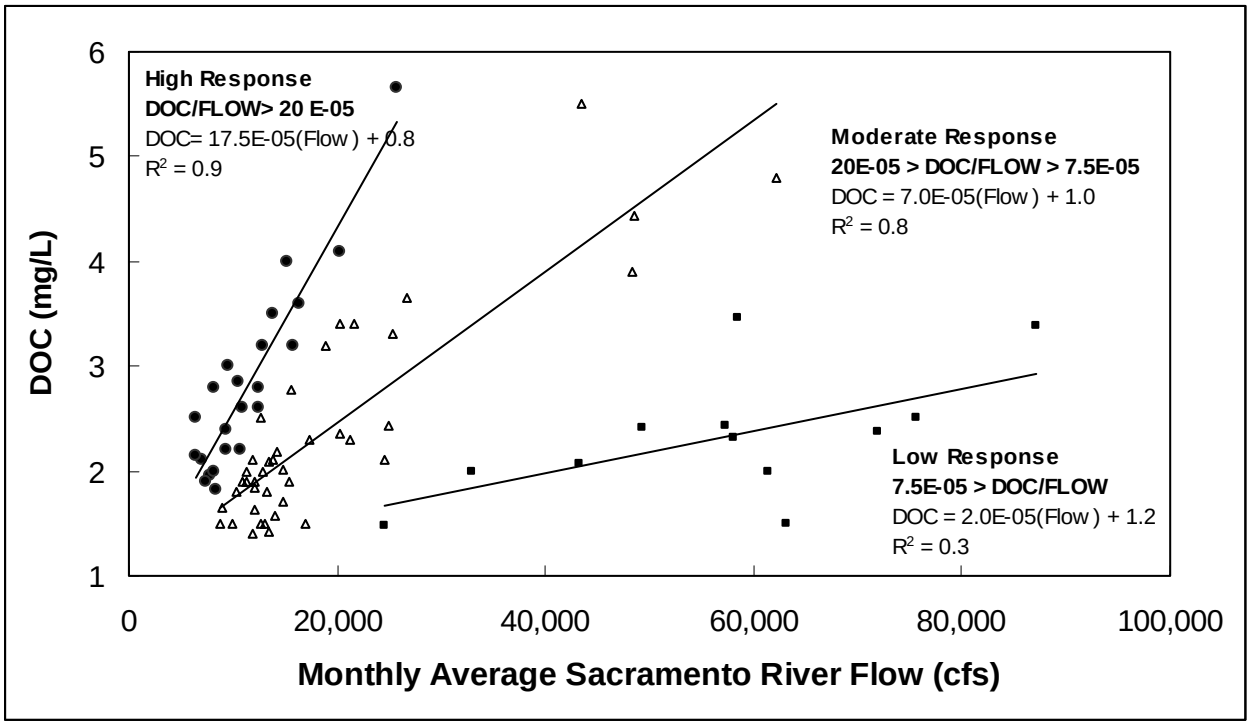

Figure 7.3: Observed DOC and Flow at Greens Landing Grouped by Response to Flow (Jun.–Oct. Data Removed).

Table 7.1: Classification of DOC Response to Flow at Greens Landing.

DOC Response to Flow	Criteria	Reqression Equation	R^2
Low	7.5E-05 > DOC / FLOW	DOC = 2.0E-05(FLOW) + 1.8	0.3
Moderate	20E-05 > DOC / FLOW > 7.5E-05	DOC = 7.0E-05(FLOW) + 1.0	0.8
High	DOC / FLOW > 20E-05	DOC = 17.5E-05(FLOW) + 0.8	0.9

DOC: monthly dissolved organic carbon (mg/L)
FLOW: monthly average flow in Sacramento River at Sacramento (cfs)

Historic flows at Greens Landing were then described as being associated with "low", "moderate" "high" DOC response (Figure 7.4). Observed patterns of DOC response to flow were applied to the planning period by considering current and preceding flows. This allowed each monthly flow during the planning period to be associated with either 1.81 mg/L DOC (June–October), or with one of three regressions with DOC (Figure 7.5).

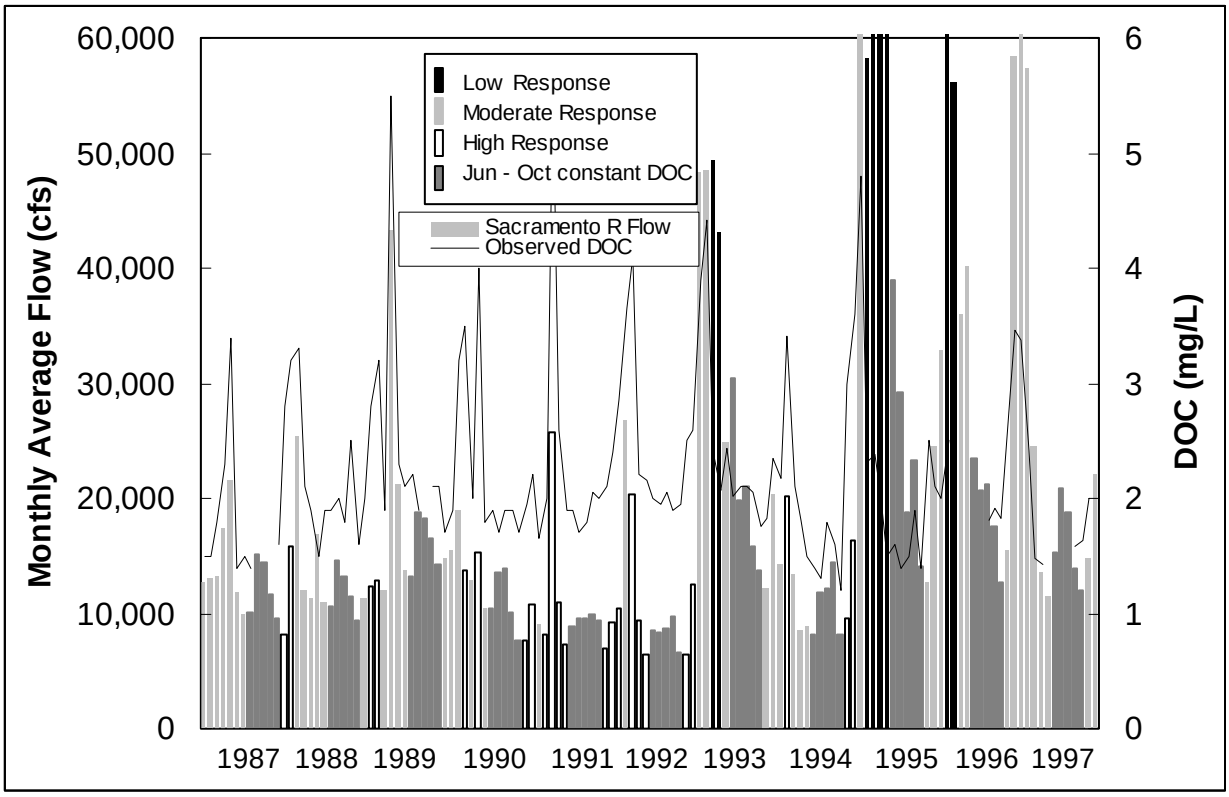

Figure 7.4: Observed DOC and Response to Flow at Greens Landing.

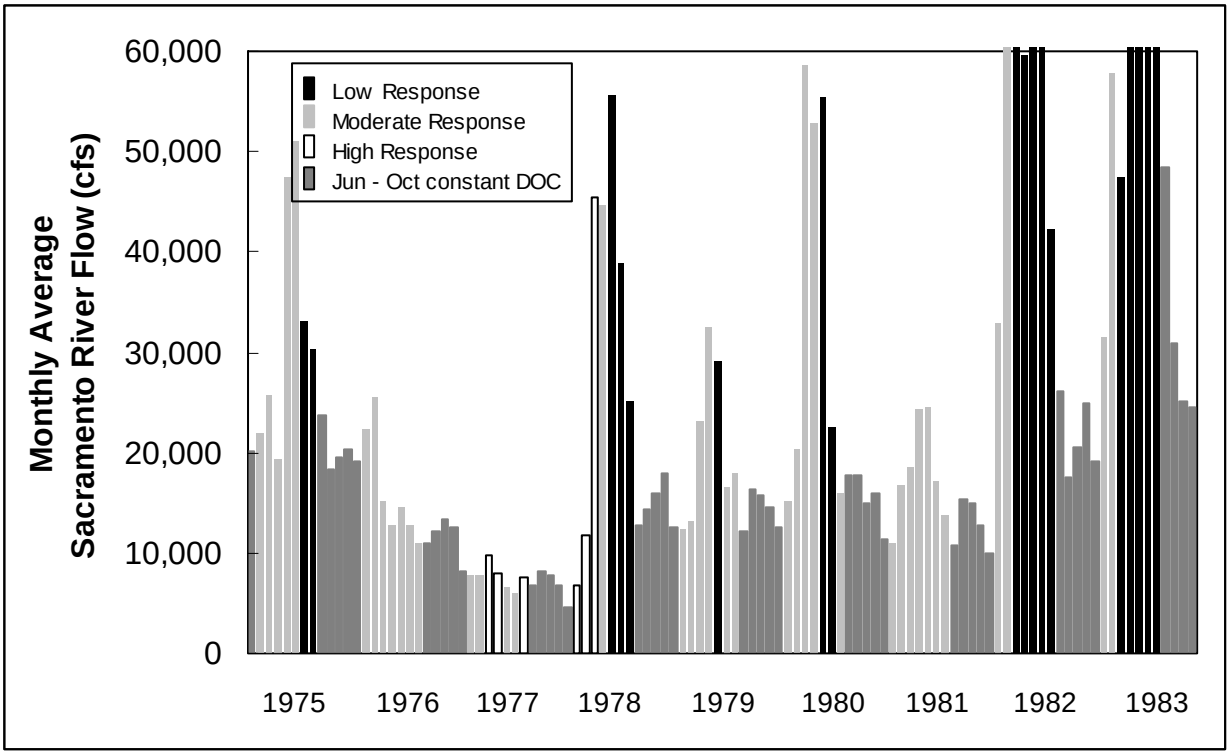

Figure 7.5a: Assignment of DOC/Flow Relationship at Greens Landing for Planning Period: 1975–1983.

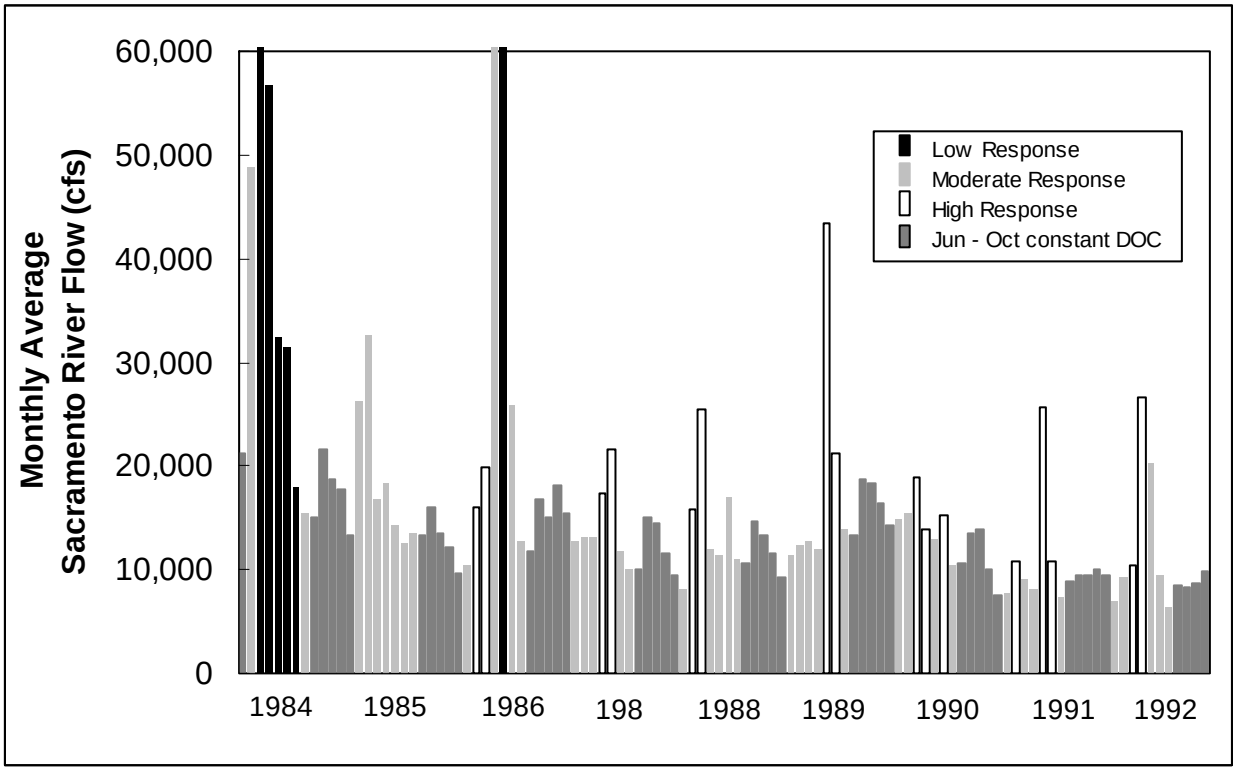

Figure 7.5b: Assignment of DOC/Flow Relationship at Greens Landing for Planning Period: 1984–1992.

After assigning a DOC of 1.81 mg/L to each month from June through October, appropriate regressions were applied to average flows from other months to generate monthly DOC. DOC derived from the regressions was limited to between 1.5 and 5.5 mg/L, the minimum and maximum values seen in the observed data. Figure 7.6 compares the historic DOC to the DOC generated by this method. Figure 7.7 and Table 7.2 show the resulting DOC over the planning period. Peak DOC occurred periodically when flow first increased in the fall or winter after several months of relatively low flow. The average DOC generated at Greens Landing by this process over the planning period was similar to the average observed DOC (Figure 7.8).

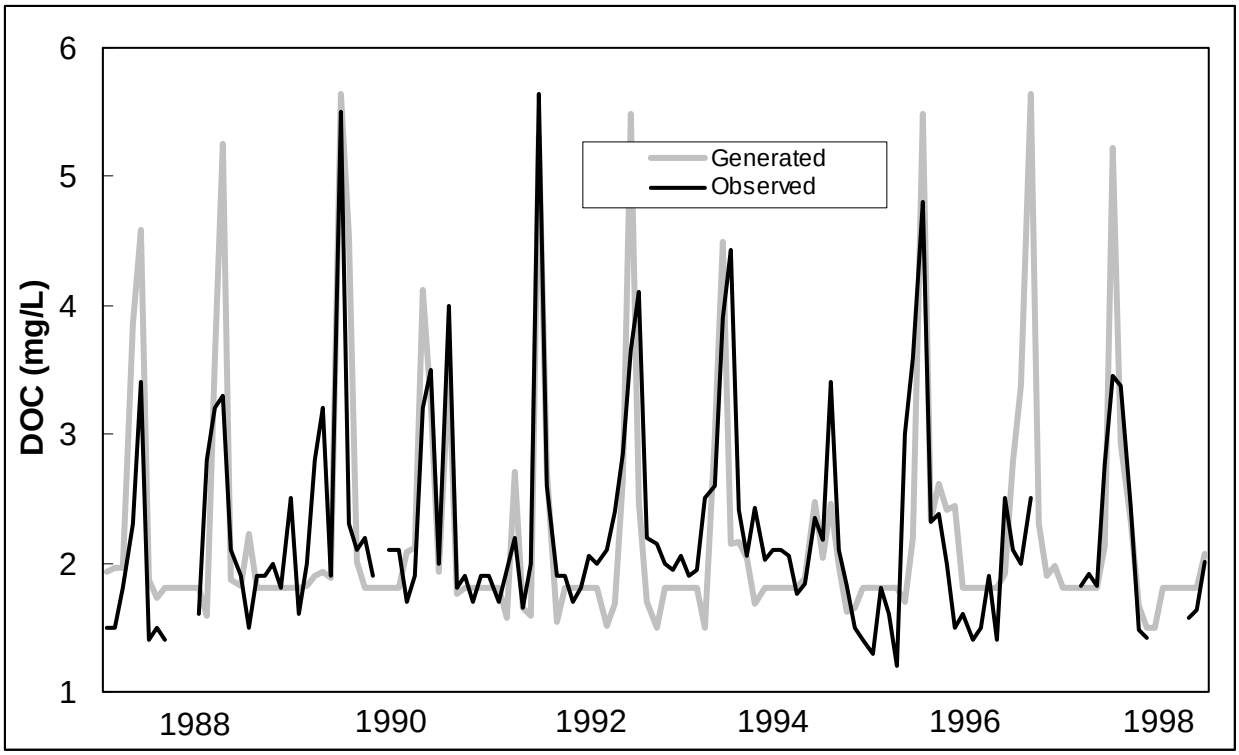

Figure 7.6: Observed and Generated DOC at Greens Landing.

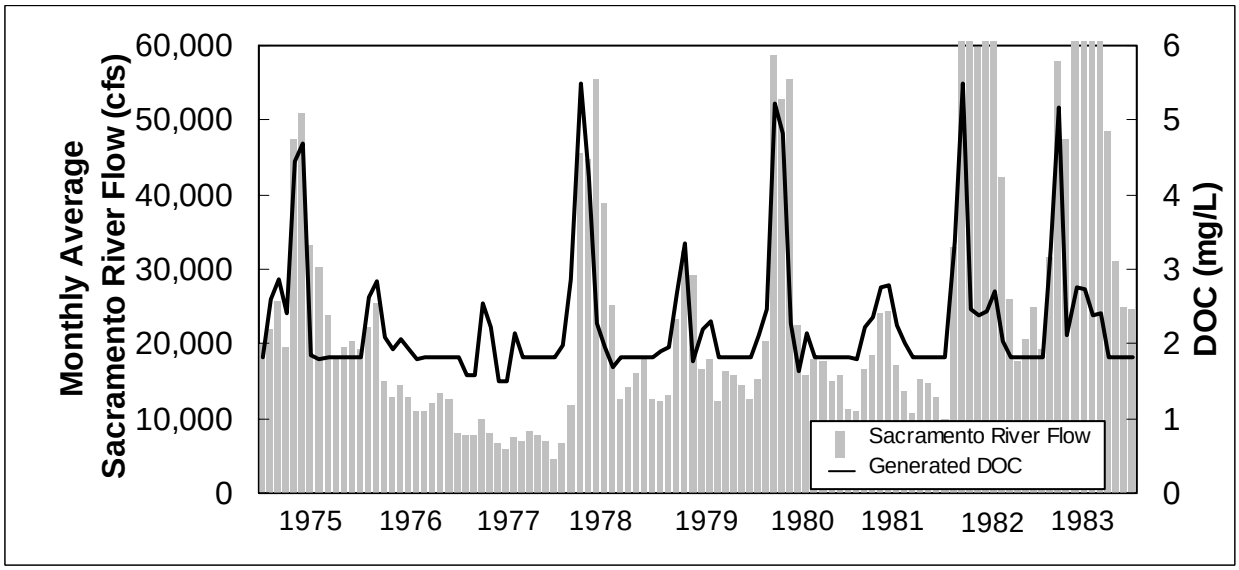

Figure 7.7a: Generated DOC at Greens Landing over the Planning Period: 1975–1983.

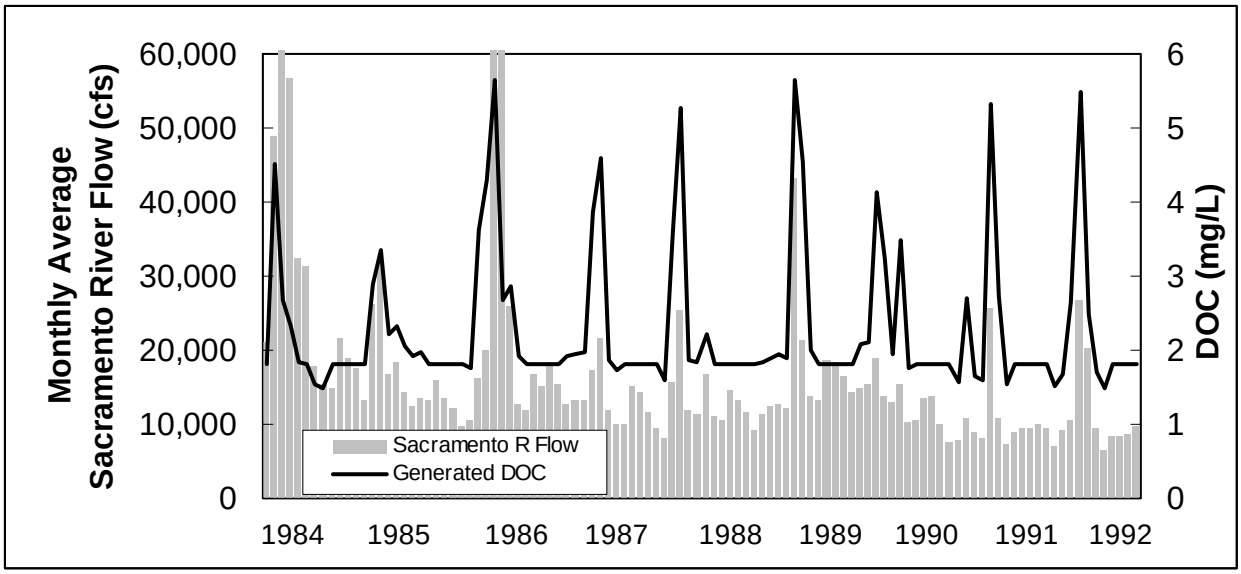

Figure 7.7b: Generated DOC at Greens Landing over the Planning Period: 1984–1992.

Table 7.2: Generated Monthly DOC at Greens Landing (values in mg/L).

Water Year	Oct	Nov	Dec	Jan	Feb	Mar	Apr	May	Jun	Jul	Aug	Sep
1975	1.81	2.60	2.86	2.41	4.43	4.68	1.84	1.78	1.81	1.81	1.81	1.81
1976	1.81	2.61	2.85	2.10	1.93	2.06	1.93	1.80	1.81	1.81	1.81	1.81
1977	1.81	1.58	1.57	2.53	2.22	1.50	1.50	2.15	1.81	1.81	1.81	1.81
1978	1.81	1.99	2.87	5.50	4.23	2.29	1.96	1.68	1.81	1.81	1.81	1.81
1979	1.81	1.91	1.96	2.68	3.35	1.76	2.20	2.31	1.81	1.81	1.81	1.81
1980	1.81	2.11	2.47	5.23	4.82	2.28	1.63	2.16	1.81	1.81	1.81	1.81
1981	1.81	1.80	2.21	2.34	2.76	2.78	2.25	2.00	1.81	1.81	1.81	1.81
1982	1.81	3.38	5.50	2.47	2.37	2.43	2.71	2.03	1.81	1.81	1.81	1.81
1983	1.81	3.28	5.17	2.13	2.76	2.74	2.39	2.42	1.81	1.81	1.81	1.81
1984	1.81	4.53	2.69	2.31	1.83	1.81	1.54	1.50	1.81	1.81	1.81	1.81
1985	1.81	2.90	3.36	2.22	2.33	2.04	1.91	1.98	1.81	1.81	1.81	1.81
1986	1.81	1.76	3.64	4.31	5.65	2.68	2.87	1.93	1.81	1.81	1.81	1.81
1987	1.81	1.92	1.96	1.96	3.86	4.59	1.86	1.73	1.81	1.81	1.81	1.81
1988	1.81	1.60	3.57	5.26	1.87	1.83	2.23	1.80	1.81	1.81	1.81	1.81
1989	1.81	1.83	1.90	1.94	1.88	5.65	4.54	2.01	1.81	1.81	1.81	1.81
1990	1.81	2.08	2.12	4.13	3.23	1.94	3.49	1.76	1.81	1.81	1.81	1.81
1991	1.81	1.57	2.71	1.66	1.60	5.32	2.72	1.54	1.81	1.81	1.81	1.81
Avg	1.81	2.32	2.91	3.01	3.01	2.85	2.33	1.92	1.81	1.81	1.81	1.81

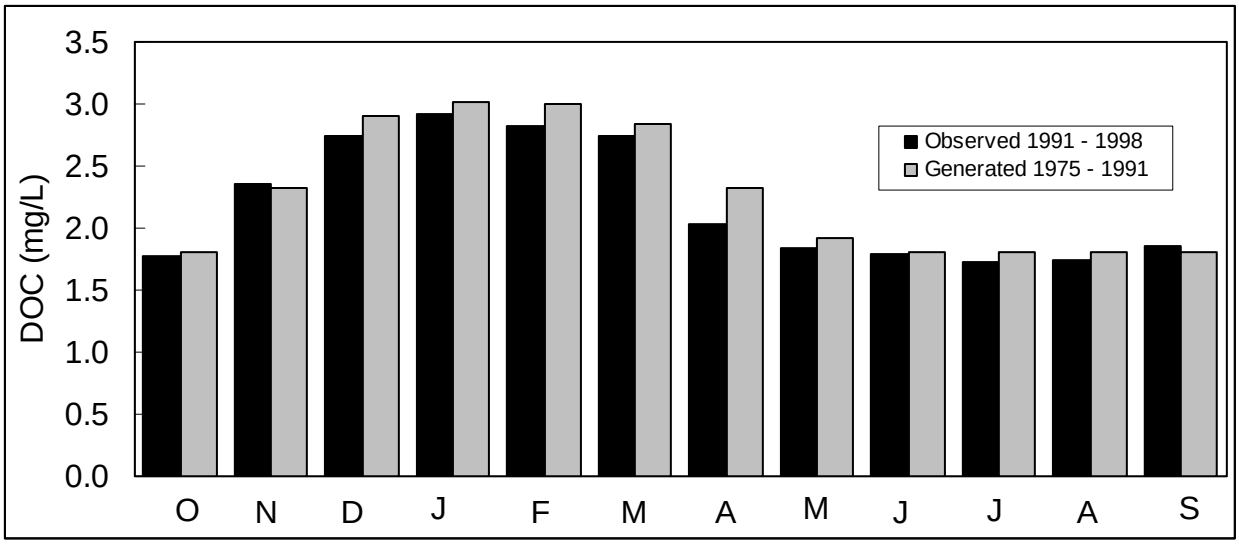

Figure 7.8: Monthly Average Observed and Generated DOC at Greens Landing.

7.3.2 Ultraviolet Absorbance at Greens Landing

UVA at Greens Landing was generated by applying a regression based on observed DOC and UVA at Greens Landing (Figure 7.9) to the generated DOC (Table 7.3).

$$UVA = 0.039DOC - 0.03 \qquad \text{[Eqn. 7-1]}$$
$$R^2 = 0.8$$

Where UVA is in units of 1/cm and DOC is in mg/L.

Average generated UVA at Greens Landing over the planning period was consistent with the average observed UVA at Greens Landing (Figure 7.10).

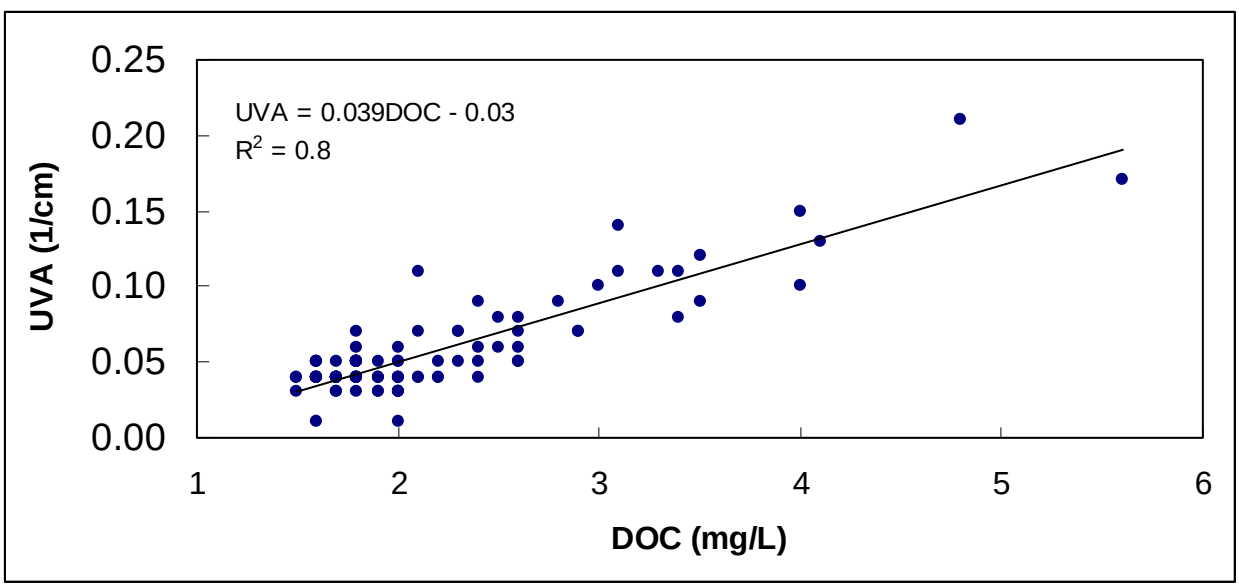

Figure 7.9: Observed UVA versus Observed DOC at Greens Landing.

Table 7.3: Generated Monthly UVA at Greens Landing (values in 1/cm).

Water Year	Oct	Nov	Dec	Jan	Feb	Mar	Apr	May	Jun	Jul	Aug	Sep
1975	0.04	0.07	0.08	0.07	0.14	0.15	0.04	0.04	0.04	0.04	0.04	0.04
1976	0.04	0.07	0.08	0.05	0.05	0.05	0.05	0.04	0.04	0.04	0.04	0.04
1977	0.04	0.03	0.03	0.07	0.06	0.03	0.03	0.06	0.04	0.04	0.04	0.04
1978	0.04	0.05	0.08	0.19	0.14	0.06	0.05	0.04	0.04	0.04	0.04	0.04
1979	0.04	0.05	0.05	0.08	0.10	0.04	0.06	0.06	0.04	0.04	0.04	0.04
1980	0.04	0.05	0.07	0.18	0.16	0.06	0.04	0.06	0.04	0.04	0.04	0.04
1981	0.04	0.04	0.06	0.06	0.08	0.08	0.06	0.05	0.04	0.04	0.04	0.04
1982	0.04	0.10	0.19	0.07	0.06	0.07	0.08	0.05	0.04	0.04	0.04	0.04
1983	0.04	0.10	0.17	0.05	0.08	0.08	0.06	0.07	0.04	0.04	0.04	0.04
1984	0.04	0.15	0.08	0.06	0.04	0.04	0.03	0.03	0.04	0.04	0.04	0.04
1985	0.04	0.08	0.10	0.06	0.06	0.05	0.05	0.05	0.04	0.04	0.04	0.04
1986	0.04	0.04	0.11	0.14	0.19	0.08	0.08	0.05	0.04	0.04	0.04	0.04
1987	0.04	0.05	0.05	0.05	0.12	0.15	0.04	0.04	0.04	0.04	0.04	0.04
1988	0.04	0.03	0.11	0.18	0.04	0.04	0.06	0.04	0.04	0.04	0.04	0.04
1989	0.04	0.04	0.05	0.05	0.04	0.19	0.15	0.05	0.04	0.04	0.04	0.04
1990	0.04	0.05	0.05	0.13	0.10	0.05	0.11	0.04	0.04	0.04	0.04	0.04
1991	0.04	0.03	0.08	0.04	0.03	0.18	0.08	0.03	0.04	0.04	0.04	0.04
Avg	0.04	0.06	0.08	0.09	0.09	0.08	0.06	0.05	0.04	0.04	0.04	0.04

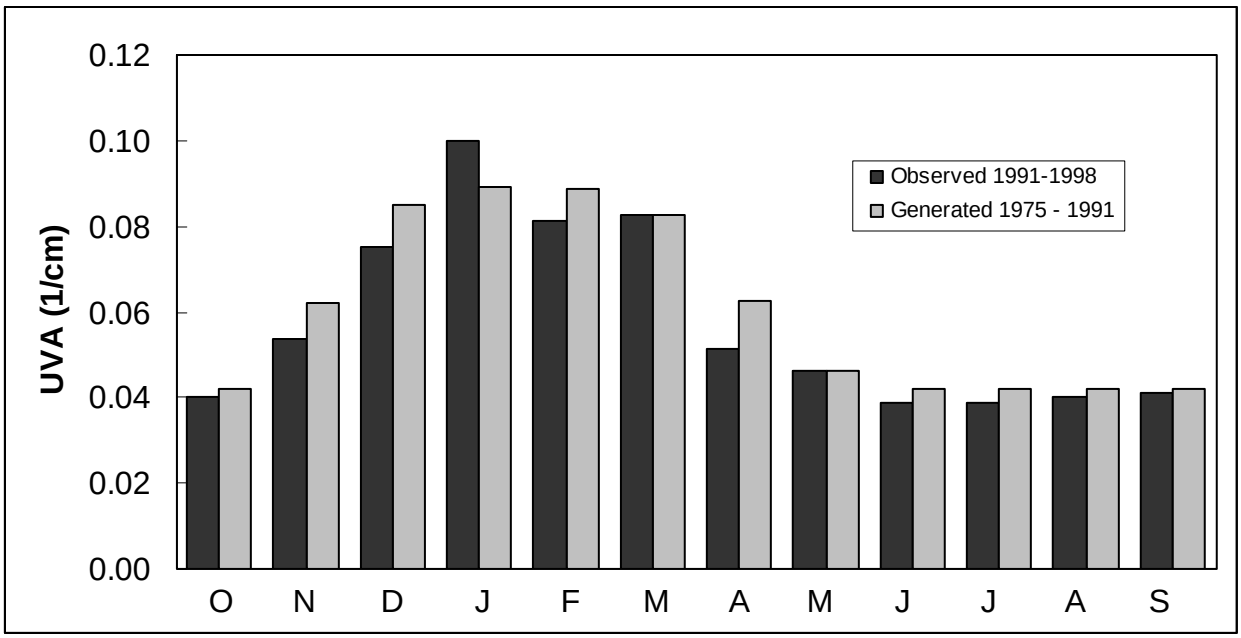

Figure 7.10: Monthly Average Observed and Generated UVA at Greens Landing.

7.4 San Joaquin River at Vernalis

7.4.1 Dissolved Organic Carbon at Vernalis

The method of generating DOC and UVA at Vernalis was similar to that described for Greens Landing. Figure 7.11 shows historic DOC and flow in the San Joaquin River at Vernalis. DOC

from Mossdale was used if available during times when Vernalis data was missing. Average observed DOC from June through October, 3.83 mg/L, approximated the monthly DOC over this interval for the planning period (Figure 7.12). DOC from other months again exhibited a pattern of high values associated with the first large flows of the fall/winter and low values after sustained high flows. The Vernalis/Mossdale DOC was partitioned according to DOC / flow values into four classifications, labeled “low”, “moderate-low”, “moderate-high”, or “high” DOC response to flow. Figure 7.13 and Table 7.4 show that, after excluding the June-October data, reasonable regressions could be found between DOC and flow.

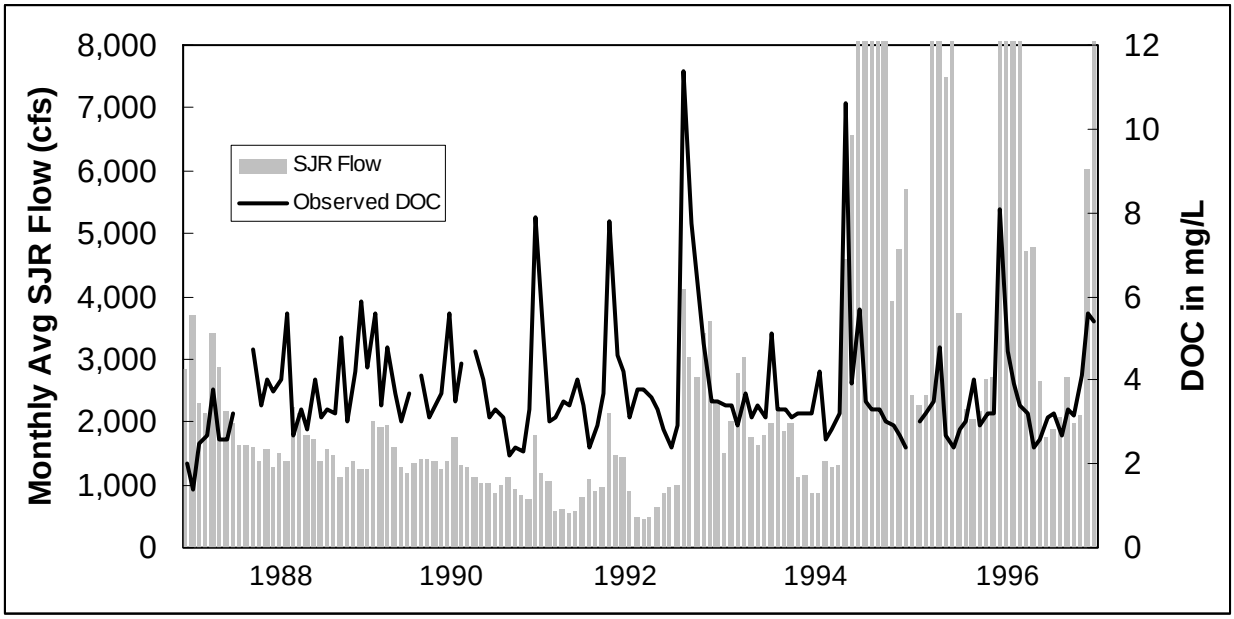

Figure 7.11: Observed DOC and Flow at Vernalis.

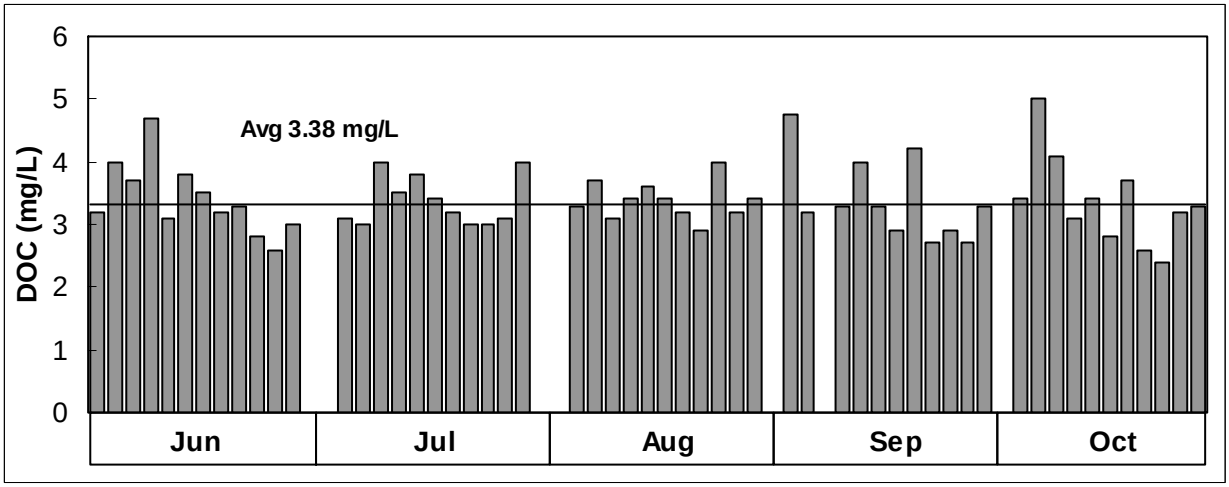

Figure 7.12: Observed DOC at Vernalis, 1987–1997 (Grouped by Month).

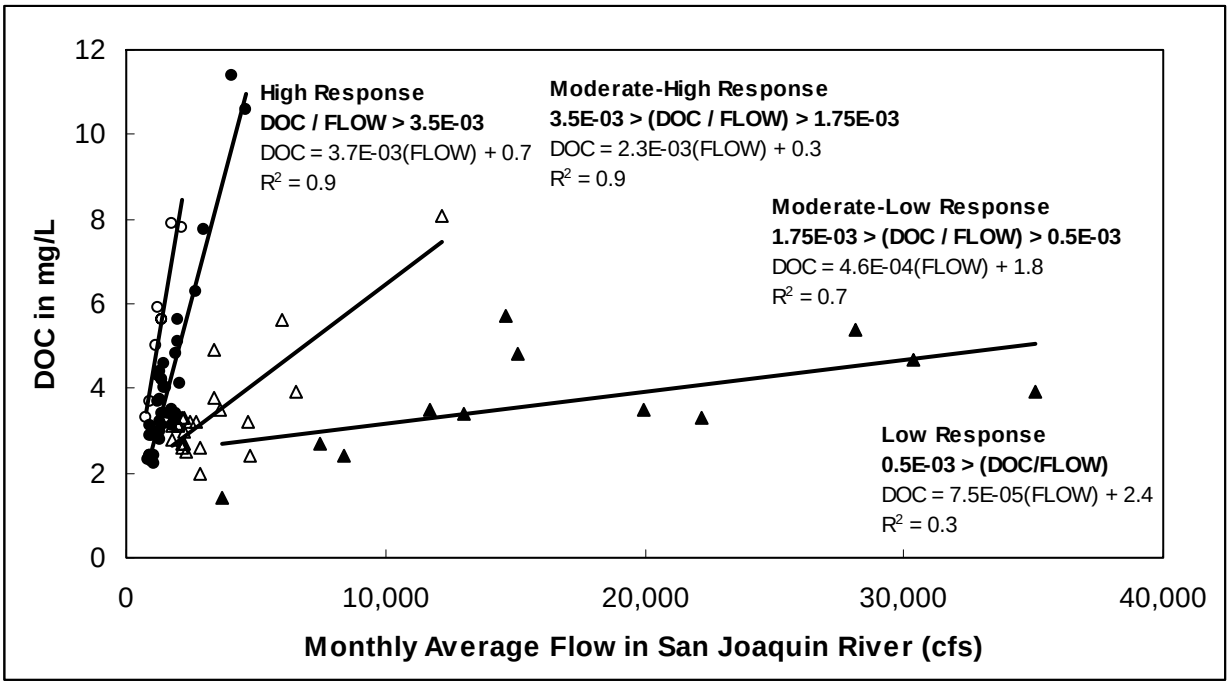

Figure 7.13: Observed DOC and Flow at Vernalis (Jun.–Oct. Data Removed).

Table 7.4: Classification of DOC Responses to Flow at Vernalis.

DOC Response to Flow	Criteria	Reqression Equation	R^2
Low	0.5E-03 > DOC / FLOW	DOC = 7.5E-05(FLOW) + 2.4	0.3
Moderate-Low	1.75E-03 > DOC / FLOW > 0.5E-03	DOC = 4.6E-04(FLOW) + 1.8	0.7
Moderate-High	20E-03 > DOC / FLOW > 1.75E-03	DOC = 2.3E-03(FLOW) + 0.3	0.9
High	DOC / FLOW > 20 E-03	DOC = 3.7E-03(FLOW) + 0.7	0.9

DOC: monthly dissolved organic carbon

FLOW: monthly average flow in San Joaquin River at Vernalis (cfs)

Historic DOC was then associated with "low," "moderate-low," "moderate-high", or "high" response to flow (Figure 7.14). The "high" DOC response to flow tended to be associated with the first significant flow after many months of low flow. Categories of DOC response to flow displayed in Figure 7.14 were assigned to the planning period by considering similar patterns in flow. This allowed each monthly flow during the planning period to be associated with either 3.83 mg/L DOC (June–October), or with one of four regressions with DOC (Figure 7.15).

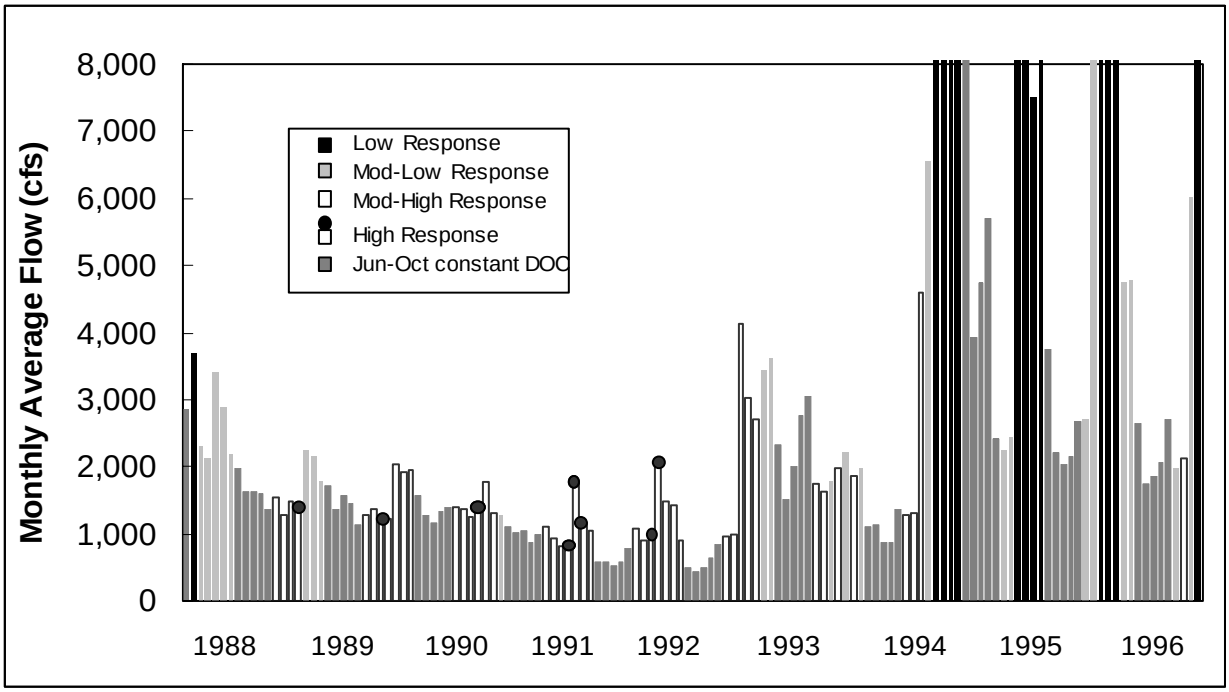

Figure 7.14: Historic SJR Flow at Vernalis Categorized by DOC Response to Flow.

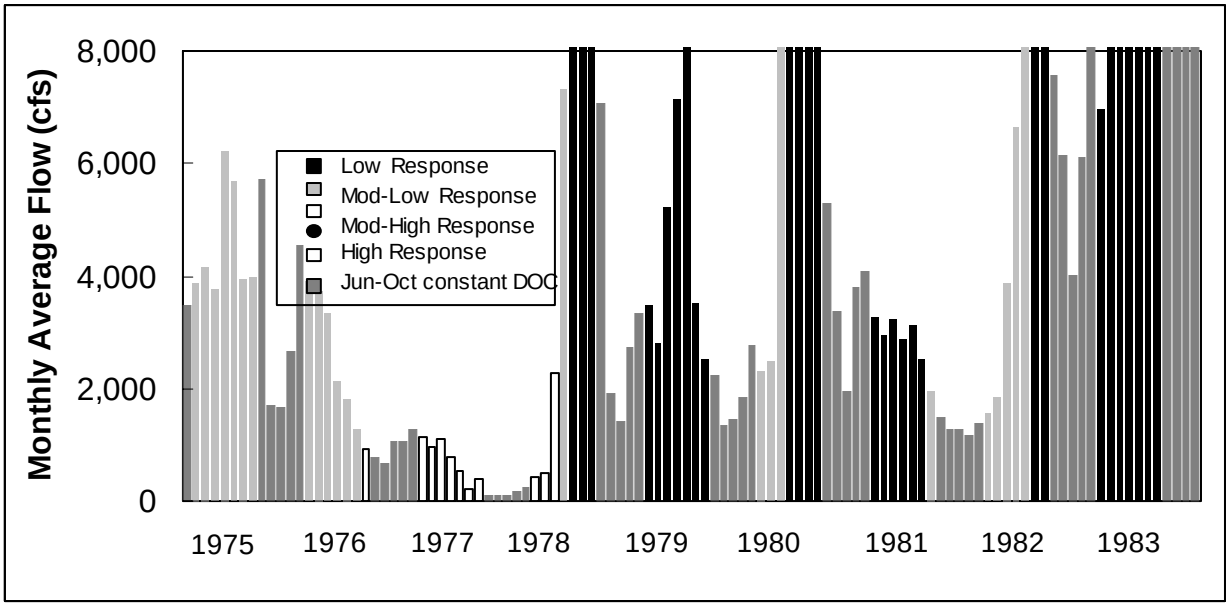

Figure 7.15a: Assignment of DOC/Flow Relationship at Vernalis for Planning Period: 1975–1983.

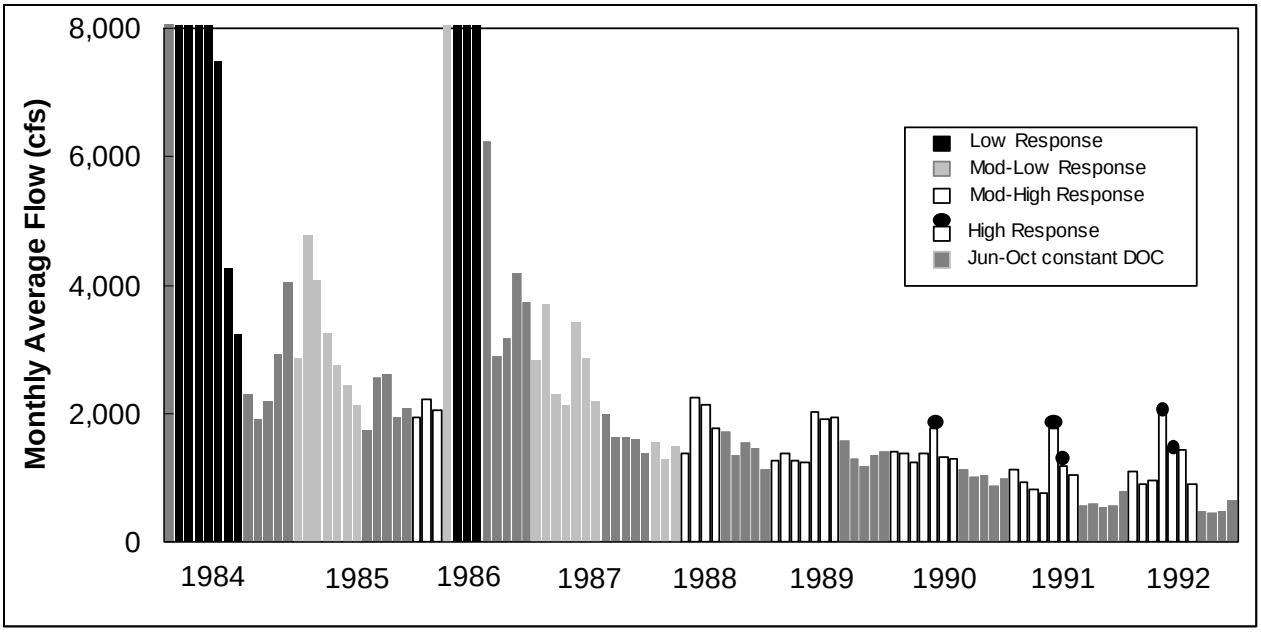

Figure 7.15b: Assignment of DOC/Flow Relationship at Vernalis for Planning Period: 1984–1992.

After assigning a DOC of 3.83 mg/L to each month from June though October, regressions were applied to average flows from other months to generate DOC. DOC derived from the regressions was limited to between 2.4 and 11.4 mg/L, the minimum and maximum values seen in the observed data. Figure 7.16 compares the historic Vernalis/Mossdale DOC to the DOC generated by this method. Figure 7.17 and Table 7.5 show the resulting generated DOC over the planning period. The average DOC generated at Vernalis by this process over the planning period was similar to the average observed DOC (Figure 7.18).

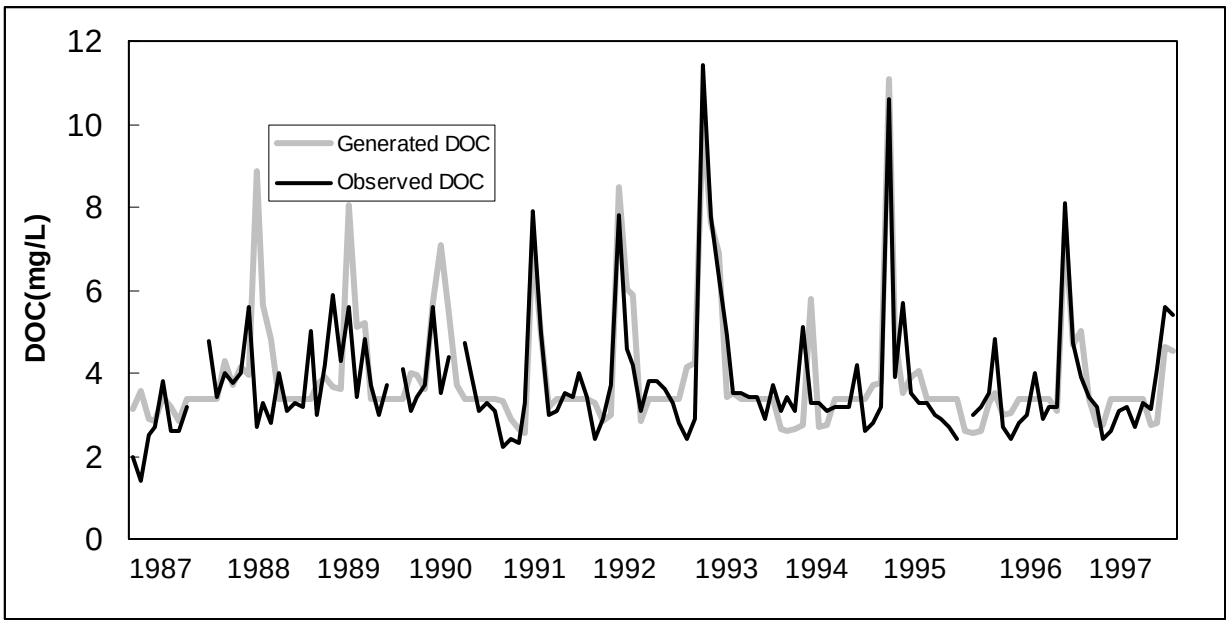

Figure 7.16: Observed and Generated DOC at Vernalis.

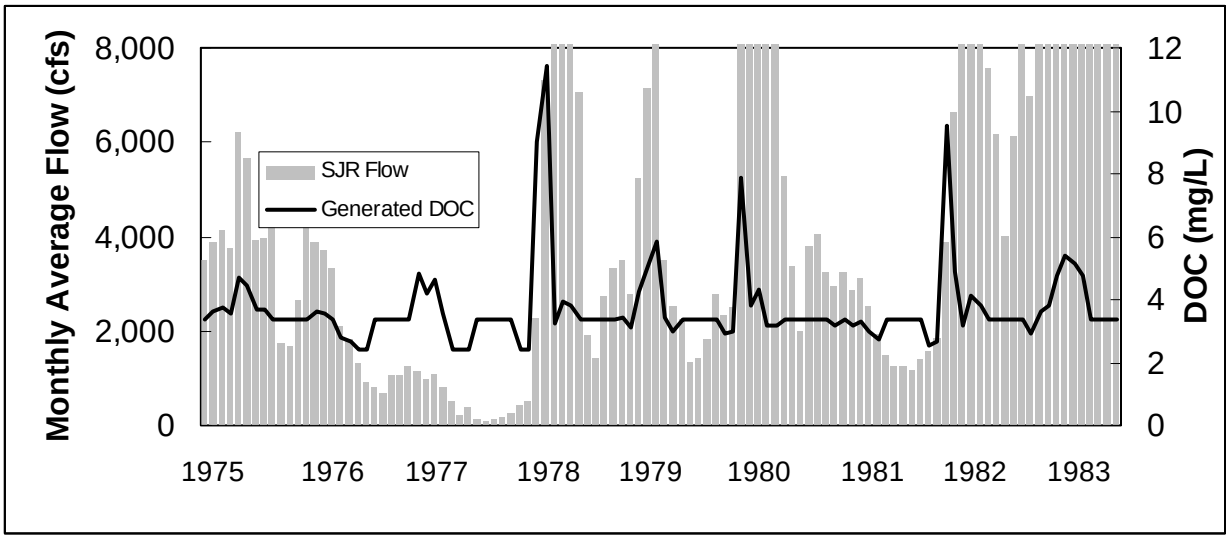

Figure 7.17a: Generated DOC at Vernalis over the Planning Period: 1975–1983.

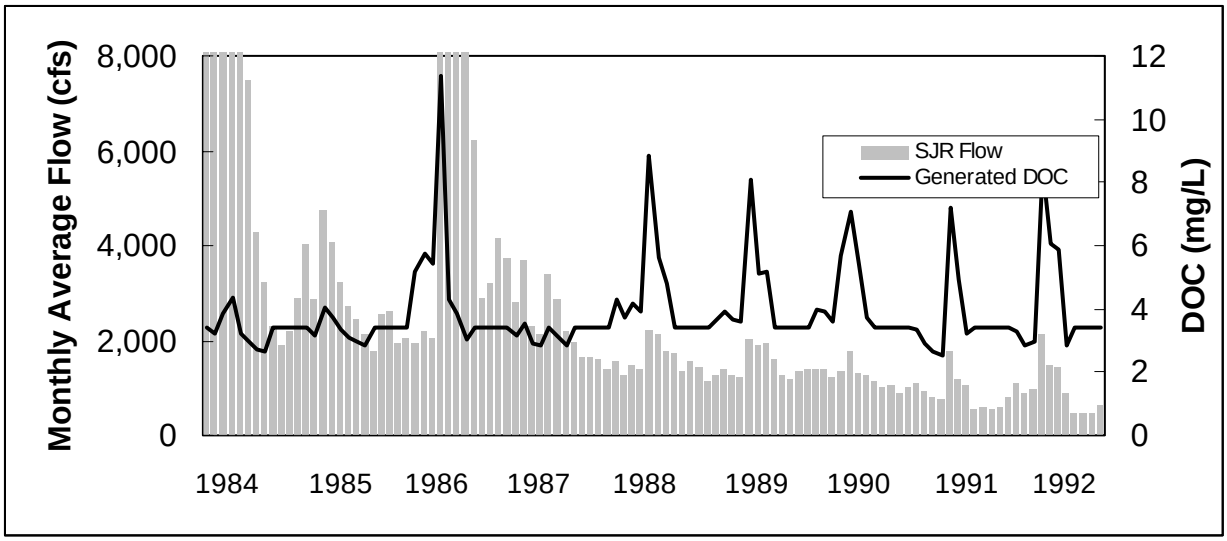

Figure 7.17b: Generated DOC at Vernalis over the Planning Period: 1984–1992.

Table 7.5: Generated DOC at Vernalis (values in mg/L).

Water Year	Oct	Nov	Dec	Jan	Feb	Mar	Apr	May	Jun	Jul	Aug	Sep
1975	3.38	3.64	3.76	3.58	4.71	4.47	3.67	3.68	3.38	3.38	3.38	3.38
1976	3.38	3.65	3.57	3.38	2.82	2.68	2.44	2.40	3.38	3.38	3.38	3.38
1977	3.38	4.83	4.20	4.66	3.56	2.40	2.40	2.40	3.38	3.38	3.38	3.38
1978	3.38	2.40	2.40	8.99	11.40	3.27	3.91	3.84	3.38	3.38	3.38	3.38
1979	3.38	3.46	3.14	4.26	5.14	5.84	3.46	3.01	3.38	3.38	3.38	3.38
1980	3.38	2.91	2.99	7.89	3.80	4.30	3.17	3.15	3.38	3.38	3.38	3.38
1981	3.38	3.35	3.20	3.34	3.17	3.28	3.01	2.75	3.38	3.38	3.38	3.38
1982	3.38	2.56	2.69	9.51	4.91	3.16	4.13	3.80	3.38	3.38	3.38	3.38
1983	3.38	2.93	3.64	3.84	4.78	5.41	5.14	4.79	3.38	3.38	3.38	3.38
1984	3.38	3.22	3.84	4.34	3.21	2.97	2.73	2.65	3.38	3.38	3.38	3.38
1985	3.38	3.16	4.05	3.72	3.34	3.11	2.97	2.82	3.38	3.38	3.38	3.38
1986	3.38	5.15	5.76	5.44	11.40	4.28	3.87	3.06	3.38	3.38	3.38	3.38
1987	3.38	3.15	3.55	2.90	2.83	3.42	3.16	2.85	3.38	3.38	3.38	3.38
1988	3.38	4.30	3.70	4.16	3.93	8.86	5.63	4.82	3.38	3.38	3.38	3.38
1989	3.38	3.69	3.91	3.65	3.60	8.06	5.12	5.19	3.38	3.38	3.38	3.38
1990	3.38	3.98	3.93	3.62	5.66	7.10	5.46	3.70	3.38	3.38	3.38	3.38
1991	3.38	3.34	2.90	2.67	2.54	7.17	4.94	3.19	3.38	3.38	3.38	3.38
Avg	3.38	3.51	3.60	4.70	4.75	4.69	3.84	3.42	3.38	3.38	3.38	3.38

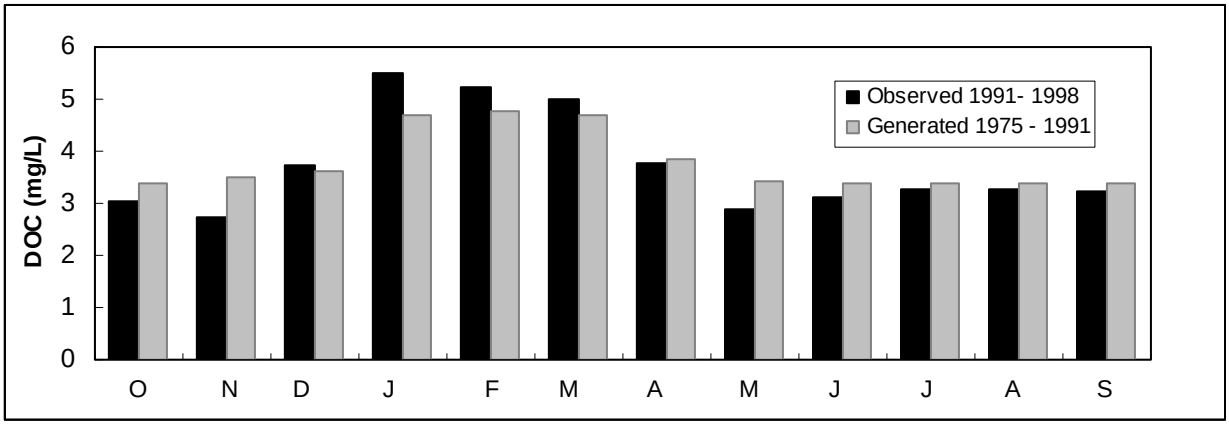

Figure 7.18: Monthly Average Observed and Generated DOC at Vernalis.

7.4.2 Ultraviolet Absorbance at Vernalis

UVA at Vernalis was generated by applying a regression based on observed DOC and UVA at Vernalis (Figure 7.19) to the generated DOC (Table 7.6):

$$UVA = 0.037DOC - 0.035 \qquad \text{[Eqn. 7-2]}$$
$$R^2 = 0.9$$

Average generated UVA at Vernalis over the planning period was consistent with the average observed UVA at Vernalis (Figure 7.20).

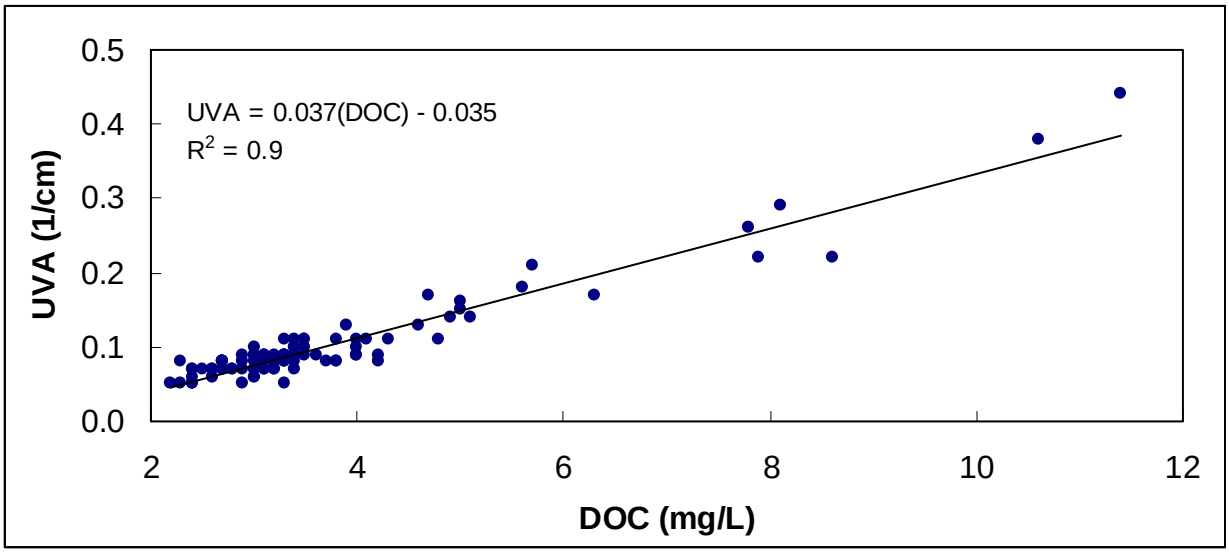

Figure 7.19: Observed UVA versus Observed DOC at Vernalis/Mossdale.

Table 7.6: Generated UVA at Vernalis (values in 1/cm).

Water Year	Oct	Nov	Dec	Jan	Feb	Mar	Apr	May	Jun	Jul	Aug	Sep
1975	0.09	0.10	0.10	0.10	0.14	0.13	0.10	0.10	0.09	0.09	0.09	0.09
1976	0.09	0.10	0.10	0.09	0.07	0.06	0.06	0.05	0.09	0.09	0.09	0.09
1977	0.09	0.14	0.12	0.14	0.10	0.05	0.05	0.05	0.09	0.09	0.09	0.09
1978	0.09	0.05	0.05	0.30	0.39	0.09	0.11	0.11	0.09	0.09	0.09	0.09
1979	0.09	0.09	0.08	0.12	0.16	0.18	0.09	0.08	0.09	0.09	0.09	0.09
1980	0.09	0.07	0.08	0.26	0.11	0.12	0.08	0.08	0.09	0.09	0.09	0.09
1981	0.09	0.09	0.08	0.09	0.08	0.09	0.08	0.07	0.09	0.09	0.09	0.09
1982	0.09	0.06	0.06	0.32	0.15	0.08	0.12	0.11	0.09	0.09	0.09	0.09
1983	0.09	0.07	0.10	0.11	0.14	0.16	0.15	0.14	0.09	0.09	0.09	0.09
1984	0.09	0.08	0.11	0.13	0.08	0.07	0.07	0.06	0.09	0.09	0.09	0.09
1985	0.09	0.08	0.11	0.10	0.09	0.08	0.07	0.07	0.09	0.09	0.09	0.09
1986	0.09	0.16	0.18	0.17	0.39	0.12	0.11	0.08	0.09	0.09	0.09	0.09
1987	0.09	0.08	0.10	0.07	0.07	0.09	0.08	0.07	0.09	0.09	0.09	0.09
1988	0.09	0.12	0.10	0.12	0.11	0.29	0.17	0.14	0.09	0.09	0.09	0.09
1989	0.09	0.10	0.11	0.10	0.10	0.26	0.15	0.16	0.09	0.09	0.09	0.09
1990	0.09	0.11	0.11	0.10	0.17	0.23	0.17	0.10	0.09	0.09	0.09	0.09
1991	0.09	0.09	0.07	0.06	0.06	0.23	0.15	0.08	0.09	0.09	0.09	0.09
Avg	0.09	0.09	0.10	0.14	0.14	0.14	0.11	0.09	0.09	0.09	0.09	0.09

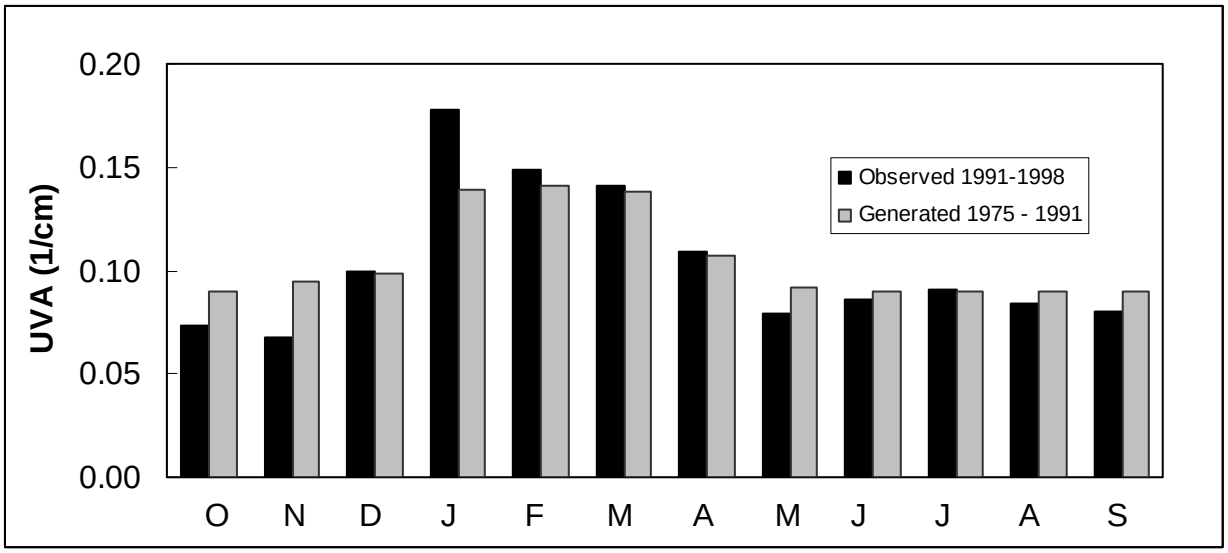

Figure 7.20: Monthly Average Observed and Generated UVA at Vernalis.

7.5 Mokelumne River

7.5.1 Dissolved Organic Carbon

Due to insufficient data, observed DOC from the American River was used to generate DOC for the Mokelumne River. Figure 7.21 shows historic DOC and flow in the American River. DOC from June through October was averaged to yield a single value of 1.66 mg/L to approximate monthly DOC each year during this interval for the planning period (Figure 7.22). Unlike Greens Landing and Vernalis, DOC in the American River in other months exhibited no apparent pattern with flows and therefore was simply averaged to yield two alternative values of DOC (Figure 7.23):

Low DOC = 1.74 mg/L
High DOC = 3.95 mg/L

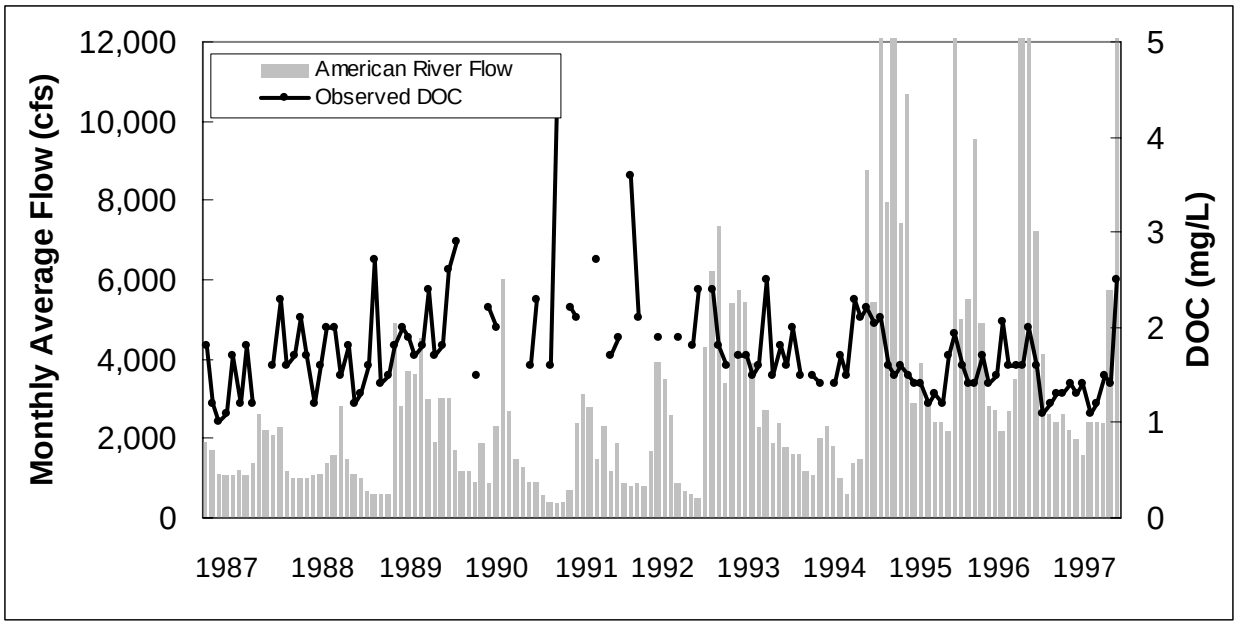

Figure 7.21: Observed DOC and Flow in the American River.

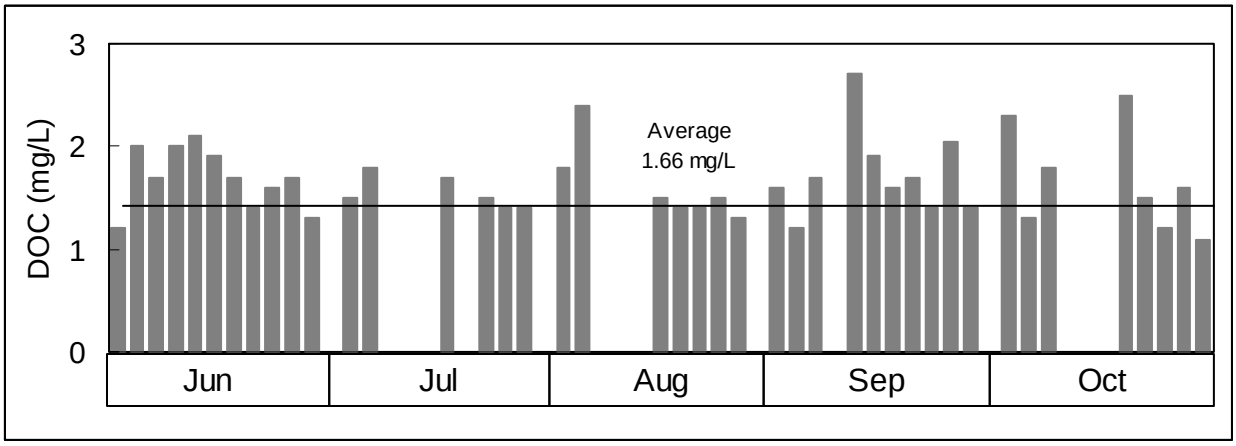

Figure 7.22: Observed DOC in the American River, 1987-1997 (Grouped by Month).

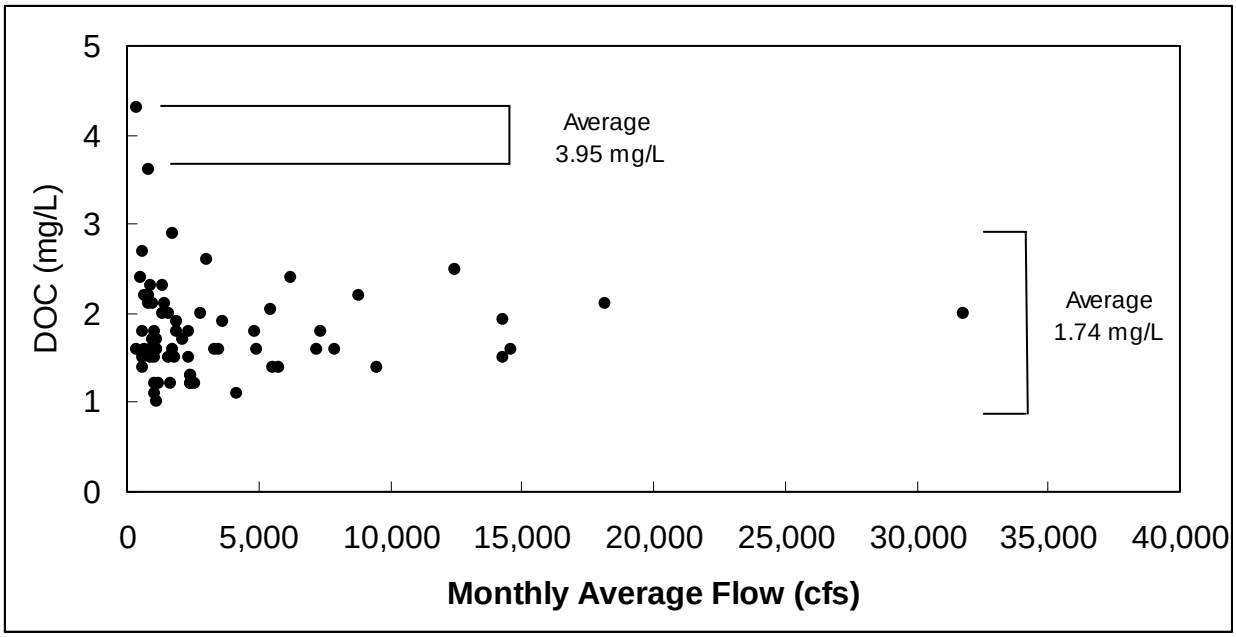

Figure 7.23: Flow and Observed DOC in the American River (Jun.–Oct. Data Removed).

These DOC values were then associated with flow in the Mokelumne River over the planning period, with 3.95 mg/L assigned to the first higher flows in the winter, 1.66 mg/L to June through October, and 1.74 mg/L to all other months (Figure 7.24, Table 7.7). The average DOC generated in the Mokelumne River by this process over the planning period was similar to the average observed DOC (Figure 7.25).

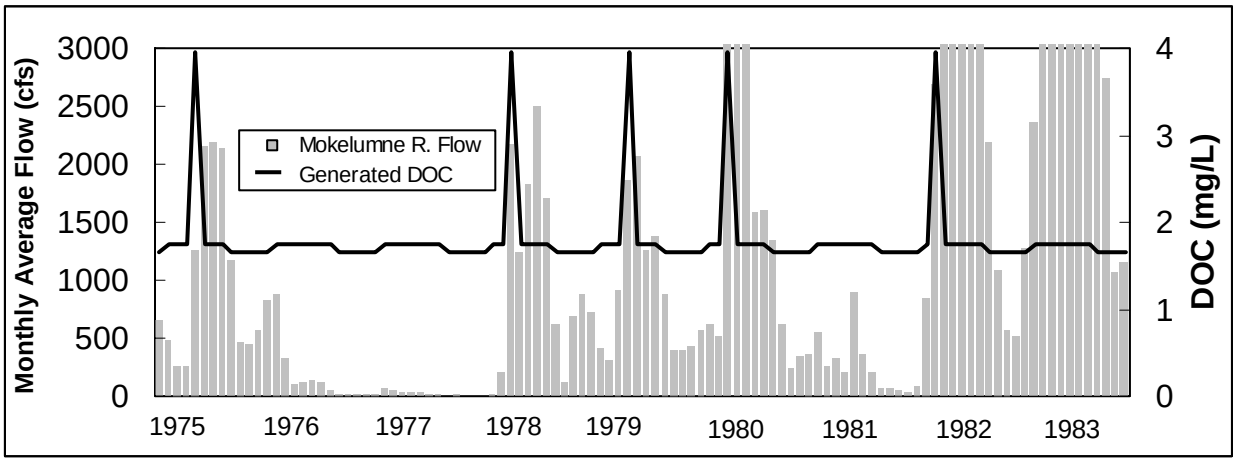

Figure 7.24a: Generated DOC in the Mokelumne River over the Planning Period: 1975–1983.

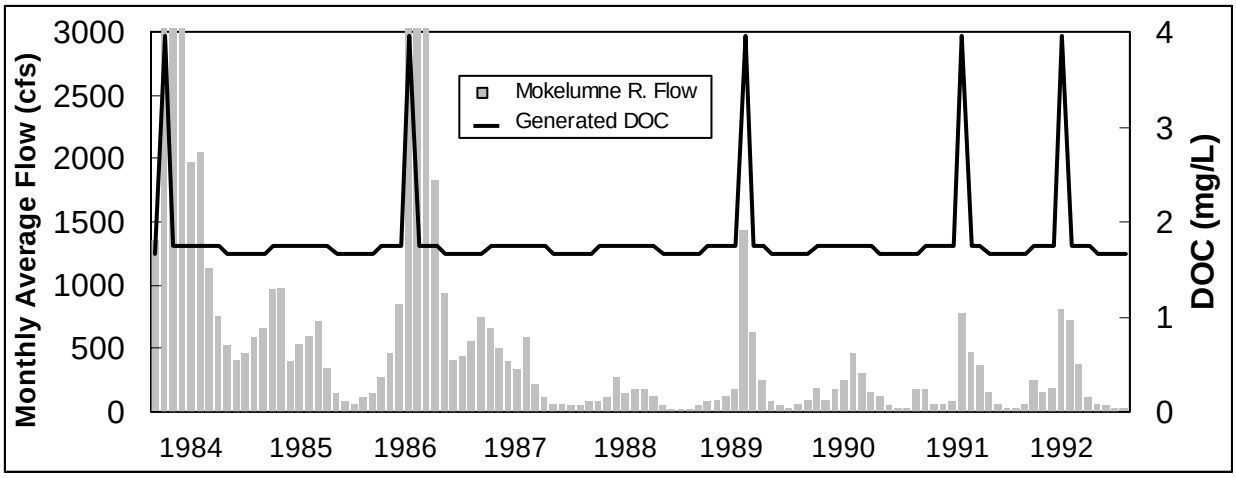

Figure 7.24b: Generated DOC in the Mokelumne River over the Planning Period: 1984–1992.

Table 7.7: Generated DOC in Mokelumne River (values in mg/L).

Water Year	Oct	Nov	Dec	Jan	Feb	Mar	Apr	May	Jun	Jul	Aug	Sep
1975	1.66	1.74	1.74	1.74	3.95	1.74	1.74	1.74	1.66	1.66	1.66	1.66
1976	1.66	1.74	1.74	1.74	1.74	1.74	1.74	1.74	1.66	1.66	1.66	1.66
1977	1.66	1.74	1.74	1.74	1.74	1.74	1.74	1.74	1.66	1.66	1.66	1.66
1978	1.66	1.74	1.74	3.95	1.74	1.74	1.74	1.74	1.66	1.66	1.66	1.66
1979	1.66	1.74	1.74	1.74	3.95	1.74	1.74	1.74	1.66	1.66	1.66	1.66
1980	1.66	1.74	1.74	3.95	1.74	1.74	1.74	1.74	1.66	1.66	1.66	1.66
1981	1.66	1.74	1.74	1.74	1.74	1.74	1.74	1.74	1.66	1.66	1.66	1.66
1982	1.66	1.74	3.95	1.74	1.74	1.74	1.74	1.74	1.66	1.66	1.66	1.66
1983	1.66	1.74	1.74	1.74	1.74	1.74	1.74	1.74	1.66	1.66	1.66	1.66
1984	1.66	3.95	1.74	1.74	1.74	1.74	1.74	1.74	1.66	1.66	1.66	1.66
1985	1.66	1.74	1.74	1.74	1.74	1.74	1.74	1.74	1.66	1.66	1.66	1.66
1986	1.66	1.74	1.74	1.74	3.95	1.74	1.74	1.74	1.66	1.66	1.66	1.66
1987	1.66	1.74	1.74	1.74	1.74	1.74	1.74	1.74	1.66	1.66	1.66	1.66
1988	1.66	1.74	1.74	1.74	1.74	1.74	1.74	1.74	1.66	1.66	1.66	1.66
1989	1.66	1.74	1.74	1.74	1.74	3.95	1.74	1.74	1.66	1.66	1.66	1.66
1990	1.66	1.74	1.74	1.74	1.74	1.74	1.74	1.74	1.66	1.66	1.66	1.66
1991	1.66	1.74	1.74	1.74	1.74	3.95	1.74	1.74	1.66	1.66	1.66	1.66
Avg	1.66	1.87	1.87	2.00	2.13	2.00	1.74	1.74	1.66	1.66	1.66	1.66

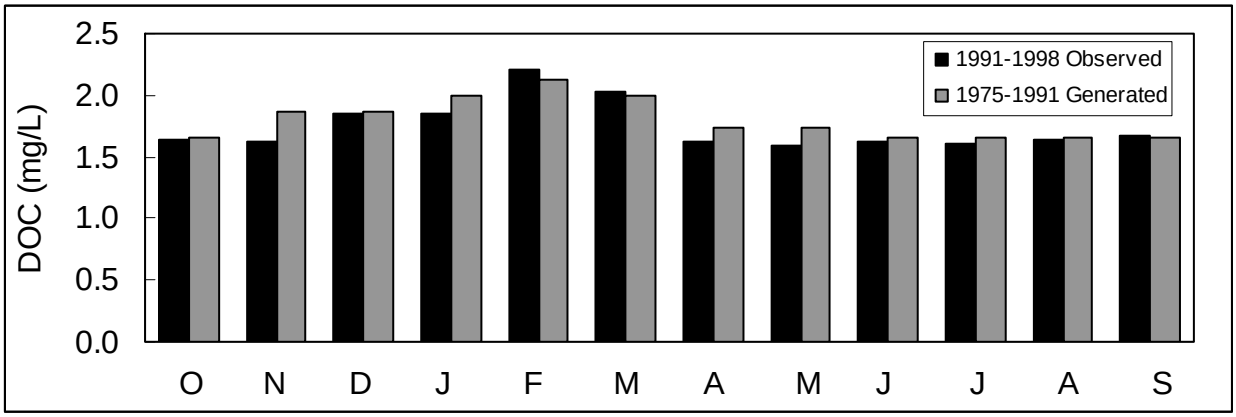

Figure 7.25: Monthly Average Observed and Generated DOC in the Mokelumne River.

7.5.2 Ultraviolet Absorbance

UVA in the Mokelumne River was generated by applying a regression based on historic DOC and UVA to the generated DOC (Figure 7.26, Table 7.8). Average generated UVA in the Mokelumne River over the planning period was consistent with the average observed UVA (Figure 7.27).

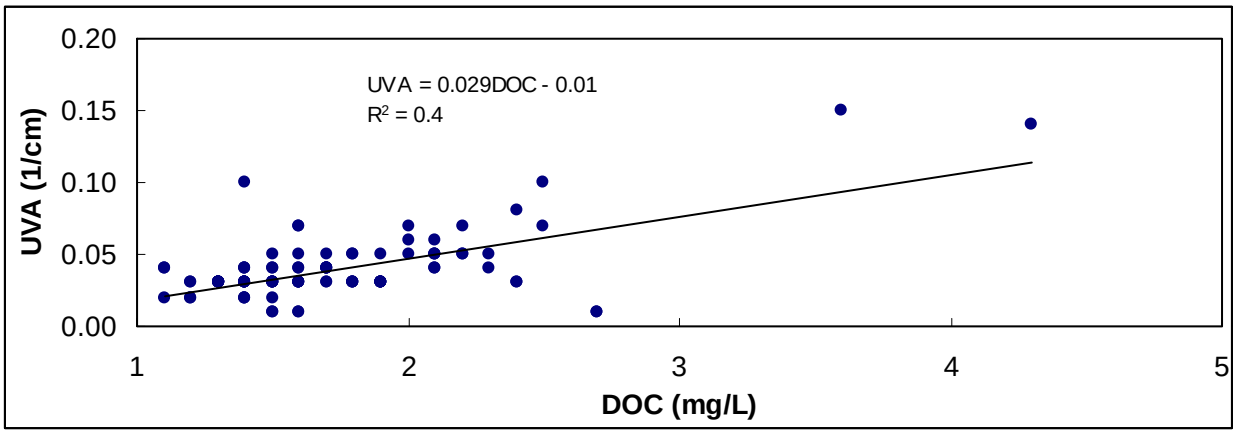

Figure 7.26: Observed UVA versus Observed DOC in the Mokelumne River.

Table 7.8: Generated UVA in Mokelumne River (values in 1/cm).

Water Year	Oct	Nov	Dec	Jan	Feb	Mar	Apr	May	Jun	Jul	Aug	Sep
1975	0.04	0.04	0.04	0.04	0.10	0.04	0.04	0.04	0.04	0.04	0.04	0.04
1976	0.04	0.04	0.04	0.04	0.04	0.04	0.04	0.04	0.04	0.04	0.04	0.04
1977	0.04	0.04	0.04	0.04	0.04	0.04	0.04	0.04	0.04	0.04	0.04	0.04
1978	0.04	0.04	0.04	0.10	0.04	0.04	0.04	0.04	0.04	0.04	0.04	0.04
1979	0.04	0.04	0.04	0.04	0.10	0.04	0.04	0.04	0.04	0.04	0.04	0.04
1980	0.04	0.04	0.04	0.10	0.04	0.04	0.04	0.04	0.04	0.04	0.04	0.04
1981	0.04	0.04	0.04	0.04	0.04	0.04	0.04	0.04	0.04	0.04	0.04	0.04
1982	0.04	0.04	0.10	0.04	0.04	0.04	0.04	0.04	0.04	0.04	0.04	0.04
1983	0.04	0.04	0.04	0.04	0.04	0.04	0.04	0.04	0.04	0.04	0.04	0.04
1984	0.04	0.10	0.04	0.04	0.04	0.04	0.04	0.04	0.04	0.04	0.04	0.04
1985	0.04	0.04	0.04	0.04	0.04	0.04	0.04	0.04	0.04	0.04	0.04	0.04
1986	0.04	0.04	0.04	0.04	0.10	0.04	0.04	0.04	0.04	0.04	0.04	0.04
1987	0.04	0.04	0.04	0.04	0.04	0.04	0.04	0.04	0.04	0.04	0.04	0.04
1988	0.04	0.04	0.04	0.04	0.04	0.04	0.04	0.04	0.04	0.04	0.04	0.04
1989	0.04	0.04	0.04	0.04	0.04	0.10	0.04	0.04	0.04	0.04	0.04	0.04
1990	0.04	0.04	0.04	0.04	0.04	0.04	0.04	0.04	0.04	0.04	0.04	0.04
1991	0.04	0.04	0.04	0.04	0.04	0.10	0.04	0.04	0.04	0.04	0.04	0.04
Avg	0.04	0.04	0.04	0.05	0.05	0.05	0.04	0.04	0.04	0.04	0.04	0.04

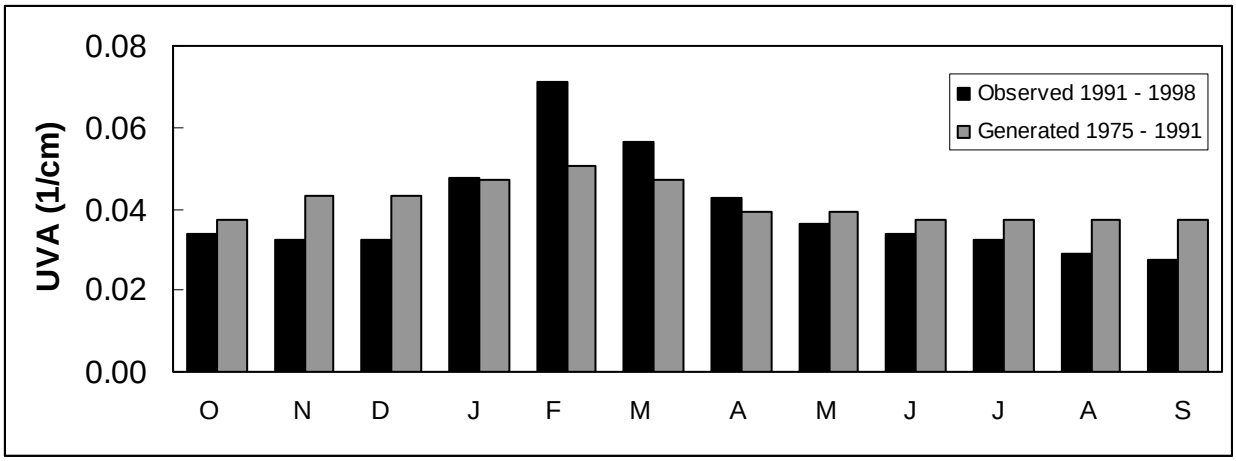

Figure 7.27: Monthly Average Observed and Generated UVA in the Mokelumne River.

Methodology for Flow and Salinity Estimates in the Sacramento-San Joaquin Delta and Suisun Marsh

23rd Annual Progress Report
June 2002

Chapter 8:
CALSIM Water Quality Operating Rules to Meet Delta Wetlands Water Quality Management Plan

Author: Tara Smith

8 CALSIM Water Quality Operating Rules to Meet Delta Wetlands Water Quality Management Plan

8.1 Introduction

CALSIM II requires operating rules to release flows to meet water demands and water quality standards. For the Delta water quality standards, CALSIM II uses an Artificial Neural Network (ANN) to determine if salinity standards are being met and adjusts the water supply in the Delta to meet those standards.

The operation of the proposed In-Delta Storage Project would affect water quality in a way that cannot currently be addressed by the ANN. ANN is trained using rimflows, exports, and Delta Cross Channel gate operations and provides salinity water quality results at select locations. The ANN has not been trained to provide salinity water quality results using a Delta hydrology that includes flows being taken and released from In-Delta Storage islands.

Additionally, there are other water quality criteria that have been listed in the Water Quality Management Plan (2000) for the In-Delta Storage project that are not addressed in CALSIM II. These also include criteria for total organic carbon (TOC), total trihalomethanes (TTHM), bromate (BRM), disolved oxygen (DO), and temperature. Figure 8.1 shows a summary of the criteria. All of the water quality constraints are described in greater detail in Hutton (2001).

The water quality criteria for the In-Delta Storage project requires that the water releases from the project islands do not adversely impact the ecosystem (temperature and DO) and do not degrade drinking water quality (TOC, Cl, TTHM, and BRM). This paper will address the preliminary work done in determining operating rules for CALSIM II that will address the In-Delta Storage Water Quality criteria. Developing these water quality rules will be an iterative process.

WATER QUALITY CRITERIA, IN-DELTA STORAGE PROGRAM

CRITERIA	JAN	FEB	MAR	APR	MAY	JUN	JUL	AUG	SEP	OCT	NOV	DEC
TOTAL ORGANIC CARBON (TOC)												
All export Locations (14-day average) (1)						<4.0 mg/L limit						
All export locations and Water TP intakes (14-day average) (2)					Incremental Increase <1.0 mg/L							
If TOC of stored water > TOC of channel water (3)		Discharge from Webb Tract or Bacon Island ranges from 40 cfs to 1,500 cfs depending on TOC										
CHLORIDE												
CCWD's intake and any urban water intake in the Delta (4)					< 10 mg/L Chloride							
Any urban intake in the Delta (5)					< 90% of salinity std.							
Limit discharge from Webb Tract and Bacon Island (6)			For chloride 0 - 250 mg/L, discharge 3,000 - 80 cfs									
DISINFECTION BYPRODUCTS (TTHM)												
Urban intake or treatment plant outlet (7)						< 64 µg/L TTHM						
BROMATE												
Urban intake or treatment plant outlet (8)						< 8 µg/L Bromate						
DISOLVED OXYGEN (DO)												
No discharge if DO in stored water is less than: (9)						< 6 mg/L						
No discharge if depressesDO of channel water to less: (10)						< 5.0 mg/L						
No discharge if DO in San Joaquin (Turner Cut to Stockton) (11)									< 6.0 mg/L			
TEMPERATURE												
No discharge if temperature differential (12)						>20º F						
For channel temp. 55º F to 66º F, limit increase to (13)						< 4º F						
For channel temp. 66º F to 77º F, limit increase to (14)						< 2º F						
For channel temp. > 77º F, limit increase to (15)						< 1º F						

FOOTNOTES

(1) Releases from storage reservoir ahould not cause the TOC concentration at any of the intakes of SWP, CVP, CCWD pumping plant, or urban water treatment plant (ALL INTAKES) to exceed 4.0 mg/L (14-day average).

(2) Incremental increase of TOC concentration at ALL INTAKES should not exceed 1.0 mg/L (14-day average).

(3) Discharge from Bacon Island and Webb Tract is limited to a declining scale if TOC concentration of stored water is higher than TOC of channel water

(4) Chloride concentrations at ALL INTAKES shall not ecxeed 10.0 mg/L.

(5) Operation of Delta Wetlands Project should not cause or contribute to salinity increase at ALL INTAKES if salinity at the intake is at 90% of an adopted standard.

(6) If chloride concentration of stored water is higher than of the channel water, the conbined discharge from storage islands will be limited depending on the incremental differencial.

(7) Modeled or predicted TTHM concentration at ALL INTAKES or the outlet of a water treatment plant should be caused by the Project to exceed 64 µg/L.

(8) Modeled or predicted bromate concentration at ALL INTAKES or the outlet of a water treatment plant should be caused by the Project to exceed 8 µg/L.

(9) Stored water will not be discharged if DO is less than 6 mg/L.

(10) Stored water will not be discharged if it would cause the DO of the mixture with channel water to drop less than 5.0 mg/L.

(11) Stored water will not be discharged if the operation would decrease the DO of San Joaquin River between Turner Cut and Stockton to less than 6.0 mg/L.

(12) Stored water will not be discharged in the channels if the temperature differential is more than 20º F .

(13) No discharge of stored water if it will increase the channel water temperature by more than 4º F when the channel water temperture is between 55º F and 66º F.

(14) No discharge of stored water if it will increase the channel water temperature by more than 2º F when the channel water temperture is between 66º F and 77º F.

(15) No discharge of stored water if it will increase the channel water temperature by more than 1º F when the channel water temperture is higher than 77º F.

Figure 8-1: Water Quality Criteria, In-Delta Storage Program (Bindra, 2001).

8.2 CALSIM II

Because CALSIM II is not designed for water quality modeling, determining if water quality standards are exceeded in the Delta is not an easy task. As previously discussed, CALSIM II uses an ANN to determine salinity at selected locations based on flows and Delta Cross Channel operation. Other water quality constraints would also require using information available from CALSIM II such as flows and would require implementing water quality modules within the code. In these situations, the processes affecting water quality would be simplified and would be a gross estimate of the effects of project operations.

There are several possible combinations of factors that can influence the operation of the projects. The various possible operations of the project to limit TOC at the urban intake locations are used to illustrate this point. To reduce the amount of TOC released from the islands the following operations could be considered:

- Water diverted onto the island could be constrained by the quality of intake water.
- The time the water is stored on the island, the temperature of the water and its depth will affect the quality of the water. The amount of release and when it is released could be based on these island storage factors.
- When the water is released from the project islands, it will have to meet water quality criteria at the urban intake locations. This meeting of the criteria could be addressed in the previous steps but could also be addressed by adjusting the amount of water that can be released.

Determining the operation that will optimize the quality and quantity of water released from the project islands will require iterations and analysis with DSM2. Discussed below are the various water quality criteria and factors that should be considered in determining operating rules.

8.3 Chloride

Diversions onto the project islands and releases from the islands will affect the hydrodynamics of the Delta system and could affect the transport of ocean salinity. This transport would affect the chloride levels. To address this issue, the ANN would be trained with project island releases and diversions.

The amount of flow diverted onto the reservoir islands in CALSIM II should be inversely proportional to the chloride levels at Old River at Rock Slough (the station closest to the project islands where that ANN determines quality). As the chloride levels increase, the amount of diversion decreases. This decrease in diversion is done to maintain low salinity levels within the reservoir. Because not all of the water may be diverted at one time, CALSIM II will need to calculate the changing concentration in the project reservoirs due to inflows and evaporation/precipitation.

The amount of water released will be determined by the effect that the release water has on quality. If the water has low levels of chloride, then the chloride quality will not be a controlling factor. If releasing the water results in a violation of the standard at Rock Slough, then the amount of water released will be less. A preliminary equation to prevent the standard from being violated was proposed by Wang (2001). The concept presented by Wang was further refined and modified by Easton (2002). The proposed operation is shown in Figure 8-2 and is described in the following paragraphs.

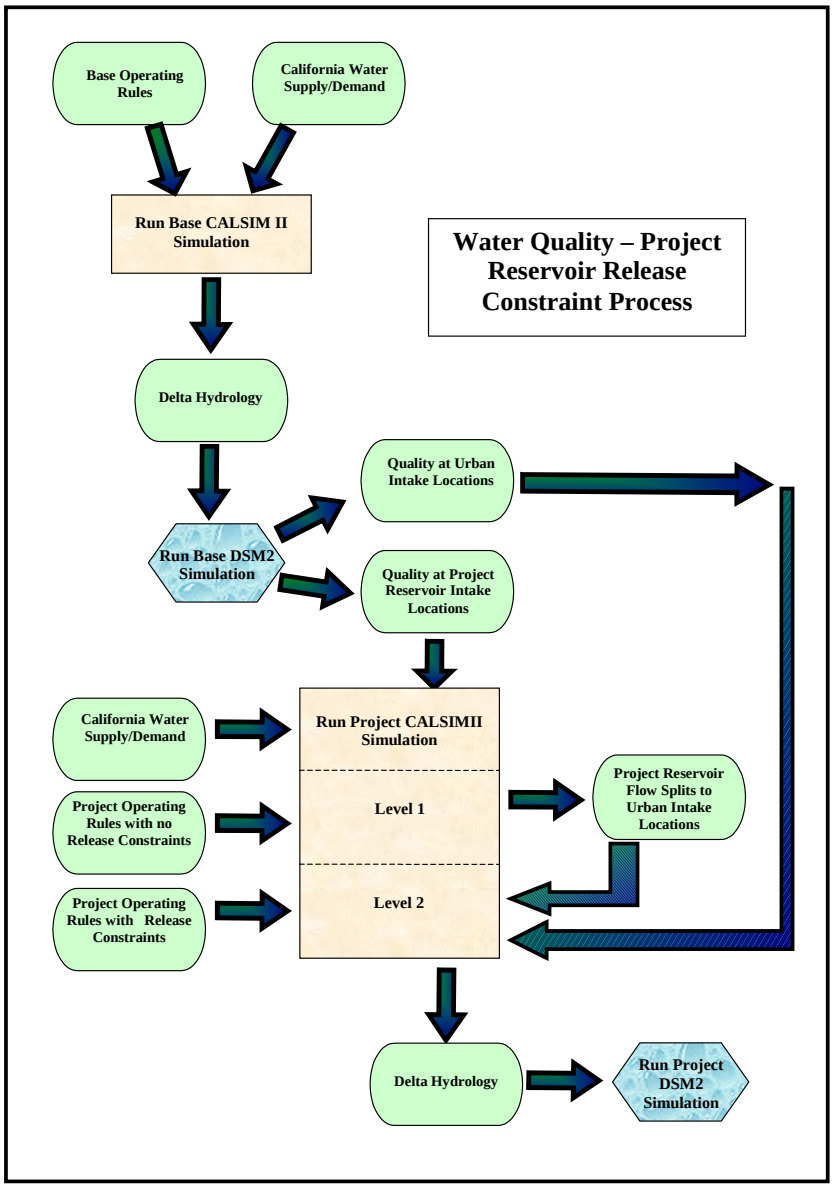

Figure 8-2: Water Quality – Project Reservoir Release Constraint Process.

8.3.1 Base Chloride Study

Begin the operation by running the CALSIM II base simulation. Using the Delta hydrology generated in that simulation, run a base DSM2 simulation. This simulation will generate a chloride concentration time series at various water quality locations in the Delta.

Use the base DSM2 chloride concentration time series generated at project intake locations as the island diversion concentrations in the CALSIM II project simulation. Also, use the base DSM2 chloride concentration time series generated at the Delta export locations as the chloride constraint basis of measure in the CALSIM II project simulation.

8.3.2 Project Study Using Chloride Constraints

Continue the operation by running the CALSIM II project simulation. This simulation is a multi-layered model that generates a dispersion mechanism in one layer for the application of the chloride constraints in another. Dispersion of chloride released from the islands is based on the split of exports without the chloride constraints.

For example, say Delta exports are pumped at the following rates without the chloride constraints: Tracy, 4,200 cfs; Banks, 5,600 cfs; and Contra Costa Water District (CCWD), 200 cfs. In the following model layer, island discharge and its associated chloride concentration would be fractionally dispersed to the three export locations as follows: Tracy 42%, Banks 56%, and CCWD 2%. Chloride constraints would be based on the resulting mixture of Delta water and island discharge at each export intake. It is assumed that all water coming off islands will go to one of the exports. This assumption is not necessarily true (especially for Webb Tract). Future modifications to the constraint equations could be made to account for water not being exported.

The constraint will limit the concentration of the project water at the urban intakes to be less then the base concentration plus 10 mg/L. Under the Water Quality Management Plan (WQMP), the project cannot exceed the base concentration by 10 mg/L.

Constraints for Tracy:

$$\frac{Q_1' C_1 + f_1 \left(Q_4 C_4 + Q_5 C_5 \right)}{Q_1} \leq C_1 + 10 \qquad \text{[Eqn. 8-1]}$$

$$Q_1' = Q_1 - f_1 \left(Q_4 + Q_5 \right) \qquad \text{[Eqn. 8-2]}$$

Constraints for Banks:

$$\frac{Q_2' C_2 + f_2\left(Q_4 C_4 + Q_5 C_5\right)}{Q_2} \le C_2 + 10 \qquad \text{[Eqn. 8-3]}$$

$$Q_2' = Q_2 - f_2\left(Q_4 + Q_5\right) \qquad \text{[Eqn. 8-4]}$$

Constraints for CCWD:

$$\frac{Q_3' C_3 + f_3\left(Q_4 C_4 + Q_5 C_5\right)}{Q_3} \le C_3 + 10 \qquad \text{[Eqn. 8-5]}$$

$$Q_3' = Q_3 - f_3\left(Q_4 + Q_5\right) \qquad \text{[Eqn. 8-6]}$$

where,

Q_1 = Tracy export rate (cfs),
Q_2 = Banks export rate (cfs),
Q_3 = Contra Costa export rate (cfs),
Q_4 = Bacon Island Release Rate (cfs),
Q_5 = Webb Tract Release Rate (cfs),
Q_1' = Export of water not released from IDS islands at Tracy (cfs),
Q_2' = Export of water not released from IDS islands at Banks (cfs),
Q_3' = Diversion of water not released from IDS islands at CCWD (cfs),
C_1 = Chloride Concentration at Tracy (mg/L) from base DSM2 simulation,
C_2 = Chloride Concentration at Banks (mg/L) from base DSM2 simulation,
C_3 = Chloride Concentration at CCWD (mg/L) from base DSM2 simulation,
C_4 = Concentration of Bacon Island Water (mg/L),
C_5 = Concentration of Webb Tract Water (mg/L),
f_1 = Dispersion fraction at Tracy,
f_2 = Dispersion fraction at Banks, and
f_3 = Dispersion fraction at CCWD.

From preliminary DSM2 simulations that were made previously to evaluate the In-Delta Storage project, the 10 mg/L change in the chloride constraint was violated during time periods that did not have significant project reservoir diversions or releases. The violation occurred because of a general reoperation of the system. To address this, additional operational rules were

implemented. In these rules, chloride quality in the project simulation could not exceed the CALSIM II base case quality by 10 mg/L or more. Due to differences in how DSM2 and ANN calculate quality, the 10 mg/L chloride constraint was still occasionally exceeded in the DSM2 simulation. Future work may tighten the rules in CALSIM II so that no degradation of water quality in the project simulation occurs.

8.4 Total Organic Carbon

There are three areas that have to be considered when looking at TOC quality and its effects on drinking water quality. The first is the quality of the water diverted onto the project islands, the second is the increase in TOC in the project reservoirs due to the interaction with the peat soil and bioproductivity, and the third area is the release quality and quantity from the project islands.

Diversion of water onto the reservoir islands takes place in excess flow conditions. TOC levels tend to be high during the first major precipitation event. Water diverted to the reservoir island during this time will have higher TOC than the water in the channels during times of reservoir island release. Operating rules may need to consider limiting the amount of water diverted during these events.

While the water stays in the project island reservoir, it interacts with the peat soil and the TOC levels increase (Jung, 2001). Additionally, TOC increases due to bioproductivity (Duvall, 2001). This increase depends on the length of time the water is stored, the depth of the water, and the temperature of the water, among other factors. Operating rules may need to consider these factors in determining when and how much water can be released. A possible operating rule to limit the increase of TOC would be to release the project island water first to meet south of Delta demands instead of releasing from upstream reservoirs (which would decrease the retention time on the island reservoirs). Furthermore, a rule to retain a small amount of water in the project island may be made to limit bioproductivity.

Since CALSIM II does not model the changing TOC or dissolved organic carbon (DOC) levels in the Delta channels, an attempt was made to correlate DOC[1] with Delta island consumptive use (DICU) with the intention of using the relationship to develop project island diversion rules. No strong correlation was found (Anderson, 2001).

Using a relationship developed by Jung (2001), the interaction between the peat soil and the water can be modeled in CALSIM II (Pandey, 2001). Jung's relationship is already incorporated into DSM2, as described in Chapter 9.

Similar to the rules for chloride, the amount of water released will be determined by the release water's effect on TOC. If the release has lower levels of TOC, then the TOC quality will not be a controlling factor. If releasing the water results in a violation of the WQMP change in TOC 1 mg/L criteria, then the amount of water released will be reduced. As a preliminary estimate of release flows that will not violate the TOC criteria, Equations 8-7 through 8-9 could be used.

[1] DOC is used as a surrogate for TOC in the simulations.

8.4.1 Base DOC Study

Begin the operation by running the CALSIM II base simulation. Using the Delta hydrology generated in that simulation, run a base DSM2 simulation. This simulation will generate concentration time series at the project reservoir intake locations and at the urban intake locations.

Use the base study DOC concentration time series generated at project intake locations as reservoir island diversion concentrations in the CALSIM II project simulation. Also, use base study DOC concentration time series generated at Delta export locations as the DOC constraint basis of measure in the CALSIM II project simulation.

8.4.2 Project Study Using DOC Constraints

Continue the operation by running the CALSIM II project simulation. This simulation is a multi-layered model that generates a dispersion mechanism in one layer for the application of the DOC constraints in another. Dispersion of DOC released from the islands is based on the split of exports without the DOC constraints.

For example, say Delta exports are pumped at the following rates without the DOC constraints: Tracy, 4,200 cfs; Banks, 5,600 cfs; and CCWD, 200 cfs. In the following model layer, island discharge and its associated DOC concentration would be fractionally dispersed to the three export locations as follows: Tracy 42%, Banks 56%, and CCWD 2%. DOC constraints would be based on the resulting mixture of Delta water and island discharge at each export intake. It is assumed that all water coming off islands will go to one of the exports. This assumption is not necessarily true (especially for Webb Tract). Future modifications to the DOC constraint equations will be made to account for water not being exported.

Calculate the constraint for each location. The constraint will limit the concentration of the project water at the urban intakes to less than the base concentration plus 1 mg/L. Under the WQMP, the project cannot exceed the base concentration by 1 mg/L.[2]

Constraint for Tracy:

$$\frac{Q_1' C_1 + f_1 \left(Q_4 C_4 + Q_5 C_5 \right)}{Q_1} \leq C_1 + 1 \qquad \text{[Eqn. 8-7]}$$

[2] The 1 mg/L constraint applies except when the base case concentrations are between 3-4 mg/L. When the concentrations are between 3-4 mg/L, the constraint limits the increase in TOC such that it does not exceed 4 mg/L.

Constraint for Banks:

$$\frac{Q_2{}'C_2 + f_2\left(Q_4C_4 + Q_5C_5\right)}{Q_2} \le C_2 + 1 \qquad \text{[Eqn. 8-8]}$$

Constraint for CCWD:

$$\frac{Q_3{}'C_3 + f_3\left(Q_4C_4 + Q_5C_5\right)}{Q_3} \le C_3 + 1 \qquad \text{[Eqn. 8-9]}$$

where,

C_1 = DOC Concentration at Tracy (mg/L) from base DSM2 simulation,

C_2 = DOC Concentration at Banks (mg/L) from base DSM2 simulation,

C_3 = DOC Concentration at CCWD (mg/L) from base DSM2 simulation,

C_4 = Concentration of Bacon Island Water (mg/L), and

C_5 = Concentration of Webb Tract Water (mg/L).

8.5 Bromate

Using the Ozekin equation in attachment 3 of the Water Quality Management Plan (2000), which was further derived and simplified in Hutton (2001), bromate can be described as a function of DOC and bromide.

$$Bromate = C_2 \times DOC^{0.31} \times Br^{0.73} \qquad \text{[Eqn. 8-10]}$$

Both DOC and bromide can be determined using relationships between TOC (Hutton, 2001) and electrical conductivity and chloride (Suits, 2001). When water is diverted, stored, and released, bromate will also have to be incorporated into the CALSIM II operating constraints if after preliminary simulations, it is discovered that bromate is a controlling constituent.

8.6 Total Trihalomethanes (TTHM)

Using the Malcolm Pirnie equation in attachment 3 of the WQMP, which was further derived and simplified in Hutton (2001), TTHM can be described as a function of DOC, and bromide, ultraviolet light absorbance (UVA), and temperature (T).

$$TTHM = C_1 \times DOC^{0.228} \times UVA^{0.534} \times \left(Br + 1\right)^{2.01} \times T^{0.48} \qquad \text{[Eqn. 8-11]}$$

When water is diverted, stored, and released, TTHM will also have to be incorporated into the CALSIM II operating constraints if, after preliminary simulations, it is discovered that TTHM is a controlling constituent.

8.7 Temperature and DO

Adequate temperature and DO rules in CALSIM II will be difficult to implement due to some precise release rules criteria. Accurately modeling temperature and DO changes due to diversions and releases in DSM2 will be difficult due to inadequate amounts of observed data to calibrate DSM2.

Analysis of the effects of releases on temperature and DO levels is currently being accomplished by using a spreadsheet model to evaluate the local effects (Yokoyama, 2001).

8.8 References

Anderson, J. (2001). "Simulated DOC to Historical DICU Correlations". Memo dated May 15, 2001. California Department of Water Resources. Sacramento, CA.

Bindra, A. (2001). Email dated August, 2001, with Water Quality and Operations Criteria Attachment. California Department of Water Resources. Sacramento, CA.

Duvall, R. (2001). ERA Draft Bioproductivity Report.

Easton, D. (2002). Discussion between T. Smith and D. Easton on implementation of DOC Operating Rules. California Department of Water Resources. Sacramento, CA.

Hutton, P. (2001). "ISI In-Delta Storage: CALSIM Water Quality Constraints to Meet Delta Wetlands WQMP". Draft memo dated May 29, 2001. California Department of Water Resources. Sacramento, CA.

Jung, M. (2001). "Reservoir Island Organic Carbon Model, Executive Summary". Consultant's Report to the California Department of Water Resources In-Delta Storage Investigations Program.

Pandey, G. (2001). "Implementation of DOC Growth Module in DSM2-QUAL". Memo dated Nov. 19, 2001. California Department of Water Resources. Sacramento, CA.

Suits, B. (2001). "Relationships Between EC, Chloride, and Bromide at Delta Export locations". Memo dated May 29, 2001. California Department of Water Resources. Sacramento, CA.

Wang, C. (2001). " Release Constraints". Fax to T. Smith at California Department of Water Resources. Metropolitan Water District of Southern California.

Water Quality Management Plan. (2000). "Protest Dismissal Agreement between CCWD and Delta Wetlands Properties, Exhibit B."

Yokoyama, K. (2001). "Water Temperature and Dissolved Oxygen Studies". Draft Report. United States Bureau of Reclamation.

Methodology for Flow and Salinity Estimates in the Sacramento-San Joaquin Delta and Suisun Marsh

23rd Annual Progress Report
June 2002

Chapter 9:
Implementation of DOC Growth in DSM2-QUAL

Author: Ganesh Pandey

9 Implementation of DOC Growth in DSM2-QUAL

9.1 Background

The Municipal Water Quality Investigations (MWQI) Program of DWR conducted field experiments to determine the changes in dissolved organic carbon (DOC) concentrations due to water contact with peat soil. Based on the experimental findings, Jung (2001) proposed a set of logistic type equations to characterize the growth of DOC on a flooded Delta island. The proposed set of equations primarily account for the amount of DOC coming out of peat soil due to leaching and microbial decay. The water on a flooded island, which has a higher DOC content due to growth, would be released back into the Delta. Much of this released water would eventually find its way to urban diversion. Due to formation of disinfection byproducts during the drinking water treatment process, the Delta Wetlands Water Quality Management Plan restricts the amount of DOC impact due to in-Delta storage reservoir releases. This has created the need to assess the impact of DOC increases at urban diversion due to increased DOC on the flooded islands. This chapter summarizes the methodology used to implement the logistic equations in the DSM2-QUAL and describes the results used to verify the validity of the implemented algorithm.

9.2 Implementation Detail

9.2.1 Logistic Equation

The logistic equation proposed to simulate the concentration of DOC in the stored water due to initial concentration and growth is expressed as (Jung, 2001):

$$Y(t) = \frac{A}{1 + Be^{-kt}} \qquad \text{[Eqn. 9-1]}$$

in which Y(t) represents the DOC concentration in mg/l at time t, “A” represents the maximum DOC concentration in mg/l, “k” is the growth rate in days^{-1}, and “t” is the water storage duration in days. “B” is a dimensionless parameter that is calculated from the initial DOC concentration. The values of constants “A” and “k” depend on reservoir specific characteristics, such as type and depth of the peat soil, antecedent flooding conditions, temperature, etc. Thus they are considered as input variables in the formulation. See Jung (2001) for details.

The magnitude of “B” is dictated by the concentration of the incoming water and is internally determined within the DSM2-QUAL. With t=0, Equation (1) leads to C_0=A/(1+B), where C_0 is the initial DOC concentration of the water diverted to the island. The value of C_0 is dynamically determined in DSM2. Knowing the value of C_0 and “A”, the value of “B” can be determined. During the filling period, the exchange of mass between peat soil and water body takes place, starting with the first parcel of water entering the reservoir. The filling process is not

instantaneous however. This means that the concentration of the diverted water keeps on changing over the filling period. Thus, during the filling of the reservoir, two aspects of DOC concentration changes must be accounted for: (1) the growth of DOC as governed by Equation 9-1, and (2) conservative mixing of water diverted from the channel into the reservoir. The first aspect usually represents a gradual change, whereas the second can potentially be an abrupt change, especially if the quality of the diverted water is highly variable. In order to model both aspects, the constant "B" is adjusted dynamically each time step to account for the changes in DOC due to channel diversions. Once filling has been completed, no more conservative mixing takes place and "B" is held constant. During the draining period, no changes to "B" are necessary.

9.2.2 Depth Adjustment

All model parameters A, B, and k are specified with respect to a given reference depth which is currently set at 2 feet. To find the other depth of the stored water, the results from Equation 9-1 need to be adjusted for depth. To adjust DOC growth for varying water depths, Jung (2001) recommends an inverse power law transformation, as shown in Equation 9-2:

$$y_d = y_2 \left(\frac{2}{d} \right)^{1.01} \qquad \text{[Eqn. 9-2]}$$

in which y_d is the adjusted DOC concentration, y_2 is the DOC concentration per Equation 9-1 with model parameters based on a 2 feet water depth, and d is the actual water depth. During the first phase of model implementation, the dynamically calculated water depth was used to represent "d". However, it was discovered that during the early cycles for the filling, very low water depths could lead to unreasonably high DOC adjustments. As a possible remedy, it was decided to set "d" equal to the maximum water depth during each filling cycle. However, the maximum water depth, which is computed by the model, is not known until the filling cycle has been completed. To work around this problem, a default value of 15 feet is used for "d" during the filling cycle until the actual water depth exceeds the default value. Once the default value is exceeded, the dynamically calculated value is used in Equation 9-2.

9.2.3 Timing of Filling and Draining

During each cycle of filling and draining, it is assumed that the exchange of mass between peat soil and water takes place immediately after the arrival of the first parcel of water. The value of t in Equation 9-1 must be initialized at the beginning of each filling cycle. To avoid ambiguities, it was decided that a filling cycle was initiated when the rate of inflow exceeds a certain default flow rate (currently set at 100 cfs). It was also decided to stop the growth contribution from Equation 9-1 once the depth becomes smaller than a minimum specified depth, currently set at 1.5 feet.

9.3 Results

The DOC module was first tested with the Delta Wetland Project (Mierzwa, 2001). In this study, Webb Tract and Bacon Island were used as storage reservoirs. In past efforts, the DOC concentration of the water returned to the river was predetermined using a "book-end" (upper

and lower limit) approach. With the new DOC module, these values are dynamically determined. The operation schedule was specified as monthly varying. Two model runs were conducted. In the first run, the return quality was determined using the newly developed DOC module. Table 9.1 shows the model parameters used in the first run. In the second run, DOC was modeled as a conservative substance. Any difference between these two runs can be attributed to the growth term incorporated in the DOC module.

Table 9.1: DOC Model Input Parameters.

Island Resevoir	A (mg/l)	k	Min. Depth (ft) to trigger a stop in DOC growth
Webb Tract	217	0.0216	1.5
Bacon Island	107	0.0256	1.5

Figure 9.1 shows a comparison between the predicted DOC concentrations in the Webb Tract for the two runs for the period covering January 1979 to September 1981. The water exchange is also shown on the same plot (with diversions shown as positive flows onto the island and the releases as negative flows leaving the island). Model results follow the same path in the first filling cycle. Once the filling cycle is completed in March 1979, predicted values quickly diverge, illustrating the growth of DOC in the first run. The largest differences occur right before the beginning of the next filling cycle. Model results appear to converge again with the start of the new filling cycle. The convergence and divergence cycles continue throughout the simulation period consistent with the operation schedule for the filling cycle. The peak expected DOC concentration in the first run approaches the value of "A", adjusted for depth using Equation 9-2.

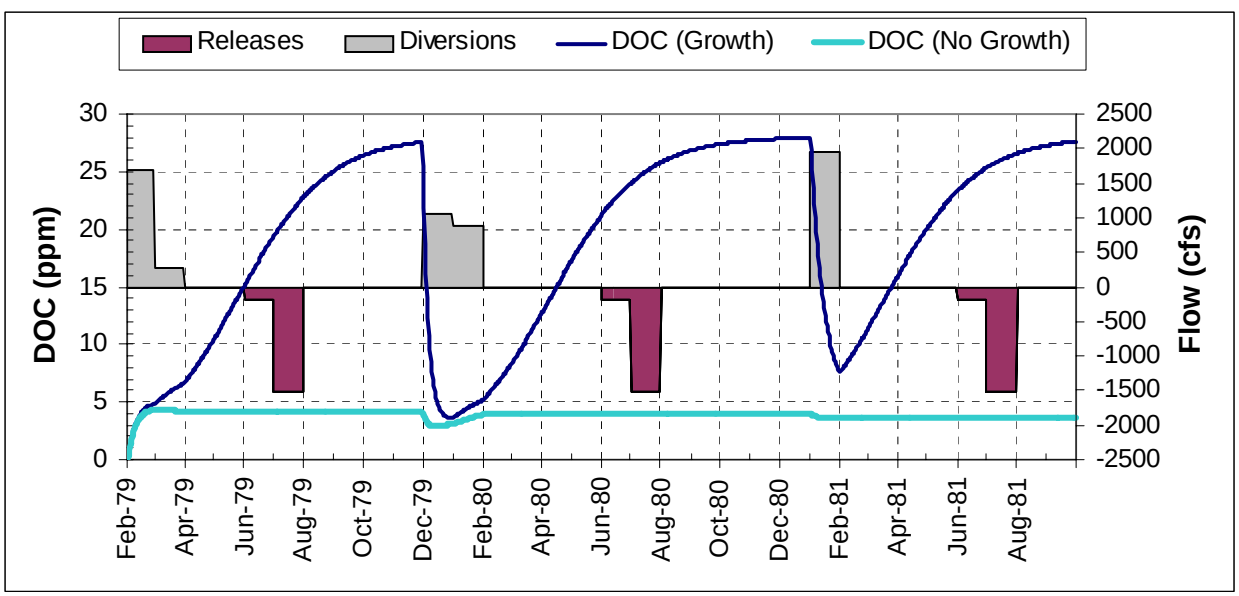

Figure 9.1: Time Series Plots of DOC Concentrations and Flow Exchange at Webb Tract.

Figure 9.2 shows a similar comparison between the two runs for the predicted channel DOC values near the Webb Tract reservoir release site. Model results correctly predict that the DOC concentrations during the filling and storage cycles are very similar. The model results then diverge with the start of a draining cycle. The model results then start merging one to two months after the end of the draining cycle.

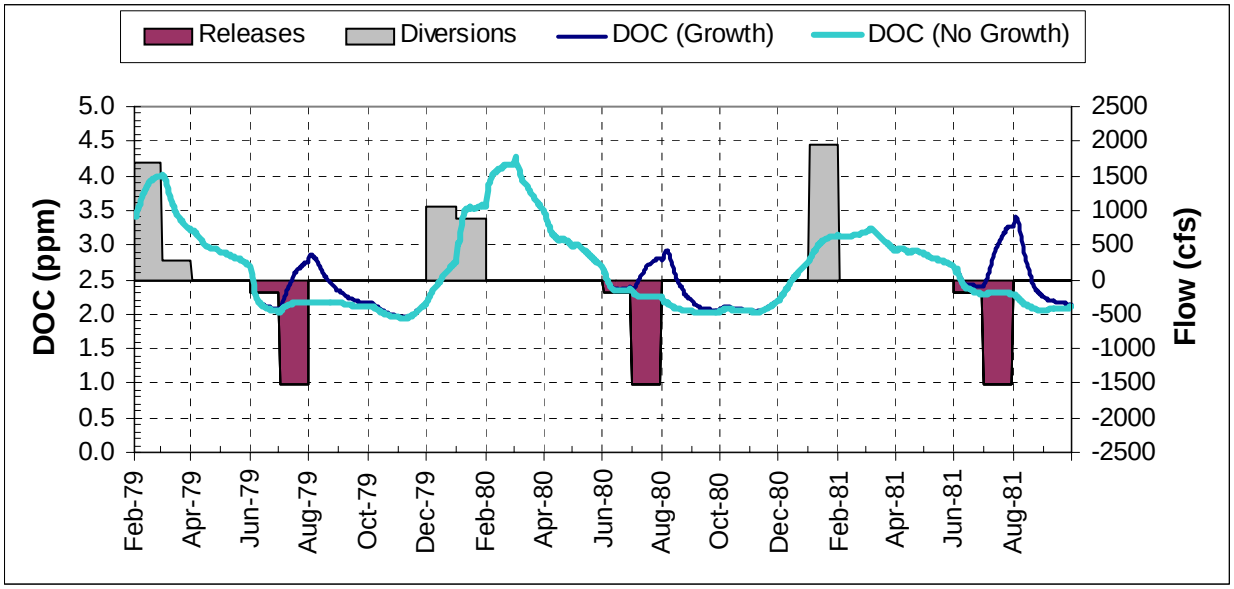

Figure 9.2: Time Series Plots of the Variations in DOC Concentrations at San Joaquin River near Mokelumne River Junction and Flow Exchange at Webb Tract.

9.4 Summary

Marvin Jung proposed a governing logistic equation for the growth of DOC in the storage reservoirs (Equations 9-1 and 9-2). These equations were implemented dynamically into DSM2-QUAL. The algorithm requires three input variables from the user. A test case was carried out assuming two islands as storage reservoirs. The test case showed that the model was behaving as expected and the DOC growth in the islands were consistent with Marvin Jung's algorithm. The changes in the DOC concentrations in the reservoir and channels appear to be consistent and reasonable.

9.5 References

Jung, Marvin. (2001). "Consultants Report to the Department of Water Resources In-Delta Storage Investigations Program Executive Summary." Municipal Water Quality Investigations, California Department of Water Resources. Sacramento, CA.

Mierzwa, Michael. (2001). "Delta Wetlands DSM2 CALSIM Studies." Presentation to In-Delta Storage Water Quality Stakeholders, October 30. Delta Modeling Section, California Department of Water Resources. Sacramento, CA.

Methodology for Flow and Salinity Estimates in the Sacramento-San Joaquin Delta and Suisun Marsh

23rd Annual Progress Report
June 2002

Chapter 10:
Optimal Control of Delta Salinity

Author: Eli Ateljevich

10 Optimal Control of Delta Salinity

[NOTE: In a project funded by DWR's Delta Modeling Section, Section member Eli Ateljevich completed a civil engineering doctoral dissertation on December 19, 2001. This chapter is a summary of that work; a complete copy of his dissertation is on file with the University of California, Berkeley.]

10.1 Introduction

Efficient control of salinity in the Delta is a subject that pervades the work of the Department's Modeling Support Branch. Water quality constraints are important in current State Water Project (SWP) operations, and even more so under the high-growth scenarios considered in water project planning. Because of this broad context in which salinity control plays a role, studies of salinity compliance have traditionally been incorporated into a larger modeling problem that goes something like this:

- Create a model of water project operations (CALSIM), and
- Include a module to model salinity intrusion and stipulate minimum inflows required to meet salinity standards (ANN, G-Model, etc). This constraint will be active during a fraction of the simulation period.

Two important simplifications are represented in this approach. The first is that the salinity module is, by computational necessity, an empirical surrogate for a physical model such as DSM2. The second is that the inflow requirement is calculated one time step at a time. The flow history up to the current time step is accepted as a *fait acompli*, and the calculations for the current step do not reckon the costs of putting the system into a costly position later. In optimization, this is known as a *greedy* treatment of time. In the present case, it is compounded by the use of large computational time steps.

Ateljevich (2001) tackles salinity control using a tack that is complementary to the traditional one: the SWP context is simplified, but the physics and the time component are treated in more detail. Under these assumptions, the *optimal water cost compliance problem* is an optimal control problem, the solution to which is the optimal schedule of upstream releases into the Delta and exports. The technical details of this problem make up the bulk of the dissertation.

10.2 Minimum Water Cost Compliance

The minimum water cost compliance problem is posed over a fixed time interval of several weeks or months. Salinity appears as an important operating constraint, and stochastic influences are neglected. The features of the problem are as follows:

- The cost function is the sum or cost over time of upstream releases.
- The volume of pumping over the optimization interval is fixed as a constraint
- Salinity constraints are imposed at one or more monitoring stations in the interior of the Delta.
- Delta dynamics are modeled using physical conservation equations of mass, momentum, and salinity transport.
- Physical bounds are imposed on the control variables to represent pumping capacity, minimum outflow requirements, and uncontrolled Delta inflows.

Variants of this formulation can be devised. For instance, pumping can be priced as a benefit rather than being fixed as a constraint. The salinity constraint may also be imposed on instantaneous or period-averaged salinity (the latter is the important case in the Delta). Finally, additional *regularization* components may be required to make the problem mathematically well posed.

The results of the dissertation indicate a high degree of control over salinity, particularly over daily-averaged values. The water cost under optimization is about 10% better than the cost obtained under very careful trial-and-error experiments and about 15-20% better than that of a good guess. The minimum water cost can also help to refine definitions of water cost and carriage water, which are usually calculated with rather gross assumptions about the time trajectory of pumping and inflow. Carriage water calculations are shown to be quite sensitive to the assumption that both pumping and inflow are constant over time.

10.3 Optimal Control Solutions

Optimal control solutions can be either hard to obtain or erratic. The features that go into the formulation of a well-posed optimal control problem are discussed at length in Ateljevich (2001). One issue deserves highlighting because it is critical to understanding what types of solutions can be obtained. That issue is *consistency* – what happens to the solution as the space and time steps are refined.

When expressed in continuous time, the optimal water cost compliance problem requires an "infinite" number of decisions – upstream inflow and pumping must be determined at an infinite number of times. This level of detail is not needed in practice, but water modelers are accustomed to discrete models that, under refinement, home in on a unique, physical continuous

solution. Constrained optimal control problems are not naturally so well behaved, even when a consistent model is used for the physics. Unless the problem is properly regularized, the prescribed control (if it exists) may exhibit infinite switches between the minimum and maximum control (*chattering*) or other types of singular or impractical behavior. Discrete solvers trying to home in on such a degenerate solution will tend to stall in ways that are time-step specific and very difficult to diagnose (often the diagnosis is "local minima" even when there is no evidence that any sort of local minimum is actually achieved or even exists). Besides being impractical, such wildly fluctuating controls violate the gradually varying flow assumptions under which the flow model is formulated.

10.3.1 Parameterization

At the other end of the spectrum, the problem can be parameterized crudely by taking one control variable per large time step (say several days or weeks), and using a representation that is piecewise constant or linear. This characterization involves a small number of decision variables. The outcome of optimization over such a restricted control space will be physically reasonable because the parameterization is too crude to represent the sort of chatter and pulses that occur when optimal control solutions go awry of common sense. On the other hand, one control per week in a system dominated by 25-hour and 14-day cycles may not be refined enough – important characteristic time scales of the problem are ignored or crudely represented. The catch is that the problem cannot be refined too much without losing the stability the crude parameterization imparts on the system.

The foregoing discussion allows for physically meaningful solutions to be developed in two ways. First, we can simply toss aside the notion of the "underlying truth" and accept a parameterized solution to the unregularized problem. Formal convergence is unlikely – the solution will always be time-step dependent. However, it may be possible to verify using a sensitivity analysis that the solution is not erratically dependent on time step in some neighborhood of interest – say, comparing four-day controls to two-day controls. In this case, the character of the *actuators* of the controls (pumps, reservoir gates, etc.), which operate with restricted complexity, may physically justify the use of a crude time step.

10.3.2 Regularization

Alternatively, we can add small regularization terms to the continuous problem, so that it does have a well-behaved solution. One common way to avoid discontinuities is to add a very small quadratic penalty on the time derivative of the control variables, which penalizes extremely sharp jumps and is insignificant the rest of the time. It is then possible to develop a solution algorithm that is consistent with this regularized problem and stop at whatever level of time detail seems appropriate. The regularization approach leads to similar water cost as the parameterized approach, but not to similar control sequences (usually the regularized solution has smaller extreme values).

Regularization of the problem requires extra development time and software designed for optimal control, but when applied it is much quicker to converge. This technique cannot be applied to DSM2 because some details in the implementation of DSM2-QUAL make it difficult

to calculate the derivative of the objective function with respect to the control variables at small time steps. Such calculations are usually made using variational (adjoint) techniques. Without this possibility, finite differences approximations must be used, perturbing the controls one at a time. This method is slow and inexact compared to variational methods. Parallel computing of DSM2 can be used to reduce the calculation time enough to make finite differences practicable (Finch and Kao, 1992).

10.3.3 Comparing Parameterization and Regularization

Because of these limitations, the differences between regularization and parameterization cannot be investigated directly for DSM2, although they can be illustrated on simplified problems. Figures 10.2 and 10.3 shows results for an optimal water cost control problem on a contrived 1-channel domain (Figure 10.1). The simplified problem has an upstream inflow, mid-stream pump, period average salinity constraint, ocean boundary, and fairly large dispersion. The numerical model used for the hydrodynamics is a four-point box scheme similar to that used in DSM2-HYDRO. The numerical scheme for salinity transport is the Flux Based Modified Method of Characteristics with a MUSCL limiter as described by Roache (1992). Derivatives were obtained using variational methods. A minimum flow of 200 cfs was enforced for inflow (0 cfs for pumping); the upper bounds were very high and did not become active during the optimization.

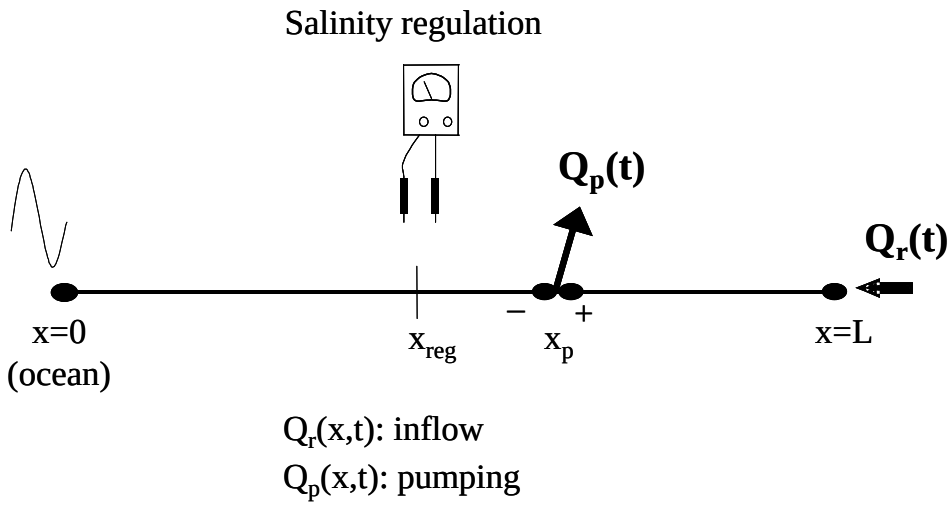

Figure 10.1: Sample 1-Channel Domain with Salinity Regulation.

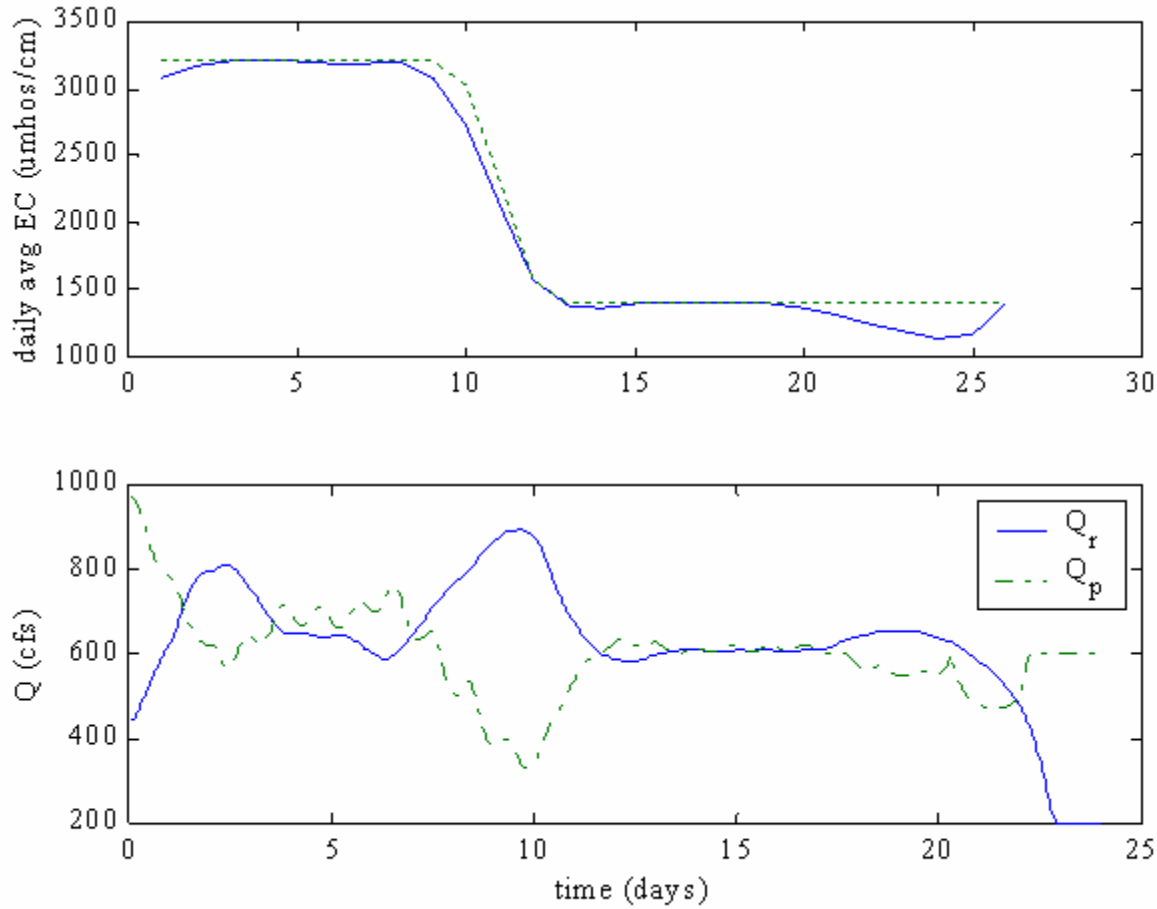

Figure 10.2: Regularization Solution to Meet Daily-Averaged Salinity Regulations with Control Trajectory for River Inflow (Q_r) and Pumping (Q_p).

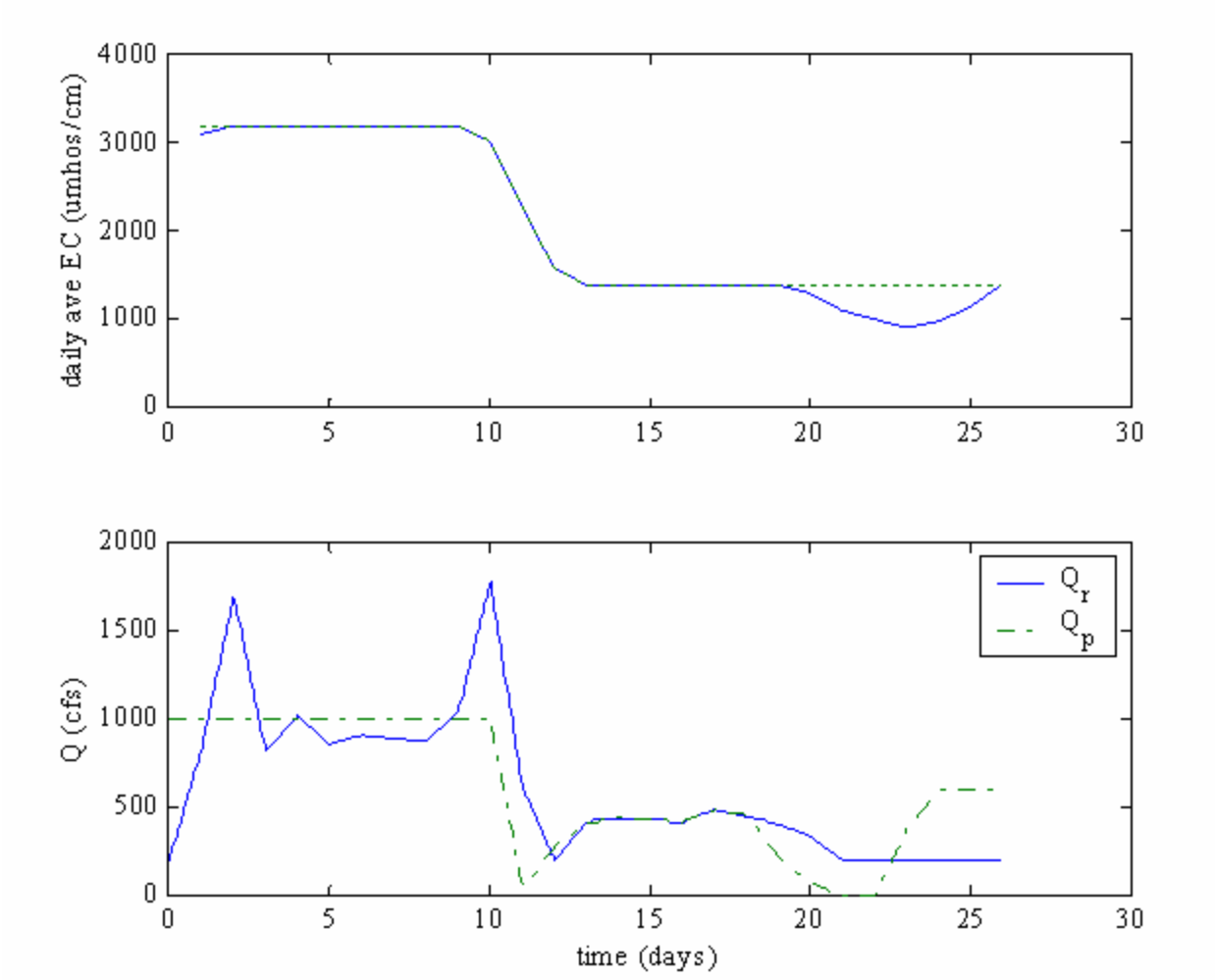

Figure 10.3: Parameterization Solution to Meet Daily-Averaged Salinity Regulations based on Piecewise Linear Controls for River Inflow (Q_r) and Pumping (Q_p).

The control solutions in the parameterized and regularized cases are not similar in character – the parameterized solution reaches greater extremes than the regularized solution. However, the water cost of the two methods is extremely close, indicating that both methods are good in a bottom-line sense. The solution to the parameterized problem degrades to wild fluctuations at time steps of fewer than four hours (not shown); the solution to the regularized problem does not change significantly under refinement.

Two features visible in Figure 10.2 are typical and will be seen again in the DSM2 applications presented in Section 10.4. First, there is a very high degree of control on salinity. The piecewise linear daily controls are sufficient to allow the salinity solution to lie almost exactly on the regulation except during transitional periods (the beginning, end and times when the regulation is changing). Such "exact compliance" was not a goal of the optimization, but it is interesting to see that it can be achieved in a deterministic modeling setting.

Second, controls produced by the optimizer in the final few days of the problem have a *greedy* character. Water released in the final time steps will not affect salinity at the monitoring station until after the optimization is over. At the same time, this water has a cost. Under optimization, releases in the final time steps will therefore naturally be set to the minimum value. This often leads to a situation where salinity in the final time step is compliant, but increasing – an infraction in the next time step is imminent. Methods for dealing with end-of-period behavior are enumerated in some detail by Ateljevich (2001), and include constraints and penalties on the final value of salinity or its time derivative. These methods generally did not work as well as just padding the problem with some extra time. Fortunately, the earlier part of the example solution (before day 15) is not particularly sensitive to the way the end-of-period effects are handled.

10.4 Experiments Using DSM2

Only the parameterized control approach was available for optimization using DSM2, where finite differences estimate derivatives. Nevertheless, it is possible to obtain solutions that are reasonably stable and exhibit most of the behavior expected from experiments using a more rigorous approach on a simplified domain.

As an example problem, Ateljevich (2001) used parameterized controls to examine a 1994 compliance problem (Creel, 2000), in which reliance on an incorrect gage allowed salinity to approach the legal limit at the Contra Costa Water District pump intake at Rock Slough (Figure 10.4). The error was discovered and pumping was curtailed for a period of about one week to bring salinity levels back down. The Sacramento River inflow and combined export pumping rates are shown in Figure 10.5. The Delta Cross Channel was open the entire time. As suggested by Figure 10.4, the pulse-like reduction in pumping overcompensated, causing salinity to drop by half.

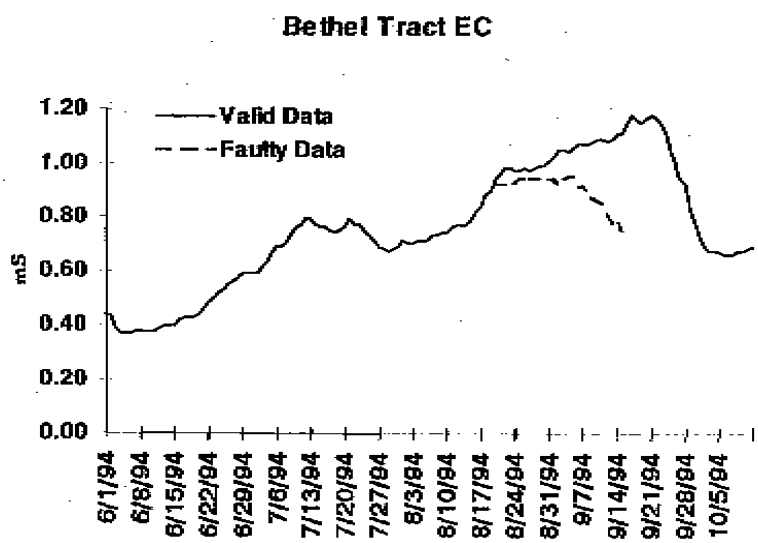

Figure 10.4: Bethel Tract Daily-Averaged EC (in mS) in Fall 1994.
(taken from Creel, 2000)

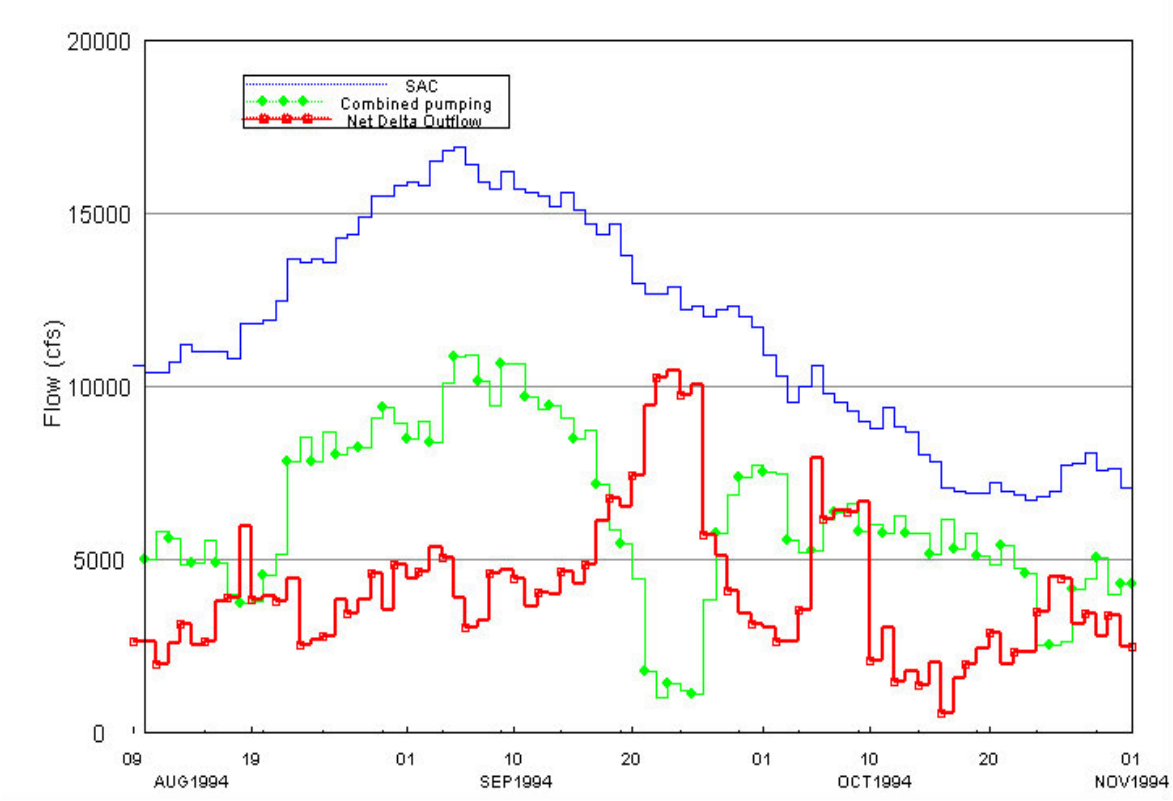

Figure 10.5: Sacramento River Flow, Combined Exports, and Net Delta Outflow in Fall 1994.

The incident has already been the subject of some retrospective water cost analysis by operators, though not with the use of optimization. They compared the abrupt historical reduction in pumping to that of a milder "adjusted" reduction begun earlier that was also adequate to achieve compliance. Figure 10.6 compares the actual and adjusted pumping strategies indirectly by means of the resulting Delta Outflow Index (DOI), a preliminary estimate of Net Delta Outflow (NDO). Sacramento inflow was held at historical levels. A comparison of the cumulative water cost of the two pumping strategies is shown in Figure 10.7. More detailed input and output from this study are not available.

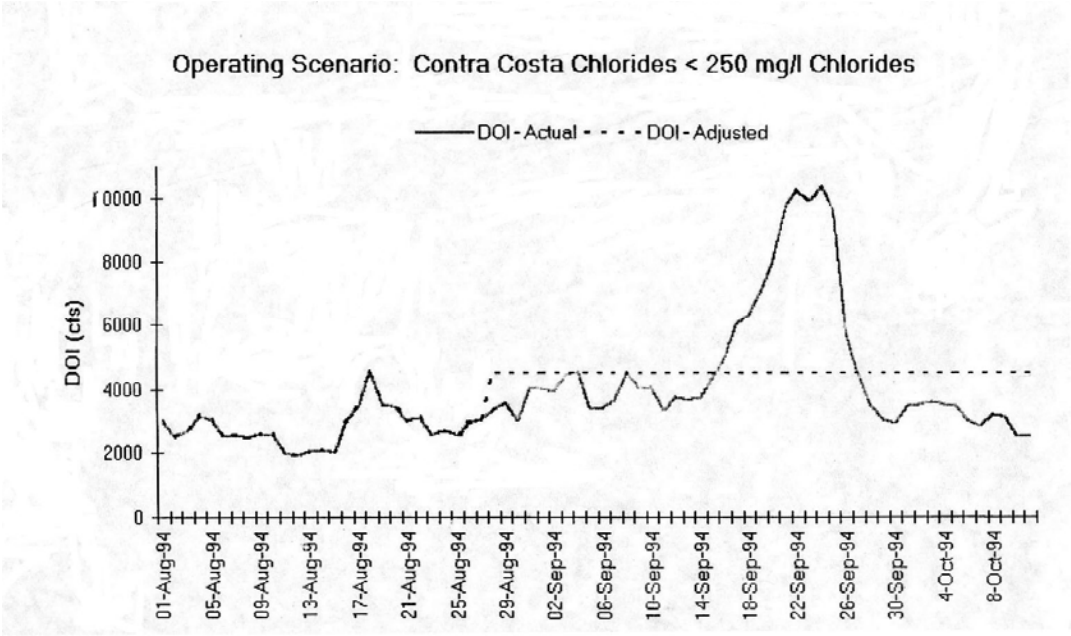

Figure 10.6: Historical and Alternative Delta Outflow Index for DWR O&M Fall 1994 Water Quality Study.
(taken from Creel, 2000)

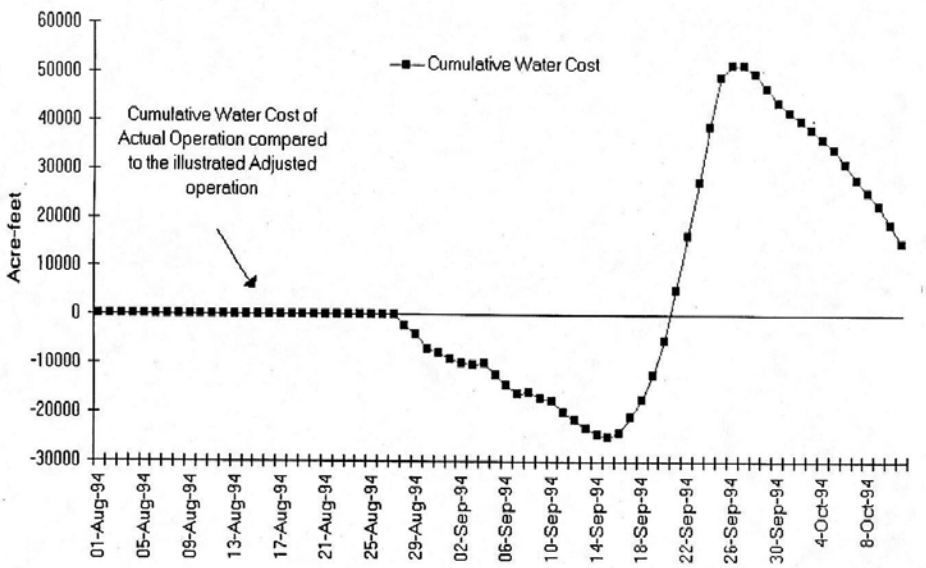

Figure 10.7: Comparison of the Cumulative Water Cost of Historical Operations to the Adjusted Operation for Fall 1994.
(taken from Creel, 2000)

Operators concluded that:

- the gentle method achieves compliance with a slightly lower water cost;
- the historical pulse achieved lower salinity with only a modest additional water cost.

The conclusion leaves open the question of the "cheapest" method, because the historical, pulse-like pump reduction had a higher cumulative water cost, but also overcompensated for salinity. Evidently, the historical pump reduction could been smaller or shorter (or timed differently).

Ateljevich (2001) extends the investigation to consider time-varying Sacramento flow and exports, using parameterized controls that are allowed to change every few days. The dynamics of the Delta were simulated using DSM2. The Sacramento River inflow and exports were treated as control variables, with other boundary conditions taken from the historical (IEP) data or DWR Delta island consumptive use (DICU) estimates. The "single step control" of 1,200 hours (50 days) was compared to finer grain controls of 50-hours and 100-hours.[1] The "salinity regulation" is an daily average EC of 1,200 μmhos/cm on Old River at Holland Tract. This is a rough surrogate for the 250 mg/l chloride standard for the Contra Costa Canal intake at Rock Slough. Average pumping was fixed, although the pumping schedule was allowed to vary as a control variable. The experiment was repeated with average combined export (Central Valley Project and State Water Project) rates of 5,000 cfs and 7,000 cfs. The optimization was carried out using a successive linear programming algorithm based on work by Zhang et al. (1985)[2]. Boundary EC at Martinez was estimated using the methods of Ateljevich (2001). Minimum outflow and E/I ratio regulations were ignored in order to study salinity control in isolation.

Figure 10.8 shows salinity and control solutions for the two levels of fixed pumping. Similar solutions were obtained from a variety of starting points. The optimization algorithm occasionally stalls, but when it does not, the minimum that it reaches is the same for all the starting points.

Just as in the simplified problem described in the previous section, the salinity trajectory lies very close to the regulation. Again, this was not a goal of the optimization, but is a reasonable result. The closeness of compliance is remarkable in light of how coarse the four-day controls are compared to the daily regulation. It is not well known in the Delta modeling community that such control over daily averaged salinity is possible, even in the sterile context of deterministic modeling.

[1] Two and four tide cycles, respectively. Due to limited computational power, the 50-hour controls contain some 100-hour periods later in the optimization period.

[2] See Ateljevich (2001) for more discussion of algorithms. This one is simple to program and is somewhat compatible with the linear programming engine of CALSIM. Somewhat more robust algorithms are available, although they tend to stall due to their use of finite differences.

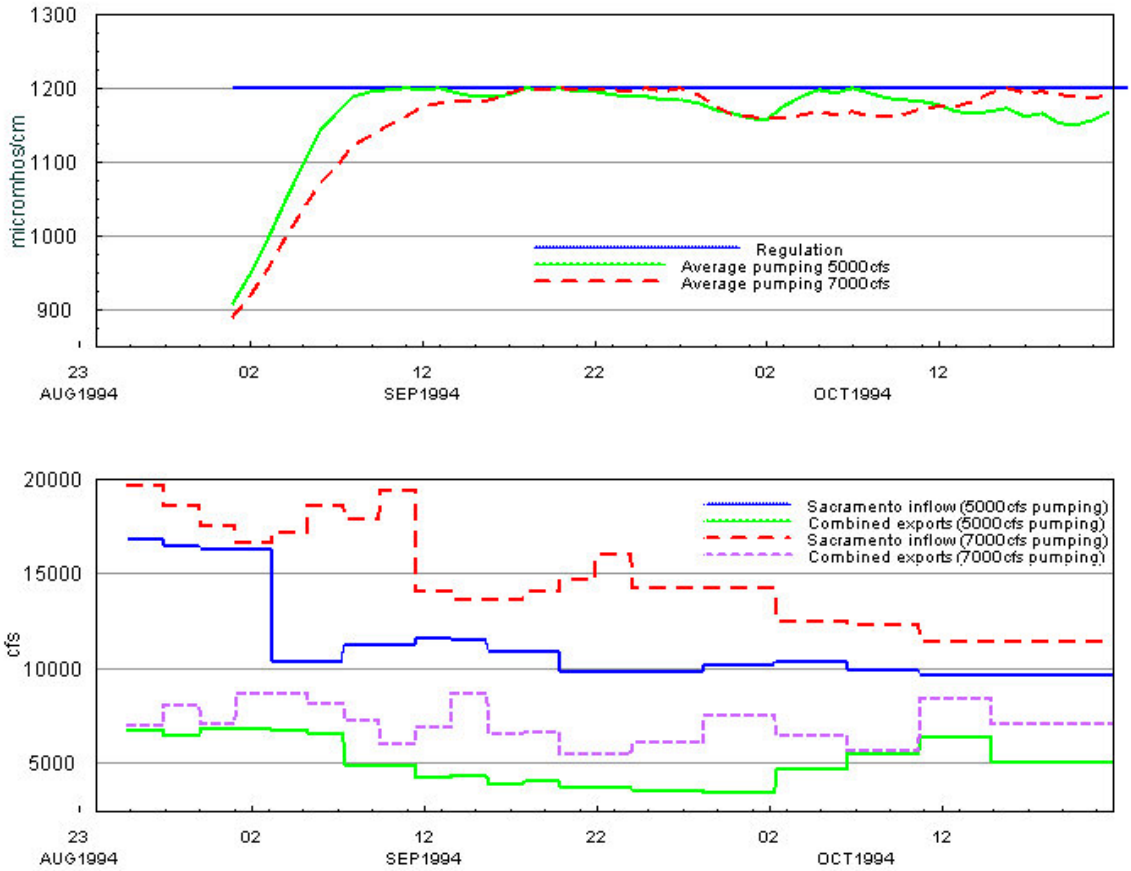

Figure 10.8: Salinity Results and Flows for Minimum Water Cost Optimization for two Cases: Average Pumping of 5,000 cfs and Average Pumping of 7,000 cfs.

The control solutions in Figure 10.8 are typical in that a decelerating pulse (high Sacramento flow and low combined exports) and relaxation is used to approach the salinity regulation at a tangent. The approach is gentler in the 7,000 cfs average pumping case than it is in the 5,000 cfs average pumping case. After the regulation is achieved, fairly steady values are observed. The spring-neap cycle and the accompanying filling and draining of the Delta have only a minor influence on the shape of the controls. One apparent influence of the spring-neap cycle or Delta filling and draining is the driving down of salinity before October 2 in order not to exceed the regulation as water levels in the Delta start to increase with the new spring tide (the tide cycle is shown in Figure 10.9).

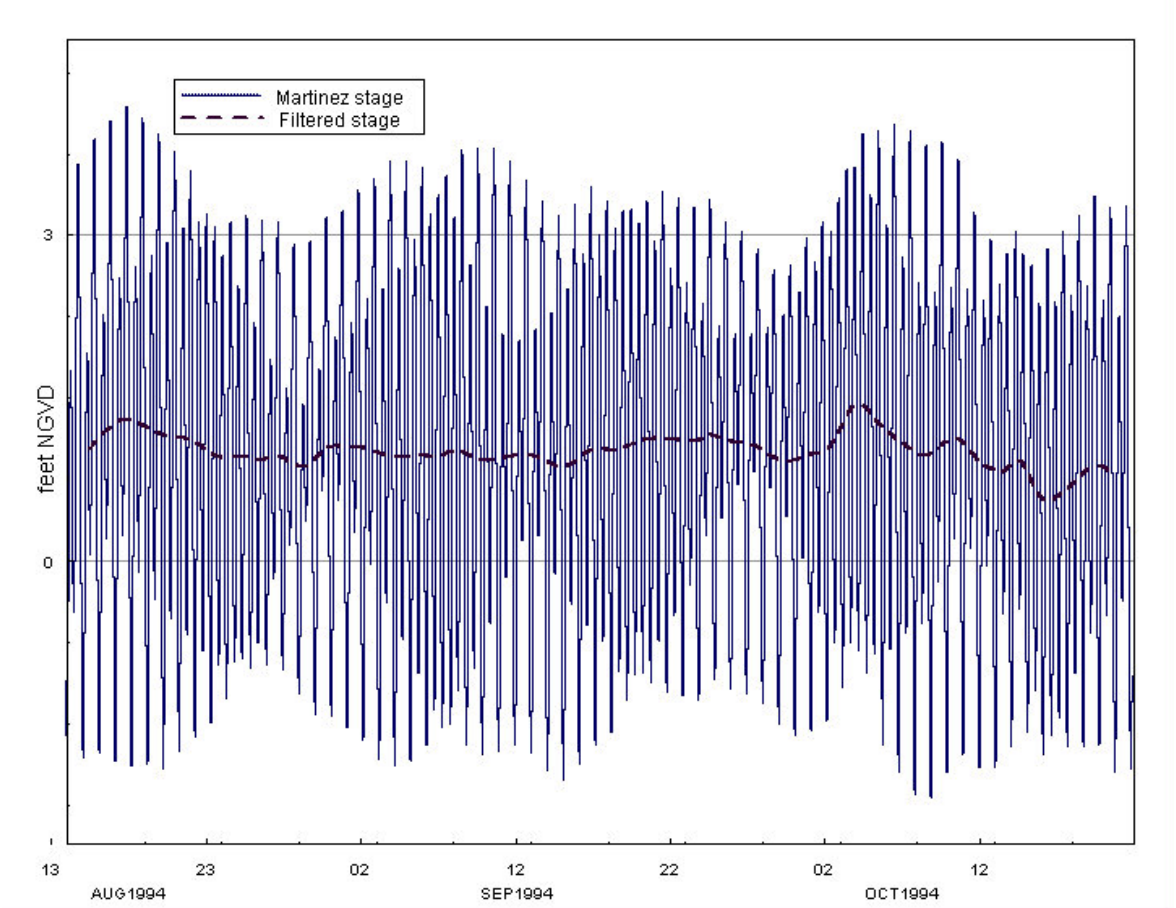

Figure 10.9: Martinez Stage and Tidal Average Using Godin Filter for Fall 1994.

Sacramento flow is more dynamic than exports. This is counter to conventional wisdom – pumping curtailment is usually treated as the main control action, on the (apparently questionable) assumption that control by means of Sacramento inflow is more expensive. Sacramento inflow tends to fluctuate in concert with exports: high flows are matched to low exports and vice versa (this is more evident in the 7,000 cfs average pumping case). This means that the E/I ratio fluctuates over a considerable range over the optimization period. In a production optimization in the Delta, the E/I ratio would have to be fixed as an additional constraint because it does not arise naturally from water quality control.

Finally, Ateljevich (2001) performs a sensitivity analysis on the time steps for inflow and pumping controls. Only controls coarser than one per day are possible for computational reasons. Given this constraint, it is interesting to question whether the solution is stable for various length control periods that are in the neighborhood of several days long and if so, at what level of detail the benefits tend to taper off. In the experiment presented here (from the 5,000 cfs average pumping case), the water cost from the 50-hour controls is only about 1% better than that resulting from the 100-hour controls and the shape of the control trajectory is similar. The incremental benefits of using a 50-hour time-step instead of a 100-hour time-step are meager compared to the 10% reduction in water costs obtained by using a 100-hour time-step instead of a single decision. The time-step sensitivity was not tested for the 7,000 cfs pumping case. However because the 7,000 cfs solution varies more over time, the difference between the

coarser and finer time steps might be larger than the 1% difference in the results for the 5,000 cfs pumping case.

10.5 Extensions

The optimization methods of Ateljevich (2001) have applications in both operational and planning models. In an operational context, optimization is able to provide an efficient reference solution for water cost. This reference solution can either be used as part of an operator decision based on multiple objectives, or it can be used as the "nominal trajectory" in a stochastic optimal control problem where the influence of uncertainty in the tide, inflows, and model are taken into account. For now, the main interest in optimal solutions will be heuristic. An example given above is the discovery that the control of salinity by means of extra Sacramento River flow may be more efficient than was previously thought.

The extension to planning models requires that the planning model CALSIM treat salinity control as a multiple-step procedure. This is a significant extension to CALSIM, and would require surrogate models (ANNs) that not only estimate salinity well at the "bottom line", but also correctly estimate the sensitivity of salinity to individual parts of the recent flow history. This is a more stringent fitting standard than the one currently in use.

The application of flow simulations to optimized CALSIM runs would also be facilitated by incorporating the formal theory of surrogates recently forwarded by Booker et al. (1998). Their methods formally tackle the idea of using a surrogate (ANNs are specifically addressed) to approximate a complicated component (DSM2) in an optimization procedure. The theory, while more expensive than a pure CALSIM-ANN implementation, is able to achieve convergence between the optimizer procedure (CALSIM) and the expensive model (DSM2) while using the surrogate for the overwhelming majority of the work.

10.6 References

Ateljevich, E. (2001). *Optimal Control of Salinity in the Sacramento-San Joaquin Delta.* Ph.D. Dissertation. University of California, Berkeley.

Booker, A.J., J.E. Dennis, Jr., P.D. Frank, D.B. Serafini, V. Torczon, and M.W. Trosset. (1998). *A Rigorous Framework for Parameterization of Expensive Functions by Surrogates.* NASA CR-1998-208735, ICASE Report TR-98-47.

Creel, C. (2000). Personal communication concerning DWR Operations and Maintenance Delta compliance issues.

Finch, R., and S. Kao. (1992). "Coarse-Grain Parallel Computing Using ISIS Tool Kit." *Journal of Computing in Civil Engineering*. 6 (2). pp. 233-44.

Roache, P.J. (1992). "A Flux-Based Modified Method of Characteristic." *International Journal of Numerical Methods in Fluids.* 15.

Zhang, J., N. Kim, and L. Lasdon. (1985). "An Improved Successive Linear Programming Algorithm." *Management Science.* 31 (1).

Methodology for Flow and Salinity Estimates in the Sacramento-San Joaquin Delta and Suisun Marsh

23rd Annual Progress Report
June 2002

Chapter 11:
16-Year DSM2 Planning Studies with Adjusted Astronomical Tides and Daily Hydrology

Author: Bijaya Shrestha

11 16-Year DSM2 Planning Studies with Adjusted Astronomical Tides and Daily Hydrology

11.1 Introduction

DWR's Delta Modeling Section uses the Delta Simulation model (DSM2) to simulate the hydrodynamics and water quality in the Sacramento-San Joaquin Delta. This chapter discusses the Section's most recent planning mode setup. Planning simulations are used to evaluate proposed long-term structural and/or operational changes in the Delta.

Traditionally, the Delta Modeling Section used a planning mode setup to conduct a 16-year simulation, covering water years 1976 to 1991, using monthly average hydrology rim input. The rationale behind the selection of this period was discussed in detail in the *Status Reports on Technical Studies for the Storage and Conveyance Refinement Process* (DWR, 1997). The monthly average hydrology input was obtained directly from the output of CALSIM. Simulations followed the following procedure:

1. A design repeating tide (which is based on the 19-year mean tide) was used as the stage boundary condition at Martinez with a 25-hour period (Nader-Tehrani, 2001).

2. A separate DSM2-HYDRO run was completed for each month. During each run, the hydrology was kept constant. The model run continued until a condition of dynamic steady state was achieved.

3. The hydrodynamic results (flow, stage, etc.) were saved in a tide file (25 hours long). These conditions were assumed to repeat every day for the entire month.

The main reason for using monthly varying hydrology with a repeating tide approach was to reduce the CPU time and storage requirements. However, due to increases in CPU speed and the drop in price of storage devices (both hard disks and CD/DVDs), these former constraints no longer applied. In summer 2001, the Delta Modeling Section initiated efforts to develop a planning study design that would incorporate daily variations of hydrology.

In the new planning mode setup the design repeating tide is replaced with an adjusted astronomical tide and the monthly hydrology is replaced with a daily hydrology. By including the spring-neap variation in the tide and by accounting for more detailed operations in the Delta, this new planning mode provides more useful results than the previous DSM2 planning studies. Furthermore, recent projects, such as the In-Delta Storage water quality studies, required the daily operations in the Delta to accurately simulate the diversions to and releases from the proposed island reservoirs.

11.2 Preprocessing Planning Runs

In order to run HYDRO and QUAL using a daily hydrology, staff addressed several new problems related to generating daily boundary conditions and dynamically changing the operation of structures within the Delta.

11.2.1 Changes in HYDRO

Daily varying hydrology input will be obtained directly from the output of a CALSIM run. Therefore, HYDRO will be used to run every day of every month, and an entire 16-year simulation will be conducted in a single run instead of individual model runs (one per month) as in the traditional planning approach. Observed tide data are not available at Martinez for the entire 16-year simulation. An adjusted astronomical tide at Martinez will be used as the stage boundary, since there are no benefits to be gained from using the design repeating tide (Ateljevich, 2001a). This tide includes the spring-neap variation that was not included in the repeating tide used in the previous studies.

As shown in Figure 11-1, flow control structures in the South Delta (Old River, Middle River, and Grant Line Canal) are operated at times to raise the stage upstream of the barriers for agricultural use (Old River at Head is a fish control structure). When all three barriers are operated simultaneously, the water upstream becomes stagnant and the water quality degrades. To prevent such stagnation and improve circulation, a special tidal operation of the flow structures has been introduced.

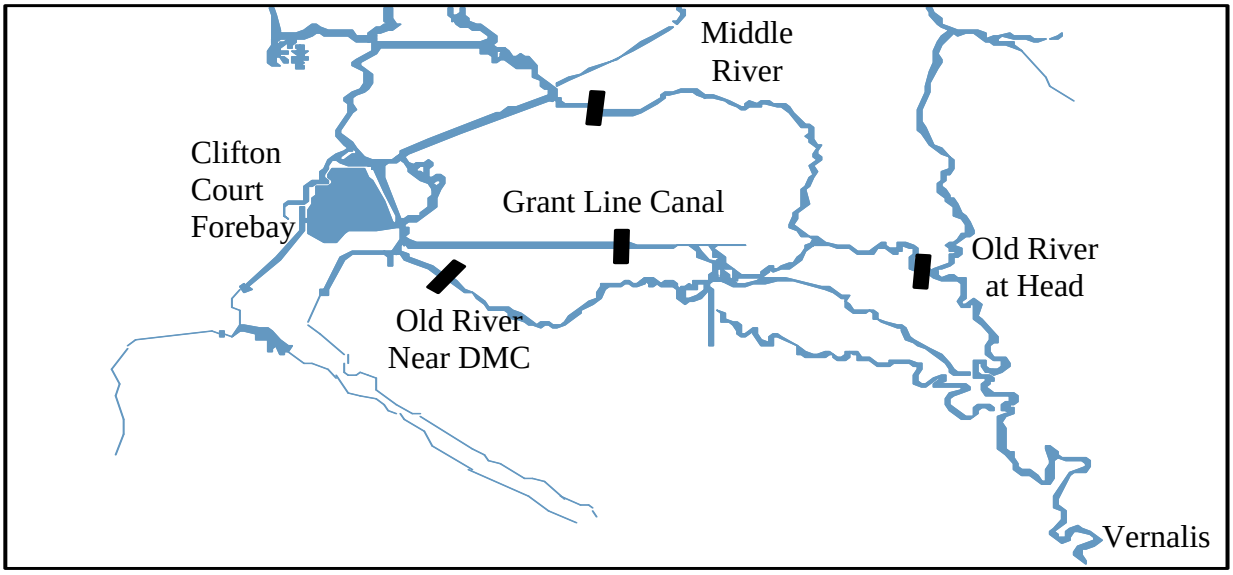

Figure 11.1: South Delta Flow Control Structures.

In the monthly planning setup, the design repeating tide has a single defined pattern that repeats every 25-hour period. Therefore, the special tidal operation of South Delta flow structures can be pre-defined in a clear way as shown in Figure 11.2.

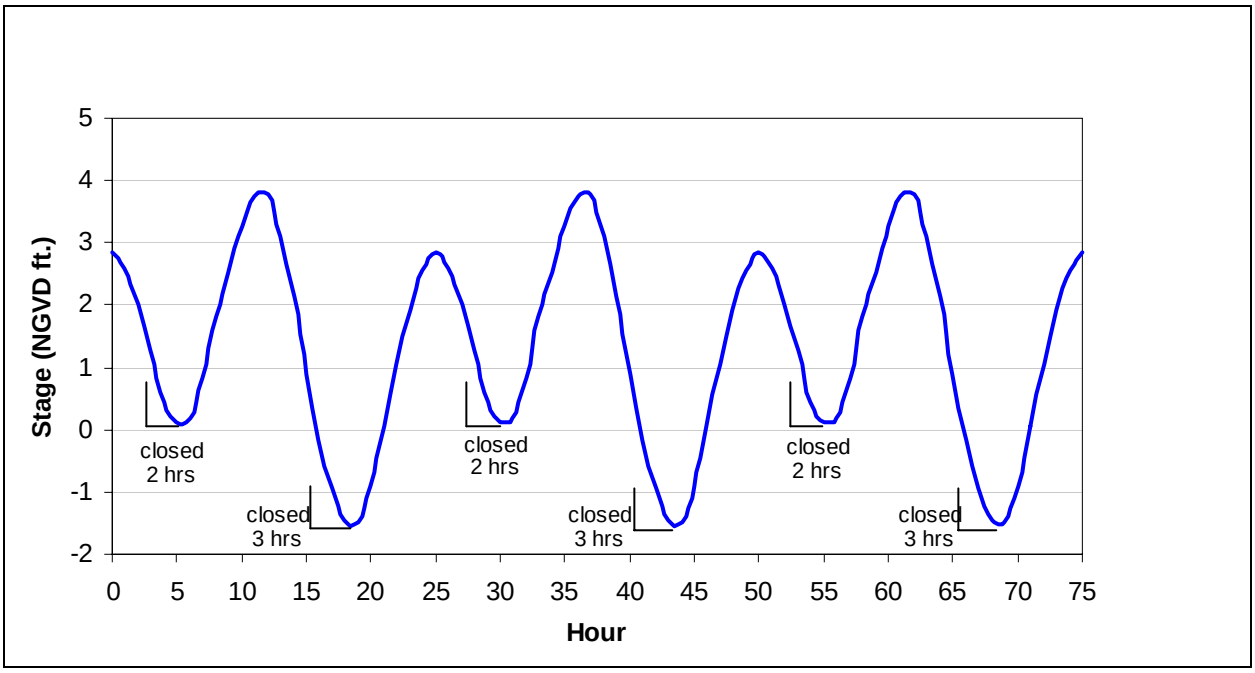

Figure 11.2: Special Tidal Operation of South Delta Flow Control Structures.
(taken from DWR, 1999)

With the new setup, the tides do not repeat, making it difficult to define a generalized schedule for the special tidal operations of the South Delta flow control structures. The new special tidal operation is defined based on the tide information (highs and lows) at Martinez and the phase difference (tide lag time) between Martinez and locations of interest in the South Delta.

In the monthly setup, gate operations changed on a monthly time-scale. Because the new planning studies are run continuously, the operation of the barriers are not limited to monthly time-scale only. The operation of the gates can be specified up to a 15-minute time-scale.

11.2.2 Changes in QUAL

In the monthly planning setup, an ANN (Artificial Neural Network) was used to estimate tidally averaged salinity (in terms of EC) as a function of Net Delta Outflow (NDO). A predetermined tidal component was added to estimate hourly variations using Kristoff coefficients. These coefficients are a series of 25 hourly values arranged in a tidal pattern that are multiplied by daily averaged salinity to produce a scaled tidal fluctuation. The tidal fluctuation was synchronized with the Martinez repeating tide (stage) so that the hydrodynamic (HYDRO) and water quality (QUAL) results were realistically phased.

Ateljevich (2001b) developed an improved method of salinity estimation for the Martinez boundary in the new daily planning setup. The new method derives 15-minute salinity estimates based on the Martinez tide and NDO.

CALSIM currently provides only average monthly values of EC for the San Joaquin River at Vernalis. The salinity at Vernalis is also an important boundary condition for QUAL. The daily EC at Vernalis is estimated using regression relationships (Equations 11-1a and 11-1b) developed by Scott Humpers (SWRCB). The regression relationships are defined separately for the irrigation and non-irrigation seasons:

Irrigation Season (April – September):

$$EC = 420,306 \times Q^{-0.5486} \qquad \text{[Eqn. 11-1a]}$$

Non-Irrigation Season (October – March):

$$EC = 2,171,698 \times Q^{-0.688} \qquad \text{[Eqn. 11-1b]}$$

where,

EC = electrical conductivity (umhos/cm), and
Q = daily flow at Vernalis (acre-ft/day).

The estimated daily EC values obtained from the regression relationship are adjusted so that the daily EC estimated from Equations 11-1a and 11-1b are consistent with the monthly EC estimated from CALSIM. The adjustment concept conserves the total salt transport. The adjustment factor, *f*, is computed as the ratio of total salt transport using monthly flow and EC values to the total salt transport in a month using the daily flow and EC values calculated in Equation 11-1.

$$f = \frac{Q_m \times EC_m \times n}{\sum_{d=1}^{n} Q_d \times EC_d} \qquad \text{[Eqn. 11-2]}$$

where,

Q_m = monthly average flow,
EC_m = monthly average EC,
Q_d = daily average flow,
EC_d = daily average EC, and
n = number of days in a month.

Using the adjustment factor calculated in Equation 11-2, the daily-adjusted EC is then described in Equation 11-3.

$$EC'_d = f \times EC_d \qquad \text{[Eqn. 11-3]}$$

11.3 Post Processing

The output from the new planning setup is extensive, and therefore a much more complex analysis may be performed. Traditionally, the Delta Modeling Section reported the monthly average flows, water quality, and monthly minimum water levels. A more detailed analysis, such as the evaluation of tidal extremes, had limited value due to the use of the design repeating tide. In fact, the table of "monthly minimum water surface elevations" presented for some of the monthly planning simulations actually represented the average minimum and not the absolute minimum.

Figure 11.3 shows an example of a typical flow output for a given month utilizing the design repeating tide. The only information recorded in the standard output is a single value representing the monthly average value.

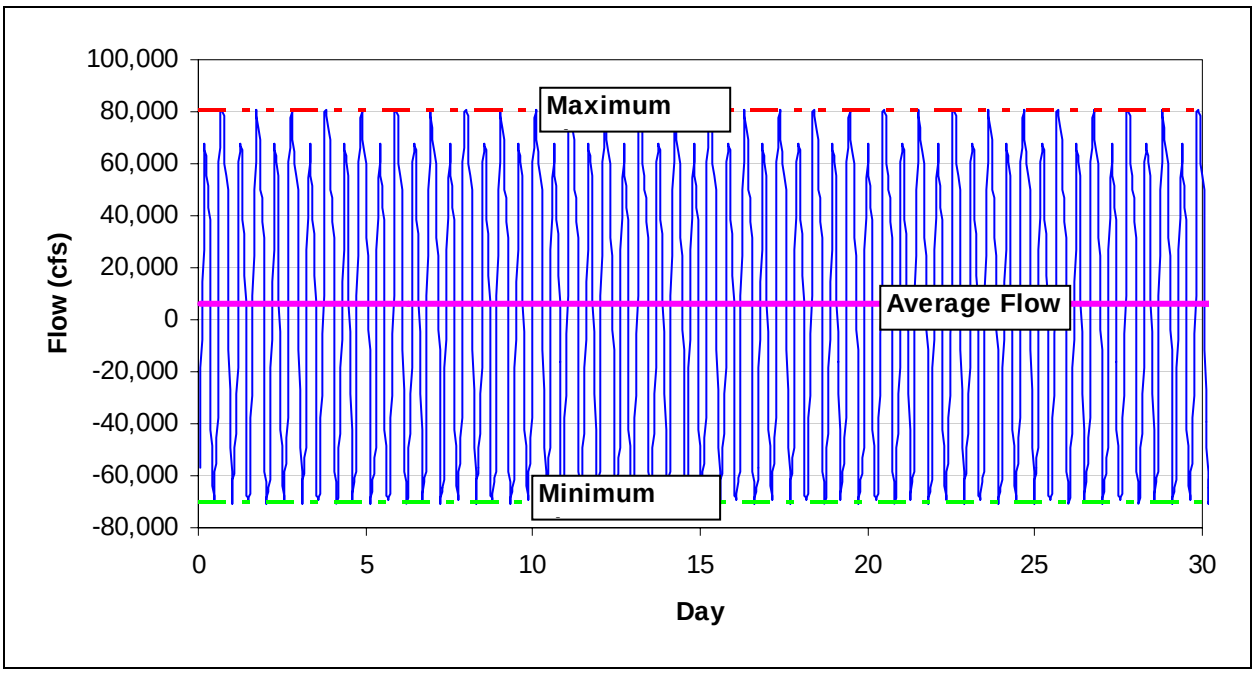

Figure 11.3: Typical Monthly Planning Study Flow Output.

Figure 11.4 represents the flow output using the adjusted astronomical tide. While it is possible to obtain and report only the monthly average statistics, a more detailed analysis may be warranted. For example, extreme value analysis can now be performed using the output that is available in a continuous time with spring neap effects due to adjusted astronomical tide.

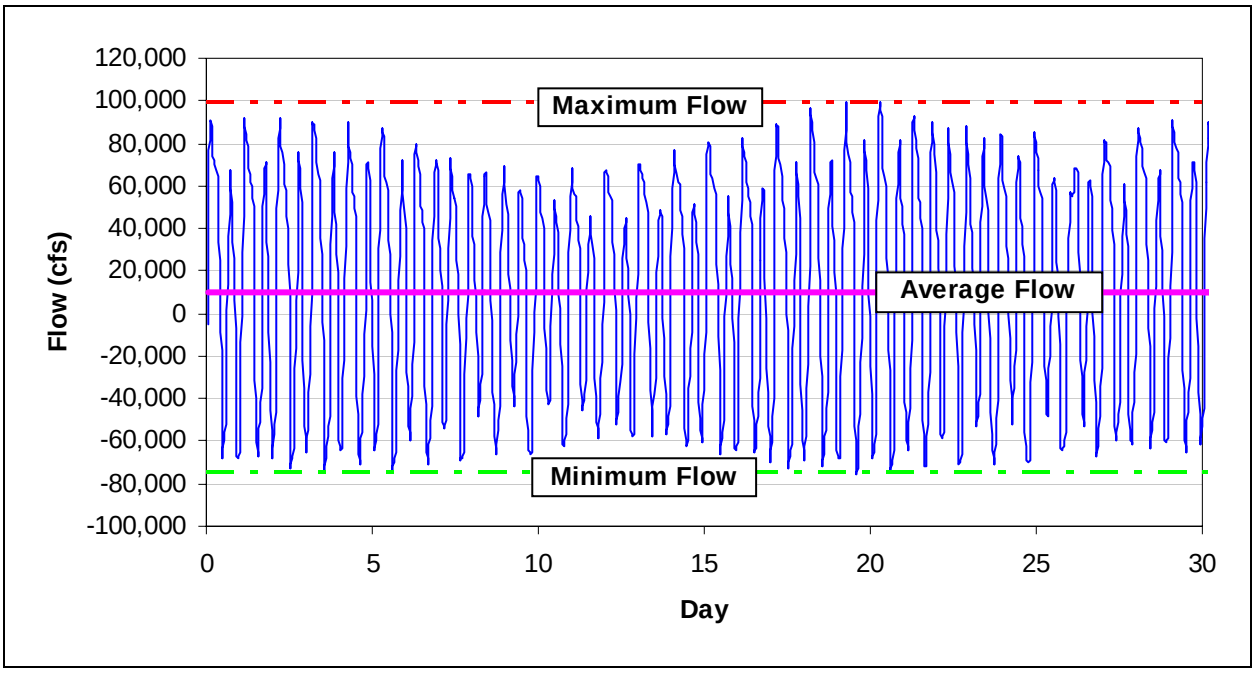

Figure 11.4: Typical New Daily Planning Study Flow Output.

A potential data presentation technique is to provide box and whisker plots as shown in Figure 11-5. The box and whisker plot gives all the statistics such as mean, median, upper and lower quartiles, and outliers in a single plot.

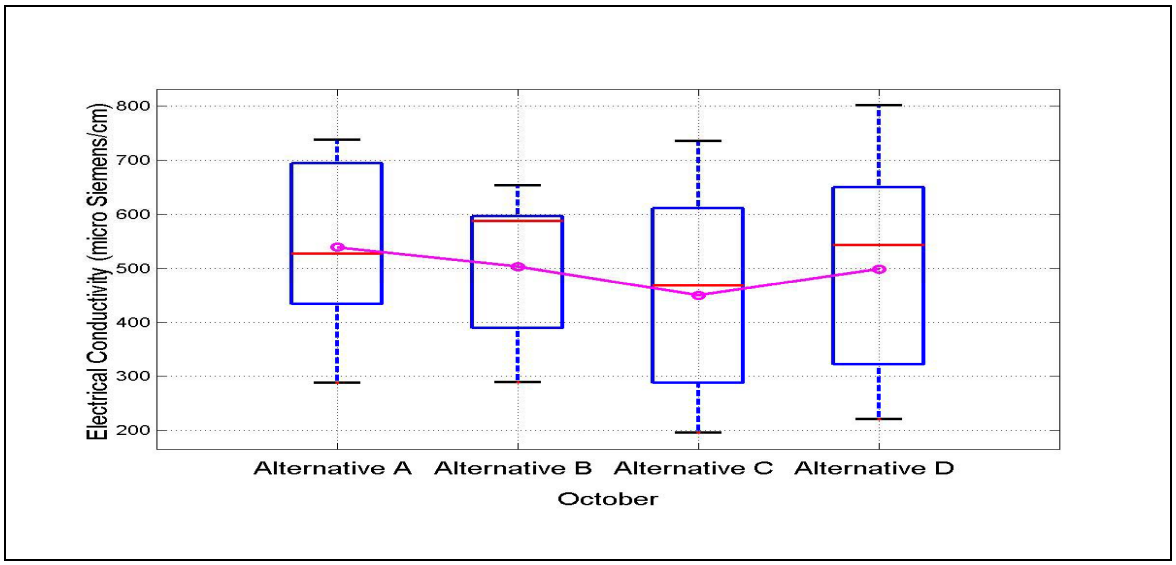

Figure 11.5: Typical Box and Whisker Plot.

The probability of exceedence plot as shown in Figure 11-6 is another potential data presentation technique that is more credible with the new planning setup. Probability plots provide information to help decision-makers select alternatives based on the alternative's risk tolerance in engineering and operational design.

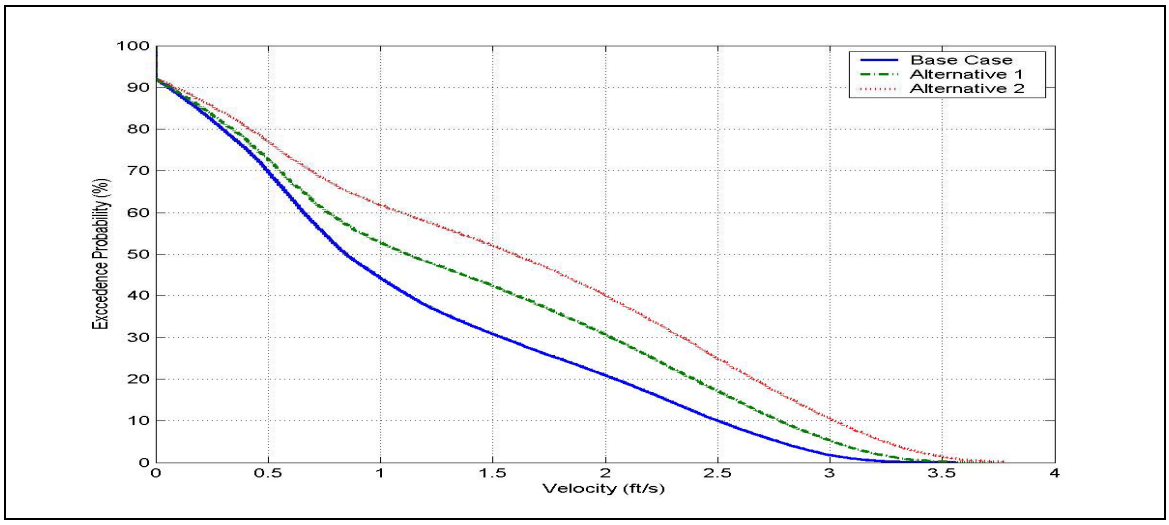

Figure 11.6: Typical Probability of Exceedence Plot.

The Delta Modeling Section is currently working on developing a post processor to provide a user-friendly analysis of the new planning study setup. The choice of data presentation techniques is expected to be an ever-evolving process based on the needs of the projects and clients.

11.4 Summary

Table 11.1 highlights the major differences between the new setup versus the traditional setup, as well as the current efforts and possible solutions for the limitations of the new setup. The comparisons made were based on a 1 GHz PC operating in the Windows 2000 environment.

Table 11.1: Comparison between Traditional Monthly Planning Studies and the New Daily Planning Studies.

	Traditional Monthly Planning Study	New Daily Planning Study	Remarks
Run Time	HYDRO and QUAL: 16 hrs	HYDRO and QUAL: 34 hrs	Current work on parallel processing of HYDRO may reduce the HYDRO run times by 50%, which is about 13 hours. However, this will require a network of computers.
Disk Space	HYDRO and QUAL output: 250 MB	HYDRO and QUAL output: 4 GB	Though a single HYDRO and QUAL run will fit on a DVD, the binary output files can be compressed to reduce the required disk space to around 3 GB.
Model Setup / Runs	Complex text-based setup, with a specific file structure. Monthly gate operations entered into a text file. Separate DSM2 runs made for each month.	Complex text-based setup, with a specific file structure. Daily gate operations generated by a series of scripts. One complete DSM2 run made for the entire simulation period.	Current work on a GUI based input database is discussed in Chapter 13.
Accuracy / Post Processing	Monthly average results only. Tide repeats over a 25-hour period.	Daily results available. Spring-neap variation accounted for in tide.	The use of daily hydrology and a tide that includes the spring-neap variation will allow for the true extremes to be analyzed.

One of the major advantages of the new setup over the traditional setup is that it simulates conditions closer to reality. This is primarily due to the fact that the new setup uses the adjusted astronomical tide at Martinez boundary, which captures the spring-neap effects. This was not possible using the traditional monthly setup when a repeating tide was used.

11.5 References

Ateljevich, E. (2001a). "Chapter 10: Planning Tide at the Martinez Boundary." *Methodology for Flow and Salinity Estimates in the Sacramento-San Joaquin Delta and Suisun Marsh. 22nd Annual Progress Report to the State Water Resources Control Board.* California Department of Water Resources. Sacramento, CA.

Ateljevich, E. (2001b). "Chapter 11: Improving Estimates of Salinity at the Martinez Boundary." *Methodology for Flow and Salinity Estimates in the Sacramento-San Joaquin Delta and Suisun Marsh. 22nd Annual Progress Report to the State Water Resources Control Board.* California Department of Water Resources. Sacramento, CA.

California Department of Water Resources. (1997). *Status Reports on Technical Studies for the Storage and Conveyance Refinement Process.* California Department of Water Resources. Sacramento, CA.

California Department of Water Resources. (1999). *Delta Simulation Model Studies, CALFED Bay-Delta Program: Vol. I.* California Department of Water Resources. Sacramento, CA.

Nader-Tehrani, P. (2001). "Chapter 9: Use of Repeating Tides in Planning Runs." *Methodology for Flow and Salinity Estimates in the Sacramento-San Joaquin Delta and Suisun Marsh. 22nd Annual Progress Report to the State Water Resources Control Board.* California Department of Water Resources. Sacramento, CA.

Methodology for Flow and Salinity Estimates in the Sacramento-San Joaquin Delta and Suisun Marsh

23rd Annual Progress Report
June 2002

Chapter 12:
DSM2 Documentation

Author: Jamie Anderson

12 DSM2 Documentation

12.1 Introduction

This chapter summarizes the Delta Modeling Section's strategy to improve documentation of the Delta Simulation Model 2 (DSM2). This chapter includes a summary of the documentation objectives, an overview of the planned documentation, an overview of the recently released DSM2 tutorial, and a review of the progress to date and future directions.

12.2 Objectives

The DSM2 documentation effort has two main objectives:

- to document the DSM2 model, and
- to standardize documentation for studies conducted using DSM2.

Details of these two objectives are described below.

12.2.1 Documenting DSM2

The primary objective of the DSM2 documentation effort is to describe the DSM2 model. Topics to be included are:

- Model formulation
- Assumptions
- Methodology
- Accuracy
- Appropriate use
- Tutorial for use

12.2.2 Standardizing Documentation of DSM2 Studies

Another objective of the DSM2 documentation effort is to standardize the documentation of studies conducted using DSM2. Topics to be included are:

- Assumptions
- Methodology
- Interpretation of results
- Dissemination of study results

12.3 DSM2 Documentation Overview

The DSM2 documentation will consist of three volumes. The first volume will review the mathematical formulation and verification of DSM2. The calibration and validation of DSM2 will be presented in the second volume. And the third volume will contain the details of how to run DSM2 and it has been given the top priority for documentation preparation.

12.3.1 Volume 1: Formulation and Verification

The first volume of the DSM2 documentation will describe the mathematical formulation used in DSM2 and the verification of the DSM2 code. Although DSM2 consists of three modules (HYDRO-hydrodynamics, QUAL-water quality, and PTM-particle tracking model), the documentation will focus on HYDRO and QUAL since PTM is documented elsewhere (see Chapter 2 of this report; Wilbur, 2001; and Smith, 1998). The mathematical formulation descriptions will include both the theory used to develop DSM2 and summaries of the algorithms that translate the theory into a numerical model.

Verification of a numerical model is the process by which the correct coding of the model algorithms is confirmed. It focuses on analysis of predicted response patterns and conservation balances. The documentation on the HYDRO verification may describe model exercises including:

- Steady, uniform flow in an open-ended channel
- Steady flow through a channel network
- Unsteady flow through a channel network
- Steady flow through a gate
- Hydrograph routing

Similarly, the documentation on the QUAL verification may describe model exercises including:

- Advection of a salinity plume
- Advection of a sharp salinity plume[1]
- Salinity penetration into a channel
- Salinity penetration into a network of channels

12.3.2 Volume 2: Calibration and Validation

The second volume of the DSM2 documentation will describe the DSM2 calibration and validation. The calibration and validation documentation will focus on HYDRO and QUAL since the calibration of PTM is documented elsewhere (see Chapter 2; Wilbur, 2001; and Smith, 1998).

Calibration is the process by which model parameters are adjusted to improve the correspondence between the simulation results and observed data for the calibration time period. Once the model is calibrated, it is validated by running the model for a second time period without adjusting any of the model parameters. The simulation results are compared to observed data to determine if the model provides acceptable results for conditions outside of the calibration time period. The assumptions, approach, and results of the Interagency Ecological Program DSM2 Project Work Team's (IEP-PWT) calibration and validation effort is currently being documented under the direction of Chris Enright of DWR's Environmental Services Office

[1] A sharp salinity plume is one in which the salinity gradient is very steep. Representation of sharp constituent gradients in numerical models is challenging due to numerical dispersion. Thus, examining both mild and sharp constituent gradients is necessary to understand how a particular model, DSM2 in this case, is affected by numerical dispersion.

(DWR-ESO). The IEP-PWT documentation will be included in this volume of the DSM2 documentation.

The second volume of the documentation will also include a section on DSM2 performance conclusions. Whereas the calibration and validation focus on comparing simulation results at specific points in the Delta, the performance conclusions will be based on a larger regional or system-wide view of model results. The accuracy and reliability of DSM2 will be evaluated in various regions under various hydrologic conditions, gate operations, and tidal conditions. Factors such as mixing patterns and flow splits will be analyzed. The performance conclusions will provide users with a better understanding of how DSM2 performs under various hydrologic and operational conditions.

12.3.3 Volume 3: Using DSM2

The third volume of the DSM2 documentation will provide instructions for running DSM2. Thus, the third volume will serve as a DSM2 user's guide. This volume has been assigned the highest priority in the documentation effort. Similar to the first two volumes, this documentation will focus on HYDRO and QUAL.

The third volume of the DSM2 documentation will be divided into three main sections: background information, basic use of DSM2, and advanced use of DSM2. The first section will contain general information that would be useful for users learning about numerical modeling of tidal systems. A brief review of tidal dynamics is provided. A general overview of topics related to modeling tidal estuaries is presented followed by information specific to the Sacramento-San Joaquin Delta and DSM2.

The second section of the DSM2 user's guide will describe basic use of DSM2. The three modes of DSM2 operation (historical, planning, and forecasting) will be discussed. Data requirements and input file structure will be presented. This documentation will evolve as the DSM2 input system evolves (see Chapter 13). Use of DSM2 will be illustrated with tutorial exercises. Sample input files for all tutorial exercises will be provided in the text and will be made available to the user on the DSM2 website.

The user's guide documentation for DSM2 use in historical simulations has been completed. As well as being incorporated into volume three, this documentation has been released as a stand-alone tutorial (see section 12.4).

The third section of the DSM2 user's guide will provide information on advanced usage of DSM2. Sample topics include gate operations, permanent and temporary barriers, object-to-object transfers, mass tracking, and fingerprinting. This section of the documentation will be based on the experience of the Delta Modeling section in actually using DSM2 for studies.

12.4 DSM2 Tutorial

The first completed product of the documentation effort is a DSM2 tutorial. The tutorial introduces the use of HYDRO and QUAL using historical simulations for November and December 1996. These time periods were selected because complete data sets for those time

periods were available. The tutorial includes sample text input files that have been annotated and exercises that illustrate common changes made to the base input files. Information is also provided on sources of observed data for comparison with simulation results. The tutorial text and the sample input files are available on the DSM2 website at http://modeling.water.ca.gov/delta/models/dsm2/index.html.

12.5 Progress and Future Directions

Progress on the DSM2 documentation effort to date includes:

- Developing an outline for all three volumes of the documentation
- Focusing effort on development of the DSM2 user's guide (volume 3)
- Creating a standalone tutorial on use of DSM2 for historical simulations (which is available at http://modeling.water.ca.gov/delta/models/dsm2/index.html)
- Completing documentation on tidal dynamics and modeling of tidal estuaries
- Beginning documentation on specific information related to modeling the Sacramento-San Joaquin Delta and DSM2
- Describing use of DSM2 for water quality fingerprinting (see Chapter 14)

Future directions for the DSM2 documentation include:

- Continuing to document DSM2
- Finishing the DSM2 user's guide (volume 3) is the top priority
- Modifying the DSM2 documentation to reflect changes in the DSM2 input system (such as those described in Chapter 13)
- Providing documentation in HTML format in addition to MS Word and PDF formats
- Incorporating HTML documentation into DSM2 in the form of online help
- Developing standardized methods for documenting DSM2 studies
- Redesigning the DSM2 website to facilitate online dissemination of information

12.6 References

Smith, Tara. (1998). "Chapter 4: DSM2 PTM." *Methodology for Flow and Salinity Estimates in the Sacramento-San Joaquin Delta and Suisun Marsh. 19th Annual Progress Report to the State Water Resources Control Board.* California Department of Water Resources. Sacramento, CA.

Wilbur, Ryan J. (2001). "Chapter 4: Validation of Dispersion Using the Particle Tracking Model in the Sacramento-San Joaquin Delta." *Methodology for Flow and Salinity Estimates in the Sacramento-San Joaquin Delta and Suisun Marsh. 22nd Annual Progress Report to the State Water Resources Control Board.* California Department of Water Resources. Sacramento, CA.

Methodology for Flow and Salinity Estimates in the Sacramento-San Joaquin Delta and Suisun Marsh

23rd Annual Progress Report
June 2002

Chapter 13:
DSM2 Input Database and Data Management System

Author: Eli Ateljevich and Tawnly Pranger

13 DSM2 Input Database and Data Management System

13.1 Introduction

A feature of DSM2 since its inception has been its flexible text input system, which improved upon the default "fixed-width FORTRAN" restrictions of previous models. There are a few shortcomings that have not been addressed, however. One is a lack of transparency. The current system allows for an excessive number of ways to accomplish some tasks. The inner workings of the model reflect this complexity as well – a significant amount of the source code is dedicated to handling switches, options, priorities, and text substitution features. A second difficulty with the text system is the problem of data management. DSM2 text input is not fully compatible with database storage nor is it easily converted to one of the newly established text standards for data such as XML. This makes version control and data standardization efforts difficult to automate using modern tools. For some kinds of studies, the standard for data acquisition is still to copy files from a colleague or previous project.

The DSM2 database project marks a transition towards more rigorous data management. This is a multifaceted effort:

- DSM2 has been reprogrammed to accept connections directly to a database,
- A normalized database structure has been devised for the input,
- An application (the "user interface") has been created for viewing and editing the data, and
- A replication scheme has been planned that will ensure data consistency across a network of users.

At the same time, every effort has been made to retain flexibility features from the original text input system that DSM2 modelers are known to use often and correctly.

In terms of data management, the goals for the DSM2 database project are as follows:

- Data standardization: users should be able to synchronize to a single, "best" version of standard input packages across a network without any bookkeeping or responsibilities on their part. The private passing of data from user to user should be discouraged (mechanically).
- Reusability: users should be able to work with bundles of standardized, frequently used components (e.g., the "Standard Delta Grid" or "South Delta Permanent Barriers").

- Security: the most important standard input should be administered and version controlled.

- Reproducibility: the user should be able to access data from the past (e.g. “as it was on March 15, 2002”).

- Externalization of quality control: data validation rules should be incorporated into the database and by the user interface. This is more efficient, reliable, and visible than the black box quality checking that goes on every time DSM2 is run.

- Modernization: the data management system should make use of high quality technology, including proprietary database applications and libraries. It is this commitment that makes such a large laundry list of goals possible under the umbrella of a single project.

The remainder of this chapter describes tools and methods that help meet these goals. Most of them are currently functional and are in beta testing at the time of writing. The chapter is not intended as a user’s manual for individual components, but rather to describe their contribution to the data management strategy.

13.2 Database and Data Management

The heart of the project is the DSM2 input database. Water resource engineers in California are accustomed to applying the term “database” to anything from a few tables in an Excel spreadsheet or Access desktop database file to large institutional databases such as the IEP data vaults or CDEC. In the case of the spreadsheet or desktop database, the data is actually on file in the user’s computer, and if the user manipulates the information and passes it to another user no data management has occurred. At the other extreme, users querying IEP or CDEC databases have no administrative control of the data. Access to the database is offered by means of custom web pages or software agents. In fact, the implementation details of the database are not known or important to the user.

The DSM2 database lies between these extremes. From the user’s point of view, the database appears like a Microsoft Access desktop database. The user will also have local copies of the DSM2 user interface and DSM2 numerical model software, which interact with the desktop database independently, as indicated in Figure 13.1. The user interface provides a graphical environment for editing data and preparing simulations. DSM2 queries this data at runtime, communicating with the database on a “read-only” basis.

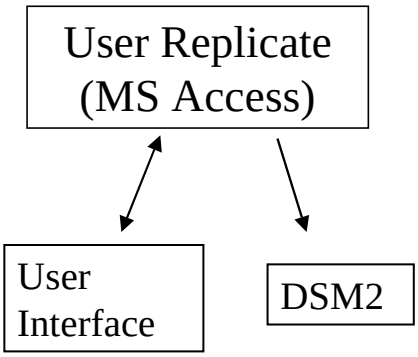

Figure 13.1: Single User Interface for Editing Data and Creating Simulations.

As implied by Figure 13.2, the desktop database is also a *replicate* in a larger, enterprise-wide data synchronization scheme. In a database context, the term *replication* refers to the sharing and synchronization of data within an organization or wider community. There are as many replication models as there are *business rules* for sharing data. The replication model for DSM2 is a consolidation model. The database *master* is a repository of the most important simulation data to which the replicates have full read access and limited (protected) write access.

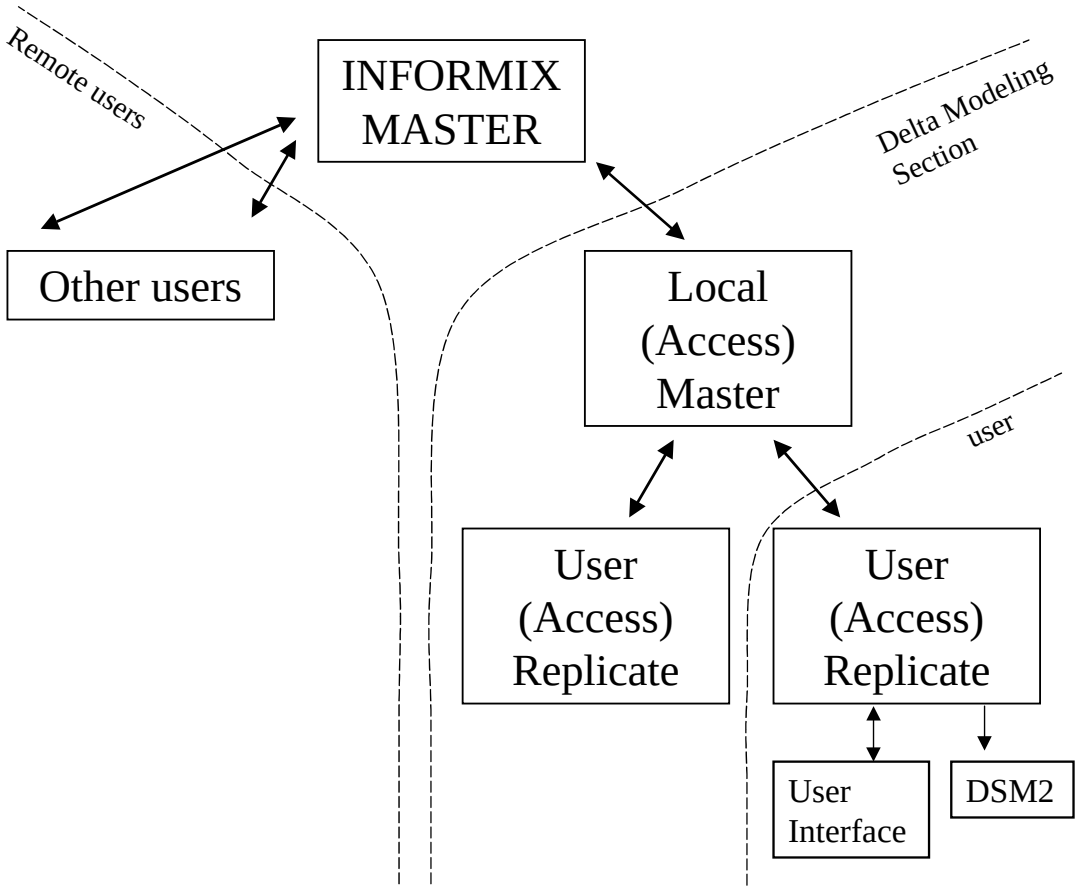

Figure 13.2: Single User in Context of a Local (MS Access) Replicate System and a Remote (Informix) Replication System.

Within the Delta Modeling Section, replication can be achieved almost entirely with Microsoft Access features. The user receives a replicate of the master database, which is a nearly full-function desktop database (the limitations can be found in the MS Access documentation; replicate status cannot be altered). The use of the Informix component has introduced two additional needs. First, it is desirable to have an Internet-capable server in order to share DSM2 data with the wider Delta modeling community. Second, Informix is an industrial strength "transactional" database that is able to log and timestamp every change made to it. Later in this chapter it will be shown that these timestamps are the key to an entirely different notion of "replicability" – the ability to reproduce earlier simulations.

The link between Informix and the Microsoft Access local master is accomplished with a Visual Basic module. Both the administration of the Informix database and the link to the local master are being carried out with the assistance of IEP database specialists.

13.3 Database Structure

The tables in the database are based on the standard relational model. The attributes of model elements such as channels and gates are stored in separate tables, using one column (also known as a *field*) per attribute. When data from different tables need to be brought together or cross-referenced, the tables can be joined during retrieval using a common field. For example, assume the database contains two tables, Channel and GridDescription, with the following fields:

Channel	**GridDescription**
ChanID	GridID
GridID	GridDescription
Length	Creator
Manning	
Dispersion	

Note: these listings are a simplification of the tables in the database.

The two tables can be joined on the GridID field to produce a result set containing information from both tables, for example ChanID, Length, and GridDescription.

In order to facilitate joins and queries, tables in the DSM2 Input Database conform to *third normal form*. Table normalization is the adherence to design rules that minimize data redundancy and prevent "anomalies" during queries (orphaning of records, contradictory entries, etc.). There are five levels of normalization described in standard texts, each indicating a stricter set of rules; third normal form is usually considered adequate by industry standards. One of the most visible consequences of data normalization is that where "one-to-many" relationships are present, a hierarchy of tables is required. A good example is the channel hierarchy. One Channel may have many Cross-sections. And each Cross-section may represent many Layers of geometry data. The hierarchy for Channels is shown in Figure 13.3.

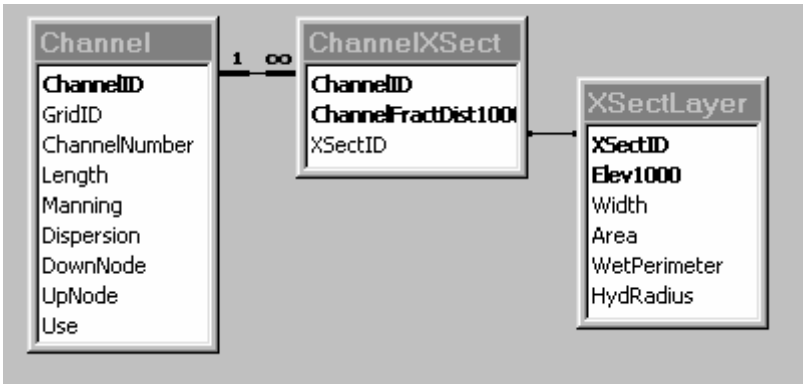

Figure 13.3: Hierarchy of the Channel Table.

Normalized tables are not intuitive to read, but they allow data from different tables to be *joined* or *linked* flexibly to form a variety of useful views. This preference of many potential views over one good immediate view underscores an important aspect of database design: **separation of the table design and the "view" of the data**.

Joining tables to form new views was described in the preceding paragraphs; *linking* tables is illustrated in Figure 13.4, a sample from the DSM2 User Interface. The tables in the top table are linked to those in the bottom panel. If the user selects a channel in the top panel, related cross-section data automatically appear.

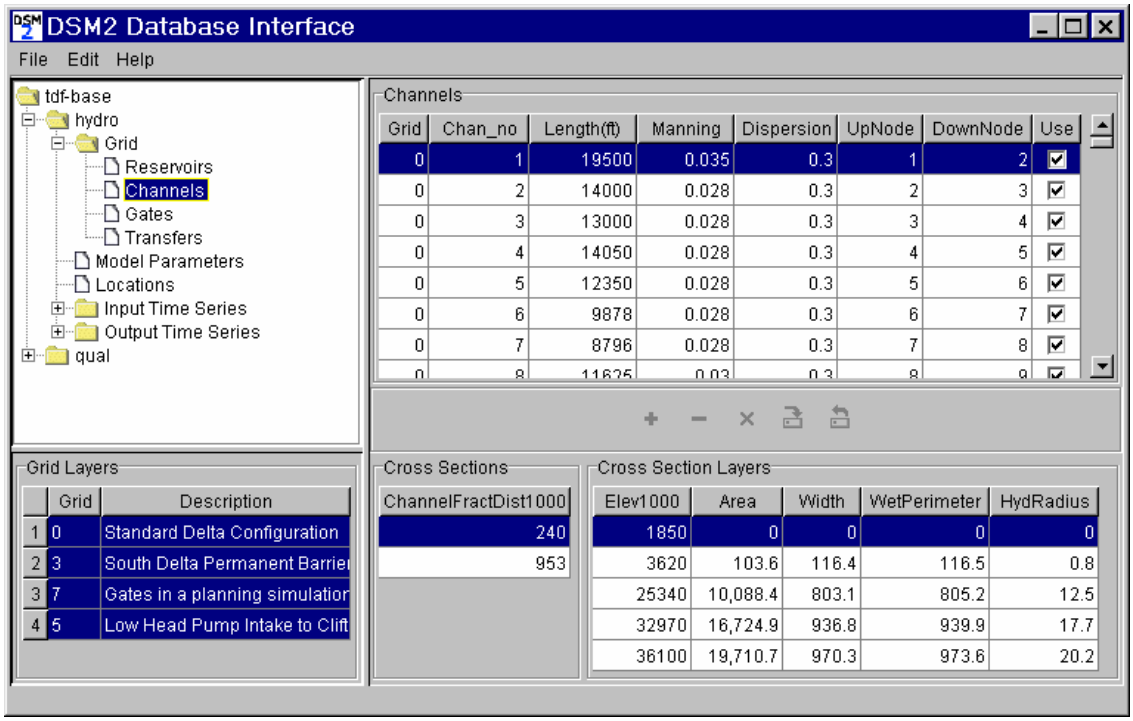

Figure 13.4: DSM2 Database Interface (Channels).

Software clients such as the new DSM2 User Interface and the DSM2 numerical model retrieve information from the database using queries written in the Structured Query Language (SQL) and implemented using software libraries designed for SQL. These libraries in turn rely on

database connectivity protocols (ODBC), which allow disparate data sources and clients to talk to one another. DSM2 connects to the input database using the CainamaSoft f90SQL library and the ODBC protocol. The user interface uses Java libraries by Borland and the JDBC:ODBC protocol. Further discussion of data normalization, SQL and ODBC is beyond the scope of this chapter; these subjects are described in most database software manuals and books.

13.4 Component Sets and Layers

There is one aspect of modeling practice that was particularly important to capture in the database design, and that is the frequent reuse of groups of components. A component is an object used by DSM2 such as a channel, a parameter, or information for inputs and outputs. To understand the importance of component reuse, one only need reflect on the type of work done by DWR (and most other institutional modelers). The bulk of the work for institutional modelers is not to pioneer new domains, but to investigate changes in a small handful of established ones. DSM2 modelers in DWR currently focus on the main Delta and an extension of the San Joaquin River.

If the number of model domains is small, the number of individual management decisions is at most medium sized – a few dozen are under active consideration at any one time. However, these components act like letters in an alphabet or notes in a scale – their permutations generate a large number of scenarios for investigation. For instance, a recent request for a study specified: standard Delta grid, CALSIM boundary input, South Delta Permanent Barriers, Through-Delta Facility, and low-head pump alternate intake to Clifton Court intake. All of the components on this list are potentially useful in other contexts.

In the new database, logically connected component groups like the standard Delta grid, the CALSIM Input set, or South Delta Permanent Barriers can be tagged together in one set. These sets may then be freely combined to construct a specific run. There are four kinds of sets:

- Grid components: Groups of channels, gates, reservoirs, and object-to-object transfers.
- Parameter sets: Groups of model parameters (grid resolution, closure parameters) that are commonly applied to numerical models.
- Input sets: Groups of input time series for boundary data (flow, stage, and water quality boundary conditions).
- Output sets: Groups of output time series commonly requested together.

All that remains is to define carefully the behavior when several component sets of a particular type (for example two sets of grid components) are used together. In the preceding example, the standard (historical) Delta grid defines temporary barriers in the south Delta, but the proposed study must overwrite these temporary barriers with the above-mentioned South Delta Permanent Barriers.

The prioritization is accomplished through a “layer” scheme similar to that used in image software such as Adobe PhotoShop™. Figure 13.5 illustrates this principle. The base layer 1 shows a model with 6 channels. The modeler wishes to alter channel 2 and extend the grid upstream of channel 3. This is accomplished by adding a new layer with only two elements: one for channel 2 and one for channel 7.

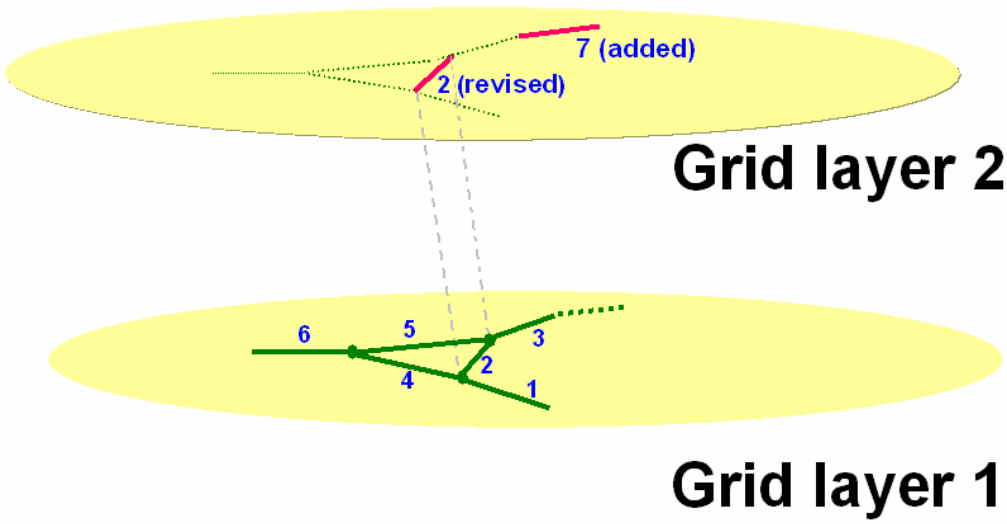

Figure 13.5: Input Layers.

In a sense, this layering scheme merely enforces good modeling practice – after all, the DSM2 text input system has always allowed overwriting. The layering system is only novel in two senses. First, it is enforceable. Users who want to dredge a channel as part of a what-if analysis cannot do so by making arbitrary changes on the standard Delta grid files. Second, overwriting is explicit. Every component carries the identification of the bundle it is defined on (e.g., the GridID field for channels shown earlier in Figure 13.4). The DSM2 User Interface is able to graphically represent:

- The input as DSM2 will see it.
- Components that have been overwritten by higher level layers.

Figure 13.6 shows how in the DSM2 User Interface entries are shaded when they are overridden by a higher-level layer, alerting the user that an entry has been overridden and allowing the user to see what the previous value was.

Some security is enforced at the level of the interface. Changes to the grid (or boundary inputs, parameters, etc.) are only allowed on one layer at a time. The interface does not allow changes until the user has selected an “editing layer”.

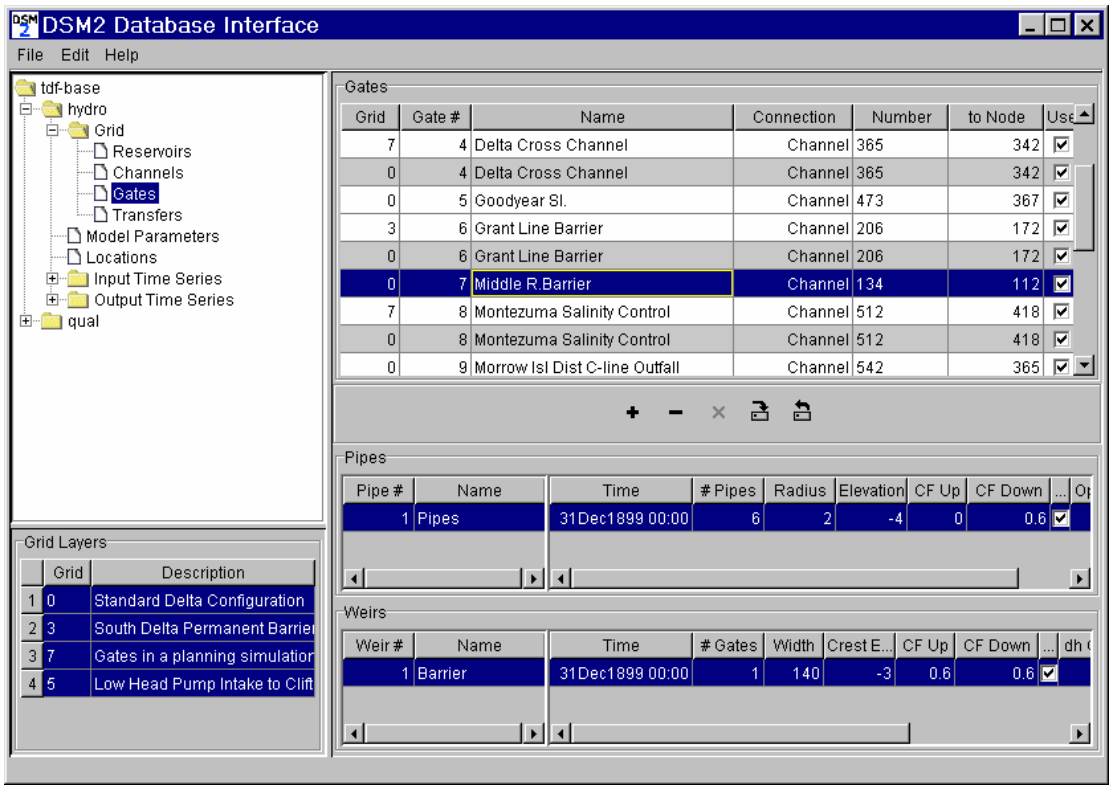

Figure 13.6: DSM2 Database Interface (Gates).

13.5 Version Control

The layering system described in the previous section is designed to facilitate experimentation, not version control. Version control is the management of refinements to the model over time. For instance, new bathymetry data may become available for channel 2, making it clear that the representation of this channel in the "standard Delta group" should be deeper. In version control, a "better" and a "worse" is usually involved. Contrast this example with an experiment: we want to analyze the outcome of dredging Channel 2. In this case, two simulations will be conducted with two different geometries for the channel, each "correct" for the scenario it represents.

Once an update has been finalized, modelers will want to make use of this correction in nearly all subsequent model runs. For the most part, distribution of the new version is effortless due to the enterprise replication scheme. The custodian of the standard Delta grid will make the necessary change and save it to the master database. The new version is then propagated to replicates upon synchronization.

In rare instances, simulations have to be performed again and replicability of a previous simulation is important (note: this discussion covers replication of an experiment, not database replication). Fortunately, the ability to roll back and view a previous version is a capability of transaction-based industrial databases, such as the Informix server. In other words, we can view "the input database as it was on March 15, 2002". As of June 2002, the Informix-based version control has not yet been implemented or tested.

13.6 Data Validation and the Externalization of Quality Control

When text is used for model input (with the exception of text that follows the XML standard), there is no choice but to validate the data inside the numerical model. This checking adds considerably to the complexity of the code, increasing the chances of software bugs. It is also a black box – without scrutiny of the source code, the user can only know from experience which items have been checked.

Externalization of quality control refers to the shifting of quality checks from DSM2 to the database and the user interface. Data validation is a standard feature of database software. The database is able to enforce field-level validation rules, such as: "channel length must be positive" or "Mannings coefficient must be between 0.0 and 1.0". It can also enforce some record-level validation rules involving more than one field, such as: "if two reservoirs have the same name, they cannot have a different reservoir number". The database passes these rules on to the user interface, so that they are enforced during data entry. The code to perform the checks is part of the underlying Microsoft, Informix, and Borland software, freeing DWR engineers to concentrate on aspects of the code in which they have better expertise and sufficient resources.

Besides being more efficient, external data validation is more transparent to the user. When data validation is internal to the numerical model, users make the error first and can only assume the internal checking will be exhaustive enough to catch them at run time. With the database and user interface, validation is pre-emptive and even interactive: graphical *picklists* are used for some input to restrict the range of entries to a prearranged data dictionary. Figure 13.7 shows the use of a picklist while selecting a *Location* for model output. This picklist displays all previously defined model locations along with descriptions, at the same time preventing the user from entering a *Location* that has not been defined yet (in another part of the interface).

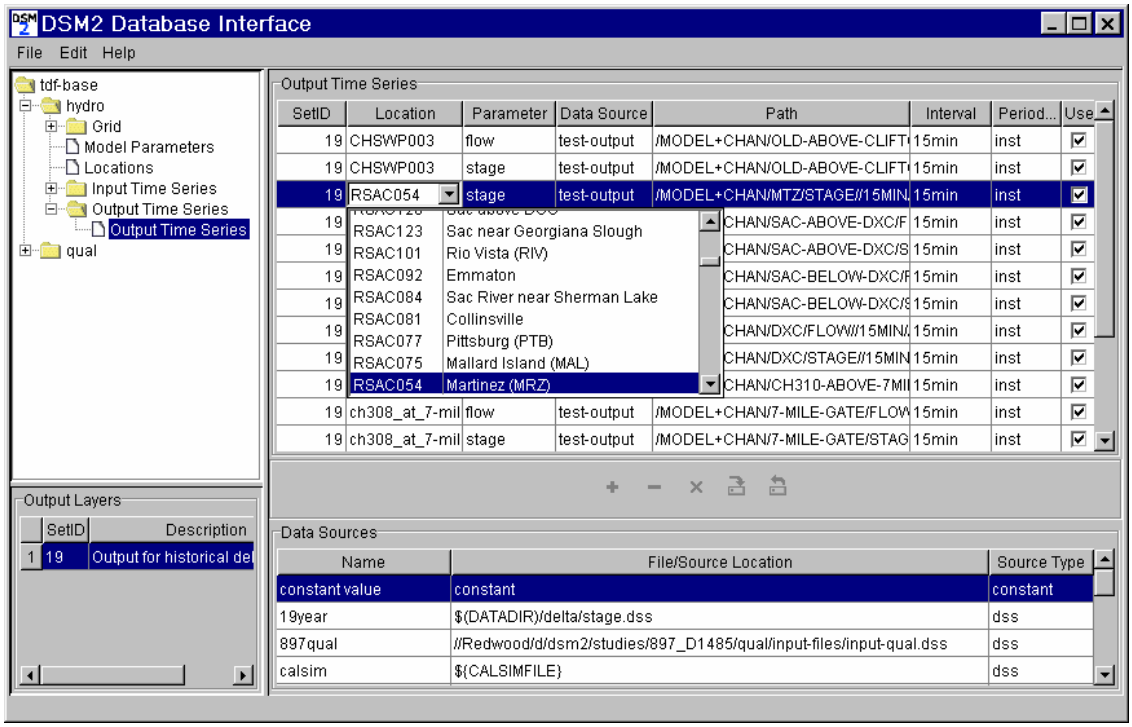

Figure 13.7: DSM2 Database Interface (Output Time Series).

13.7 Conclusions

The DSM2 Input Data project represents an effort not only to bring modern data management to DWR's Delta Modeling Section, but also to conform to the way Delta modelers do their work. The layering scheme described in this chapter is an innovation aimed at the typical institutional setting: few model domains, lots of management options. The other facets of the data management strategy – data validation, data normalization, version control and replication – simply make use of established database software features.

The database project described in this chapter is in a beta-testing state. A few DSM2 model runs have been performed using database input and checked successfully against text input equivalents. The user interface is complete, but still awaits documentation. The connection to the Informix server, which is needed for both external connectivity and version control, is still incomplete.

Finally, the database project heralds one more change in software development strategy. For the first time, a proprietary library (f90SQL by CainamaSoft) has been linked directly to DSM2. Moreover, since this library is only available for the PC, the UNIX environment must be abandoned – at least for the time being. These changes, while lamentable according to open-source philosophy, represent an excellent shift in resource allocation for DWR. The computational portion of the code is still completely open, while some of the data management chores have been shifted to specialty software that is well supported.

Methodology for Flow and Salinity Estimates in the Sacramento-San Joaquin Delta and Suisun Marsh

23rd Annual Progress Report
June 2002

Chapter 14:
DSM2 Fingerprinting Methodology

Author: Jamie Anderson

14 DSM2 Fingerprinting Methodology

14.1 Introduction

A methodology has been developed where a single simulation using the Delta Simulation Model 2 (DSM2) can be used to estimate the concentration of any conservative constituent at any specified time and location in the Delta[1]. Transport of conservative tracer constituents is simulated to determine volume contributions from various sources. These volume contributions can then be utilized to estimate concentrations of any conservative constituent. Use of DSM2 in this mode is referred to as fingerprinting. The main methods of applying the fingerprinting technique are:

- **Volume Fingerprinting** - Determine the relative contributions of water sources to the volume at any specified location.
- **Volume and Timing Fingerprinting** - In addition to determining the relative contributions of water sources to the volume at any specified location, the time period during which that water entered the system is also recorded.

Fingerprinting techniques can also be applied to a specific constituent as follows[2]:

- **Constituent Fingerprinting** - Determine the relative contributions of conservative constituent sources to the concentration at any specified location.
- **Constituent and Timing Fingerprinting** - In addition to determining the relative contributions of conservative constituent sources to the concentration at any specified location, the time period during which that constituent entered the system is also recorded.

The volume fingerprinting techniques are the most general. Volume fingerprinting can be used to estimate concentrations of any conservative constituent without rerunning DSM2. Constituent fingerprinting is a more specific method in which the results are valid for the constituent simulated. For constituent fingerprinting, the results are not easily extrapolated to other constituents.

Fingerprinting provides valuable insight into the system being modeled. Applications of fingerprinting include:

Hydrodynamics

- Determine the relative flow contribution of each source at a specified location. For example, how much of the flow at Clifton Court originated from the Sacramento River, the San Joaquin River, eastside streams[3], the ocean, and agricultural return flows? (Volume fingerprinting)

---

[1] Parviz Nader-Tehrani in DWR's Delta Modeling Section developed this methodology for volume fingerprinting.
[2] Prior to the development of volume fingerprinting, the Delta Modeling Section has used the superposition principle for specific constituent fingerprinting (see Hutton and Chung, 1992).
[3] Eastside streams include the Mokelumne, Cosumnes, and Calaveras rivers.

- Determine the relative flow contribution and timing of each source at a specified location. For example, how much of the flow at Clifton Court originated from the Sacramento River, the San Joaquin River, eastside streams, the ocean, and agricultural return flows during the current month, last month, the month before that, etc.?
  (Volume and timing fingerprinting)

Water Quality

- Estimate conservative water quality constituent concentrations at specified locations using a single DSM2 simulation.
  (Volume fingerprinting)

- Estimate conservative water quality constituent concentrations and timing at specified locations using a single DSM2 simulation.
  (Volume and timing fingerprinting)

- Determine the relative importance of sources of a water quality constituent at a specified location. For example, how much of the EC at the entrance to Clifton Court Forebay was contributed by each source?
  (Constituent fingerprinting)

- Determine the relative contributions and timing of each source of a water quality constituent at a specified location. For example, how much of the EC at the entrance to Clifton Court Forebay contributed by each source entered the Delta this month, last month, the month before that, etc.?
  (Constituent and timing fingerprinting)

14.2 Conceptualization of Volume Fingerprinting

To illustrate the concept of volume fingerprinting, consider a stream with two tributaries (Figure 14.1). If a sample of water was removed from the stream at each of the three locations indicated in Figure 14.1, the volume of water in each sample would be made up of contributions from the three streams as shown in Figure 14.2. For illustration purposes, hypothetical relative volume contributions from each source have been indicated. DSM2 fingerprinting can be used to determine the relative volume of water at a given location from specified sources.

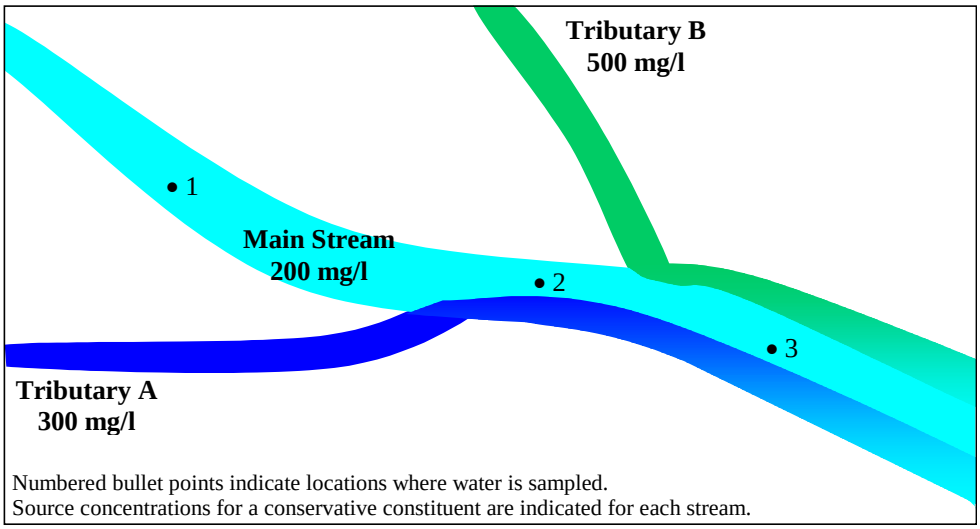

Figure 14.1: Conceptualization of a Stream with Two Tributaries.

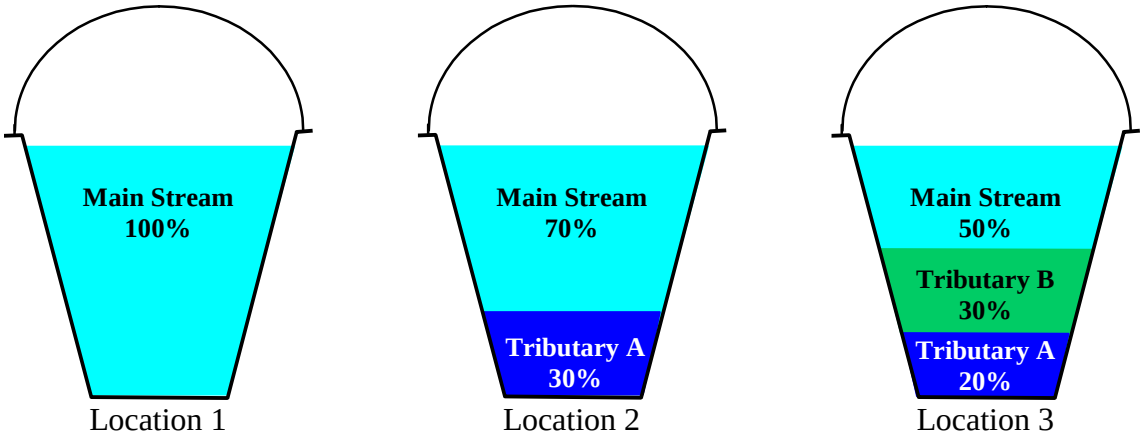

Figure 14.2: Conceptualization of Relative Volume Contributions from each Source for Water Sampled from Three Locations.

From the volume contributions and source concentrations, the concentration of a conservative constituent can be estimated by summing the volume of each source multiplied by the concentration of the constituent associated with that source (Equation 14-1).

$$C_{CC} = \sum_{i=1}^{n} \frac{V_{\%i}}{100} C_i \qquad \text{[Eqn. 14-1]}$$

where,

C_{CC} = concentration of a conservative water quality constituent at a specified location,
C_i = concentration of a conservative water quality from source *i* at the specified location,
n = total number of sources, and
$V_{\% i}$ = percent volume at a specified location contributed by source *i*.

Using the source concentrations from Figure 14.1 and the relative volume contributions from Figure 14.2, the concentration of a conservative constituent for the three sample locations can be estimated using Equation 14-1 as shown in Table 14.1 and Figure 14.3.

Using the volume fingerprinting methodology, the concentration of any conservative constituent can be estimated from the simulated volume contributions if the source concentrations are known. This methodology does not take into account any antecedent conditions. Because of the long residence time in the Delta due to tidal influences, the volume fingerprinting methodology provides a very rough estimate of conservative constituent concentrations. The timing of the sources becomes very important if the source flows or concentrations vary drastically with time. Thus for more accurate conservative constituent concentration estimates, the volume and timing fingerprinting methodology should be utilized.

Table 14.1: Estimation of Conservative Constituent Concentrations using Volume Contributions and Source Concentrations.

Source	**% Volume, $V_{\%}$**	**Source Concentration, C (mg/l)**	**$V_{\%}$/100 x C (mg/l)**
Location 1			
Main Stream	100	200	200
Tributary A	0	300	0
Tributary B	0	500	0
Total	*100*		***200***
Location 2			
Main Stream	70	200	140
Tributary A	30	300	90
Tributary B	0	500	0
Total	*100*		***230***
Location 3			
Main Stream	50	200	100
Tributary A	20	300	60
Tributary B	30	500	150
Total	*100*		***310***

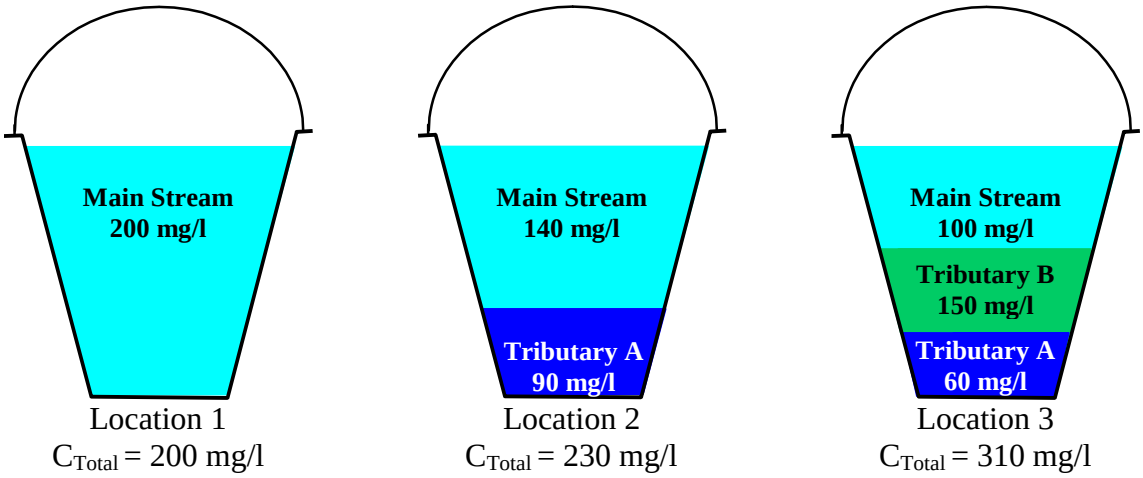

Figure 14.3: Conceptualization of Relative Concentrations Computed from Source Volumes and Source Concentrations for Water Sampled from Three Locations.

14.3 Conceptualization of Volume and Timing Fingerprinting

In some cases, it may be desirable to know not only the source of water, but also to have information of the timing when that water entered the system. In systems with long residence times, such as the Delta, the water from each source in a sample of water at a specified location may consist of water that entered the system at different times with different concentrations. Thus in addition to determining the source of the water in the sample, the timing of when that source entered the system is also useful for more accurate estimates of conservative constituent concentrations.

For illustration purposes, consider a sample of water withdrawn from a system with two sources (Figure 14.4). The sampled water could be divided both by source and by time period of entry into the system (Figure 14.5). For illustration purposes, hypothetical relative volume contributions from each source have been indicated for each time period. The number of time periods represented in the sample is referred to in this document as the system "memory". The length of the system memory will depend on the hydrologic conditions and the retention time of the system. For this example the system memory is three time periods long.

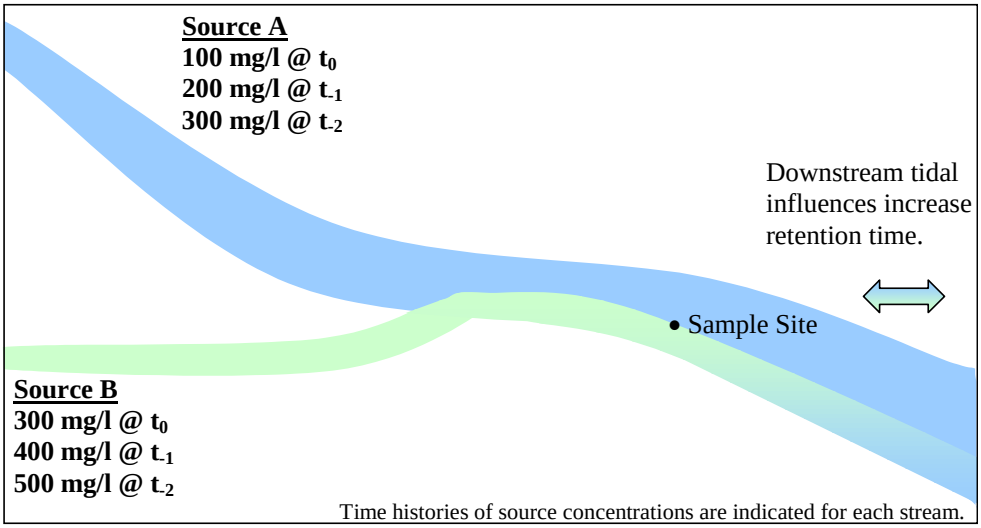

Figure 14.4: Conceptualization of Two Source Streams with a Long Retention Time after their Confluence.

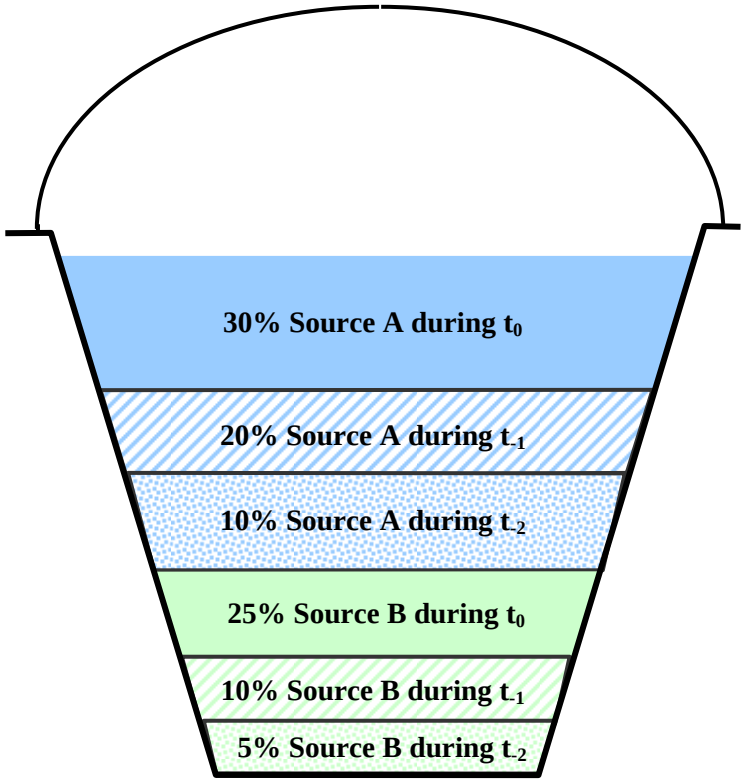

Figure 14.5: Conceptualization of Volume and Timing of Source Contributions in a Water Sample from Two Source Streams with a Long Retention Time.

From the volume contributions, source concentrations, and timing, the concentration of a conservative constituent can be estimated by summing the volume of each source for each time period multiplied by the concentration of the constituent associated with that source for that time period (Equation 14-2).

$$C_{CC}(t) = \sum_{i=1}^{n} \sum_{j=0}^{m} \frac{V_{\%i,-j}}{100} C_{i,-j} \qquad \text{[Eqn. 14-2]}$$

where,

$C_{CC}(t)$ = concentration of a conservative water quality constituent at a specified location and time,
$C_{i,-j}$ = concentration of a conservative water quality constituent from source *i* at time *-j*[4],
n = total number of sources,
m = length of the system memory, and
$V_{\%\,i,-j}$ = percent volume at a specified location from source *i* at time *-j*.

Using the source concentrations from Figure 14.4 and the relative volume contributions from Figure 14.5, the concentration of a conservative constituent for the sample location can be estimated using Equation 14-2 as shown in Table 14.2 and Figure 14.6.

Table 14-2: Estimation of Conservative Constituent Concentrations using Volume Contributions, Source Concentrations, and Source Timing.

Source	**% Volume, $V_{\%}$**	**Source Concentration, C (mg/l)**	**$V_{\%}$/100 x C (mg/l)**
Source A for t_0	30	100	30
Source A for t_{-1}	20	200	40
Source A for t_{-2}	10	300	30
Source B for t_0	25	300	75
Source B for t_{-1}	10	400	40
Source B for t_{-2}	5	500	25
Total	*100*		***240***

[4] Note that the time periods are counted backwards from the present. t_0 is the present time period, t_{-1} is one time period in the past, etc. Similarly $C_{i,0}$ is the concentration of the constituent from source *i* from the present time, $C_{i,-1}$ is the concentration of the constituent from source *i* from one time period in the past, etc.

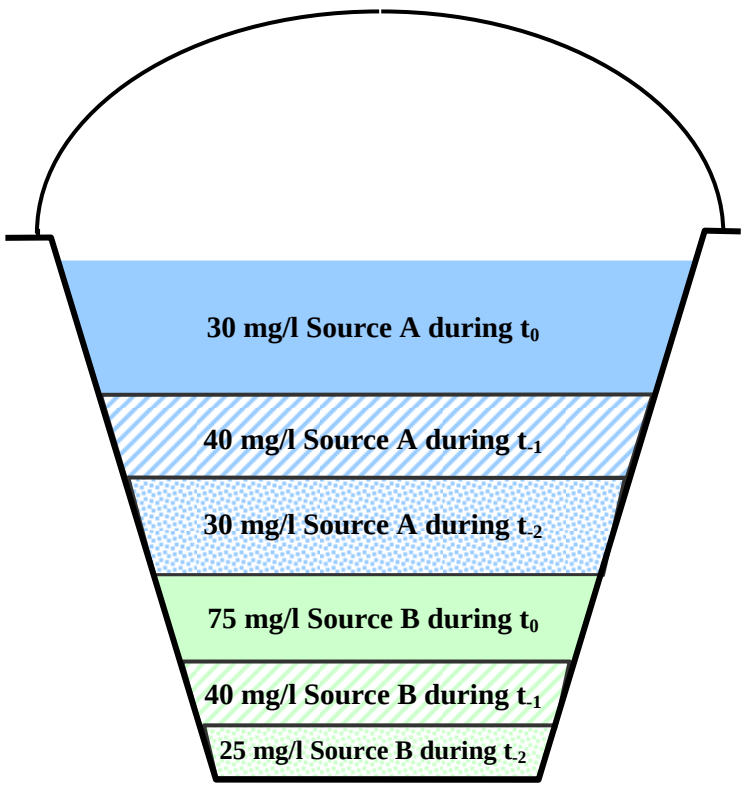

C_{Total} = 240 mg/l

Figure 14.6: Conceptual Relative Concentrations Computed from Source Volumes, Source Concentrations, and Source Timing.

Using the volume and timing fingerprinting methodology, the concentration of any conservative constituent can be estimated from the simulated timed volume contributions if the timed source concentrations are known. The volume and timing fingerprinting method should be used when boundary flows and concentrations vary drastically with time. Because of the long residence time in the Delta due to tidal influences and the varying boundary conditions, this methodology provides a better estimate of conservative constituent concentrations than the volume fingerprinting method.

To further illustrate the two different types of fingerprinting (volume fingerprinting and volume and timing fingerprinting), hypothetical fingerprinting results were generated for the three sample locations for the system shown in Figure 14.1. Pie charts for each type of fingerprinting (Figure 14.7) could represent relative contributions of either water volumes or of conservative constituent concentration depending on the type of analysis that was conducted.

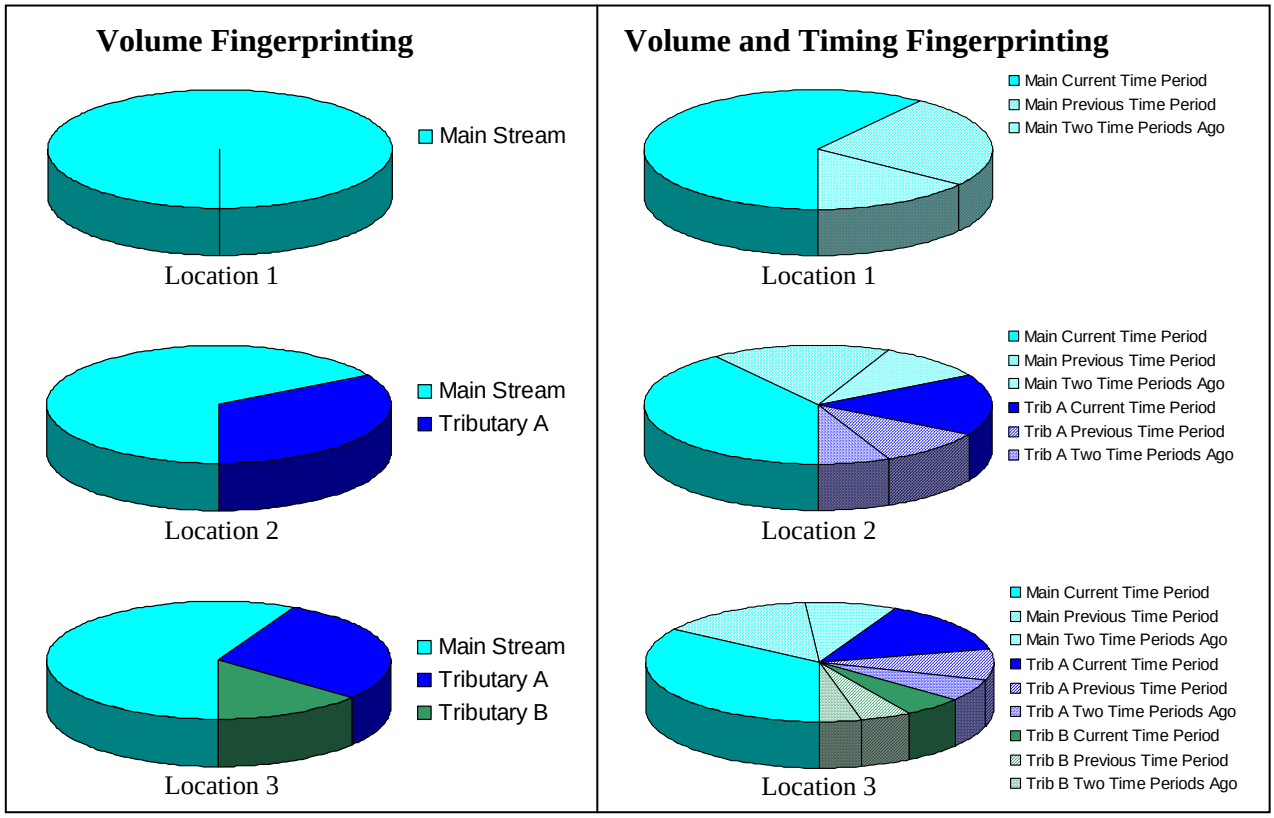

Figure 14.7: Pie Charts of Relative Contributions of Water Volume or of Conservative Constituent Concentrations using Two Fingerprinting Methods.

14.4 Constituent Fingerprinting

The volume fingerprinting methodologies described above provide a general analysis tool for water volumes and conservative constituent concentrations. Constituent fingerprinting is a specialized application of volume fingerprinting or volume and timing fingerprinting in which a specific constituent is utilized instead of a general conservative constituent. Constituent fingerprinting is discussed in more detail in section 14.6.

14.5 Application of Fingerprinting in the Delta using DSM2

Fingerprinting techniques have been utilized in DSM2 to analyze relative sources of flow and conservative constituents in the Sacramento-San Joaquin Delta. Due to the tidal flows in the Delta, the residence time or system "memory" can be up to six months depending on the hydrologic conditions. For fingerprinting studies, six main sources are typically used: the Sacramento River, the San Joaquin River, Martinez, eastside streams (all combined), agricultural drains (all combined), and the Yolo Bypass (Figure 14.9). A sample of water withdrawn from any location in the Delta contains water contributions from these sources (Figure 14.8). Similarly, the concentration of a conservative constituent at any location in the Delta is derived

from contributions from these sources. The flow and conservative constituent contributions from the various sources at a given location can be determined by conducting fingerprinting simulations utilizing DSM2.

DSM2 provides various methods for running fingerprinting simulations. These methods fall into two main categories, which are described in this chapter:

- Modify DSM2-QUAL boundary condition input files to use tracer constituents for fingerprinting analysis. This method can be used for volume fingerprinting, volume and timing fingerprinting, constituent fingerprinting, and constituent and timing fingerprinting.

- Modify DSM2-QUAL OUTPUTPATHS section to request internally computed fingerprinting results. This method can only be used for constituent or constituent and timing fingerprinting (see section 14.6.3).

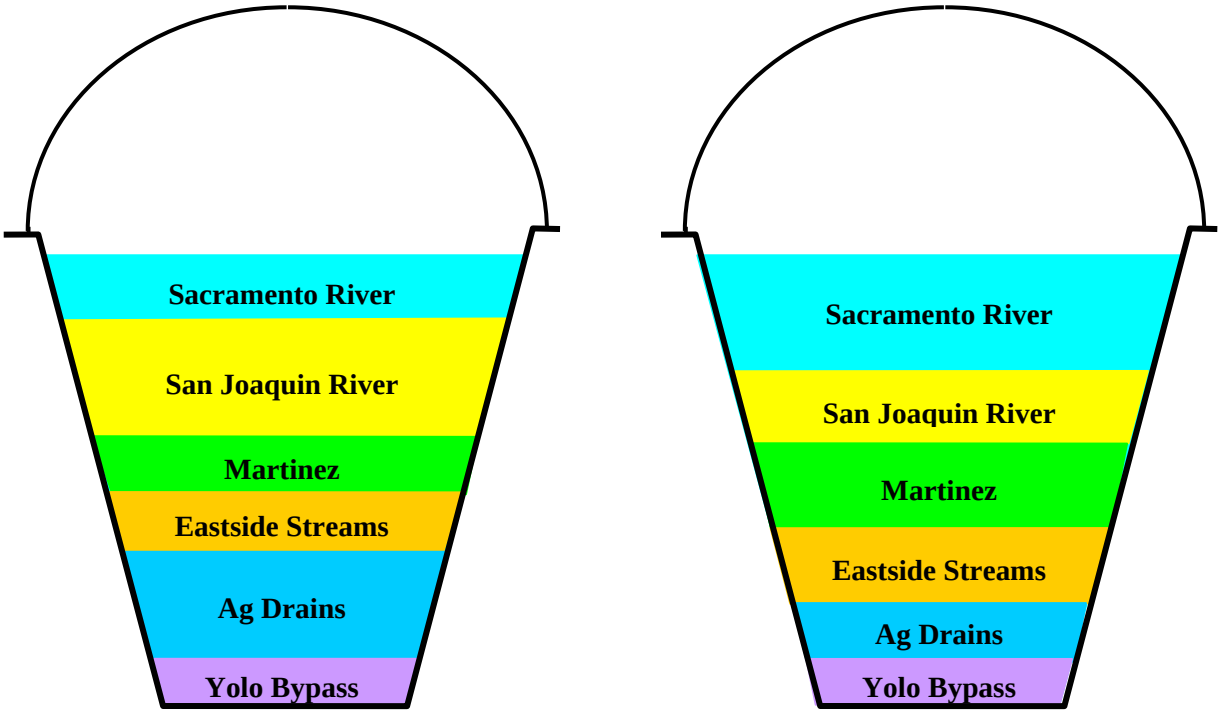

Figure 14.8: Conceptualization of Relative Contributions of Six Sources to Water Samples from Two Different Locations in the Delta.

Note: Relative contributions are for illustrative purposes only. They do not reflect actual results from the Delta.

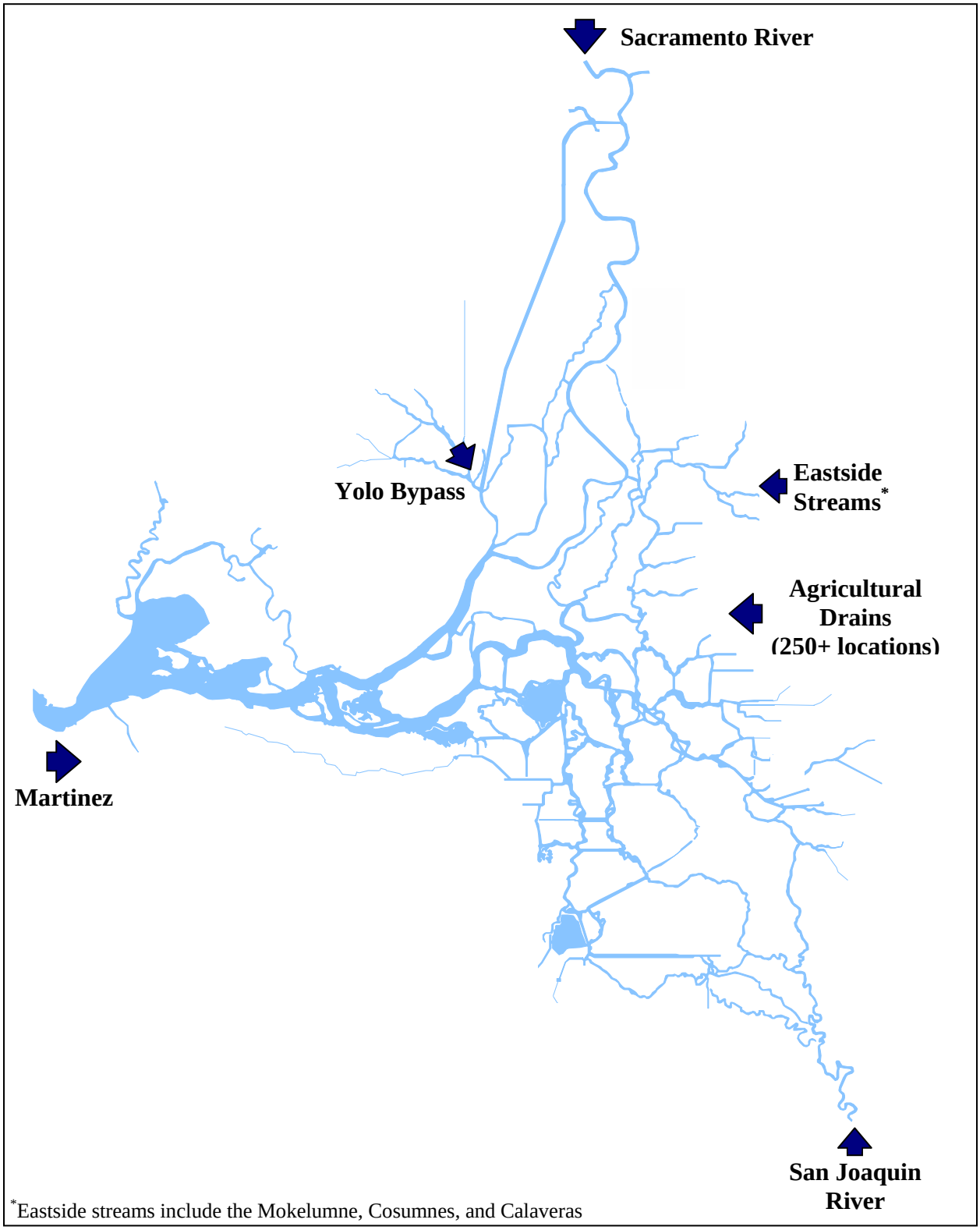

Figure 14.9: Typical Fingerprinting Source Locations for the Sacramento-San Joaquin Delta.

14.5.1 Volume Fingerprinting for Conservative Constituents by using Tracer Constituents in QUAL

Volume fingerprinting indicates the volume of water at a given location and time contributed by each source. For volume fingerprinting simulations, tracer constituents are used to represent contributions from each source. These tracers are arbitrarily defined conservative constituents in DSM2. The concentration of each tracer constituent is set to a constant value at the point of origin of each tracer. The concentration of each tracer constituent is then set equal to zero at all other locations. Thus for the six source locations typically used in DSM2 fingerprinting studies, the tracer concentrations would be set up as illustrated in Table 14.3. In this example, tracer 1 is associated with the Sacramento River, tracer 2 is associated with the San Joaquin River, etc. Additional source locations can be included by adding additional tracer constituents for each new source.

In addition, a tracer for checking mass conservation can be specified. Thus, for a six-source volume fingerprinting simulation of the Delta, seven tracer constituents would be specified: one for each source and one for mass conservation. For the mass conservation tracer, the concentration at each source is set equal to the constant value used for the individual source tracers (Table 14.3). If the same constant value is used at each source, the concentration of the mass conservation tracer will equal that constant value at all locations throughout the system. If mass is conserved, at any time at a specified location the sum of the tracer constituent concentrations should equal the simulated concentration of the mass conservation tracer (Equation 14-3). Although it is not necessary to use a separate mass conservation tracer, it provides a method to check that the simulation was set up correctly.

$$C_{Tmc} = \sum_{i=1}^{n} C_{Ti} \qquad \text{[Eqn. 14-3]}$$

where,

C_{Tmc} = concentration of the mass conservative tracer at a given location,
C_{Ti} = concentration of tracer constituent i at a given location,
n = total number of sources.

The value assigned for the concentration of each tracer at the source with which it is associated is arbitrary. For convenience in analysis, the same constant value is typically used for each tracer. A concentration of 10,000 is often used because percent contributions are easily determined by dividing by 100. A concentration of 10,000 is also large enough to indicate minor contributions, which can be lost in round off error if smaller values are used.

Table 14.3: Specified Tracer Concentations for Volume Fingerprinting in the Delta.

Location	Tracer 1	Tracer 2	Tracer 3	Tracer 4	Tracer 5	Tracer 6	Tracer 7 to Check Mass Conservation
Sacramento River	Constant value e.g., 10,000	0	0	0	0	0	Constant value e.g., 10,000
San Joaquin River	0	Constant value e.g., 10,000	0	0	0	0	Constant value e.g., 10,000
Martinez	0	0	Constant value e.g., 10,000	0	0	0	Constant value e.g., 10,000
Eastside Streams	0	0	0	Constant value e.g., 10,000	0	0	Constant value e.g., 10,000
Ag Drains	0	0	0	0	Constant value e.g., 10,000	0	Constant value e.g., 10,000
Yolo Bypass	0	0	0	0	0	Constant value e.g., 10,000	Constant value e.g., 10,000

Percent Volume Contributions for Volume Fingerprinting

The volume fingerprinting methodology indicates the volume of water at a given location contributed by each source represented by a tracer constituent. The percent volume contribution of a particular source, *k*, at a given location and time can be determined as shown in Equation 14-4:

$$V_{\%k} = \frac{C_{Tk}}{\sum_{i=1}^{n} C_{Ti}} \times 100\% = \frac{C_{Tk}}{C_{Tmc}} \times 100\% \qquad \text{[Eqn. 14-4]}$$

where,

C_{Ti} = concentration of the tracer constituent *i* at a given location,
C_{Tk} = concentration of the tracer constituent associated with specific source *k* at a given location,
n = total number of sources, and
$V_{\% k}$ = percent volume contribution from source *k* at a specified location.

Conservative Constituent Estimates for Volume Fingerprinting

The concentration of a conservative constituent at a specified location can be estimated from the percent volume contributions from each source if the source concentrations are known (Equation 14-5):

$$C_{CC} = \sum_{i=1}^{n} C_{Ti} \frac{V_{\%i}}{100} \qquad \text{[Eqn. 14-5]}$$

where,

C_{CC}	=	concentration of a conservative water quality constituent at a given location,
C_{Ti}	=	concentration of the tracer constituent *i* at a given location,
n	=	total number of sources, and
$V_{\%\,i}$	=	percent volume contribution from source *i* at a specified location.

Examples of volume fingerprinting results for different analysis periods are given in section 14.5.4.

Once the fraction of water contributed by each source, $\frac{V_{\%i}}{100}$, has been determined, a single DSM2 simulation can be used to estimate the concentration of any conservative constituent from the source concentrations for that constituent. However, Equation 14-5 only approximates the concentration of a conservative water quality constituent for a specific location. Antecedent conditions are not considered. This method does not account for changes in source flows and concentrations. If the residence time of the system is longer than the analysis period for the volume contributions, the volume and timing fingerprinting method provides a more accurate estimate of conservative constituent concentration estimates.

14.5.2 Volume and Timing Fingerprinting for Conservative Constituents by using Tracer Constituents in QUAL

The volume fingerprinting method presented in section 14.5.1 can be expanded to include the timing of the sources. Typically in DSM2, the volume and timing analysis is conducted on a monthly basis. An arbitrarily defined conservative tracer constituent is assigned to each source location for each month out of the year. Since the system memory for the Delta is considered to be six months or less, the volume and timing fingerprinting simulations are simplified by combining tracers for months that are six months apart. In other words, the same tracer is used to represent sources in January and July, February and August, March and September, etc. At the point of origin for each tracer, the concentration of that tracer constituent is set equal to a constant value for the two months represented by that source, and it is set equal to zero for the remaining ten months out of the year. The concentrations of the tracer constituents are set equal to zero at all other locations for all times. Thus for the six source locations typically used in DSM2 fingerprinting studies, the tracer concentrations would be set up as illustrated in Table 14.4. In this example, tracers 1-6 are associated with the Sacramento River, tracers 7-12 are associated with the San Joaquin River, etc. Additional source locations can be included in a

volume and timing fingerprinting simulation by adding six additional tracer constituents for each source. An example of the six tracer constituents that would be required to represent a single source in a volume and timing fingerprinting study is shown in Figure 14.10. For a six-source volume fingerprinting simulation of the Delta, thirty-six tracer constituents would be specified: six for each source.

Analysis of volume and timing fingerprinting results can be tricky, especially if the short cut of assigning two source time periods to each tracer is used. If two source time periods are assigned to each tracer, the source time represented by that tracer will depend upon the month for which the simulation results are analyzed. For example, consider a tracer that represents water from a given source entering the system in January and July. Simulated concentrations of that tracer represent the volume contribution by its source during January for simulation results in January through June. However, for simulation results for July through December, that tracer represents the volume contributed by its source during July. To further illustrate this concept, the source months represented by each tracer in Figure 14.10 for each simulation month are summarized in Table 14..

In addition, a tracer for checking mass conservation can be specified. Thus, for a six-source volume fingerprinting simulation of the Delta, forty-two tracer constituents would be specified: six for each source (6x6 = 36) and six for mass conservation (36+6 = 42). For the mass conservation tracer, the concentration at each source for each time period is set equal to the constant value used for the individual source tracers (Table 14.4). If the same constant value is used at each source, the concentration of the mass conservation tracer will equal that constant value at all locations throughout the system. If mass is conserved, at any time at a specified location the sum of the tracer constituent concentrations should equal the sum of the simulated concentration of the mass conservation tracers (Equation 14-6). Although it is not necessary to use a separate mass conservation tracer, it provides a method to check that the simulation was set up correctly.

$$\sum_{j=1}^{m} C_{Tmc,j} = \sum_{i=1}^{n}\sum_{j=1}^{m} C_{T(i,j)} \qquad \text{[Eqn. 14-6]}$$

where,

$C_{Tmc,j}$ = concentration of the mass conservative tracer at a given location for time period j,

$C_{T(i,j)}$ = Concentration of the tracer constituent i at a given location for time period j,

n = total number of sources, and

m = total number of time periods based on system memory.

Table 14.4: Specified Tracer Concentations for Volume and Timing Fingerprinting in the Delta.

Location	Tracers 1-6	Tracers 7-12	Tracers 13-18	Tracers 19-24	Tracers 25-30	Tracers 31-36	Tracers 37-42 to Check Mass Conservation
Sacramento River	Constant value e.g.,10,000 or zero*	0	0	0	0	0	Constant value e.g.,10,000 or zero*
San Joaquin River	0	Constant value e.g.,10,000 or zero*	0	0	0	0	Constant value e.g.,10,000 or zero*
Martinez	0	0	Constant value e.g.,10,000 or zero*	0	0	0	Constant value e.g.,10,000 or zero*
Eastside Streams	0	0	0	Constant value e.g.,10,000 or zero*	0	0	Constant value e.g.,10,000 or zero*
Ag Drains	0	0	0	0	Constant value e.g.,10,000 or zero*	0	Constant value e.g.,10,000 or zero*
Yolo Bypass	0	0	0	0	0	Constant value e.g.,10,000 or zero*	Constant value e.g.,10,000 or zero*

*Tracer is assigned a constant concentration for the two months represented by that tracer, and a value of zero is assigned for all other months.

Similar to the volume fingerprinting method, the value assigned for the concentration of each tracer at the source with which it is associated is arbitrary. For convenience, the same constant value is typically used for each tracer. A concentration of 10,000 is often used because percent contributions are easily determined by dividing by 100. A concentration of 10,000 is also large enough to indicate minor contributions, which can be lost in rounding error if smaller values are used.

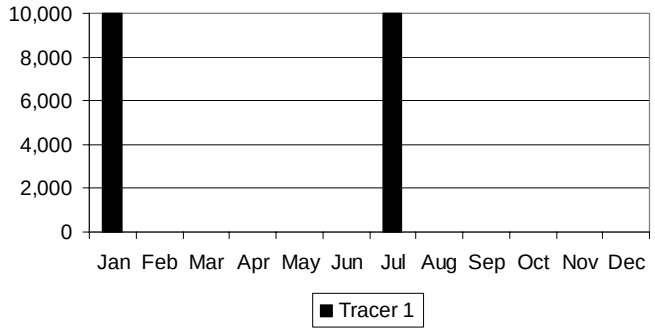
10,000
8,000
6,000
4,000
2,000
0
Jan Feb Mar Apr May Jun Jul Aug Sep Oct Nov Dec
Tracer 1

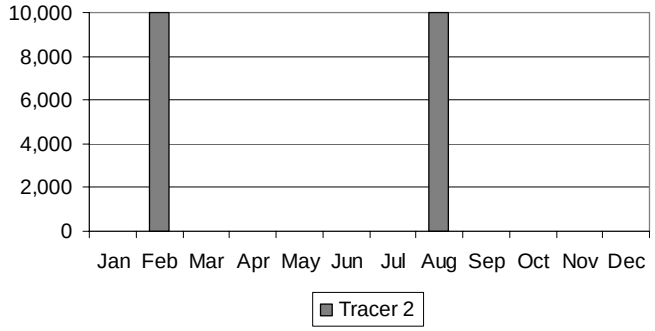
10,000
8,000
6,000
4,000
2,000
0
Jan Feb Mar Apr May Jun Jul Aug Sep Oct Nov Dec
Tracer 2

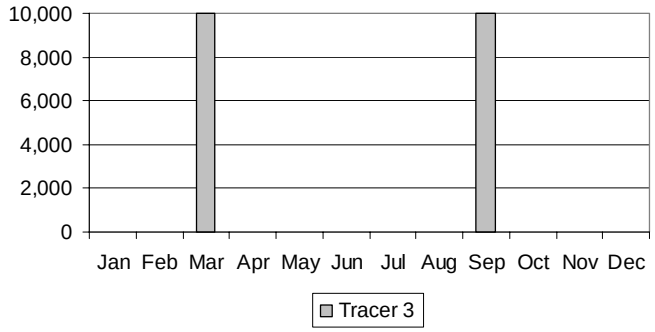
10,000
8,000
6,000
4,000
2,000
0
Jan Feb Mar Apr May Jun Jul Aug Sep Oct Nov Dec
Tracer 3

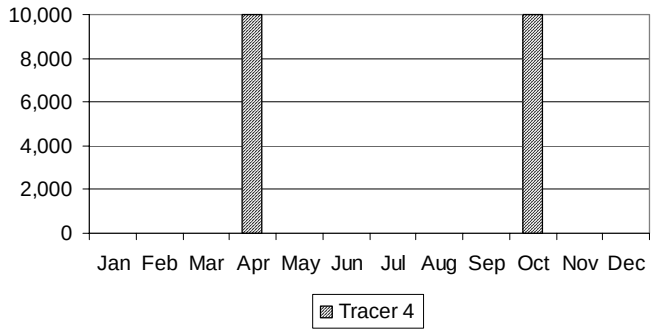
10,000
8,000
6,000
4,000
2,000
0
Jan Feb Mar Apr May Jun Jul Aug Sep Oct Nov Dec
Tracer 4

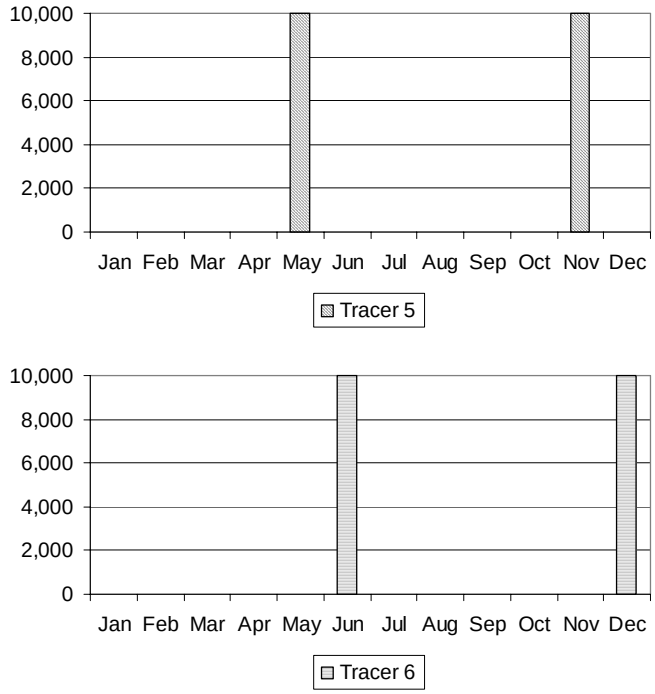

Figure 14.10: Specified Tracer Concentrations for a Single Source for Volume and Timing Fingerprinting in the Delta.

Table 14.5: Source Month Represented by each Tracer for a Specified Month in the Delta.

Simulation Results Month	**Jan**	**Feb**	**Mar**	**Apr**	**May**	**Jun**	**Jul**	**Aug**	**Sep**	**Oct**	**Nov**	**Dec**
Tracer 1	Jan	Jan	Jan	Jan	Jan	Jan	Jul	Jul	Jul	Jul	Jul	Jul
Tracer 2	Aug	Feb	Feb	Feb	Feb	Feb	Feb	Aug	Aug	Aug	Aug	Aug
Tracer 3	Sep	Sep	Mar	Mar	Mar	Mar	Mar	Mar	Sep	Sep	Sep	Sep
Tracer 4	Oct	Oct	Oct	Apr	Apr	Apr	Apr	Apr	Apr	Oct	Oct	Oct
Tracer 5	Nov	Nov	Nov	Nov	May	May	May	May	May	May	Nov	Nov
Tracer 6	Dec	Dec	Dec	Dec	Dec	Jun	Jun	Jun	Jun	Jun	Jun	Dec

Percent Volume Contributions for Volume and Timing Fingerprinting

The volume and timing fingerprinting methodology indicates the volume of water at a given location contributed by each source from a specified month. At a given location, the percent volume contribution of a particular source, *k*, from a specified time, *t*, can be determined as shown in Equation 14-7:

$$V_{\%(k,t)} = \frac{C_{T(k,t)}}{\sum_{i=1}^{n} C_{T(i,t)}} \times 100\% = \frac{C_{T(k,t)}}{C_{Tmc,t}} \times 100\% \qquad \text{[Eqn. 14-7]}$$

where,

$C_{Tmc,t}$ = concentration of the mass conservative constituent associated with specific source *m* at a given location for a specific time *t*,
$C_{T(k,t)}$ = concentration of the tracer constituent associated with specific source *k* at a given location for a specific time *t*,
$C_{T(i,t)}$ = concentration of the tracer constituent *i* at a given location for a specific time *t*,
n = total number of sources, and
$V_{\%\,(k,t)}$ = percent volume contributed from source *k* at a specified location for a specific time *t*.

For the Delta, six time periods (n = 6) represent the six-month "system memory". Because a single tracer represents two time periods for volume and timing fingerprinting, care must be taken when conducting analyses to ensure that the correct source times are associated with each tracer (see Figure 14.10 and Table 14.).

Conservative Constituent Estimates for Volume and Timing Fingerprinting

The concentration of a conservative constituent at a specified location can be estimated from the percent volume contributions from each source if the source concentrations are known (Equation 14-8):

$$C_{CC} = \sum_{i=1}^{n}\sum_{j=1}^{m} C_{T(i,j)} \frac{V_{\%(i,j)}}{100} \qquad \text{[Eqn. 14-8]}$$

where,

C_{CC} = concentration of a conservative water quality constituent at a specified location for a give time,
n = total number of sources,
m = total number of time periods based on the system memory, and
$V_{\%\,(i,j)}$ = percent volume contributed from source i at a specified location for a specific time *j*.

Once the fraction of water contributed by each source during each time period, $\frac{V_{\%(i,j)}}{100}$, has been determined, a single DSM2 simulation can be used to provide a good estimate of the concentration of any conservative constituent from the source concentrations for that constituent. Because of the long residence times in the Delta and fluctuations in boundary flows and constituent concentrations, using the volume and timing fingerprinting method provides a more accurate estimate of conservative constituent concentration estimates than using the volume fingerprinting method.

14.5.3 Accuracy of Conservative Constituent Concentration Estimates

The accuracy of conservative constituent concentration estimates using fingerprinting depends on various factors. Variations in the source flows and/or concentrations over the analysis period (hourly, daily, monthly) affect the accuracy of constituent concentration estimates using fingerprinting. For example, EC concentrations for the Sacramento River, eastside streams, and Yolo Bypass are relatively constant with time. However, EC concentrations for Martinez, the San Joaquin River, and agricultural drains vary with time. Using fingerprinting methods that include timing of the sources increases the accuracy of the constituent concentration estimates.

The relative importance of errors in a fingerprinting analysis may depend on the application. To illustrate this point, consider volume fingerprinting results for Martinez that are going to be used to estimate constituent concentrations for both EC and DOC at Rock Slough. Typical source concentrations at Martinez for these two constituents are 25,000 umhos/cm for EC and between 1.6 and 7.0 mg/l for DOC.[5] Assume that the fingerprinting analysis found the volume of water from Martinez at Rock Slough to be 2% of the total volume of water at Rock Slough.

To illustrate the impacts of errors in boundary constituent concentrations on estimates of constituent concentrations at other locations in the Delta, consider a 10% error in the Martinez source concentration. For the EC concentration estimate, a 10% error in the Martinez source concentration estimate results in a 2,500 umhos/cm error at the Martinez boundary. Based on the fingerprinting concentration volume contribution at Rock Slough, the original Martinez contribution at Rock Slough would be 500 umhos/cm, while the same contribution with a 10% increase in the Martinez concentration would be 550 umhos/cm. The 50 umhos/cm difference at Rock Slough between these two scenarios is considerably smaller than the 2,500 umhos/cm error at Martinez.

For the DOC concentration estimate, a 10% error in the Martinez source concentration estimate results in a 0.02 to 0.07 mg/l increase in the DOC concentration at Martinez. Based on the fingerprinting volume contribution, the high-end (7 mg/l) contribution at Rock Slough would be 0.14 mg/l, while the same contribution of DOC from Martinez with a 10% increase would be 0.15 mg/l. The 0.01 mg/l difference at Rock Slough is on the same order of magnitude as the difference in DOC at Martinez (0.02 and 0.07 mg/l for the low- and high-end errors).

The significance of an error in a source concentration estimate at a location of interest depends not only upon the magnitude of the error at the boundary, but also depends on the relative concentrations from the other sources and the volume contribution from the source in question. Errors related to a major source of a constituent will have more of an impact on the concentration estimate than errors related to minor sources.

14.5.4 Sample Volume Fingerprinting Results

Results from fingerprinting simulations can be analyzed in several different ways. Results can be examined on different time scales (hourly, daily, monthly, etc). Analyses can be conducted based on hydrologic conditions, such as dividing the simulation results by water year type. To illustrate the wide range of applications of fingerprinting, examples from a volume fingerprinting

[5] The DOC water quality at Martinez is based on data collected at Mallard Island (Pandey, 2001).

study of historical conditions for water years 1992-1998 are presented below. All results shown are for the entrance to Clifton Court Forebay. In Figure 14.11, monthly percent volume contributions from two sources, the Sacramento and San Joaquin rivers, are shown as a time series plot. Other sources contributed less than 20% and were omitted for illustration purposes. The time series plot indicates that it depends on the time period whether the Sacramento River or the San Joaquin River provides the majority of the volume at the entrance to Clifton Court Forebay.

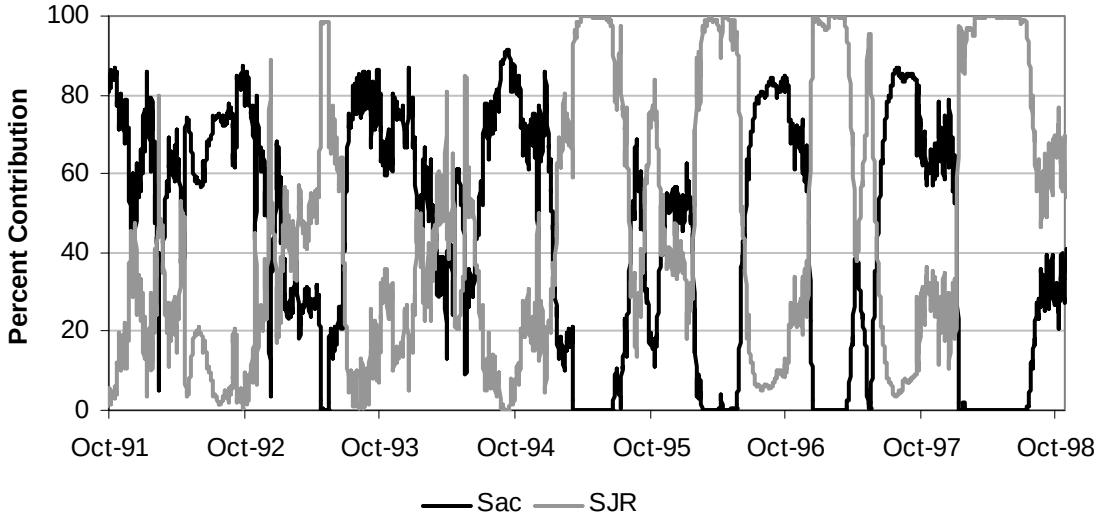

Figure 14.11: Percent Volume Contributions of the Sacramento and San Joaquin Rivers at the Entrance to Clifton Court Forebay.

As an additional analysis, the volume fingerprinting results were examined based on water year types. Pie charts illustrate the relative volume contributions from six sources by water year type (Figure 14.12). These results indicate that at the entrance to Clifton Court Forebay the Sacramento River provide the majority of the water volume during critical years, whereas the San Joaquin River provides the majority of the water volume during wet years.

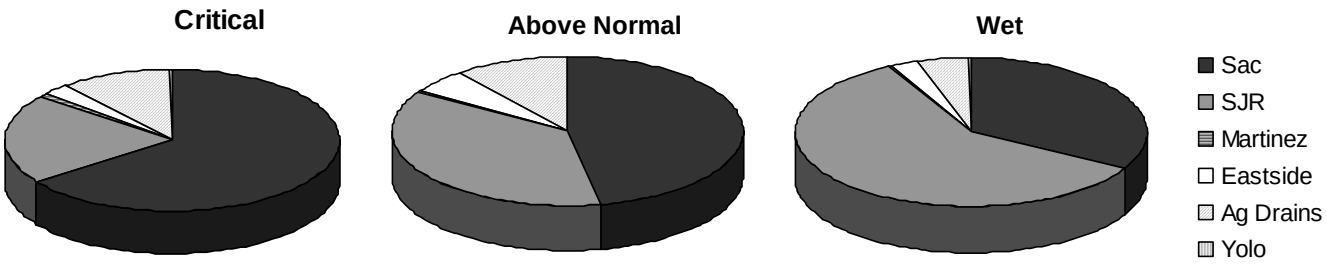

Figure 14.12: Percent Volume Contributions of the Sacramento and San Joaquin Rivers at the Entrance to Clifton Court Forebay based on Water Year Types.

Monthly average volume contributions over the seven-year period were also analyzed. The monthly average results in Figure 14.13 indicate that at the entrance to Clifton Court Forebay the Sacramento River provides the majority of the water volume during dry months, whereas the San Joaquin River provides the majority of the water volume during wet months.

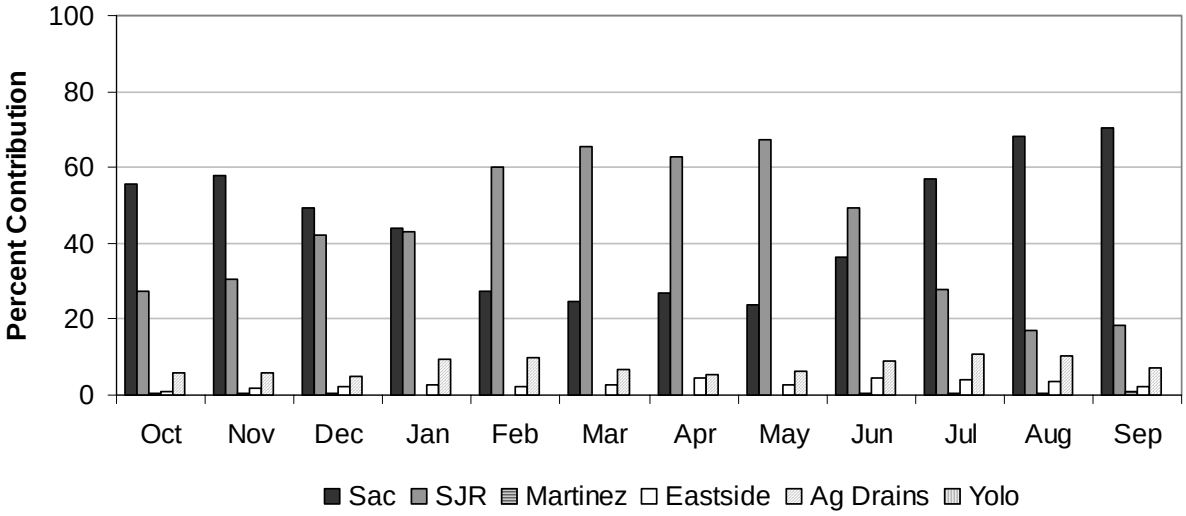

Figure 14.13: Monthly Average Percent Volume Contributions of the Sacramento and San Joaquin Rivers at the Entrance to Clifton Court Forebay.

14.6 Special Applications of Fingerprinting using DSM2

The volume-based fingerprinting methods described in section 14.5 provide a general analysis methodology that can be used to estimate the concentration of any conservative constituent. This section describes adaptations of those techniques when analysis is desired for a specific conservative constituent.

14.6.1 Constituent Fingerprinting

For the volume fingerprinting method, tracer constituents represent any conservative constituent. For the case when fingerprinting analysis is only desired for a specific constituent (e.g., EC), the arbitrary concentration of the tracer constituent (Table 14.3) can be replaced with the source concentrations of the desired constituent (Table 14.). In addition to specifying a tracer constituent for each source, the conservative constituent being investigated (e.g., EC) is simulated as its own constituent in the traditional manner. If mass is conserved, at any time at a specified location the sum of the tracer constituent concentrations should equal the simulated constituent concentration (Equation 14-9). This provides a method to check that the simulation was set up correctly.

$$C_{CC} = \sum_{i=1}^{n} C_{Ti} \qquad \text{[Eqn. 14-9]}$$

where,

C_{CC} = concentration of the conservative constituent to be simulated,
C_{Ti} = concentration of tracer constituent i, and
n = total number of sources.

Table 14.6: Specified Tracer Concentations for Constituent Fingerprinting in the Delta.

Location	Tracer 1	Tracer 2	Tracer 3	Tracer 4	Tracer 5	Tracer 6	Constituent (e.g., EC)
Sacramento River	Observed Values	0	0	0	0	0	Observed Values
San Joaquin River	0	Observed Values	0	0	0	0	Observed Values
Martinez	0	0	Observed Values	0	0	0	Observed Values
Eastside Streams	0	0	0	Observed Values	0	0	Observed Values
Ag Drains	0	0	0	0	Observed Values	0	Observed Values
Yolo Bypass	0	0	0	0	0	Observed Values	Observed Values

Percent Contributions for Constituent Fingerprinting

The constituent fingerprinting methodology indicates the relative contributions of a specified source to the constituent concentration at a given location. The percent contribution of a particular source, k, at a given location and time can be determined as shown in Equation 14-10:

$$C_{\%k} = \frac{C_{Tk}}{\sum_{i=1}^{n} C_{Ti}} \times 100\% = \frac{C_{Tk}}{C_{CC}} \times 100\% \qquad \text{[Eqn. 14-10]}$$

where,

$C_{\%k}$ = percent contribution of the conservative constituent from source k at a specified location,
C_{Tk} = concentration of tracer constituent k, and
n = total number of sources.

14.6.2 Constituent and Timing Fingerprinting

The constituent fingerprinting method described in section 14.6.1 can be extended to constituent and timing fingerprinting also by adding tracer constituents for each desired source location and time. For the case when fingerprinting analysis is only desired for a specific constituent (e.g., EC), the arbitrary concentration of the tracer constituent (Table 14.4) can be replaced with the source concentrations of the desired constituent (Table 14.7).

Table 14.7: Specified Tracer Concentations for Constituent and Timing Fingerprinting in the Delta.

Location	Tracers 1-6	Tracers 7-12	Tracers 13-18	Tracers 19-24	Tracers 25-30	Tracers 31-36	Constituent (e.g., EC)
Sacramento River	Observed values or zero*	0	0	0	0	0	Observed values
San Joaquin River	0	Observed values or zero*	0	0	0	0	Observed values
Martinez	0	0	Observed values or zero*	0	0	0	Observed values
Eastside Streams	0	0	0	Observed values or zero*	0	0	Observed values
Ag Drains	0	0	0	0	Observed values or zero*	0	Observed values
Yolo Bypass	0	0	0	0	0	Observed values or zero*	Observed values

*Tracer is assigned the observed concentration for the two months represented by that tracer, and a value of zero is assigned for all other months.

Percent Contributions for Constituent and Timing Fingerprinting

The constituent and timing fingerprinting methodology indicates the relative contributions of a specified source during a specified month to the constituent concentration at a given location.

Based on Equation 14-10, the percent contribution of a particular source, *k*, from a specified month, *t*, at a given location can be determined as shown in Equation 14-11:

$$C_{\%(k,t)} = \frac{C_{T(k,t)}}{\sum_{i=1}^{n}\sum_{j=1}^{m} C_{T(i,j)}} \times 100\% = \frac{C_{T(k,t)}}{C_{CC}} \times 100\% \qquad \text{[Eqn. 14-11]}$$

where,

$C_{\%(k,t)}$ = percent contribution of the conservative constituent *k* during time *t* at a specified location,
$C_{T(i,j)}$ = concentration of tracer constituent from source *i* at time *j* at a specified location,
$C_{T(k,t)}$ = concentration of tracer constituent *k* at time *t*,
n = total number of sources, and
m = length of the system memory.

14.6.3 Constituent or Constituent and Timing Fingerprinting for Conservative Constituents by using an OUTPUTPATHS Section in the QUAL Input

In addition to the fingerprinting methods described above, DSM2 will internally set up and run fingerprinting simulations by specifying an appropriate OUTPUTPATHS section in the QUAL input. The OUTPUTPATHS section requests fingerprinting results at specified locations. The amount of the constituent contributed by the specified source is then computed internally when QUAL is run in a process that is transparent to the user. Results are only provided for the constituents and sources specified in a QUAL OUTPUTPATHS section.

For constituent fingerprinting, an OUTPUTPATHS section is added to the QUAL input that includes one of the following key words:

- FROM_NAME tracks conservative constituents from a location name
- FROM_TYPE tracks conservative constituents from an accounting type
- FROM_NODE tracks conservative constituents from a node number
- FROM_ALL tracks conservative constituents from all sources[6]

Additional details on OUTPUTPATHS sections in the DSM2 input files can be found in the 1998 annual report (Nader-Tehrani et al., 1998).

Sample Scenario

How much of the EC at various locations in the Delta originated from the ocean (Martinez)?

[6] The FROM_ALL computation occurs automatically for any fingerprinting simulation specified by one of the above FROM_XXX keywords. However the results are only provided in the output if the FROM_ALL keyword is specified.

Sample OUTPUTPATHS Section

```
OUTPUTPATHS
NAME FROM_NAME  TYPE  INTERVAL PERIOD  FILENAME
antioch         mtz   ec       1day    ave      output-files/qual.dss
jerseypt        mtz   ec       1day    ave      output-files/qual.dss
victoria        mtz   ec       1day    ave      output-files/qual.dss
cvp             mtz   ec       1day    ave      output-files/qual.dss
END
```

Using the above OUTPUTPATHS section, DSM2 would compute the one-day average contributions of EC from Martinez at the four specified locations (Antioch, Jersey Point, Victoria, and the CVP). The results would be stored in a file called qual.dss located in the output-files directory.

14.7 Summary

Fingerprinting techniques have been used to analyze source contributions of Delta flows and conservative constituent concentrations using DSM2. Fingerprinting studies are conducted by simulating the transport of conservative tracer constituents associated with each source. The two main applications of fingerprinting are volume fingerprinting and volume and timing fingerprinting. Results from fingerprinting analyses provide:

- A method for using a single DSM2 simulation to estimate the concentration of any conservative constituent at specified locations in the Delta if the source concentrations are known. The volume and timing fingerprinting method provides the best estimate of conservative constituent concentrations.
- The relative importance of each source.
- Improved understanding of the Delta.

Use of fingerprinting techniques with DSM2 provides a powerful analysis tool for understanding both hydrodynamics and water quality dynamics in the Delta.

14.8 References

Hutton, P. and F. Chung. (1992). "Simulating THM Formation Potential in Sacramento Delta. Part II." *Journal of Water Resources Planning and Management.* American Society of Civil Engineers. 118 (5).

Nader-Tehrani, P. and R. Finch. (1998). "Chapter 5: DSM2 Input and Output." *Methodology for Flow and Salinity Estimates in the Sacramento-San Joaquin Delta and Suisun Marsh. 19th Annual Progress Report to the State Water Resources Control Board.* California Department of Water Resources. Sacramento, CA.

Pandey, G. (2001). "Chapter 3: Simulation of Historical DOC and UVA Conditions in the Delta." *Methodology for Flow and Salinity Estimates in the Sacramento-San Joaquin Delta and Suisun Marsh. 22nd Annual Progress Report to the State Water Resources Control Board.* California Department of Water Resources. Sacramento, CA.

Methodology for Flow and Salinity Estimates in the Sacramento-San Joaquin Delta and Suisun Marsh

23rd Annual Progress Report
June 2002

Chapter 15:
Short-Term Improvements to Artificial Neural Network Implementation in CALSIM

Author: Sanjaya Senevirante

15 Short-Term Improvements to Artificial Neural Network Implementation in CALSIM

15.1 Introduction

An Artificial Neural Network (ANN) was recently implemented in CALSIM II to define Delta salinity constraints. The Delta Modeling and Hydrology and Operation Sections are collaborating with the U.S. Bureau of Reclamation (USBR) staff through the CALSIM ANN Refinement Team (CART) to make systematic improvements to the model. This chapter outlines the team's objectives, current status, and future considerations. The team's goal is to implement a refined ANN in CALSIM II by mid-2003.

15.2 Objectives

The short-term objectives for the year 2002 have been identified as follows:

- Identify the best inputs for the ANN that generate the most accurate flow-salinity relationship.
- Identify better training techniques to improve the accuracy of the predicted EC.
- Increase the robustness of the ANN to take into account any variation of hydrology and Delta operations.
- Find a method to simplify the ANN implementation and reduce ANN run time in CALSIM.

15.2.1 Best Input Parameters in ANN

The existing ANN uses Sacramento and San Joaquin flows, exports (including net channel depletions) and Delta Cross Channel (DCC) operation as inputs to estimate EC at any given location. The following inputs will be considered in an attempt to improve the existing ANN:

- Use the Cross Delta Flow (flow through the DCC and Georgiana Slough), instead of DCC operation.
- Use QWEST instead of DCC operation.
- Use net channel depletions as a separate input.
- Use EC at Mallard as a new input (the existing ANN predicts EC at Mallard very well).

- Train the ANN on the differences rather than the absolute values, i.e. use flow differences to predict EC differences.

15.2.2 Better Training Techniques

The existing ANN was trained using the Stuttgart Neural Network Simulator (SNNS version 4.2). The goal is to develop the best training techniques that will yield the best results using the current SNNS. The performance of other ANN models will not be evaluated this year.

- At present, the time period between 1980–1991 is used for calibration and 1975–1979 is used for validation. Instead of a specific time period, 25% of the data will be randomly picked as the validation data set.

- At present all input data are normalized between 0.2–0.8 prior to training the ANN. Different ranges will be tested.

- To increase the accuracy of the predictions, weights in key regions will be increased.

- Different training parameters including the use of different ANN hidden will be tested.

15.2.3 Increase the Robustness of the ANN

The existing ANN performance degrades when the hydrology changes by a significant amount. This observation can be attributed to the following:

- The hydrology is outside the range of the training data set.

- The EC time series pattern in the training data set is very different from the EC time series pattern that is generated by the planning hydrology.

To eliminate these problems the following strategies will be tested:

- Multiply a given hydrology by different factors to generate a wide range of hydrologies. The perturbations should encompass all possible hydrologies that CALSIM will generate.

- Use several different known hydrologies in the training of the ANN. It is important to pick at least two hydrologies that bookend all other hydrologies.

- Synthetically generate a data set to capture all possible hydrologies.

15.2.4 Changes in ANN Implementation in CALSIM

Depending on the final form of the new ANN, the implementation of ANN in CALSIM will likely be changed. This work will begin when the new ANN is finalized.

15.3 Current Status

Most of the planned experiments are ongoing. No definite conclusions have been made. However, an improvement in predicted EC was observed when Cross Delta flow was used instead of DCC operation.

15.4 Future Considerations

The tests that are planned for this year are part of an ongoing process to achieve the best possible flow-salinity model using the least possible computation time.

Acronyms and Abbreviations

ADCP – Acoustic Doppler Current Profiler
ANN – Artificial Neural Network
BRM – Bromate
CALSIM – California Water Resources Simulation Model
CART – CALSIM ANN Refinement Team
CCC PP #1 – Contra Costa Canal Pumping Plant #1
CCWD – Contra Coast Water District
CVP – Central Valley Project
D-1485 – SWRCB Water Rights Decision 1485
D-1641 – SWRCB Water Rights Decision 1641
DAYFLOW – DWR Delta Daily Boundary Flow Model
DCC – Delta Cross Channel
DICU – Delta Island Consumptive Use
DMC – Delta Mendota Canal
DO – Dissolved Oxygen
DOC – Dissolved Organic Carbon
DOI – Delta Outflow Index
DSM1 – Delta Simulation Model 1
DSM2 – Delta Simulation Model 2
DWR – California Department of Water Resources
EC – Electrical Conductivity
E/I – Ratio of Delta Exports to Delta Inflows
ESO – DWR's Environmental Services Office
HYDRO – DSM2 Hydrodynamics Model
IEP – Interagency Ecological Program
IEP-PWT – IEP DSM2 Recalibration Project Work Team
ISI – Integrated Storage Investigation
JP – Jersey Point
MSE – Mean Squared Error
MWQI – DWR's Municipal Water Quality Investigations
NDO – Net Delta Outflow
O&M – DWR's Operation and Maintenance
PTM – Particle Tracking Model
PWT – Project Work Team (see IEP-PWT)
RS – Rock Slough
QUAL – DSM2 Water Quality Model
QWEST – Approximation of Western Flow in Delta
SNNS – Stuttgart Neural Network Simulator
SQL – Structured Query Language
SWP – State Water Project
SWRCB – State Water Resources Control Board
TDS – Total Dissolved Solids
TTHM – Total Trihalomethane
TOC – Total Organic Carbon
USBR – U.S. Bureau of Reclamation
USFWS – U.S. Fish and Wildlife Service
USGS – U.S. Geological Survey
UVA – Ultraviolet Light Absorbance
VISTA – Visualization Tool and Analyzer
WIMS – Water Information Monitoring System
WQMP – Water Quality Management Plan